

Course CT5310

Probabilistic Design in Hydraulic Engineering

June 2006

Faculty of Civil Engineering and
Geosciences

Prof. drs. ir. J.K. Vrijling
Dr. ir. P.H.A.J.M. van Gelder



Bestelnummer: 06917300051

CONTENTS

I.	Introduction	I - 1
I.1.	Course objective.....	I - 1
I.2.	The course set-up.....	I - 2
II.	Statistical description of boundary conditions and strength	II - 1
II.1.	Introduction.....	II - 1
II.2.	Extreme value distributions.....	II - 3
II.3.	Types of extreme value distributions	II - 8
II.4.	Dependence and extreme value distributions.....	II - 13
II.5.	Probability density functions and distributions from physical relations.....	II - 13
II.6.	Multi- dimensional probability density functions.....	II - 17
II.7.	Wave climate.....	II - 24
II.8.	Verification of the input data	II - 33
II.9.	Hydraulic boundary conditions for the Oosterschelde storm surge barrier.....	II - 38
II.9.1.	Introduction.....	II - 39
II.9.2.	The still water levels at both sides of the barrier.....	II - 40
II.9.2.1.	Introduction.....	II - 40
II.9.2.2.	The storm surge level: two models.....	II - 40
II.9.2.3.	The low water level.....	II - 45
II.9.2.4.	Empirical evidence.....	II - 47
II.9.2.5.	The transformation of the low water levels into basin levels.....	II - 47
II.9.3.	The surge levels and wave energy.....	II - 48
II.9.3.1.	Introduction.....	II - 48
II.9.3.2.	Foundations of the model.....	II - 49
II.9.3.3.	The mathematical wave model of the Oosterschelde.....	II - 50
II.9.3.4.	Empirical evidence.....	II - 54
II.9.3.5.	Wave direction.....	II - 55
II.9.3.6.	The processes on the North Sea.....	II - 57

II.9.3.7.	Empirical evidence.....	II - 59
II.9.3.8.	The completed model.....	II - 60
II.9.4.	The three dimensional probability density function of maximum storm surge level, wave energy and basin level.....	II - 61
II.10.	Strength.....	II - 64
II.10.1.	Some data.....	II - 64
II.11.	Methods of statistical analysis.....	II - 68
II.11.1.	Regression analysis.....	II - 69
II.11.1.1.	Working method for linear regression of two variables with constant variance.....	II - 70
II.11.1.2.	Implications of transformations.....	II - 71
II.11.2.	Correlation analysis.....	II - 72
II.11.3.	Explained variance.....	II - 73
II.12.	Estimates of statistics.....	II - 74
II.13.	Estimating distribution parameters.....	II - 77
II.13.1.	Methods for the estimation of distribution parameters.....	II - 77
II.13.2.	The method of the moments.....	II - 77
II.13.3.	Linear regression.....	II - 83
II.13.3.1.	Organisation of the observation material and transformations.....	II - 83
II.13.3.2.	The method of the least squares.....	II - 85
II.13.4.	The method of maximum likelihood.....	II - 85
II.13.5.	Bayesian parameter estimation.....	II - 88
II.13.6.	χ^2 - test.....	II - 90
II.13.6.	Kolmogorov- Smirnov test.....	II - 91
II.14.	Loads.....	II - 92
II.15.	Probabilistic determination of the load for the Oosterschelde storm surge barrier.	II - 96
II.15.1.	Introduction.....	II - 96
II.15.2.	Hydraulic boundary conditions.....	II - 97
II.15.3.	Transfer functions.....	II - 97

II.15.3.1.	Mathematical model.....	II - 97
II.15.3.2.	Description of model facilities.....	II - 99
II.15.3.3.	Series of tests.....	II - 99
II.15.3.4.	Results.....	II - 100
II.15.4.	Probabilistic load determination.....	II - 101
II.15.4.1.	General.....	II - 101
II.15.4.2.	The description of the method.....	II - 101
II.15.4.3.	Numerical transfer.....	II - 103
II.15.5.	The reliability of the method.....	II - 104
II.15.5.1.	The description of the analyses.....	II - 104
II.15.5.2.	Results.....	II - 106
II.15.6.	The applications in the design process.....	II - 106
II.15.6.1.	The design method.....	II - 106
II.15.6.2.	The application of the load distribution.....	II - 106
II.15.6.2.1.	Quasi- probabilistic design method.....	II - 106
II.15.6.2.2.	Semi- probabilistic design method.....	II - 107
II.15.7.	Conclusions.....	II - 108
APPENDIX II-1. Comparison of Gumbel distribution with Weibull distribution.....		II - 114
APPENDIX II-2. Ordinates with data sets of observations.....		II - 117
APPENDIX II-3. Comparison of linear regression (method of least linear squares) with the method of the moments.....		II - 121
III.	Probabilistic calculations	III - 1
III.1.	Comparison of probabilistic calculations at levels II and III.....	III - 1
III.2.	The weighted sensitivity analysis at level III.....	III - 1
III.3.	Transformation to standard-normally distributed variables.....	III - 2
III.3.1.	The design point in an integration procedure.....	III - 2
III.3.2.	The design point in Monte Carlo simulations.....	III - 3
III.3.2.1.	Method "centre of gravity".....	III - 4

III.3.2.1.	Method "angles".....	III - 6
III.3.2.3.	Method "nearest to mean".....	III - 8
III.3.2.4.	Comparison of the results for the chosen example.....	III - 9
III.3.2.5.	Programs in MATHCAD 7.3 and in TURBO PASCAL.....	III - 10
III.4.	Boundary conditions as a function of two phenomena.....	III - 16
III.4.1.	Extreme high water levels.....	III - 16
III.4.2.	Storm surge levels.....	III - 17
III.4.3.	River discharges.....	III - 19
III.4.4.	Equal level curves.....	III - 21
III.4.5.	Equal level curves in the "Guidelines Lower Rivers".....	III - 23
III.4.6.	Probability density of the high water levels in the basin.....	III - 25
III.4.7.	Failure of the water defence.....	III - 26
III.4.8.	Coinciding loads.....	III - 26
IV.	Failure modes in a cross-section	IV - 1
IV.1.	Failure modes.....	IV - 1
IV.2.	Examples.....	IV - 4
V.	Length effects	V - 1
V.1.	Introduction.....	V - 1
V.2.	Length effects as a result of fluctuating strength.....	V - 4
V.3.	Length and time effects.....	V - 16
VI.	Optimal safety	VI - 1
VI.1.	Norms.....	VI - 1
VI.2.	Econometric approach.....	VI - 4
VI.3.	More than one threat.....	VI - 6
VI.3.1.	General.....	VI - 6
VI.3.2.	Predominant Objection.....	VI - 8
VI.3.3.	Limited budget.....	VI - 8
VI.4.	Several modes in one cross section.....	VI - 9

VI.5.	Consequence varying as a function of the high water level and of the location of the breach.....	VI - 10
VII.	Budgeting and time planning	VII - 1
VII.1.	Introduction and definitions..	VII - 1
VII.2.	The classical approach to budget estimates and time planning.....	VII - 3
VII.3.	Uncertainty concerning budget estimates and time planning.....	VII - 7
VII.3.1.	Classification of uncertainty.....	VII - 8
VII.4.	Time planning and budget estimates in level II calculations.....	VII - 13
VII.5.	Visualisation of uncertainty.....	VII - 22
VII.6.	Quantification of the item unforeseen.....	VII - 23
VII.6.1.	Experiences with exceedences of costs.....	VII - 23
VII.7.	Comparison of an estimate containing special events with experience on cost exceedences.....	VII - 25
VII.8.	Risk control measures	VII - 26
VII.8.1.	Description of concepts.....	VII - 26
VII.8.2.	Analysis of the influence of risk control measures.....	VII - 29
VII.8.3.	Analysis of the influence of risk control measures on the accuracy of an estimate (or the sensitivity of the costs for risk control measures).....	VII - 31
VII.9.	Literature.....	VII - 36
VIII.	Safety coefficients	VIII -1
VIII.1.	Boundary conditions and other basic variables.....	VIII -1
VIII.2.	The acceptable probability of failure.....	VIII- 2
VIII.3.	The format of the proposed code.....	VIII- 2
VIII.4.	The results.....	VIII- 3
VIII.5.	Tentative proposal.....	VIII- 4
VIII.6.	Discussion points.....	VIII -5
IX.	Maintenance theory	IX -1
IX.1.	Introduction.....	IX -1
IX.2.	Terminology.....	IX- 4

IX.2.1.	Time dependent strength.....	IX- 4
IX.2.2.	Probability of failure.....	IX -4
IX.2.3.	Deterioration models.....	IX -5
IX.2.4.	Life-span of a structure without maintenance.....	IX -6

I. INTRODUCTION

I.1 COURSE OBJECTIVE

The objective of this course is to convey knowledge and experience of probabilistic techniques that were acquired during large scale hydraulic projects such as:

- ◆ creation of an artificial island in the Beaufort Sea (to the North of Alaska, see Figure I-1)
- ◆ port construction in Karwar (on the westcoast of India, see Figure I-2)
- ◆ the design of the Jamuna Bridge in Bangladesh (idem)
- ◆ the Oosterschelde storm surge barrier (see Figure I-3)
- ◆ the Nieuwe Waterweg storm surge barrier (idem)
- ◆ the design of the Pump Accumulation Station (the Lievense Plan)
- ◆ water defences; most importantly the latter refers to a study carried out for the Technical Advisory Committee on Water Defences (TAW). The Advisory Committee's tasks include giving guidelines for the construction, management and maintenance of water defences (not only for dykes).

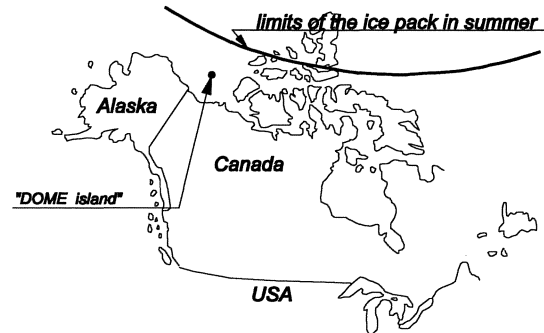


Figure I-1

This course will also treat the guidelines.

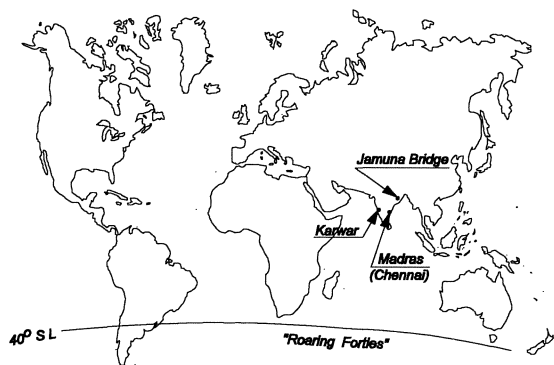


Figure I-2

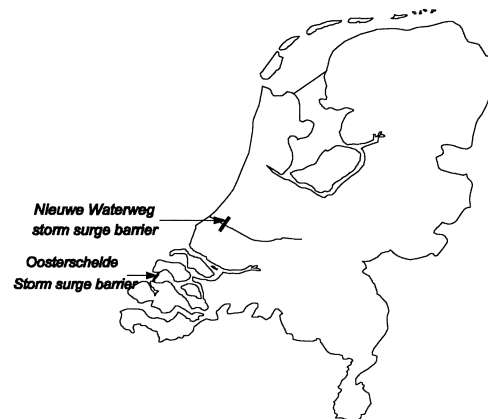


Figure I-3

Using fault trees and other probabilistic techniques sometimes leads to a better grasp of the problem, as became evident during the design of the Jamuna Bridge and the breakwater design for Karwar and Madras (Chennai).

The aforementioned techniques were used for the risk analysis for existing breakwaters, carried out for PIANC. The objective was to define guidelines for breakwater design. For the design of armour units safety factors were determined.

I.2. THE COURSE SET-UP

The following subjects will be treated during the course:

- ◆ Statistical description of boundary conditions and strength.
- ◆ Selecting probability functions and the related parameters. Correlation.
- ◆ Probabilistic calculations for ultimate limit states (U.L.S.) and serviceability limit states (S.L.S.). Calculations at levels III, II and I and further refinements. Selecting methods and testing. Boundary conditions with two or more variables such as water levels in the transitory area between the river and the sea and load by waves, where wave heights and periods in the wave field are of significance.
- ◆ Failure modes in a section. Stability for a great number of possible failure modes. Fault- and event trees. Examples of U.L.S. and S.L.S..
- ◆ Length effects. Length effects resulting from boundary conditions and loads on the one hand and from fluctuating strength on the other hand.
- ◆ Analysis of the complete design using examples. Correspondence with quality assurance.
- ◆ Regulations, guidelines etc.

Though not directly in the hydraulic domain, the following issue is also covered:

- ◆ Risk- analysis of the costs and planning.

II. STATISTICAL DESCRIPTION OF BOUNDARY CONDITIONS AND STRENGTH

II.1. INTRODUCTION

High water levels, wave climates (which concern the directions, heights and periods of the waves, as well as the possible relations between these aspects), discharges etc. are often presented as exceedance frequency curves or probability distributions. If observations concerning the variable to be examined are available, one should first consider with which objective the data is to be analysed. There is a difference between looking for:

- ◆ an extreme load (an ultimate limit state - U.L.S. - with an expected occurrence of for example 0,01 or less in one year) and
- ◆ a frequently occurring load (a serviceability limit state - S.L.S. - which occurs a considerable amount of the time.)

When analysing statistical data, one should first consider the form of the process (natural phenomenon) (see Figure II-1):

- a Is it a constant process? b do seasons play a role? c are there more than one phenomena?
 (Is the process STATIONARY? ¹) (E.g. monsoons) (E.g. a cyclone during a monsoon)

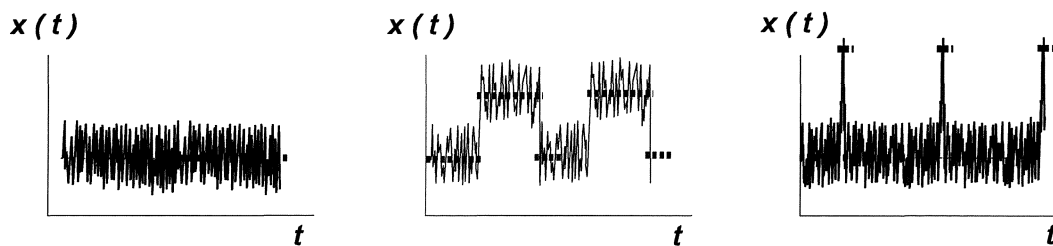


Figure II-1

Ad a.

If the observations originate from one stationary process, an uninterrupted observation period of for example one year gives sufficient information for the statistical description of the phenomenon. The distribution of the phenomenon can be determined from observations. If 3-hourly observations (of wind velocities, significant wave heights, etc.) are concerned, as is often the case with wave registrations, the function found is an estimated probability that phenomenon x

(the significant wave height determined from wave registrations during 20 minutes, measured with intervals of 3 hours, is assumed equal to the significant wave height during those 3 hours) is smaller than or equal to a certain value x . This distribution is usable

for S.L.S. considerations such as wear, workable days (under weather conditions), etc..

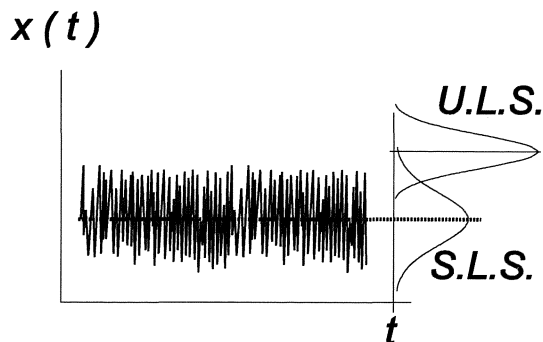


Figure II-2

¹ A process is stationary if the expected value is constant, i.e. $E[x(t)] = E[x(t + \tau)] = c$, where τ denotes a time interval. The term process indicates that the random variable is time dependent. If the random variable is place dependent (in x-, y- and/or z- direction) a so called field is involved. For the sake of brevity these notes only mention a random process.

Ad b.

In the case of seasonal influences, it is sometimes possible to carry out the analysis for every process that is (more or less) stationary during the season. Seasons last a considerable percentage of time, so this analysis will also be for an S.L.S.. An example of such a process is the wave height in a monsoon region. During the northeastern monsoon (on the northern hemisphere) circumstances are more or less stationary, likewise during the southwestern monsoon (also on the northern hemisphere). The considered S.L.S. could be the calm location of ships behind a breakwater.

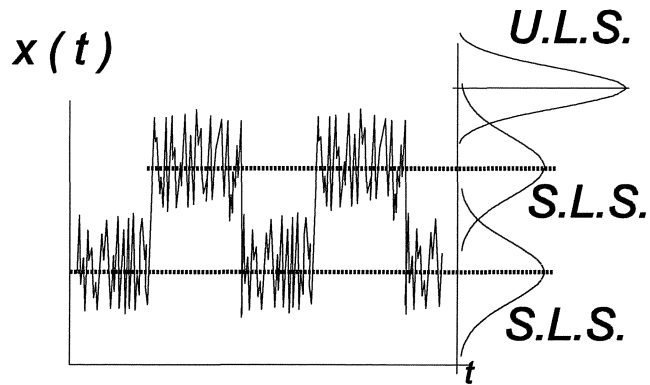


Figure II-3

Exceptions are cyclones or hurricanes which are "superposed" on monsoon circumstances. In that case the phenomena are as is indicated in Figure II-1c.

Ad c.

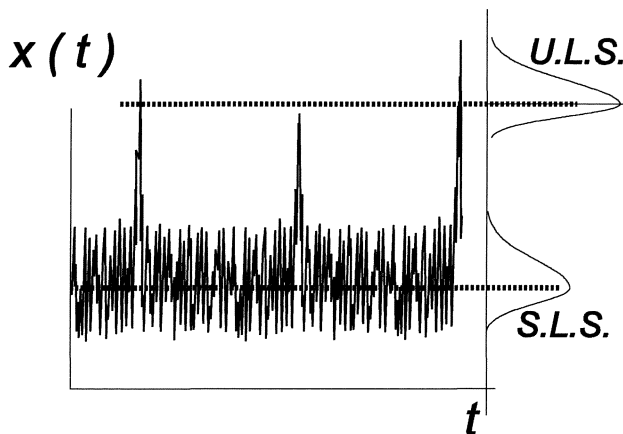


Figure II-4

Often extreme phenomena occur during the stationary process. From a certain point of view these cases entail more than one process. Cyclones and storm depressions (extreme phenomena) during a southwestern monsoon or the winter season on the northern hemisphere (the stationary process) are examples of these cases.

The extreme loads caused by these processes are analysed for the U.L.S. During storm circumstances ships don't need a calm shelter behind a breakwater. Some disturbance in the port is acceptable. The breakwater must, however, stay intact (or damages may not exceed a small percentage according to requirements).

If several storms occur per year, as is the case on the coasts of western Europe, three types of analysis are possible:

- Firstly, considering every year's greatest storm and applying the statistics of yearly maxima. Unfortunately, the periods during which measurements take place are usually rather short. By applying this method one is left with very few measurements.
- Secondly, considering storms that cause wave heights above a certain threshold value as statistically independent realisations (Peak Over Threshold or P.O.T.).
- The third possibility (a physical consideration) is distinguishing between wind directions (and possibly also the course of the depression which causes the storm). Determining the probability function of extremes selected by this method, is only suitable for U.L.S. analysis.

With given 3-hourly observations of a stationary process, the most simple assumption is that these observations are independent of each other. In that case the number of observations in one year is: $N = \frac{365 \cdot 24}{3} = 2920$.

The highest of these values is normative. The distribution of the highest (significant) wave can be derived by using the extreme value theorem (see § II-2). This highest (significant) wave is used in an U.L.S. analysis.

The assumption of independence of the 3-hourly observations is incorrect, but it is a safe assumption. Dependence is disregarded so probabilities are overestimated. Weather conditions usually continue for more than 3 hours. Weather can be ascribed a certain persistence. The number of "sea states", affected by the weather situation (i.e. by H_s) will be smaller than assumed. If $N > M$, the expected value of the highest of N (significant) waves is greater than that of the highest of M (significant) waves, as long as both samples are taken from the same basic distribution.

II.2. EXTREME VALUE DISTRIBUTIONS

With the given distribution $F_{\underline{x}}(x)$ the probability¹⁾ that the random variable \underline{x} is smaller than or at most equal to a certain given value x per definition equals $F_{\underline{x}}(x)$:

$$P(\underline{x} \leq x) = F_{\underline{x}}(x)$$

Wanted: the probability that the highest of N realisations from the distribution $F_{\underline{x}}(x)$ is smaller than a certain value x .

The probability that the first realisation is smaller than or at most equal to x equals $F_{\underline{x}}(x)$.

The probability that the second realisation is smaller than or at most equal to x equals $F_{\underline{x}}(x)$.

The probability that the first and the second realisations are smaller than or at most equal to x equals: $F_{\underline{x}}(x) * F_{\underline{x}}(x)$ as long as the realisations are *independent*.

Further realisations are analogous, so for N realisations:

$$\text{Probability that all } N \text{ realisations } \leq x = F_{\underline{x}}(x) * F_{\underline{x}}(x) * \dots = F_{\underline{x}}^N(x).$$

The distribution of the highest of N realisations from a basic distribution is called an extreme value distribution $F_E(x)$ for maxima²⁾:

$$F_E(x) = F_{\underline{x}}^N(x)$$

The probability density function (p.d.f.) $f_E(x)$ of the extreme value distribution for maxima is acquired by differentiation:

$$f_E(x) = N \cdot f_{\underline{x}}(x) \cdot F_{\underline{x}}^{N-1}(x)$$

An example of an extreme value distribution type I for maxima (a Gumbel distribution) is given in Figure II-5.

¹ Note that the *probability* is *without dimensions*. The *probability density* generally *does* have a dimension, namely the reciprocal of that of the considered random variable.

² Note that the capital letter E as an index refers to the extreme value distribution, whilst the underlined letter (in dit case: \underline{x}) indicates a random variable. The variable which is *not* underlined (x) is the "current value" or the "dummy variable" of the distribution. An average value of a random variable \underline{x} is denoted by $\mu_{\underline{x}}$. The estimated average calculated from observations (x_i) is denoted by \bar{x} .

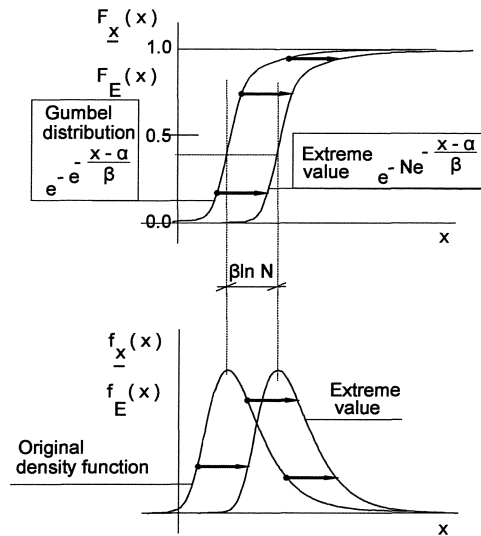


Figure II-5

To find the distribution of extreme minima the procedure is analogous:

$$\text{Probability that all } N \text{ realisations } > x = \{1 - F_x(x)\} * \{1 - F_x(x)\} * \dots = \{1 - F_x(x)\}^N.$$

The mathematical adaptations, applied to the extreme value distributions for minima lead to results analogue of those for maxima. The figure below shows this for an extreme value distribution type I for minima:

$$F_x(x) = 1 - e^{-e^{\frac{x-\alpha}{\beta}}} \quad \beta > 0$$

The extreme value distribution for this is::

$$F_E(x) = \left\{ 1 - e^{-e^{\frac{x-\alpha}{\beta}}} \right\}^N$$

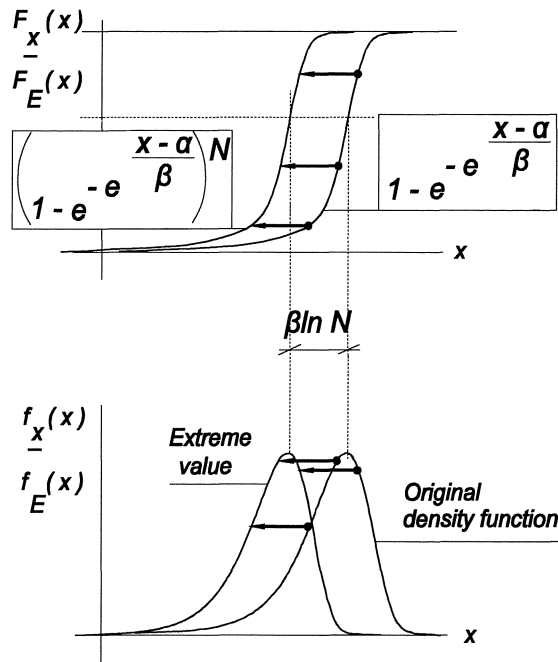


Figure II-6

EXAMPLE: EXTREME VALUE DISTRIBUTION OF A FINITE DISCRETE DISTRIBUTION

The chosen process is throwing an unbiased six-sided dice. Wanted are the probability density function and the distribution of the throw with the highest outcome when it is thrown N times. N.B. The probability density function concerns a variable that can only equal discrete values, in this case 1, 2, ..., 6, and thus is the equivalent of the p.d.f..

The probability density function consists of so called Dirac- functions (also known as "nails"). With one dice one throws either a one or a two etc.. In between there are no values of the variable: "outcome of throw ". The probability density is defined only for whole numbers: one, two, etc.. In a graph this is expressed by infinitely small widths Δx_i with heights $f_{\underline{x}}(x_i) = \frac{1}{6 \cdot \Delta x_i}$ (the "nails"), such that the surface of each nail is $1/6$. In case $N = 1$ (one throw) the probability that $M = 1, 2, 3$, etc. (outcome of throw) when throwing an unbiased six-sided dice always equals: $f_{\underline{x}}(x_i) \cdot \Delta x_i = \frac{1}{6}$. The probability density could be represented by Dirac- functions or distributions. (See Figure II-7 left.)

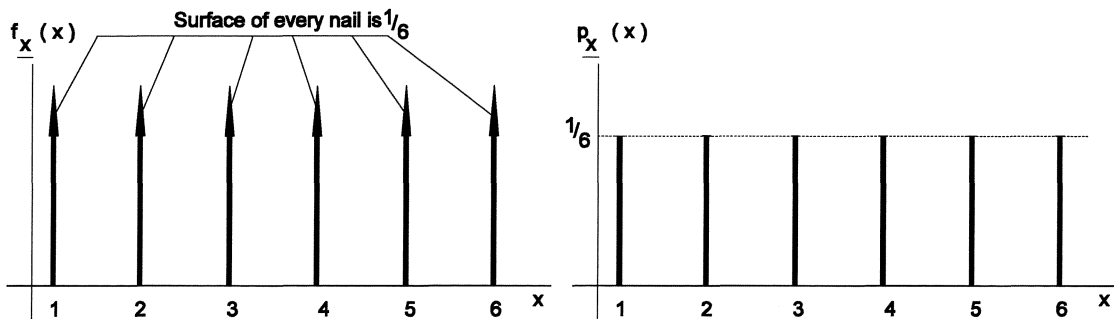


Figure II-7

We can define a probability density function: $p_{\underline{x}}(x) = P(\underline{x} = x)$. The right side of figure II-7 shows the probability density function of all possible outcomes of throwing an unbiased six-sided dice.

The distribution function of a continuous random variable can be obtained from the p.d.f. by integration. The distribution function of a discrete random variable follows from the probability density function by addition.

$$F_{\underline{x}}(x) = \int_{-\infty}^x f_{\underline{x}}(x) dx \quad \text{of} \quad F_{\underline{x}}(x) = \sum_{\text{all } x_i \leq x} p_{\underline{x}}(x)$$

Integrating Dirac- functions is not simple, so the second definition of the distribution will be used.

For extreme value distributions $F_E(x) = F_{\underline{x}}^N(x)$ continues to be valid (page II-3, halfway), so for throwing a six-sided dice:

$$F_E(x) = \left\{ \sum_{\text{all } x_i \leq x} p_{\underline{x}}(x) \right\}^N$$

The distributions of the probabilities of throwing M or less in N throws and the probabilities of throwing a maximum of M in one out of a total of N throws, are presented in the table in Figure II-8. The right side of Figure II-8 shows the probability distributions $F_E(x) = F_x^N(x)$.

Explanation (see shaded square in the table in Figure II-8):

The probability of the event "a 5 or less is thrown" ($M = 5$) occurring when a dice is thrown once ($N = 1$) is the probability that "a 5 is thrown" or that "a 4 is thrown" or that ... or that "a 1 is thrown". According to the rule for "independent or-probabilities" (see lecture notes CTOW4130 /b3¹) the probability of the event "a 5 or less is thrown" occurring with one throw equals $5 * \frac{1}{6}$.

When there are 4 throws ($N = 4$), this probability is valid for the first throw and the second throw and the third throw and the fourth throw. According to the rule for "independent and-probabilities" (see lecture notes CTOW4130/b3) the probability of the event "a 5 or less is thrown every time" occurring with 4 throws equals $\left(\frac{5}{6}\right)^4 \approx 0.48$.

Analogously, one finds that the probability of the event "a 4 or less is thrown every time" ($M = 4$) occurring when a dice is thrown 4 times ($N = 4$) equals $\left(\frac{4}{6}\right)^4 \approx 0.20$.

The two calculated probabilities lead to the probability of the event "the maximum throw is 5" when a dice is thrown 4 times, as this equals the difference between "a 5 or less is thrown" in four throws and "a 4 or less is thrown" in four throws: $0.48 - 0.20 = 0.28$.

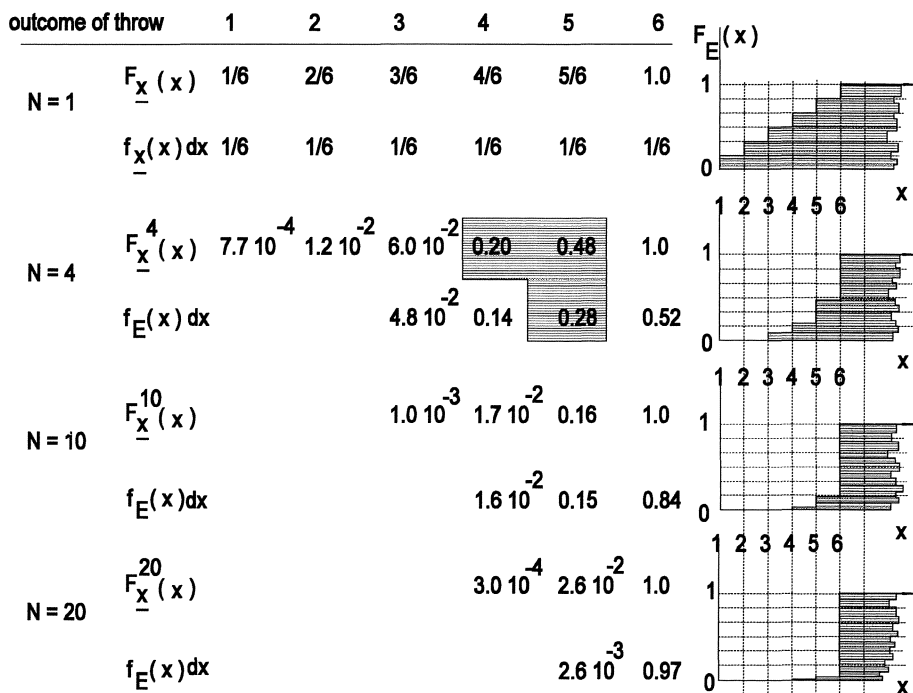


Figure II-8

¹ Vrijling, J.K. and A.C.W.M. Vrouwenvelder, Lecture notes b3, Probabilistic Design, Faculty of Civil Engineering of the Technical University Delft (in Dutch)

EXAMPLE: EXTREME VALUE DISTRIBUTION OF A UNIFORM DISTRIBUTION

The probability density function of a uniform distribution is:

$$f_x(x) = \frac{1}{\beta - \alpha} \text{ for } \alpha < x \leq \beta \text{ and } 0 \text{ elsewhere.}$$

The distribution function follows from this by integration:

$$F_x(x) = \frac{x - \alpha}{\beta - \alpha}$$

The corresponding extreme value distribution is:

$$F_E(x) = \left(\frac{x - \alpha}{\beta - \alpha} \right)^N$$

Differentiation gives:

$$f_E(x) = \frac{N}{\beta - \alpha} \cdot \left(\frac{x - \alpha}{\beta - \alpha} \right)^{N-1}$$

If, after the analogy of the dice, one takes: $\alpha = 1$ and $\beta = 6$, the following extreme probability density functions $f_E(x)$ apply for various values of N :

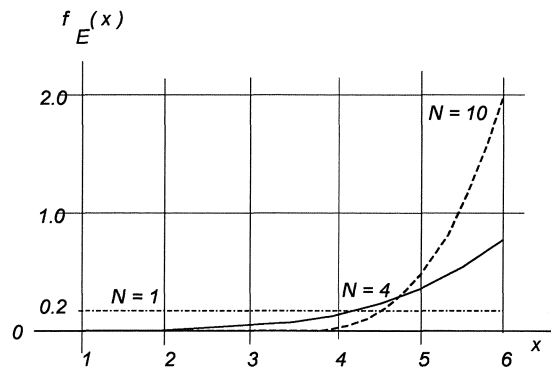


Figure II-9

Figure II-10 shows the corresponding probability distributions.

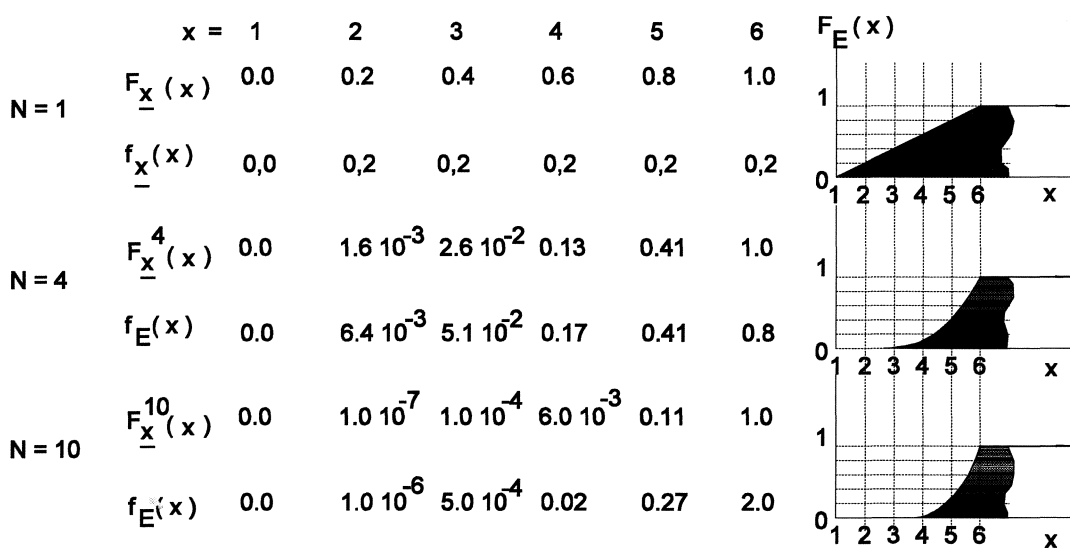


Figure II-10

II.3. TYPES OF EXTREME VALUE DISTRIBUTIONS

Observations can be clustered and set out in a histogram. This histogram can be matched with a mathematical description which serves as an estimate for the probability density function of the considered statistical phenomenon (see Figure II-11). A number of techniques that can be used for this purpose are discussed in more detail in § II.11 and further. By adapting the found probability density function as described in § II.2, the corresponding extreme value distribution is determined.

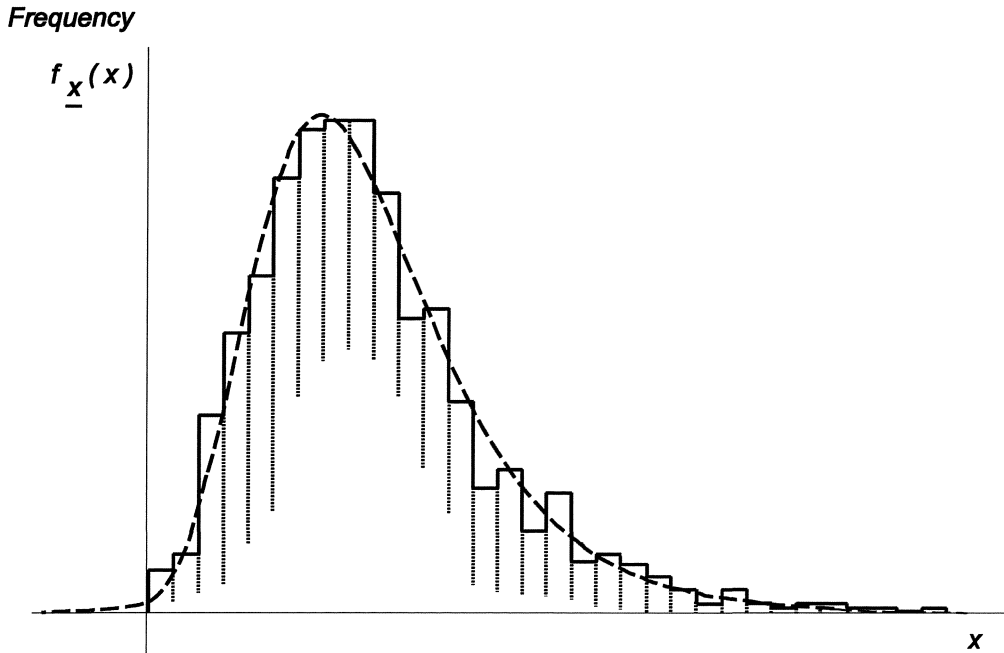


Figure II-11

Depending on the behaviour of the "extreme tail" of the original p.d.f., (for maxima this is on the right side) the extreme value distribution converges to type I, II or III. A standard publication concerning extreme value distributions is:

E. J. Gumbel, *Statistics of Extremes*, Columbia University Press, New York and London, 1958.

For yearly maxima of wave heights, river discharges, high water levels, etc., an extreme value distribution type I for maxima is often used, a so-called Gumbel- distribution:

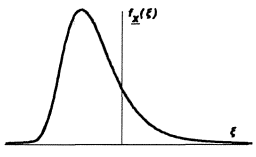
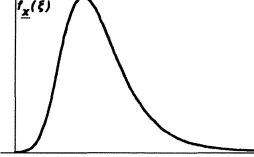
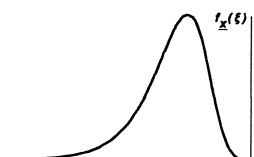
$$F_x(x) = e^{-e^{-\frac{x-a}{\beta}}} = \exp\left(-e^{-\frac{x-a}{\beta}}\right)$$

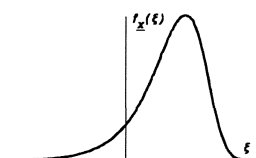
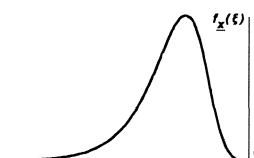

One can demonstrate quite simply ¹⁾, that the extreme value distribution of N observations taken from a Gumbel distribution is in fact another Gumbel- distribution, which is congruent with the original distribution, but displaced over $\beta \cdot \ln N$. One might say: the extremes of a Gumbel distribution are Gumbel distributed.

¹⁾ Suppose the two derivatives (of the original distribution and of the extreme value distribution) equal zero. The difference in intercept values for which the second derivatives are zero is $\beta \cdot \ln N$. (See also Figure II-5. Naturally the comment also stands for the extreme value distribution type I for minima: see Figure II-6.)

N.B. Note that assuming the second derivative equals zero, gives the intercept of the point of inflection of the probability distribution, i.e. the maximum of the probability density function. From this the modal value follows.

SUMMARY OF EXTREME VALUE DISTRIBUTIONS

	Type I maxima (Gumbel)	Type II maxima (Fréchet)	Type III maxima
$F_{\xi}(\xi)$	$\exp [-e^{-\alpha(\xi-u)}]$	$\exp [-(\xi/u)^k]$	$\exp [-(\xi/u)^k]$
$f_{\xi}(\xi)$	$\alpha \exp [-\alpha(\xi-u)-e^{-\alpha(\xi-u)}]$	$(k/u)(\xi/u)^{k-1} \exp [-(\xi/u)^k]$	$-(k/u)(\xi/u)^{k-1} \exp [-(\xi/u)^k]$
range	$-\infty < \xi, -\infty < u < +\infty, \alpha > 0$	$\xi, u, k > 0$	$u, \xi < 0, k > 0$
μ_{ξ}	$\mu = u + 0,577/\alpha$	$\mu = u \Gamma(1-1/k) (k > 1)$	$\mu = u \Gamma(1+1/k)$
σ_{ξ}	$\sigma = \pi/\alpha \sqrt{6}$	$\sigma^2 + \mu^2 = u^2 \Gamma(1-2/k) (k > 2)$	$\sigma^2 + \mu^2 = u^2 \Gamma(1+2/k)$
$x = \max y_i$ $i = 1 \dots n$	$\alpha_x = \alpha, u_x = u + \{\ln(n)\}/\alpha$	$k_x = k, u_x = u, n^{1/k}$	$k_x = k, u_x = u, n^{1/k}$
			

	Type I minima	Type II minima	Type III minima (Weibull)
$F_{\xi}(\xi)$	$1 - \exp [-e^{+\alpha(\xi-u)}]$	$1 - \exp [-(\xi/u)^k]$	$1 - \exp [-(\xi/u)^k]$
$f_{\xi}(\xi)$	$\alpha \exp [\alpha(\xi-u)-e^{+\alpha(\xi-u)}]$	$-(k/u)(\xi/u)^{k-1} \exp [-(\xi/u)^k]$	$(k/u)(\xi/u)^{k-1} \exp [-(\xi/u)^k]$
range	$-\infty < \xi, -\infty < u < +\infty, \alpha > 0$	$\xi, u < 0, k > 0$	$u, \xi, k > 0$
μ_{ξ}	$\mu = u - 0,577/\alpha$	$\mu = u \Gamma(1-1/k) (k > 1)$	$\mu = u \Gamma(1+1/k)$
σ_{ξ}	$\sigma = \pi/\alpha \sqrt{6}$	$\sigma^2 + \mu^2 = u^2 \Gamma(1-2/k) (k > 2)$	$\sigma^2 + \mu^2 = u^2 \Gamma(1+2/k)$
$x = \max y_i$ $i = 1 \dots n$	$\alpha_x = \alpha, u_x = u - \{\ln(n)\}/\alpha$	$k_x = k, u_x = u, n^{1/k}$	$k_x = k, u_x = u, n^{1/k}$
			

Notes:

1. The type II and III distributions are given with lower (upper) boundary 0; by translation an arbitrary different boundary can be introduced.

2. The gamma function is defined as: $\Gamma(r) = \int_0^{\infty} t^{r-1} \cdot e^{-t} dt$. with $\Gamma(r) = (r-1)!$ (for $r \geq 0$).

Furthermore, the following applies to r: $\Gamma(r+1) = 1 \cdot 2 \cdot 3 \cdot \dots \cdot r$, the faculty function.

The extreme value distribution type II for maxima is also known as the Fréchet distribution. The distribution function is:

$$F_{\underline{x}}(x) = \exp\left\{-\left(\frac{x-\alpha}{\beta}\right)^{-\gamma}\right\} \quad x > \alpha, \beta > 0, \gamma > 0$$

- The relation between the Gumbel distribution and the Fréchet distribution is an analogue of the relation between the normal distribution and the log-normal distribution: if \underline{y} is Fréchet distributed, then $\underline{x} = \ln \underline{y}$ is Gumbel distributed, as long as the parameter α is equal to 0 (zero) in both distributions.

This can be interpreted as follows. The Fréchet distribution is taken:

$$F_{\underline{y}}(y) = \exp\left\{-\left(\frac{y}{\beta}\right)^{-\gamma}\right\} \quad (\text{Assuming: } \alpha = 0.)$$

Assume: $\underline{x} = \ln \underline{y}$, so, for the "dummy variables": $y = e^x$.

Substitution of this in the Fréchet- distribution gives:

$$\begin{aligned} F_{\underline{x}}(x) &= \exp\left\{-\left(\frac{e^x}{\beta}\right)^{-\gamma}\right\} = \exp\left\{-\left(\frac{e^x}{e^{\ln \beta}}\right)^{-\gamma}\right\} \\ &= \exp\left\{-\left(e^{x-\ln \beta}\right)^{-\gamma}\right\} \end{aligned}$$

$$F_{\underline{x}}(x) = \exp\left\{-e^{-\gamma(x-\ln \beta)}\right\} \quad \dots \text{Gumbel.}$$

- The extremes of a Fréchet- distribution are Fréchet distributed. For the Fréchet distribution of significant wave heights \underline{H}_s :

$$F_{\underline{H}_s}(H) = \exp\left\{-\left(\frac{H-A}{B}\right)^{-C}\right\}$$

The extreme value distribution becomes:

$$F_E(H) = \exp\left\{-\left(\frac{H-A}{B \cdot N^{\frac{1}{C}}}\right)^{-C}\right\}$$

So $A_E = A, B_E = B \cdot N^{\frac{1}{C}}$ and $C_E = C$.

Often, a Weibull distribution is used for the long term distribution of significant wave heights. This is not based on the extreme value theory (see § II.2) and it has no physical background. Usually, a good fit is found between the data (observations) and the Weibull distribution. The Weibull distribution is the extreme value type III distribution for *minima*. However, the distribution is often used to model *maximum* significant wave heights.

$$F_{\underline{x}}(x) = 1 - \exp\left\{-\left(\frac{x-\varepsilon}{u}\right)^k\right\} \quad x \geq \varepsilon, u > 0, k > 0 \quad \text{Weibull}$$

For the values 1 and 2 of exponent k , the Weibull distribution is known by separate names:

$$k = 1: \quad F_{\underline{x}}(x) = 1 - \exp\left\{-\frac{x-\varepsilon}{u}\right\}: \text{exponential distribution.}$$

$$k = 2: \quad F_{\underline{x}}(x) = 1 - \exp\left\{-\left(\frac{x}{\sqrt{2 \cdot m_0}}\right)^2\right\}: \text{Rayleigh distribution.}$$

EXAMPLE: THE DISTRIBUTION OF THE SIGNIFICANT WAVE HEIGHT AT KARWAR DURING THE SOUTHWEST MONSOON

The significant wave heights during a southwest monsoon period at Karwar (on the westcoast of India, see Figure II-47 on page II-32) can be described with a Gumbel distribution¹). The 3-hourly observations satisfy:

$F_{H_s}(H) = \exp\left(-e^{-\frac{H-A}{B}}\right)$ with $A = 1.941 \text{ m}$ and $B = 0.284 \text{ m}$. The modal value of the significant wave is thus 1.941 m.

Assuming each monsoon period lasts 3 months, each of those periods would contain:

$$N = \frac{3 \text{ mth.} \cdot 30 \text{ day.} \cdot 24 \text{ hr.}}{3 \text{ hr. obs.}} = 720$$

independent realisations of the significant wave height.

The extreme value distribution to be considered is the distribution of the highest significant wave in a year. This will be another Gumbel distribution with:

$A_E = A + B \ln 720 = 3.81 \text{ m}$ and $B_E = 0.284 \text{ m}$. The modal value of the maximum significant wave in a year is thus 3.81 m.

Assuming that observations every 6 hours (instead of every 3 hours) are independent, due to persistence of the waves, then $N = 360$ and calculations lead to: $A_E = 3.61 \text{ m}$. The difference with the last A_E is only 0.20 m. The significance of persistence for A_E is academic rather than practical.

If one wishes to determine the distribution of the highest significant wave during the life of a breakwater (presumed 50 years) the procedure will have to be repeated with $N = 50$:

$A_{EL} = A_E + B \cdot \ln 50 = 3.81 + 0.284 \cdot 3.91 = 4.92 \text{ m}$. The modal value of the highest significant wave at Karwar in the southwestern monsoon period (without hurricanes) is 4.92 m in 50 years.

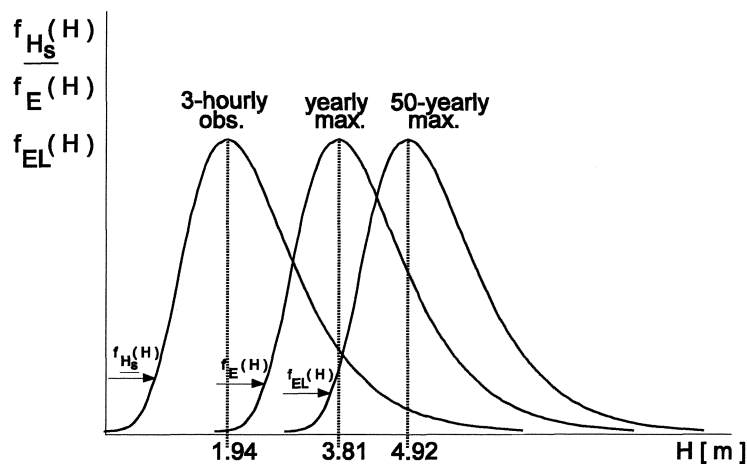


Figure II-12

¹ In Figure II-38 on page II-29 the significant wave heights during the southwestern monsoon are approximated using a Weibull distribution. That distribution for the significant wave heights during the southwestern monsoon will be used in the rest of these lecture notes. In Appendix II-I at the end of this chapter (page II-113 and further), the approximations are compared (Gumbel and Weibull distributions based on *the same* measurements).

EXAMPLE: THE DISTRIBUTION OF THE SIGNIFICANT WAVE HEIGHT AT KARWAR DURING CYCLONES

The significant wave heights during cyclones in the southwestern monsoon period in Karwar appeared to satisfy a Fréchet distribution by good approximation:

$$F_{H_s}(H) = \exp\left\{-\left(\frac{H-A}{B}\right)^{-C}\right\} \quad \text{Frechet}$$

Based on the observations of the significant wave height during twenty five cyclones, it appeared that: $A = 0.00 \text{ m}$, $B = 2.498 \text{ m}$ and $C = 3.388$ (see Figure II-52 on page II-34).

Assume that a construction (breakwater) in Karwar must withstand a certain wave attack and that this wave attack is characterised by the significant wave height. If a cyclone were to occur every year and the "life" of the construction was 50 years, then the parameters of the Fréchet distribution of the highest significant wave in that lifetime would be:

$$A_E = 0.00 \text{ m}, B_E = 2.498 \cdot 50^{\frac{1}{3.388}} = 7.93 \text{ m} \text{ and } C_E = 3.388.$$

The problem is more complicated. A cyclone does not occur every year. Counting over a number of years gives an estimated probability $P(\text{cyclone})$ of 0.5 that a cyclone occurs in a year. Significant waves during a cyclone occur *on condition* that a cyclone occurs.

The probability of a significant wave occurring as a result of a cyclone in a year (*probability of significant waves AND a cyclone*) is made up of two "contributions":

- 1 the probability of "no cyclone" occurring in a particular year (in which case there is no significant wave caused by the cyclone):

$$P(\text{no cyclone}) = 1 - P(\text{cyclone})$$

- 2 the probability of a significant wave height occurring in a particular year whilst a cyclone is taking place¹). This is the conditional probability of a significant wave height given that a cyclone is occurring, multiplied by the probability of a cyclone taking place:

$$P(H_s \cap \text{cyclone}) = P(H_s | \text{cyclone}) * P(\text{cyclone})$$

The probability density and the distribution of H_s can be presented as is shown in Figure II-13:

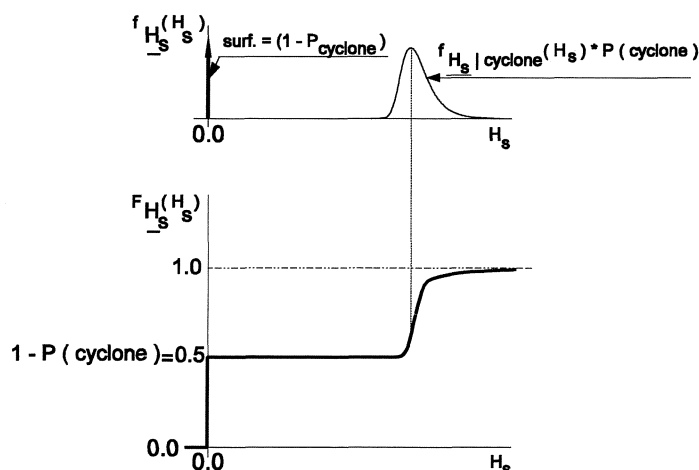


Figure II-13

¹ If a cyclone is taking place, one can assume that the total energy in the wave field originates from wind waves. Other sources of energy (swell) are disregarded.

In Figure II-13 $f_{H_s|cyclone}(H_s)$ is the probability density function of H_s , which has been calculated (fitted) from observations of H_s during cyclones. (See Figure II-52 for the conditional distribution function $F_{H_s|cyclone}(H_s)$.)

In this case it is easier to work with the exceedance frequency curve:

$$P(\underline{H}_s > H_s) = 1 - F_{\underline{H}_s}(H_s) = \left(1 - F_{H_s|cyclone}(H_s)\right) \cdot P(cyclone)$$

The probability distribution is:

$$P(\underline{H}_s \leq H_s) = F_{\underline{H}_s}(H_s) = 1 - \left(1 - F_{H_s|cyclone}(H_s)\right) \cdot P(cyclone)$$

II.4. DEPENDENCE AND EXTREME VALUE DISTRIBUTIONS

Assume a dyke in the storm direction ("op de stormstreek") on a lake with a fixed water level. The "load" is formed by wave attack. The "strength" is the crest level of the dyke. The regarded failure mode is "wave overtopping".

The distribution of the highest wave in a year and the distribution of the crest level are given. The probability of failure (probability of wave overtopping) P_f in a year can then be calculated. The highest wave in M years can be derived from the given distribution for wave heights. The probability of failure in M years becomes:

$$P_f^M = 1 - (1 - P_f)^M \approx M \cdot P_f \text{ as long as } P_f \text{ is sufficiently small.}$$

This expression for the probability of failure in M years (the life or the period between maintenance works) is valid for independent failure probabilities in all years. The maximum waves in various years are independent but the height of a dyke in one year is not independent of the height in the preceding year. The probabilities of failure in various years are thus dependent on the crest level of the dyke. A good procedure is to determine the probability distribution of the highest wave in the lifetime for the load and then calculate the probability of failure during the lifetime of the structure.

II.5. PROBABILITY DENSITY FUNCTIONS AND DISTRIBUTIONS FROM PHYSICAL RELATIONS

If possible, the determination of a mathematical relation between quantities based on measurements ("fitting" a relation between physical quantities or adapting a p.d.f.) should *not* be based solely on statistical techniques. It is at least as important to take the physical process into consideration.

The wave height on a (short) shallow foreshore bordering a (deep) sea is used as an example ¹⁾. The wave height is limited by the water depth. In deep water the significant wave is: H_{s_0} . On the shallow foreshore the significant wave is: H_s (see Figure II-14). Given the p.d.f. of the significant wave height in deep water, one wants to determine the p.d.f. of the significant wave in shallow water.

¹ The foreshore must be short and the sea must be deep, because otherwise an "onshore wind", necessary for the occurrence of wave attack, would cause wind set up. The wave height would then be influenced by the water depth in a special way. This influence is disregarded here.

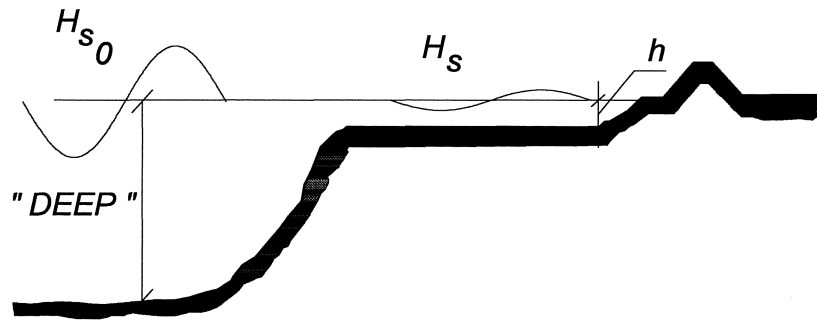


Figure II-14

The mathematical relation (the mathematical model) between the significant wave "in deep water" and the significant wave on the shallow foreshore is:

$$H_s = \begin{cases} H_{s_0} & \text{for } H_{s_0} \leq 0,5 * h \text{ (} h = \text{waterdepth)} \\ 0,5 * h & \text{for } H_{s_0} > 0,5 * h \end{cases}$$

This model is illustrated in Figure II-15. The p.d.f. of the significant wave in shallow water is acquired by transforming the wave in deep water. Provided the wave doesn't break, the wave height on the shallow foreshore equals the significant wave height in deep water. In Figure II-15 that transformation is represented by short black arrows between the cross hatched surfaces in the p.d.f.s. Waves higher than half the water depth break until the height (approximately) equals half the depth. The broken waves *conserve* the wave length they had before breaking.

The distribution of deep water waves is, as far as the distribution of significant waves on the shallow foreshore is concerned, *censored* by the breaker depth. In Figure II-15 this is marked by the darker spotted surface that transforms into the "nail" in the p.d.f. of the significant wave on the shallow foreshore.

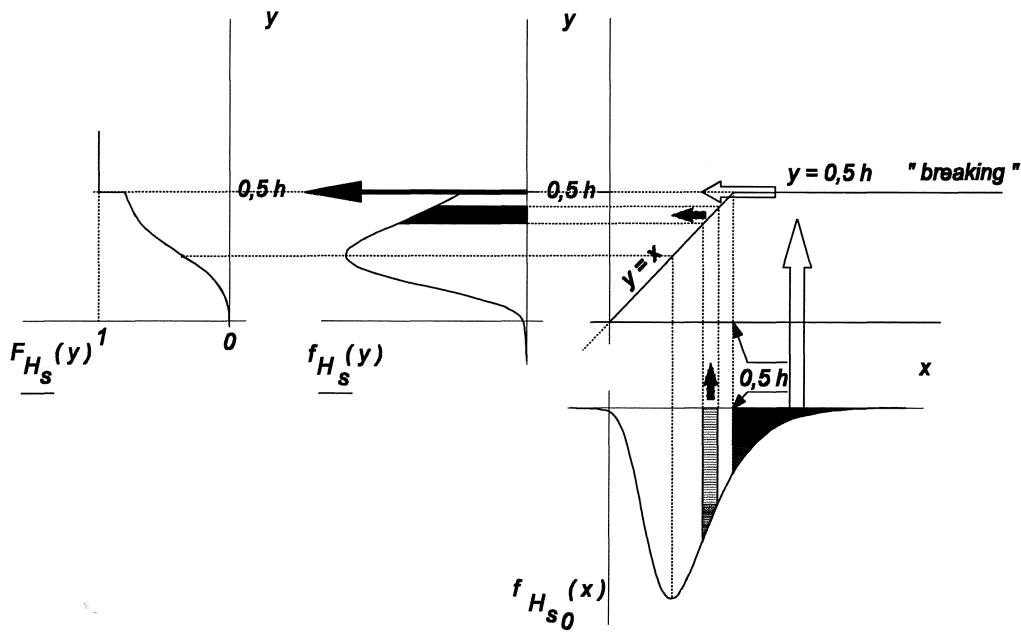


Figure II-15

The distribution of the significant waves on the shallow foreshore is a so-called *censored distribution*. This distribution function has a gap where the probability density function is censured. (In Figure II-15: for $y = 0,5 h$.) This gap is easily missed if one only considers the observations.

Another way to "cut down" a distribution is applied in the case of the so-called *truncated distribution*. This way the reduced a^{th} part of the basic probability density function is proportionally distributed among the ordinates of the rest of the probability density function so that:

$$\int_{-\infty}^{\text{Point of truncation}} f_T(x) dx = 1$$

The ordinates become:

$$f_T(x) = \frac{1}{1-a} * f_y(x); \quad a = \int_{\text{point of truncation}}^{+\infty} f_y(x) dx \Rightarrow 0 < a \leq 1, \quad x \leq \text{point of truncation in } f_T(x)$$

In this $f_T(x)$ is the truncated probability density function, see Figure II-16.

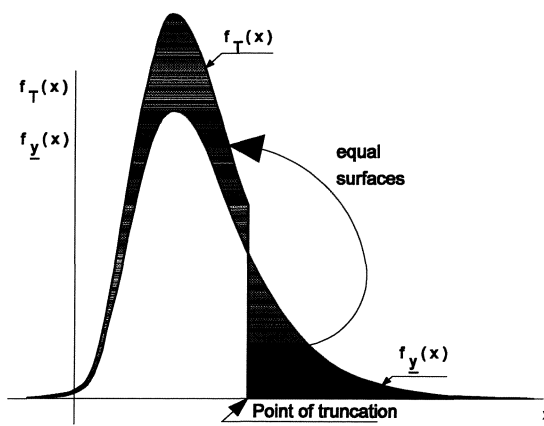


Figure II-16

Such a distribution can be used to model the probability of occurrence of weights of stones from a quarry. The largest stones are removed from the population or, alternatively, are broken into smaller stones.

A different discontinuity can be found in the exceedance frequency curves for high water levels in a river. If any present flood plains are not taken into account, one extrapolates high water levels as follows:

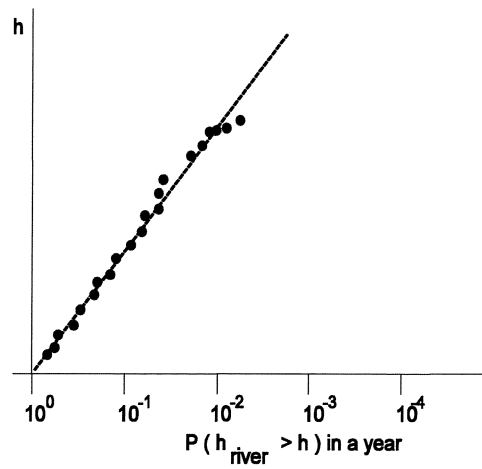


Figure II-17

However, at the highest measured water levels the riverbed that leads the current may differ from the bed used at lower water levels.

That way the river's discharge- water level relation (Q- h or rating curve) changes. The high water level exceedance frequency curve shows a bend at h_{crit} , i.e. the height at which the flow profile changes size. (Compare Figure II-18 with Figure II-19.) During processing or interpretation of the data of observed high water levels this easily escapes attention. (Compare Figure II-17 with Figure II-19.)

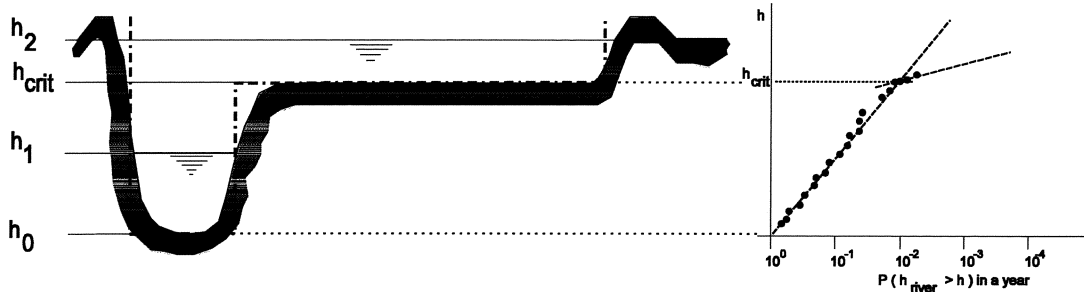


Figure II-18

Figure II-19

The relation between discharge and water level is shown analogously to the $H_{s0} - H_s$ relation for waves breaking on a high foreshore. The p.d.f. of the discharge can often be assumed continuous. The corresponding high water level, however, shows a "leap" where the flood plains are inundated as a result of the slope difference in the Q- h- curve.

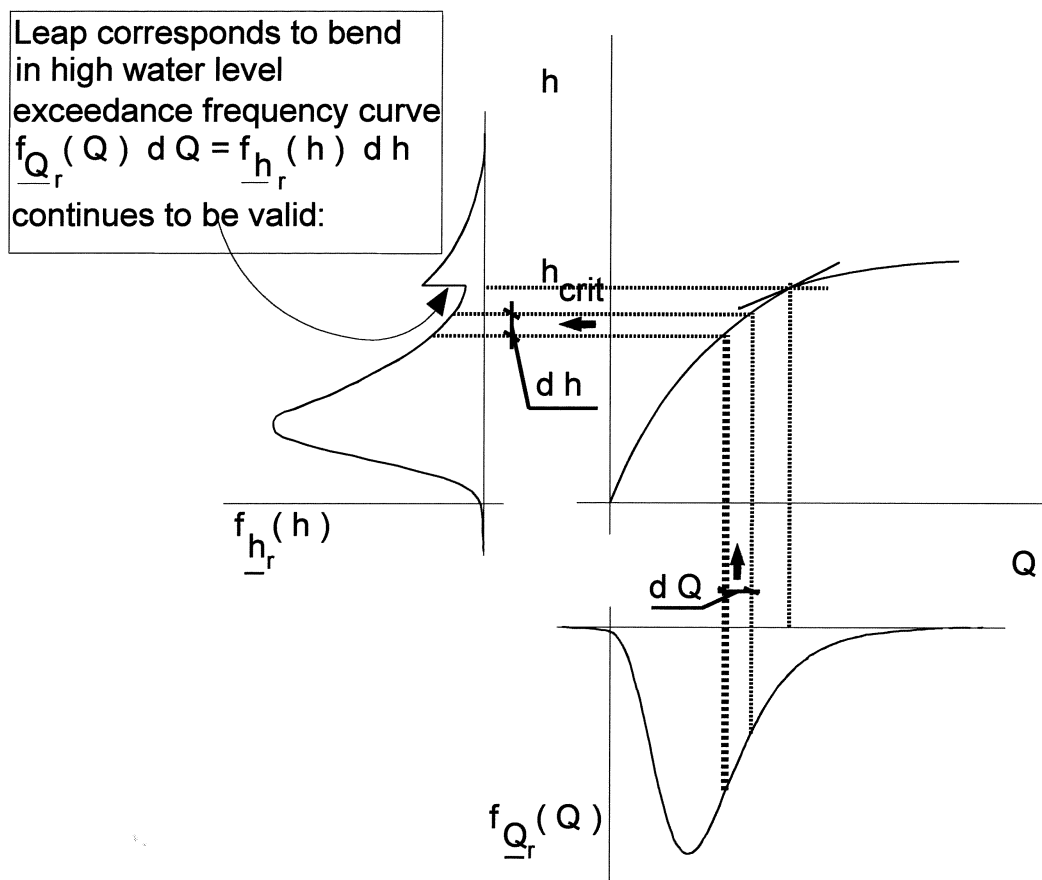


Figure II-20

II.6. MULTI-DIMENSIONAL PROBABILITY DENSITY FUNCTIONS

When a phenomenon is described by more than one random variable, the probability density function of this phenomenon is multi-dimensional. The variables each have a marginal probability density. The phenomenon has the probability density of all variables together. It is usual to illustrate a joint probability density function for two variables with normal marginal probability density functions:

$$f_{\underline{x}_1}(x) = \frac{1}{\sigma_{\underline{x}_1} \sqrt{2\pi}} \cdot \exp^{-\frac{1}{2} \left(\frac{x - \mu_{\underline{x}_1}}{\sigma_{\underline{x}_1}} \right)^2}$$

$$f_{\underline{x}_2}(y) = \frac{1}{\sigma_{\underline{x}_2} \sqrt{2\pi}} \cdot \exp^{-\frac{1}{2} \left(\frac{y - \mu_{\underline{x}_2}}{\sigma_{\underline{x}_2}} \right)^2}$$

If the parameters \underline{x}_1 and \underline{x}_2 are statistically independent, then the joint probability density function is the product of the marginal probability density functions:

$$f_{\underline{x}_1, \underline{x}_2}(x, y) = \frac{1}{2\pi \sigma_{\underline{x}_1} \sigma_{\underline{x}_2}} e^{-\frac{1}{2} \left\{ \left(\frac{x - \mu_{\underline{x}_1}}{\sigma_{\underline{x}_1}} \right)^2 + \left(\frac{y - \mu_{\underline{x}_2}}{\sigma_{\underline{x}_2}} \right)^2 \right\}}$$

Lines of equal probability density are determined by assuming the exponent is a constant:

$$\left(\frac{x - \mu_{\underline{x}_1}}{\sigma_{\underline{x}_1}} \right)^2 + \left(\frac{y - \mu_{\underline{x}_2}}{\sigma_{\underline{x}_2}} \right)^2 = \text{Constant} \Rightarrow \text{ellipses}$$

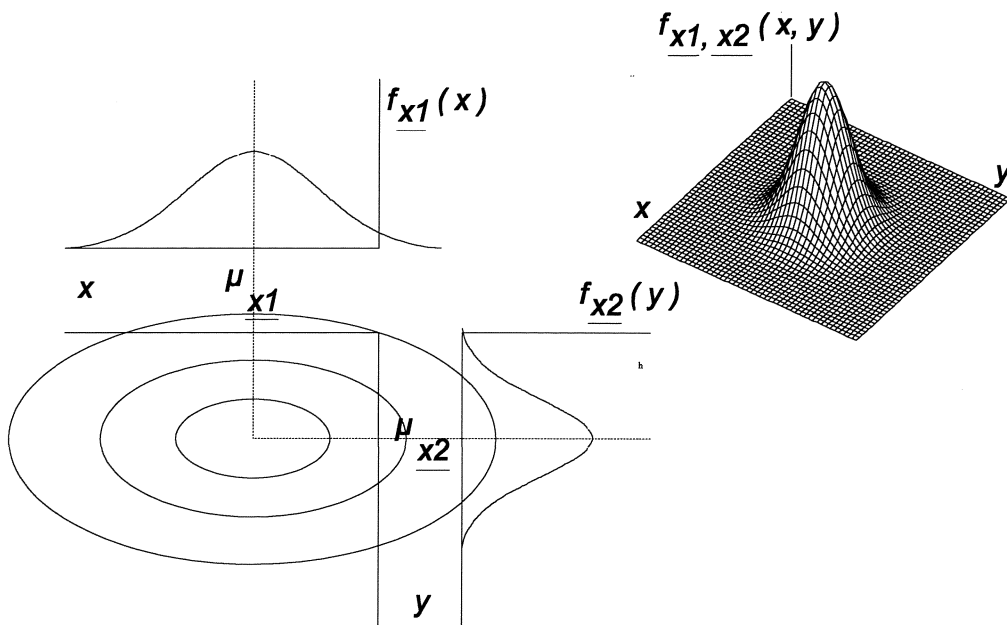


Figure II-21

In this figure one recognises the frequently presented "Gauss- hat".

The variables x_1 and x_2 are not always independent and they are not always normally distributed either. In case they are *linearly dependent and normally distributed*¹⁾ the joint probability density function can be denoted as:

$$f_{x_1, x_2}(x, y) = \frac{1}{2\pi\sigma_{x_1}\sigma_{x_2}\sqrt{1-\rho_{x_1, x_2}^2}} e^{-\frac{1}{2(1-\rho_{x_1, x_2}^2)}\left\{\left(\frac{x-\mu_{x_1}}{\sigma_{x_1}}\right)^2 - 2\rho_{x_1, x_2}\frac{(x-\mu_{x_1})(y-\mu_{x_2})}{\sigma_{x_1}\sigma_{x_2}} + \left(\frac{y-\mu_{x_2}}{\sigma_{x_2}}\right)^2\right\}}$$

In this case lines of equal probability density are determined by the ellipses:

$$\left(\frac{x-\mu_{x_1}}{\sigma_{x_1}}\right)^2 - 2\rho_{x_1, x_2}\frac{(x-\mu_{x_1})(y-\mu_{x_2})}{\sigma_{x_1}\sigma_{x_2}} + \left(\frac{y-\mu_{x_2}}{\sigma_{x_2}}\right)^2 = \text{Constant}$$

Tangents of these ellipses are derived from:

$$y' = -\frac{\frac{\partial f}{\partial x}}{\frac{\partial f}{\partial y}}$$

Vertical tangents of these ellipses are found from:

$$\frac{\partial f}{\partial y} = 0 = -2\rho_{x_1, x_2}\frac{x-\mu_{x_1}}{\sigma_{x_1}\sigma_{x_2}} + 2\frac{y-\mu_{x_2}}{\sigma_{x_2}} \cdot \frac{1}{\sigma_{x_2}} \Rightarrow y-\mu_{x_2} = \rho_{x_1, x_2}\frac{\sigma_{x_2}}{\sigma_{x_1}}(x-\mu_{x_1})$$

(See Figure II-22.)

The following is a formula of the regression line with x as an independent variable ("regression of y on x"), as estimated with linear regression using the Least Square Method (see § II.11.1 and further):

$$y - \bar{y} = r_{x,y} \frac{s_y}{s_x} (x - \bar{x})$$

The direction of this regression line relative to the x-axis (the axis for the independent variable) is estimated as follows:

$$\text{tg } \alpha = \frac{\text{cov}(x,y)}{s_x^2} = \frac{r_{x,y}s_x s_y}{s_x^2} = r_{x,y} \frac{s_y}{s_x}$$

Based on observations, the (empirical) regression line is thus an estimate of the connections between the points and the vertical tangent on the contour ellipses (the theoretical regression line). (See Figure II-22.)

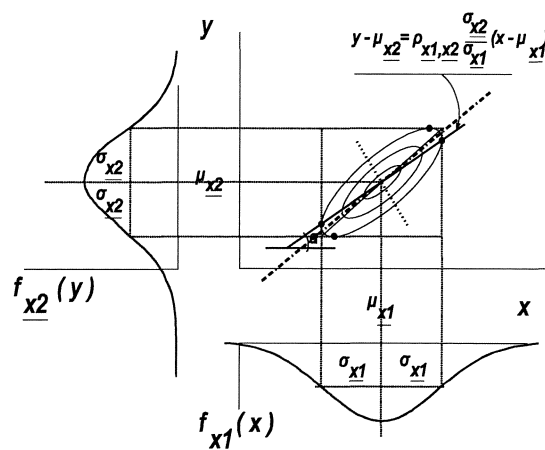


Figure II-22

¹ If the dependence is *not linear*, the meaning of the correlation coefficient, ρ_{x_1, x_2} (see Figure II-22), can not be interpreted unambiguously. Estimates of statistics are treated further in §II.12.

Often, marginal probability density functions are not normal. Suppose that both the wind set up on a sea and the high discharge of a river in that sea are exponentially distributed. If the wind set up and discharge are both independent, the joint probability density function for a station on the river, where the tidal influence is still noticeable, is as follows:

For the wind set up (storm surge) assume:

$$f_{\underline{HW}}(SV) = \frac{1}{C1} e^{-\frac{SV}{C1}}$$

and for the discharge:

$$f_{\underline{Q}_r}(Q) = \frac{1}{C2} e^{-\frac{Q}{C2}}$$

The joint probability density is the product of the marginal probability density functions *provided they are independent*¹⁾:

$$f_{\underline{HW}, \underline{Q}_r}(SV, Q) = \frac{1}{C1 \cdot C2} e^{-\left(\frac{SV}{C1} + \frac{Q}{C2}\right)}$$

In this case lines of equal probability density are denoted by:

$$\frac{SV}{C1} + \frac{Q}{C2} = \text{Constant} \Rightarrow \text{straight lines}$$

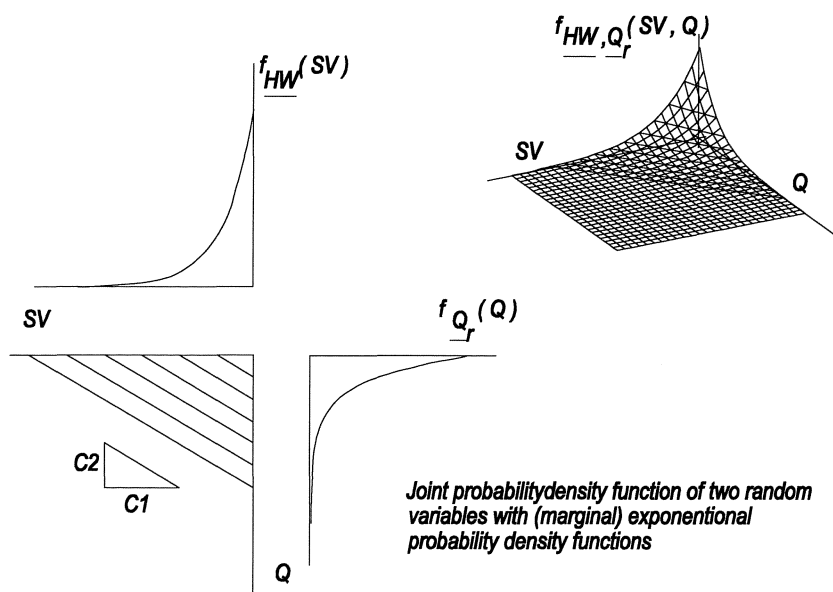


Figure II-23

1

For wind set up on the North Sea and discharges of the Rhine Van Der Made (1969) demonstrated that wind set up and discharges are not totally independent.

(Van Der Made, J. W. , Design levels in the transition zone between the tidal reach and river regime reach. Actes des Colloque de Bucarest: Hydrologie des Deltas, mai, 1969.)

Another example is the (incorrect) assumption that the wind velocity, \underline{u} , and the wind direction, $\underline{\varphi}_w$, are independent ¹).

The marginal probability density functions could be:
for the wind velocity:

$$f_{\underline{u}}(v) = \frac{1}{C} \cdot e^{-\frac{v}{C}} \quad \text{exponential}$$

and for the wind direction:

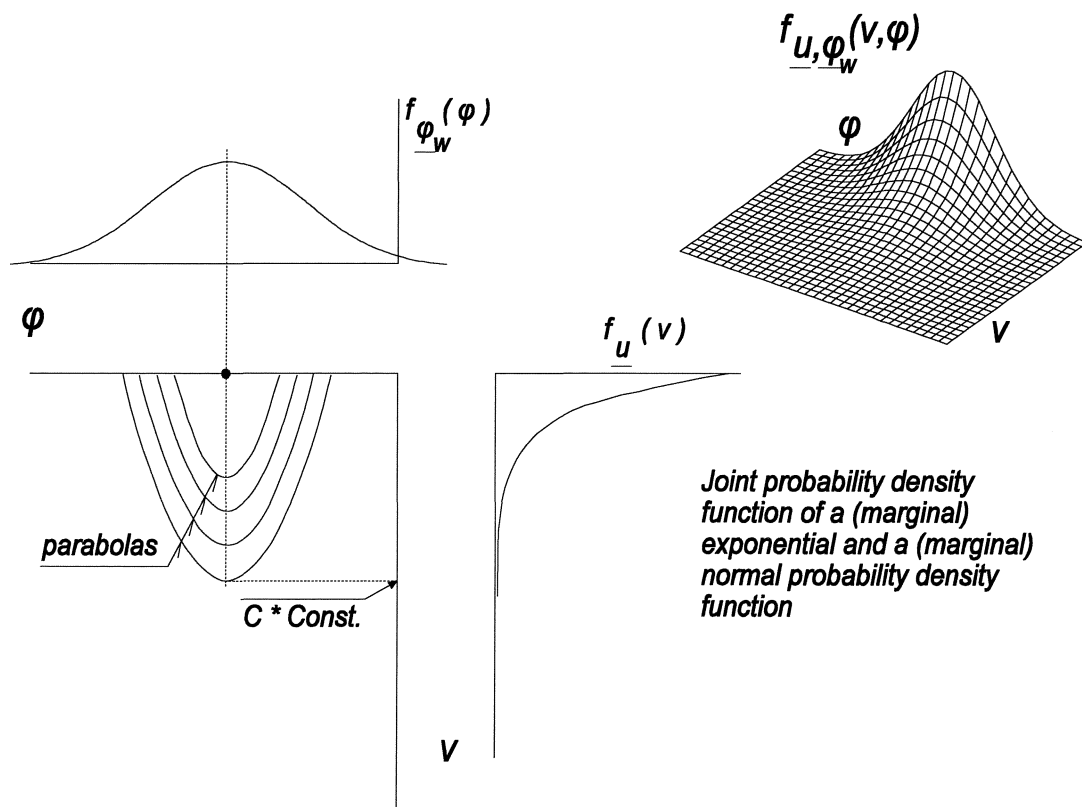
$$f_{\underline{\varphi}_w}(\varphi) = \frac{1}{B\sqrt{2\pi}} e^{-\frac{1}{2}\left(\frac{\varphi-A}{B}\right)^2} \quad \text{normal}$$

The joint probability density function would then become:

$$f_{\underline{u}, \underline{\varphi}_w}(v, \varphi) = \frac{1}{BC\sqrt{2\pi}} e^{-\left\{\frac{v}{C} + \frac{1}{2}\left(\frac{\varphi-A}{B}\right)^2\right\}}$$

The lines of equal probability density are acquired by assuming the exponent is a constant:

$$\frac{v}{C} + \frac{1}{2}\left(\frac{\varphi-A}{B}\right)^2 = \text{Constant} \quad \Rightarrow \quad \text{parabolas}$$



Joint probability density function of a (marginal) exponential and a (marginal) normal probability density function

Figure II-24

¹ Particularly for the Netherlands this is not true. Storms from the northwest are usually stronger (see Figure II-28) than those from the east northeast.

EXAMPLE: TWO DIMENSIONAL P.D.F. OF WIND VELOCITY AND WIND DIRECTION.

To determine the joint p.d.f. of wind directions and wind velocities 3- hourly observations of (usually) 20 minutes are used, so that a year is presumed to give 2920 independent observations. These observations can be classified according to direction sectors of for example $11^\circ 15'$. (Giving 32 sectors or points of the compass to be considered). The number of times a year the wind blew from a certain direction sector is counted. Assume the number of times equals N_i . This number is divided by the total number of observations (2920). The fraction of the total number of observations concerning "wind from a certain direction sector" can be displayed according to the direction sectors in a histogram:

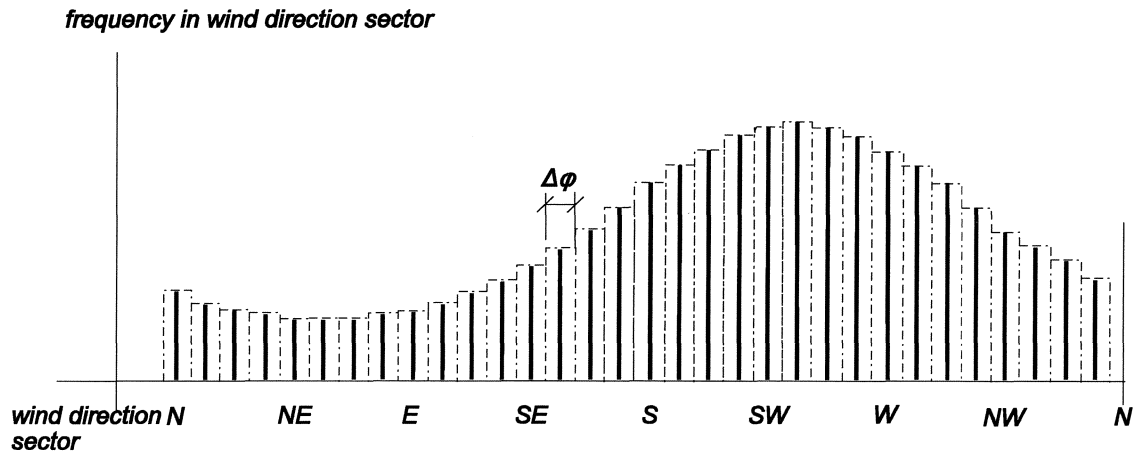


Figure II-25

This histogram can be perceived as an approximation of the probability density function of "wind from a certain direction" in a year. Per direction sector: $p_{\varphi_i} \{ \varphi_i \} \approx \frac{N_i}{\sum_{i=1}^M N_i}$. M Denotes the number of selected

direction sectors (in this example 32). A mathematical description of the frequency diagram can be obtained using a Fourier analysis.

For every selected direction sector, the wind velocity has to be established for every time the wind blew from that direction. Thus, per direction sector a wind velocity exceedance frequency curve can be determined, based on the N_i observations for every i^{th} direction sector. This conditional wind velocity exceedance frequency curve can be denoted as:

$$P\{(\underline{v} > v) | (\varphi_i < \varphi \leq \varphi_i + \Delta\varphi)\} = 1 - F_{\underline{v} | (\varphi_i < \varphi \leq \varphi_i + \Delta\varphi)}(v)$$

The order of work given above:

- 1 classifying observations according to direction
- 2 determining wind velocity exceedance frequency curve on condition of wind from a certain direction

is preferable to:

- 1 estimating the probability distribution of wind velocities from all observation data
- 2 determining the marginal probability distribution of wind directions.

The observation data is more homogenous after classification according to direction sectors.

For a good description of the conditional p.d.f. of wind velocities and wind directions in a certain place on earth, observations need to be gathered over a longer period of time (e.g. 30 years).

In practice, the probability of exceedance of wind velocities from certain directions in one year are often presented graphically (see for example Figures II-26 and II-28):

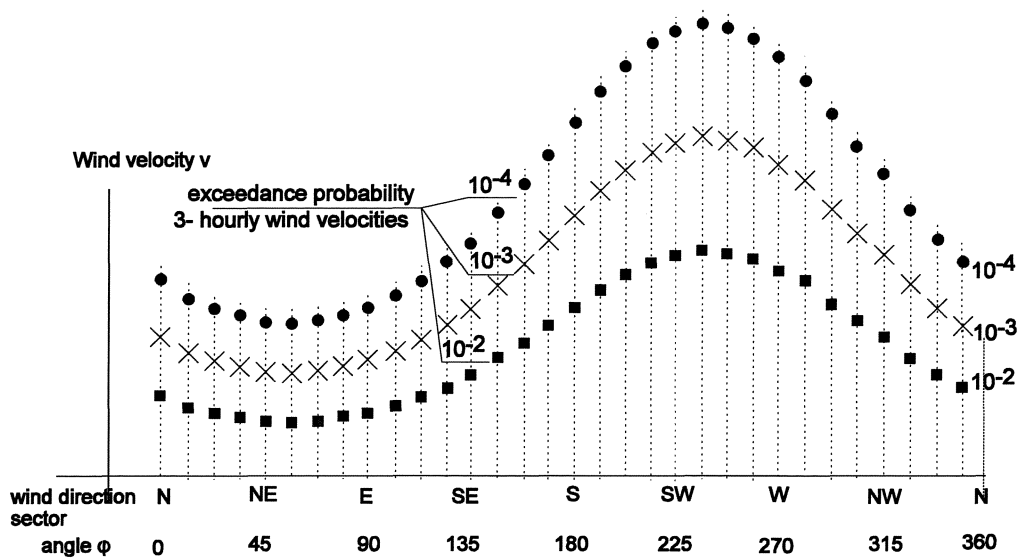


Figure II-26

$$P\{(\underline{v} > v) \cap (\varphi_i < \varphi \leq \varphi_i + \Delta\varphi)\} = (1 - F_{\underline{v} | (\varphi_i < \varphi \leq \varphi_i + \Delta\varphi)}(v)) \cdot p_{\varphi_i}(\varphi_i)$$

Note, that the probabilities of exceedance (and corresponding wind velocities) are only defined separately for the distinguished direction sectors. The above formula is valid for one separate direction. The probability of exceedance of 3-hourly wind velocities from a particular direction has a distribution (and a probability density) *per discrete direction sector*.

The exceedance frequency curve of the wind velocity for all direction sectors is:

$$1 - F_{\underline{v}}(v) = \sum_{i=1}^M \{1 - F_{\underline{v} | (\varphi_i < \varphi \leq \varphi_i + \Delta\varphi)}(v)\} \cdot p_{\varphi_i}(\varphi_i)$$

This exceedance curve is always above the exceedance curve per wind direction because the exceedance frequency curve of the wind velocities for all directions is an addition of the curves per direction sector.

$1 - F_{\underline{v}}(v) > 1 - F_{\underline{v} | (\varphi_i < \varphi \leq \varphi_i)}(v)$ for all φ_i continues to be valid

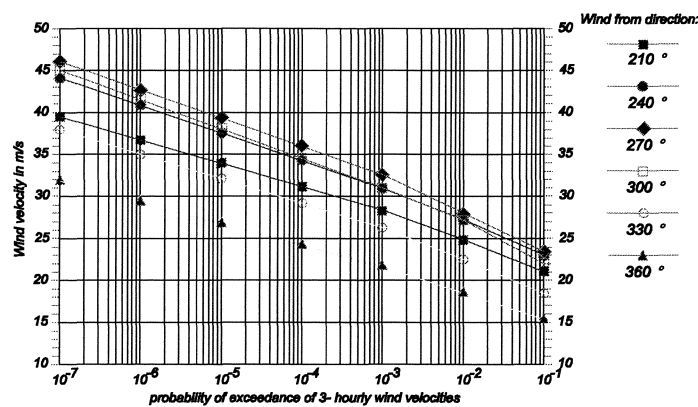


Figure II-27

The parameters of the conditional distributions of the wind velocities should be determined per direction sector (centrally for 36 sectors of 10° or 32 sectors of 11° 15' or 12 sectors of 30° or 8 sectors of 45°) (E.g. two parameters for an exponential distribution or three parameters for a Weibull distribution). A maximum of 32 (sectors) * 3 (parameters for a Weibull distribution) = 96 parameters are necessary to establish the joint p.d.f..

Sometimes, multiplication with $p_{\varphi_i}(\varphi_i)$ leads to a simple translation of the conditional wind velocity exceedance frequency curve :

$$p_{\varphi_i}(\varphi_i) \cdot e^{-\frac{v-A}{B}} = e^{-\frac{v-A-B \cdot \ln p(\varphi_i)}{B}}$$

or:

$$p_{\varphi_i}(\varphi_i) \cdot \exp\left(-\frac{v-A}{B}\right)^C = \exp\left\{\left(-\frac{v-A}{B}\right)^C + \ln p(\varphi_i)\right\}$$

Observations Lightship Goeree
 Period 1949 - 1955 (incl.) (total 57513 hours)
 Distribution wind direction and windforce
 No. Hours exceedance of a certain
 wind force in degrees Beaufort

WINDSCALE OF BEAUFORT		
Wind force	Wind velocity (m/s)	Name
0	0 - 0.5	calm
1	0.6 - 1.7	
2	1.8 - 3.3	light breeze
3	3.4 - 5.2	
4	5.3 - 7.4	moderate breeze
5	7.5 - 9.8	
6	9.9 - 12.4	strong breeze
7	12.5 - 15.2	
8	15.3 - 18.2	fresh gale
9	18.3 - 21.5	
10	21.6 - 25.1	whole gale
11	25.2 - 29.0	
12	> 29.0	hurricane

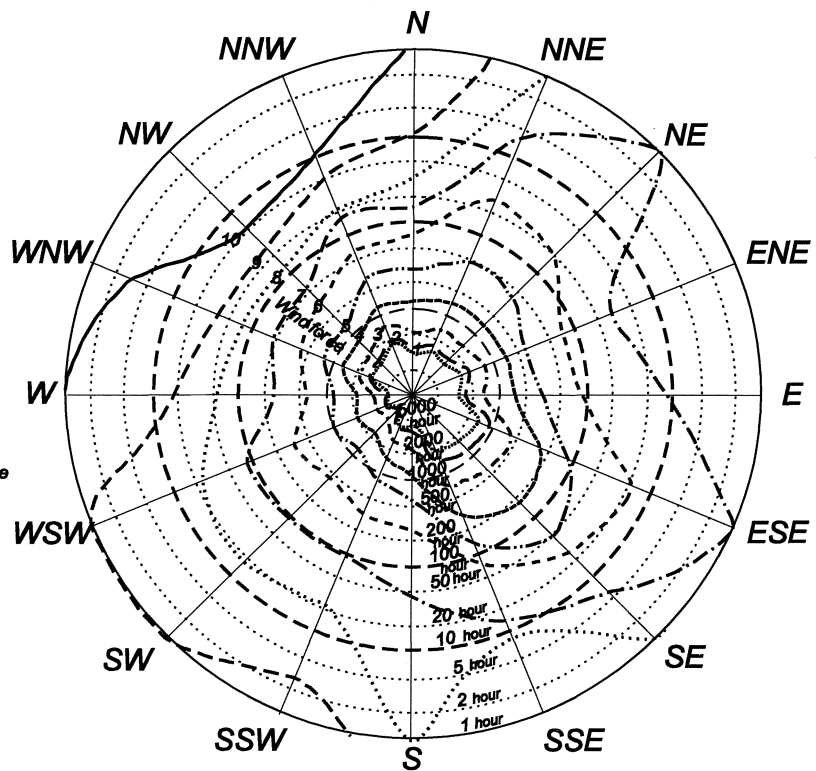


Figure II-28

Sometimes, Figure II-26 is presented in the same format as Figure II-28. Figure II-28 suggests a classification in (M =) 16 direction sectors and one- hourly (outer circle) independent(?) observations of the wind velocity.

The joint p.d.f. of wind velocity and wind direction, presented above, is valid for the S.L.S. because it is based on all observations in a year. If one wishes to establish the joint p.d.f. for the U.L.S., one must determine the extreme value distribution per direction sector.

In order to establish the joint p.d.f. of wind direction and wind velocity one can also work with the yearly maxima of the wind velocity per sector (measured during a number of years). See Figure II-29:

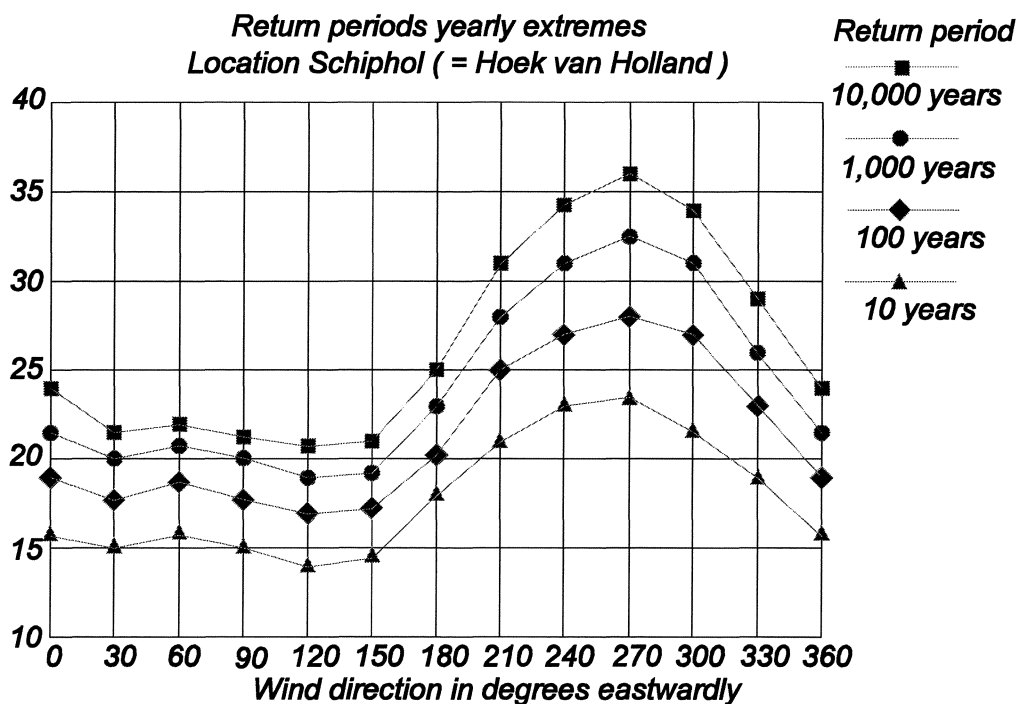


Figure II-29

If the wind velocity is Gumbel distributed, Figure II-29 will match Figure II-26. For other distributions it generally does NOT hold that the reciprocal of the exceedance probability in a year is the return period in years.

II.7. WAVE CLIMATE

Waves are created on the plane dividing two media (e.g. water and air) which flow with different relative velocities. As a rule, the height and length of sea waves increase with the wind velocity. The wind transfers energy to the water surface, which causes waves to grow and to increase their velocity until the propagation velocity equals the wind velocity. The fact that waves no longer grow can also be attributed to decreasing wind velocity. Sometimes the water depth limits the propagation velocity and/or the height.

The wave record under the influence of wind (this wave record is called swell) does not consist of a series of monotonous, uniform waves, but of a scala of waves of different heights and periods, which run through and over each other. Figure II-30 gives the irregular wave record which is created by the superposition (momentary recordings) of six different monotonous wave series.

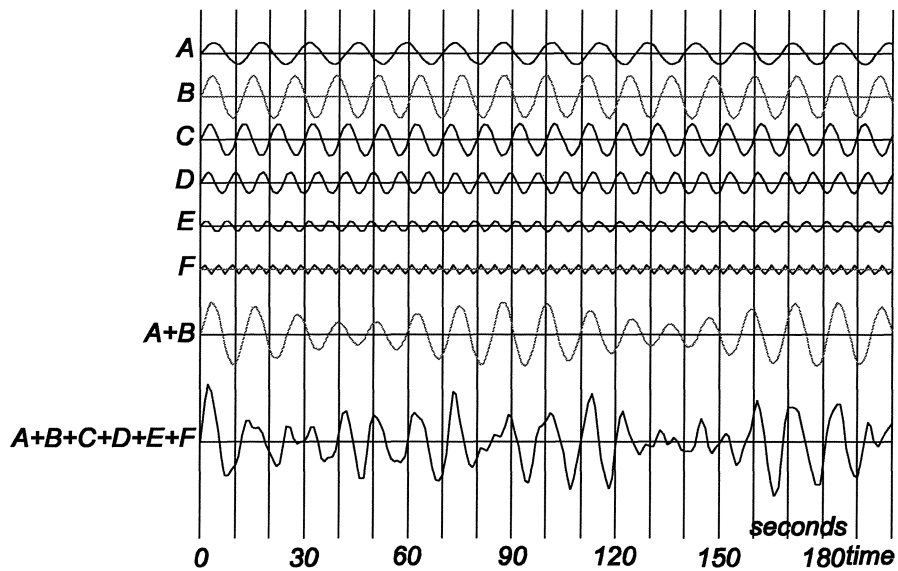


Figure II-30

Some data concerning the above wave series:

wave component	period T (seconds)	radial frequency ω (s^{-1})	amplitude (m)
A	14	0.42	1
B	12	0.52	2
C	10	0.63	1.5
D	8	0.79	1
E	6	1.05	0.5
F	4	1.57	0.4

Though only six monotonous wave series were added, the superposition already gives a rather "wild" wave record.

The square of the amplitude, η , is a measure for the energy per m^2 which is present in a wave field. Plotted against the period, T, or against the frequency, $f = \frac{1}{T}$, or against the radial frequency, $\omega = \frac{2 \cdot \pi}{T}$, this leads to the energy spectrum (Figure II-31) of the waves treated above, leaving the factors ρ (mass density) and g (acceleration due to gravity) and a constant undefined.

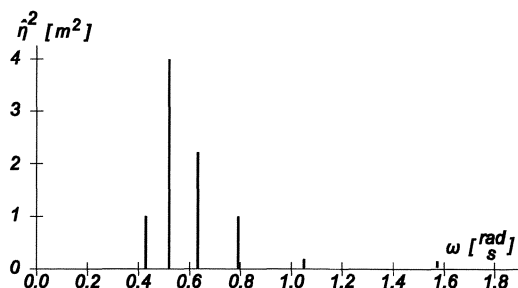


Figure II-31

As a rule, all radial frequencies are generated in a wind field. It is hence no longer possible to speak of the energy in one particular wave component. One refers to the energy in a radial frequency band $\Delta\omega$ or in a frequency band Δf .

In a variance density spectrum the variance (a measure for the energy) of the wave amplitudes is conveyed as a function of the (radial) frequency ($\omega = \frac{2\pi}{T}$ respectively $f = \frac{1}{T}$, with T = wave period).

Several spectra have been described in formulae: Neumann (outdated), Pierson-Moscowitz, JONSWAP. (See Lecture notes b 78 Wind waves, september 1989 (in Dutch).)

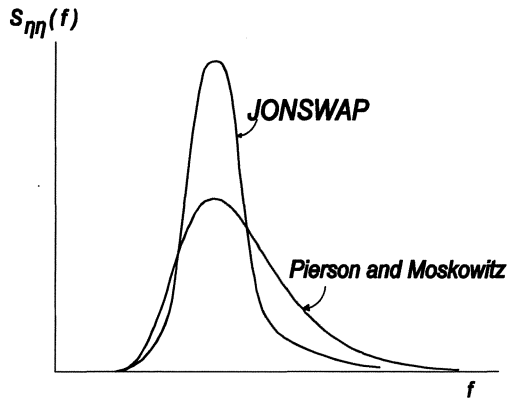


Figure II-32

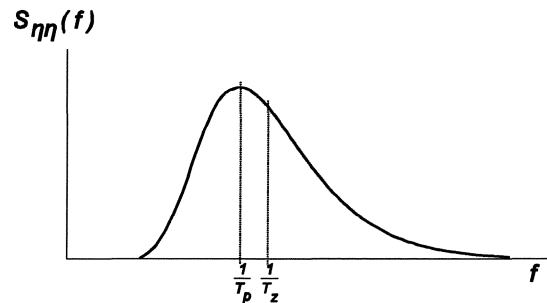


Figure II-33

The variance or energy density spectrum describes the short term wave record. A spectrum is determined by the shape, the surface below the curve and the peak period. During a storm the wave heights are assumed to be distributed according to Rayleigh. The distribution during a storm is the short term wave height distribution.

From the energy density spectrum the following long term wave statistics are of importance:

- H_s = significant wave height ($H_s = 4\sqrt{m_0}$ with m_0 = surface of the variance density spectrum).
 - = average height of the highest one third of the waves
 - = wave height which is exceeded by approximately 13% of the waves (with a Rayleigh- distribution)
- T_p = peak period
 - = period with which the energy density is maximum
- φ = the angle of incidence.

The peak period can usually be indicated directly. The average period T_z ("centre of gravity" of the energy density spectrum) is more difficult to define because this centre is very much dependent on the shape of the spectrum (selected: Pierson- Moskowitz, JONSWAP, etc.). For the P-M spectrum:

$$\frac{T_p}{T_z} \approx 1.4 \text{ is valid, for the JONSWAP spectrum: } \frac{T_p}{T_z} \approx 1.2.$$

Often, in practice, the spectra are not indicated as "tidily" as the "standard spectra". Double peak spectra and spectra with different shapes exist. The peak period can be recognized more clearly in the spectrum than the average period. The use of the peak period (see Figure II-33) is therefore preferable.

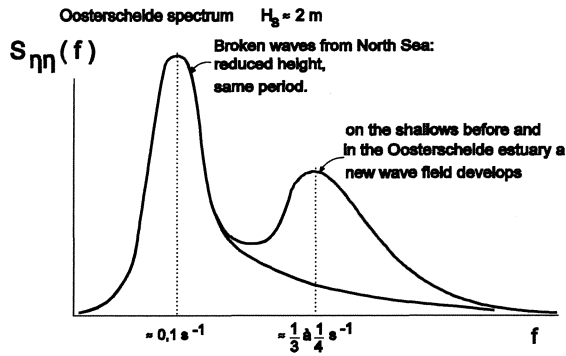


Figure II-34

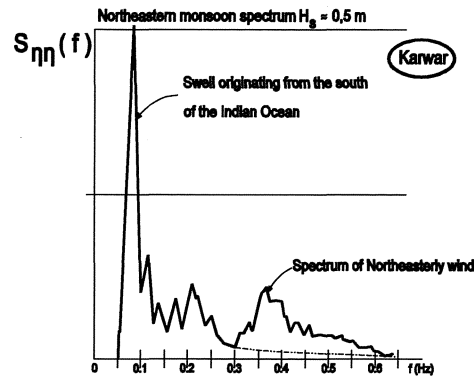


Figure II-35 = Figure II-36-1-a

From the measured energy density spectrum and from the measured directions spectrum much can be deduced concerning the "physical backgrounds" of waves. Often there is one "high frequency peak", caused by "local events" (wind over shallows located nearby, wind along the coast, etc.) and a "low frequency peak", caused by the swell, which is influenced by breaking. Often the direction of the "high frequency waves" is determined by the wind direction, whilst the "low frequency waves" get their direction from the combination of the "deep water wave climate" and the geometry of the seabed in front of the coast. T_p corresponds to the "main phenomenon", T_z is influenced by all phenomena.

The next pages display the monsoon-spectra for Karwar.

Figure II-36-1 and Figure II-36-2 concern wave data collected during the northeastern monsoon. (Recordings are from November 12 and 13 1988.)

Figure II-37-1 and Figure II-37-2 concern data collected during the southwestern monsoon. (Recordings are from June 19 and 20 1988.)

Figures II-36/37-1/2-a (top figures) give the variance densities in m^2s (as a function of the frequency in Hz).

Figures II-36/37-1/2-b (bottom figures) give the angles of incidence of the waves.

During the northeastern monsoon, the waves with a maximum density of the variance of the amplitude (represented by approximately $0.2 m^2s$ - on 12/11/88 - to $0.37 m^2s$ - on 13/11/88) come from the direction 210° eastwardly, or roughly from the south southwest. This is obvious if one is aware that their source is in the south of the Indian Ocean somewhere near Capetown. The waves with maximum variance density (waves with the "peak frequency" T_p) thus travel "against the prevailing northeasterly wind". During the southwestern monsoon the waves which are generated by the local wind field are from the same direction as the (low frequency) swell. (See Figures II-37-1/2,a,b.) Because the wind velocity is a little higher than during the northeastern monsoon, the constituent parts of the spectrum can be distinguished less clearly than in Figures II-36-1/2,a,b.

Wavec i*1988 11-12 12:30
 Steepness S_p: .022
 T_m : 4.5 s T_p : 11.7 s
 H_s : .49 m T_z : 3.7 s

Wavec i*1988 11-13 11:30
 Steepness S_p: .011
 T_m : 6.5 s T_p : 13.3 s
 H_s : .52 m T_z : 5.4 s

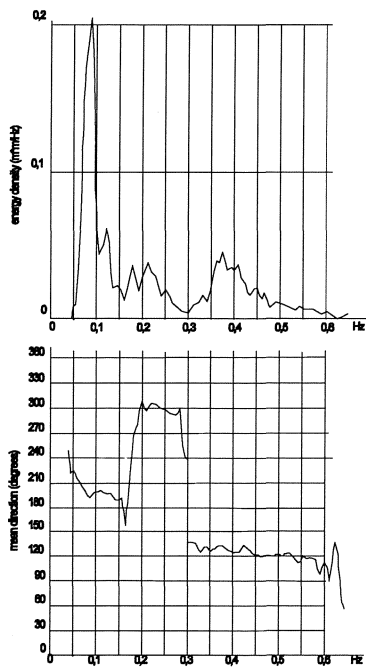


Figure II-36-1-a,b

Wavec i*1988 06-19 01:30
 Steepness S_p: .025
 Tm: 8.4 s Tp: 10.5 s
 Hs: 1.84 m Tz: 7.67 s

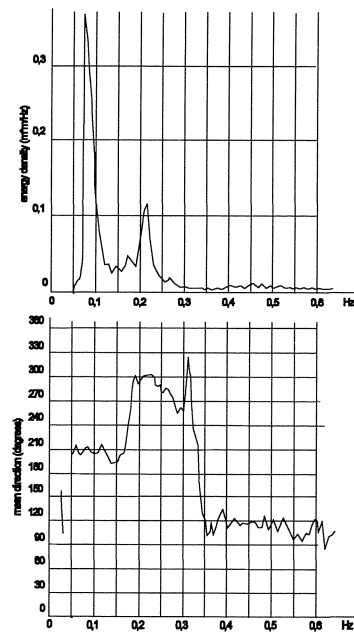


Figure II-36-2-a,b

Wavec i*1988 06-20 12:30
 Steepness S_p: .03
 Tm: 7.1 s Tp: 10.5 s
 Hs: 1.78 m Tz: 5.4 s

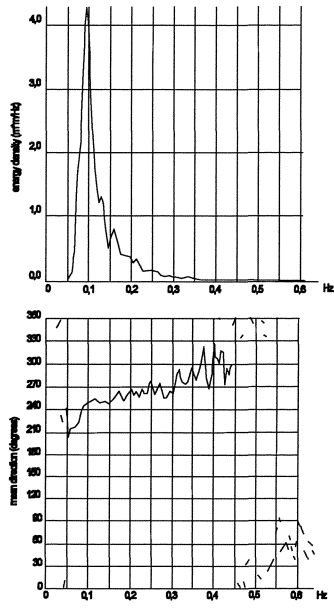


Figure II-37-1-a,b

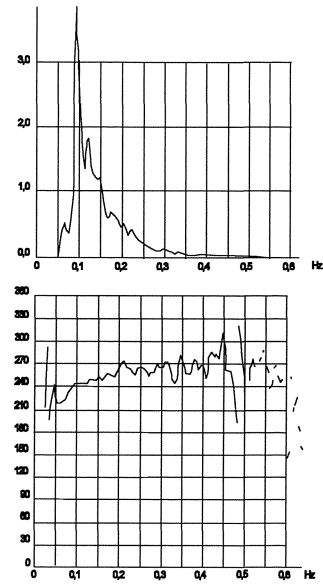


Figure II-37-2-a,b

For long term wave statistics (description of the wave climate) three elements are of importance: H_s (significant wave height), T_p (peak period) and φ (direction from which the wave originates). Often wind directions can be distinguished from which the majority of the waves originate. For those wind directions only the H_s and the T_p are of importance. Traditionally, a lot of attention is paid to the statistical description of H_s . For this description a Weibull- (exponential), Gumbel- or log- normal distribution is often selected. However, the (peak) period, $T_{(p)}$ is of equal importance.

Some data that result from measurements on location in Karwar are noted in the following tables and figures:

For the southwestern monsoon:
 Significant wave height in m.
 Analysis of 291 data

$$F_{H_s}(H) = 1 - e^{-\left(\frac{H-1.500}{0.675}\right)^{1.866}}$$

MEAN = 2.103 m
 ABS. DEVIATION = 0.298 m
 ST. DEVIATION = 0.347 m
 SKEWNESS = 0.513
 KURTOSIS = 2.270
 H_{s_max} = 3.180 m
 H_{s_min} = 1.550 m

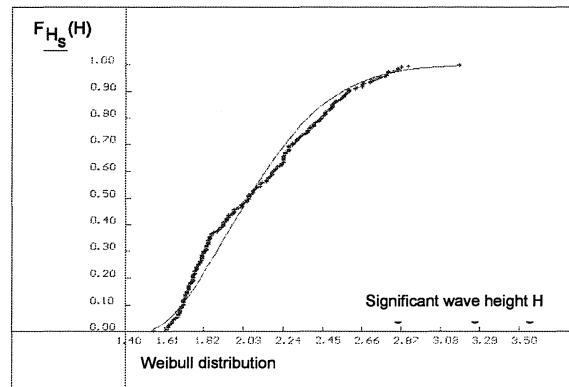


Figure II-38

For the southwestern monsoon:
 Period during which maximum energy density in s
 Analysis of 291 data

$$F_{T_p}(T) = \int_0^T \frac{1}{0.095 \cdot \xi \cdot \sqrt{2\pi}} \cdot e^{-\frac{1}{2} \left(\frac{\ln \xi - 2.408}{0.095}\right)^2} d\xi$$

MEAN = 11.15 s
 ABS. DEVIATION = 0.679 s
 ST. DEVIATION = 1.019 s
 SKEWNESS = 1.593
 KURTOSIS = 12.926
 T_{p_max} = 18.100 s
 T_{p_min} = 8.300 s

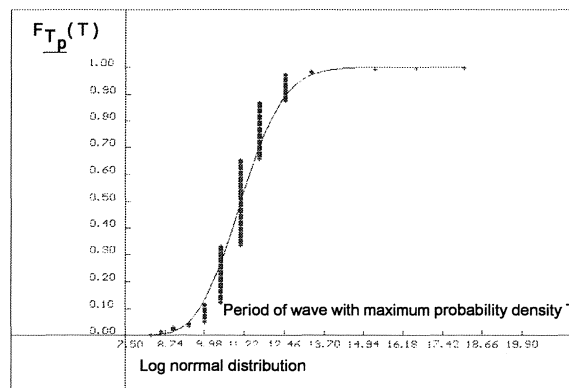


Figure II-39

For the southwestern monsoon:
 Wave steepness
 Analysis of 291 data

$$F_{s_p}(s) = e^{-e^{-\frac{s-1.000}{0.167}}}$$

MEAN = 1.095%
 ABS. DEVIATION = 0.149%
 ST. DEVIATION = 0.205%
 SKEWNESS = 1.211%
 KURTOSIS = 7.714%
 s_{p_max} = 2.205%
 s_{p_min} = 0.415%

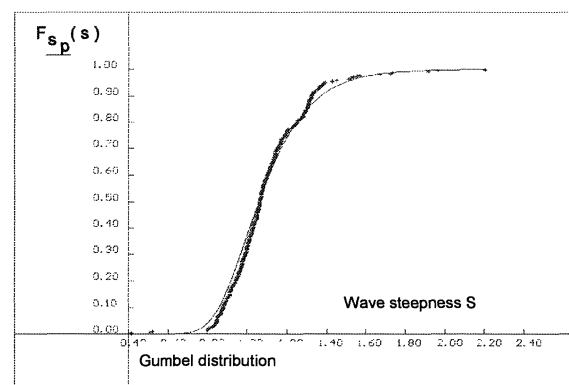


Figure II-40

An important question is, how to describe the joint p.d.f. of H_s and T_p . For the calculation of quasi-static wave loads on constructions or for use in combination with recently developed formulas for stone stability (formulas by Van Der Meer, for example) the peak period, T_p , is at least as important as H_s .

The joint probability density function of H_s and T_p can be determined. In literature one often finds that the marginal p.d.f.s of H_s and T_p are modelled with Weibull or log normal p.d.f.s. If H_s and T_p were not correlated, the joint p.d.f. could look as shown in Figure II-41.

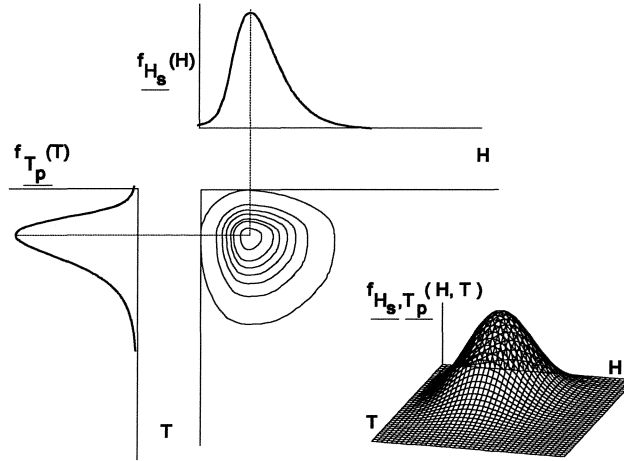


Figure II-41

However, the joint p.d.f. can NOT be derived from the marginal p.d.f.s because H_s and T_p are certainly correlated. High waves usually have long periods, low waves usually have short periods. Figure II-42 (taken from Lecture notes Wind waves, b 78, Station "INDIA" (in Dutch: Collegehandleiding Windgolven, b78, Station "INDIA"), Battjes, 1970, 1972) clearly shows this dependency.

Figure II-42 is generated by determining the marginal probability density of the period with maximum energy density per class of significant wave height (and also per direction sector from which the waves arrive):

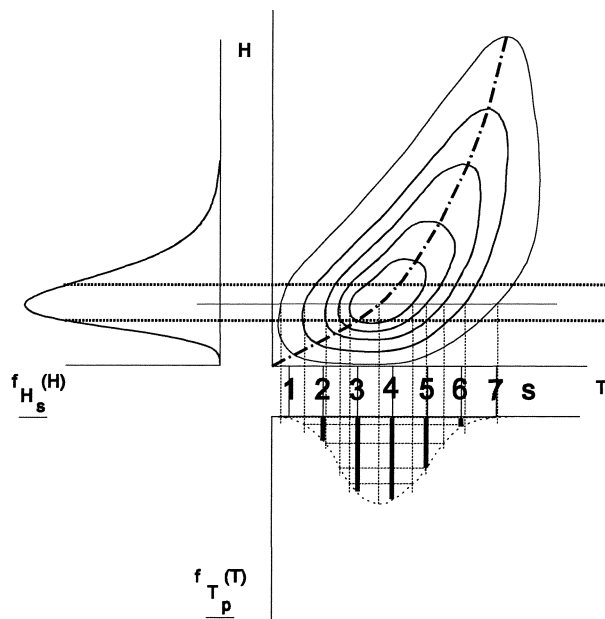


Figure II-42

The relation between H_s and T_p can be described (modeled) in many ways. This course maintains a preference for the consideration of $\underline{H_s}$ and $\underline{s_p}$ as independent random variables.

s_p = wave steepness (for wave length and height see the definition diagram: Figure II-43.)

$$s_p = \frac{H_s}{L_p} = \frac{H_s}{\frac{g T_p^2}{2 \pi}}$$

L_p = length of the wave with period T_p

g = acceleration caused by gravity.

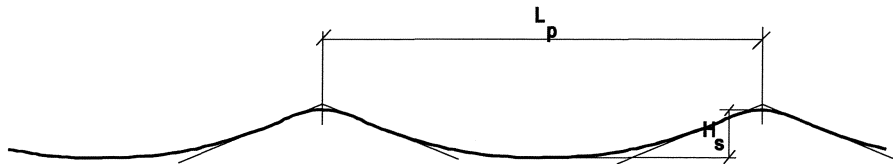


Figure II-43

In the $H_s - T_p$ plane lines of constant wave steepness are presented as parabolas:

$$s_p = \frac{H_s}{\frac{g T_p^2}{2 \pi}} = \text{constant} \Rightarrow H_s = C * T_p^2, \text{ parabolas for different } C = \frac{s_p \cdot g}{2 \cdot \pi}.$$

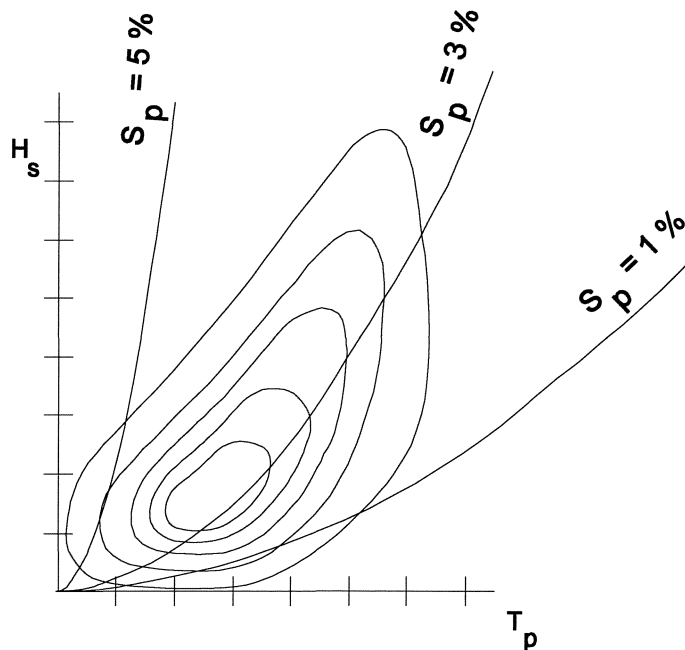


Figure II-44

This is a verification of the input data (observations) concerning H_s and T_p . In nature waves with a steepness greater than 5 to 6% don't or rarely exist. Waves with this steepness break. On the other hand, waves with a steepness less than approximately 1% rarely exist either. A steepness that small is found, for example, for swell that originates from a far away source.

II.8. VERIFICATION OF THE INPUT DATA

Firstly, the independence of the input data (i.e. s_p and H_s) has to be tested. Subsequently, one has to consider whether or not the results of this test can be explained physically.

To test whether H_s and s_p are independent, the calculated steepnesses are plotted against the significant wave height. If H_s and s_p are independent, no clear relation can be revealed. The diagram opposite serves as an example of independent H_s and s_p .

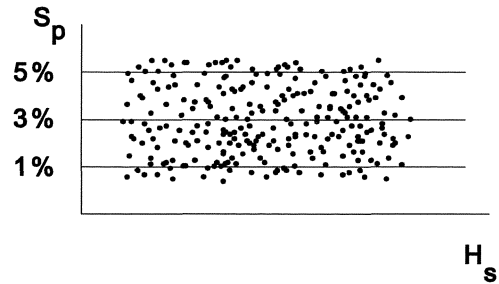


Figure II-45

The position of the cloud of points serves as a test of the input data (observations) of H_s and T_p .

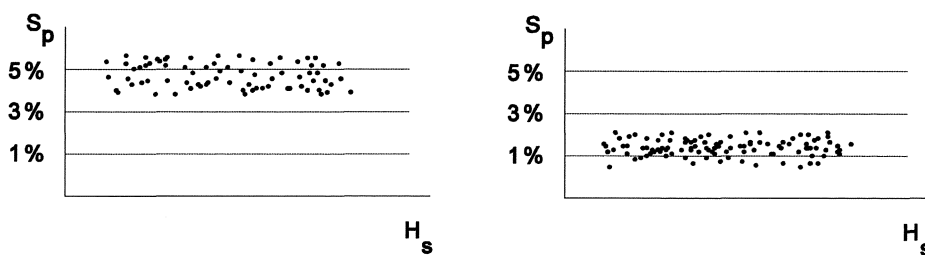
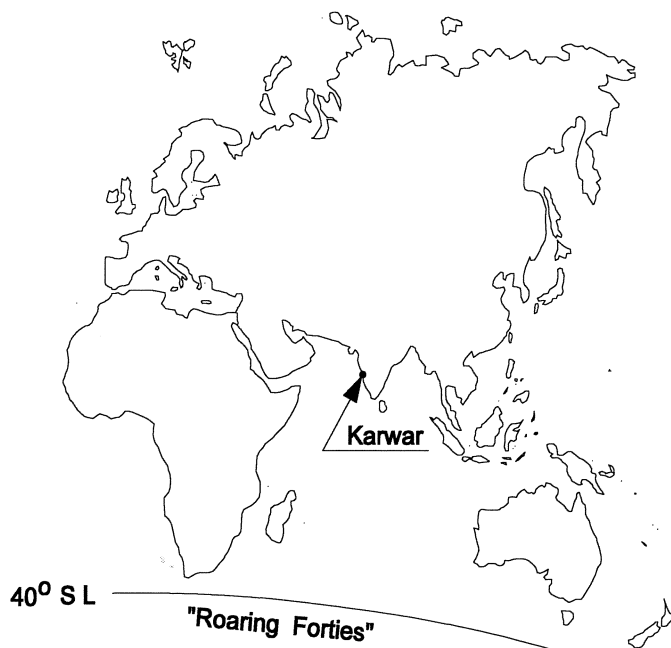


Figure II-46

Subsequently, consideration should be given as to whether the acquired diagrams are explicable. Waves in a lake (no swell, surface of the lake small compared with that of a depression, so that one wind field is to be considered) will have a wave steepness of around 5%, independent of the wave height. This is known as young swell. The cloud of points will be around the $s_p = 5\%$ line. (For example, figure II-46 left could have been based on wave data from the IJsselmeer.)



In Karwar the steepnesses found during a southwestern monsoon generally were approximately 0.8 to 1%. (see Figures II-51 and II-56, comparable with Figure II-46 right.) The waves (mainly swell) transpired to originate from the south of the Indian Ocean ("Roaring Forties").

Figure II-47

In nature, the conditions for the generation of a long significant wave are less easily met than those for the generation of a high significant wave. Hence, the peak periods of spectra are usually relatively short.

Significant wave heights with periods of 15 to 20 seconds demand very large fetches and very high wind velocities. The approximation of independence of H_s and s_p is a conservative one considering that high steep waves are assumed as likely as low steep waves.

When a deep depression passes, as is indicated in Figure II-48, the swell entering the North Sea from the Atlantic Ocean is broken on the Doggersbank. In the North Sea new waves are generated. During a storm on the North Sea, the wave steepness near the indicated measuring point (BG II, see also Figure II-66) is around 3.5%.

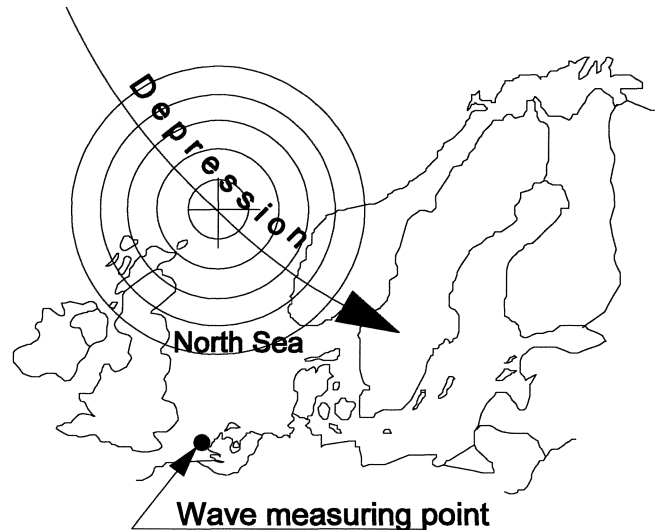


Figure II-48

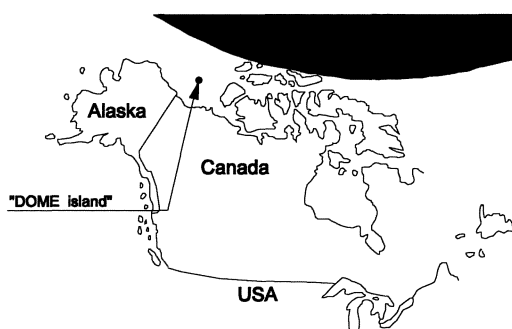


Figure II-49

Around 1980 the former oil company DOME built an oilrig in the Beaufort Sea to the north of Alaska. For this purpose a "sand hill" was created. To prevent the drilling installations from being pushed off the island by ice packs in the winter, a square of caissons was placed. The space within the square was filled with sand. On top of that the drilling installations were placed. One believed to have found, from measurements, that the (significant) waves had steepnesses of around 2% with a height of $H_s \approx 2\text{ m}$. Considering the reflection against the vertical restriction, formed by the caissons, the caissons were given a height of 2 m above still water.

Taking into account the distance between the border of the ice pack in summer and the coast of Alaska, the then prevailing northern wind and the size of the centres of the depressions, one would expect a wave steepness of 5% (young swell). The Beaufort Sea is "deep enough" everywhere, so breaking would not take place. (Breaking reduces the height, but the wave period remains practically the same.) It appeared that the expected wave steepness was better than the measurements. A mistake had been made during the registration of the wave height. The waves on the Beaufort Sea turned out to be 4 m instead of 2 m high, so, reflected by the caissons, the waves around the island were 8 m high. The sand that had been dumped between the caissons washed away very quickly! Only with great improvisations (supplying parts for steel sheet piling by plane from mainland and importing a polypropylene cloth from the Netherlands to hold the sand) the island could be saved. The costs, however, were considerable!

EXAMPLES OF RELATIONS BETWEEN H_s AND T_p

The steepness of the waves near Karwar during the **SOUTHWESTERN MONSOON** can be modelled with a Gumbel distribution (see next to Figure II-40):

$$P\{s_p < s\} = F_{s_p}(s) = e^{-e^{-\frac{100 \cdot s - 1.000}{0.167}}}$$

The heights of the significant waves are given in % of the lengths of those waves, i.e. the steepness is expressed in %.

The wave steepness which is not attained by 10% of the waves follows from:

$$e^{-e^{-\frac{100 \cdot s - 1.000}{0.167}}} = 0.1 \Rightarrow s \approx 0.861\%$$

For $s_p = s = 0.00861$ (see the definition of s_p on the top of page II-31):

$$H_s \approx 0.01344 \cdot T_p^2$$

This line is plotted in Figure II-50. The line is labelled $s_{10\%}$.

Analogously:

$$H_s \approx 0.02149 \cdot T_p^2, \text{ labelled } s_{90\%} \text{ and } H_s \approx 0.01657 \cdot T_p^2, \text{ labelled } s_{50\%}.$$

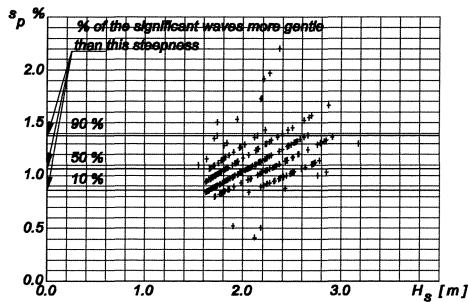


Figure II-51

Data gathered from measurements on location in Karwar during **HURRICANES**, are presented in the following tables and figures:

For hurricanes during the southwestern monsoon:

Significant wave height in m.

Analysis of 25 data points:

$$F_{H_s}(H) = e^{-\left(\frac{H}{2.498}\right)^{-3.388}}$$

MEAN = 3.075 m

ABS. DEVIATION = 0.797 m

ST. DEVIATION = 1.042 m

SKEWNESS = 0.880

KURTOSIS = 3.072

H_{s_max} = 5.770 m

H_{s_min} = 1.530 m

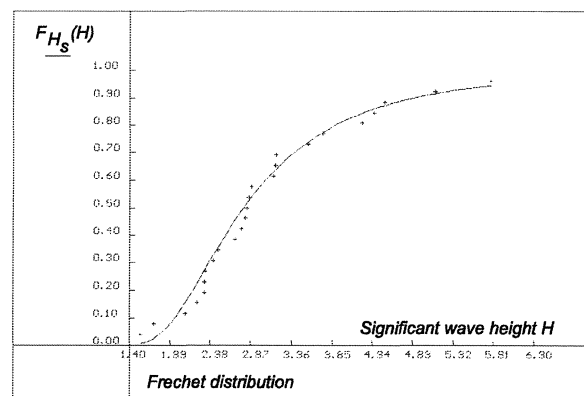


Figure II-52

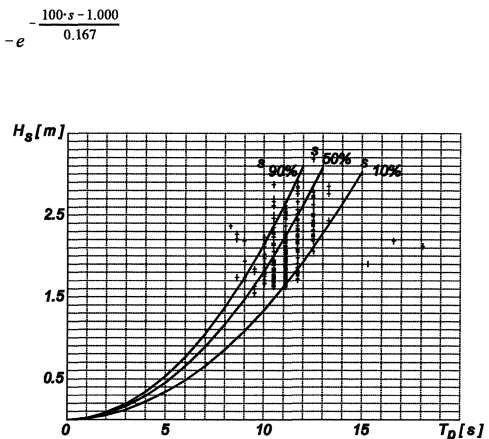


Figure II-50

To check whether the wave steepness is independent of the significant wave height, s_p can be plotted against H_s . This was done in Figure II-51. The lines $s_p = 0.861\%$ (probability of non-exceedance 10%), $s_p = 1.061\%$ (probability of non-exceedance 50%) and $s_p = 1.376\%$ (probability of non-exceedance 90%) are plotted in the diagram. The regularity that seems to appear from the figure is deceptive because the peak periods were "supplied" in classes. (Compare Figure II-39.)

For hurricanes during the southwestern monsoon:
 Period T_p for which the energy density is maximum in s.

Analysis of 25 data points

$$F_{T_p}(T) = \int_0^T \frac{1}{0.151 \cdot \xi \cdot \sqrt{2\pi}} \cdot e^{-\frac{1}{2} \left(\frac{\ln \xi - 2.110}{0.151} \right)^2} \cdot d\xi$$

MEAN = 8.323 s
 ABS. DEVIATION = 0.881 s
 ST. DEVIATION = 1.136 s
 SKEWNESS = 0.508
 KURTOSIS = 2.374
 $T_{p_max} = 10.610$ s
 $T_{p_min} = 6.780$ s

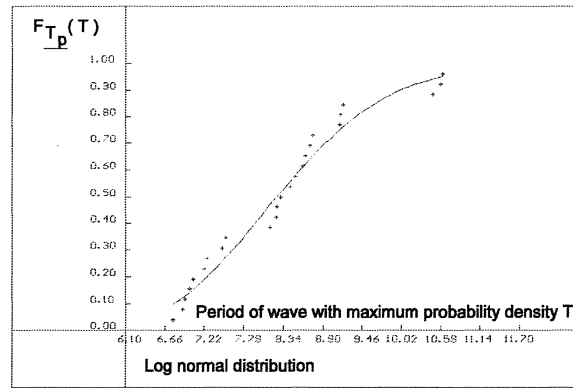


Figure II-53

For hurricanes during the de southwestern monsoon:

Wave steepness.

Analysis of 25 data points

$$F_{s_p}(s) = \frac{1}{0.724 \cdot \sqrt{2\pi}} \int_{-\infty}^s e^{-\frac{1}{2} \frac{(\xi - 2.820)^2}{0.724^2}} d\xi$$

MEAN = 2.820%
 ABS. DEVIATION = 0.517%
 ST. DEVIATION = 0.644%
 SKEWNESS = 0.475%
 KURTOSIS = 2.974%
 $s_{p_max} = 4.536\%$
 $s_{p_min} = 1.753\%$

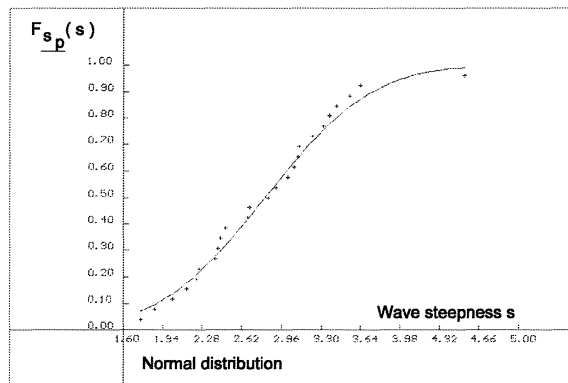


Figure II-54

In this case it is possible to model the wave steepness during hurricanes with a normal distribution (see adjacent to Figure II-54):

$$P\{s_p \leq s\% \} = F_{s_p}(s) = \frac{1}{0.724 \cdot \sqrt{2\pi}} \int_{-\infty}^s e^{-\frac{1}{2} \frac{(100 \cdot \xi - 2.820)^2}{0.724^2}} d\xi$$

The wave steepness that is not attained by 10% of the waves follows from:

$$\frac{1}{0.724 \cdot \sqrt{2\pi}} \int_{-\infty}^s e^{-\frac{1}{2} \frac{(100 \cdot \xi - 2.820)^2}{0.724^2}} d\xi = 0.1 \Rightarrow \frac{100 \cdot s - 2.820}{0.724} = -1.28 \Rightarrow s = 1.89\%$$

For $s = 0.0189$:

$$H_s \approx 0.02951 \cdot T_p^2$$

This line is drawn in the opposite figure. The line is labelled $s_{10\%}$.

Analogously:

$$H_s \approx 0.04404 \cdot T_p^2, \text{ labelled } s_{50\%} \text{ and}$$

$$H_s \approx 0.05872 \cdot T_p^2, \text{ labelled } s_{90\%}.$$

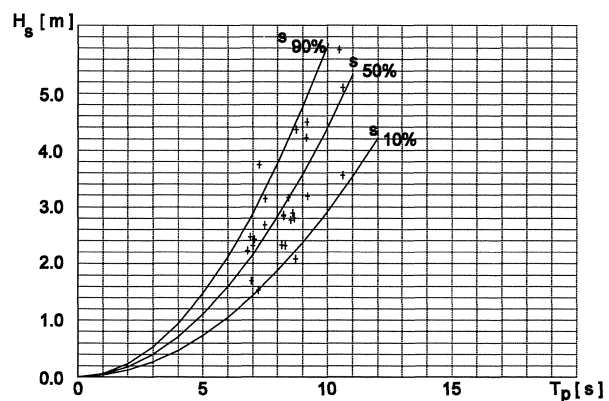
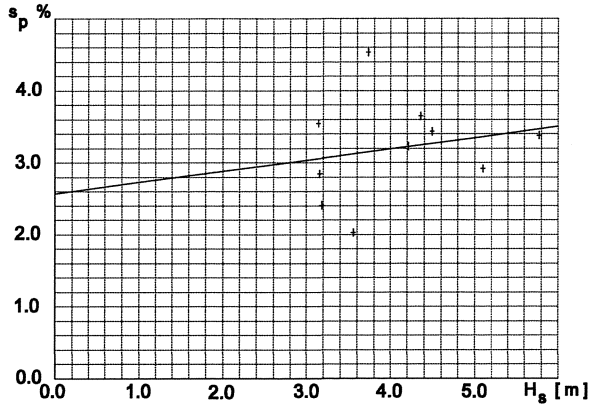


Figure II-55



To check whether the wave steepness is independent of the significant wave height, again, plot s_p against H_s . This has been done in the opposite diagram. The calculated regression line has a small gradient and the points are widely spread around it. From this a strong suggestion of independence arises. (A strategic test could also be carried out. Due to the small number of observations - only waves with $H_s > 3$ m were considered - the visual evaluation of the diagram opposite will suffice.)

Figure II-56

BG II- observations (see below: the peak frequency, f_p , plotted against the significant wave height, H_s) originate from a measuring pole in the Oosterschelde estuary at a depth of 10 m. The very curved lines are drawn for statistical reasons. The lines with constant gradients have also been included in the figure.

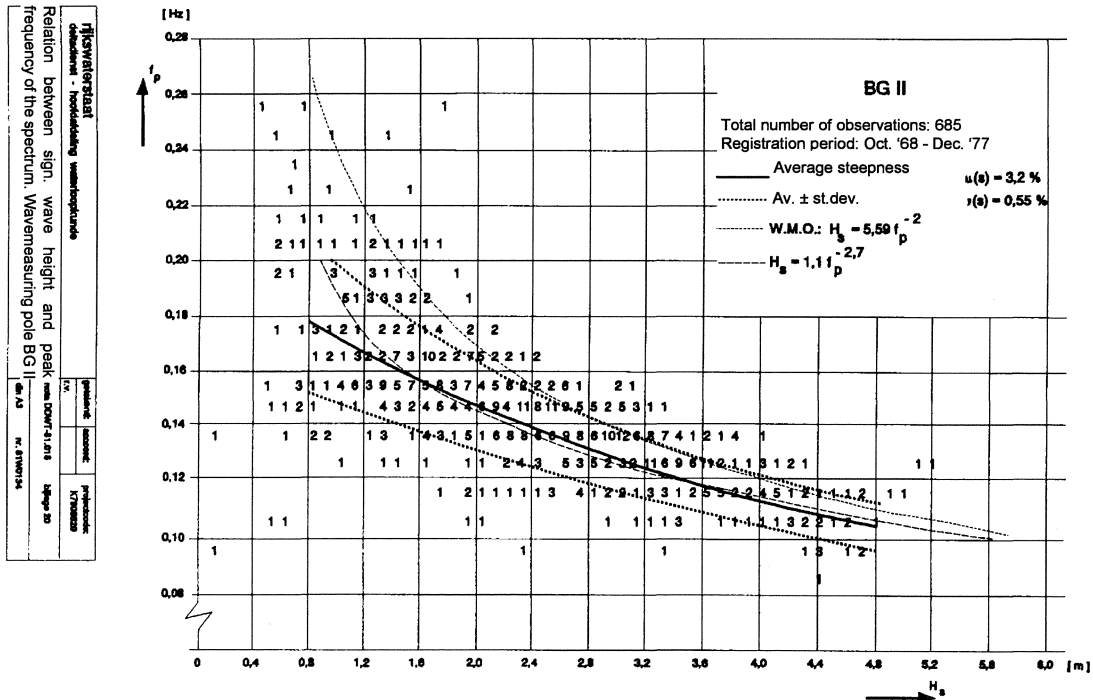


Figure II-57

II.9. HYDRAULIC BOUNDARY CONDITIONS FOR THE OOSTERSCHELDE STORM SURGE BARRIER

The following article, titled Hydraulic Boundary Conditions and written by Vrijling, J.K. and Bruinsma, J. is taken from a contribution to the Symposium on Hydraulic Aspects of Coastal Structures.

SYNOPSIS

In the design of the Oosterschelde storm surge barrier semi-probabilistic methods have been used. The probabilistic load calculation requires knowledge of the three dimensional probability density function of storm surge level, basin level and wave energy.

However especially in the interesting regions of low probability of occurrence the consequent lack of measured data prevents a reliable estimate of this function.

In this paper a combination of purely statistical models and mathematical models, based on physical laws and checked with measured data, has been used. The probability density function of the storm surge level is based on a purely statistical model. A simple mathematical model, based on physical facts, is used to derive the conditional probability density function of the basin level on the storm surge level. The conditional probability density function of the wave energy on the storm surge level is found along the same lines. A mathematical model is developed based on the hypothesis, that the typical double peaked form of the wave spectrum is caused by the fact, that the wave energy originates from two sources: waves, entering the estuary from deep water via the shoals and waves generated locally, form together the seastate at the barrier site. The required three dimensional probability density function of storm surge level, basin level and wave energy is derived as the product of the probability density functions referred to above.

CONTENTS

1. Introduction
2. The still water level at both sides of the barrier
 - 2.1. Introduction
 - 2.2. The storm surge level, two models
 - 2.3. The low water level
 - 2.4. Empirical evidence
 - 2.5. The basin level
3. The storm surge levels and wave energy
 - 3.1. Introduction
 - 3.2. Analysis and foundation of the model
 - 3.3. The mathematical wave model of the Oosterschelde
 - 3.4. Empirical evidence
 - 3.5. Wave direction
 - 3.6. The mathematical model of the North Sea
 - 3.7. Empirical evidence
 - 3.8. The completed model
4. The three dimensional probability density Function of storm surge level, basin level and wave energy

II.9.1. INTRODUCTION

In the design of the Oosterschelde storm surge barrier semi-probabilistic methods have been used (Mulder and Vrijling, 1980). The probabilistic load calculation requires knowledge of the three dimensional probability density function of storm surge level, wave energy, and basin level. Basically there are two ways of extrapolating the measured data of these parameters and their correlations into the regions of low probability of occurrence, where measured data are not available.

1. A purely statistical extrapolation.
2. A statistical extrapolation supplemented by mathematical models based on physical laws and checked with measured data.

A combination of these methods has been used in finding the probability density function of the storm surge level and the conditional probability density functions of wave energy and basin level, from which the three dimensional probability function is derived. A schematic diagram for the development of this three dimensional function has been given in Figure II-58.

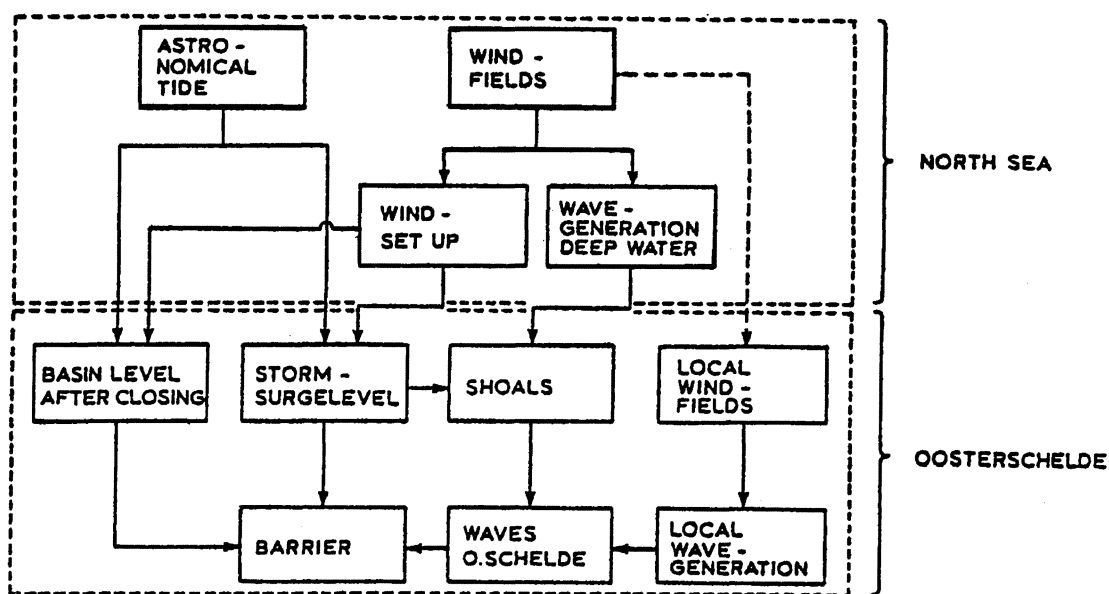


Figure II-58 A schematic diagram of the physical relations used for the derivation of the three dimensional probability function of storm surge level, wave energy and basin level.

The probability density function of the storm surge level is based on 68 years of historical data; extremes are predicted by statistical extrapolation. The knowledge of the physical laws governing this phenomenon has been used to see whether predicted extremes could be reached (ch. II.9.2).

The conditional probability density function of the basin level depends at least partly on the closing strategy of the barrier during storm surges. A simple model was developed based on the fact that a storm surge is formed by a random combination of wind set up and astronomical tide (ch. II.9.2.). From this model the conditional probability density function of the basin level (conditional on storm surge level) could be derived for different closing strategies. The basin level was found to be virtually statistically independent of the wave energy.

It appeared from the data that a loose correlation exists between the storm surge level and the energy of the wave spectrum. Lack of data, however prevented a reliable extrapolation of this two dimensional probability function by purely statistical methods. Therefore a mathematical model has been developed (ch. II.9.3.). It is based on the hypothesis that the typical double peaked form of the wave spectrum is caused by the fact, that the wave energy originates from two sources. Waves, entering the estuary

from deep water via the shoals, are influenced by the processes of breaking, bottom dissipation and refraction by depth and current. The remaining wave energy reaching the barrier depends strongly on the storm surge level. In addition, waves are generated by local windfields, showing a loose relation to the general storm intensity. The model, which incorporates all these effects, is tested in a hindcast of several storms. Being in good agreement, the model is used in extrapolating the conditional two dimensional probability density of storm surge level and wave energy.

The required three dimensional probability density function of storm surge level, wave energy and basin level is derived as the product of the probability density functions referred to above (ch. II.9.4). It has been used as input in the calculations of the probability distribution of the hydrodynamic load on the storm surge barrier.

II.9.2. THE STILL WATER LEVELS AT BOTH SIDES OF THE BARRIER

II.9.2.1. INTRODUCTION

As the storm surge level, the basin level and the wave energy will be considered as stochastic entities, it is possible to construct the three dimensional probability density function of these quantities. Throughout this paper the stochastic variables will be underscored. In this chapter the still water levels at both sides of the barrier during a storm surge will be studied.

The probability density function of the maximum storm surge level has to be based on the frequency of exceedance curve of such level published in the Delta-report (1960), regulating the design of the Dutch sea defenses. However in addition a model is used, that relates the maximum storm surge level to its fundamental origins, viz. the windfield above the North Sea and the astronomical tide. It is shown that extreme storm surge levels can only be reached by North Westerly storms.

Further a model is developed that incorporates the available stochastic information on wind set up, storm duration and astronomical tide. The model is tested by comparing the calculated probability of exceedance curve of maximum storm surge levels to the empirical curve as published in the Delta report. Subsequently it is used to find the set of low waters preceding a storm surge that necessitates the closure of the barrier. This set is also gathered from historical storm surge data and shows good resemblance to the calculated set.

Finally the two dimensional probability density function of maximum storm surge level and basin level is evaluated.

II.9.2.2 THE STORM SURGE LEVEL; TWO MODELS

The probability density function of the storm surge level is based on the frequency of exceedance curve presented by the Delta-committee (1960) as a criterion for the design of the Delta works. This curve is based on historical data collected in the period 1888-1956 and corrected for influences due to the Delta works. It is given by:

$$P(\underline{z}_m > z) = e^{-\frac{2.94 - z}{0.3026}} \quad (1)$$

where: \underline{z}_m = the highest still water level during a storm in metres above reference plane (NAP)

However, to see whether predicted extremes could be reached, the underlying physical phenomena have been analysed and modelled by Schalkwijk (1947) and Weenink (1958). They show, that a storm surge is the resultant of two stochastically independent phenomena, viz.:

1. wind set up
2. astronomical tide

The wind set up is caused by the wind fields of a cyclone above the North Sea. If the form of the cyclone and the 9-hour uninterruptedly exceeded wind speed are known, the model of Weenink calculates the maximum wind set up (s_m) in the region of the Oosterschelde.

Applying the model for two schematised storms, the following expression can be derived.

North Westerly storm:

$$s_m \approx 3.47 \cdot 10^{-2} W_9^2 / g \quad (2)$$

South Westerly storm:

$$s_m \approx 1.50 \cdot 10^{-2} W_9^2 / g \quad (3)$$

where:

- s_m = maximum wind set up near the Oosterschelde [m]
- W_9 = 9-hour uninterruptedly exceeded wind speed [m/s]
- g = acceleration of gravity [m/s²]

These expressions show that any given wind set up caused by a South Westerly storm can be equalled by the set up due to a North Westerly storm having a 1.5 x lower wind speed.

A common way to get an impression of the maximum storm surge level (z_m) is simply to add the maximum wind set up and the astronomical high water level. Analysing the historical storm surge of 1953 and the design "Delta" storm ($z = 5.50$ m), assuming different astronomical high waters (h_{HW}), one finds the following figures for the wind set up and the required wind speed as a function of wind direction (α).

Storm	z_m [m]	tide	h_{HW} [m]	s_m [m]	α	W_9 [m/s]
1953	4.20	neap	1.20	3.00	NW	28
Delta	5.50	neap	1.10	4.40	NW	34
Delta	5.50	average	1.50	4.00	NW	33
Delta	5.50	spring	1.90	3.60	NW	31
Delta	5.50	spring	1.90	3.60	SW	49

The table shows, that the dramatic storm surge of 1953 can be easily surpassed, if the same wind velocities coincide with spring tide.

The conclusion can also be drawn from the table, that an exceedance of the deterministic design storm level NAP + 5.50 m may indeed be caused by an extreme North Westerly storm. An exceedance of this level during a South Westerly storm seems however very improbable, given the wind statistics for the North Sea region.

By simply adding the astronomical high water and the maximum wind set up, the model developed above excludes phase shifts and interactions between the two phenomena. The effect of possible phase shifts will be studied next by treating the wind set up and the astronomical tide as independent functions of time.

The properties of the wind set up as a function of time have been studied by subtracting the astronomical tide from the still water level variations recorded during 38 selected storms in the period 1921-1970. It turned out that the variation of the wind set up with time could be roughly approximated by:

$$s(t) = s_m \cos^2\left(\frac{\pi t}{D}\right) \quad (4)$$

for $0 \leq t \leq D$

where:

s_m = the maximum wind set up during the storm
 D = the duration of the wind set up

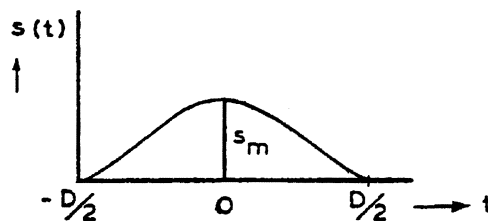


Figure II-59 The wind set up as a function of time.

In this study it was found that the probability of exceedance of the maximum wind set up during a storm, after correction for the Delta works, can be given by:

$$P(s_m > s) = e^{\frac{1.53 - s}{0.3026}} \quad [s] = m \quad (5)$$

As already shown by Van Dantzig (1960) the probability of exceedance curve of wind set up is parallel to the probability of exceedance curve of storm surge level (compare eqs. 1 and 5).

The duration of the wind set up of the 38 storms is found to be log-normally distributed.

$$p(D) = \frac{1}{D \ln(1.4) \sqrt{2\pi}} e^{-\frac{1}{2} \left(\frac{\ln(D) - \ln(51.3)}{\ln(1.4)} \right)^2} \quad [D] = hrs \quad 1) \quad (6)$$

Although Rijkooort (1960) proves a positive correlation between the maximum wind speed and the duration of a storm, the wind set up data show virtually no correlation between the maximum and the duration of the wind set up ($r_{s_m, D}^2 = 0.02$). Therefore it is assumed, that these two parameters are stochastically independent.

1) This notation is used in contrast to that in other parts of these lecture notes

The astronomical tide is caused by the gravity forces of the celestial bodies. Thus, the astronomical tide has no causal relation with the wind set up. In this study the astronomical tide is modelled as a periodical fluctuation of the water level \underline{h} with a period $T_o = 12.4$ hrs, and with a Gaussian distributed random amplitude (\underline{h}_{HW}). This randomness embodies the daily inequalities. The mean and standard deviation of \underline{h}_{HW} are given by:

$$E\{\underline{h}_{HW}\} = 1.480 \text{ m} \quad \sigma\{\underline{h}_{HW}\} = 0.195 \text{ m}$$

In addition the low water level amplitude \underline{h}_{LW} is found to be linearly dependent on \underline{h}_{HW} :

$$\underline{h}_{LW} = 0.897 \underline{h}_{HW} - 0.22 \quad [h] = m \quad (7)$$

A storm surge is now represented as a linear superposition of a random wind set up and a random astronomical tide, whose maxima occur at a random time shift $\underline{\phi}$ with respect to the maximum of the wind set up (see Figure II-60).

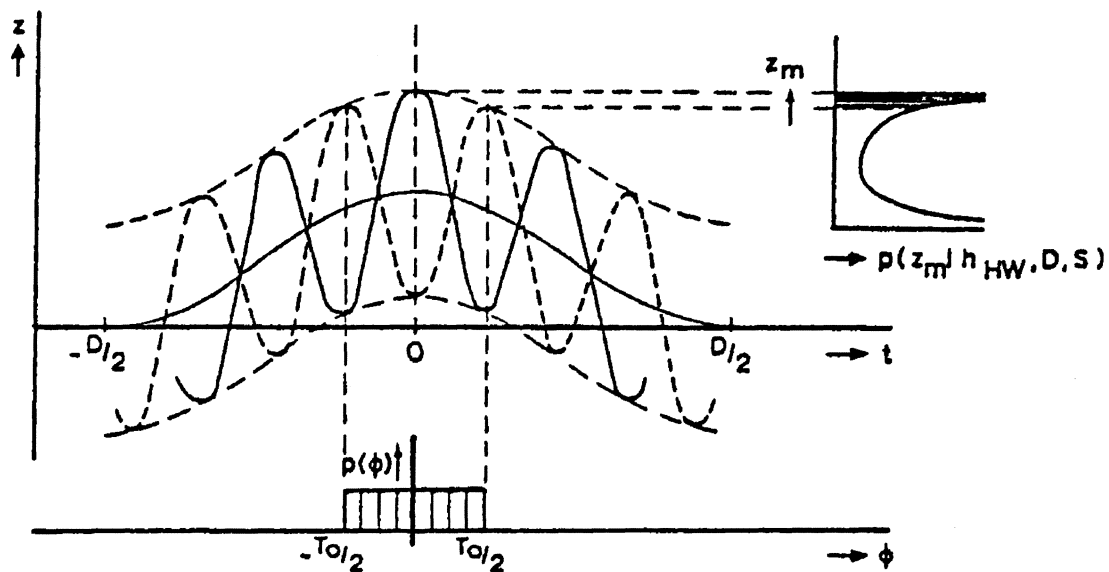


Figure II-60 A storm surge level as a linear superposition of wind set up and tidal fluctuation

$$z(t) = \underline{h}(t) + \underline{s}(t) \quad (8)$$

where:

- $\underline{z}(t)$ = storm surge level in reference to NAP
- $\underline{h}(t)$ = astronomical tide in reference to NAP
- $\underline{s}(t)$ is given in equation 4

$$\underline{h}(t) = \frac{\underline{h}_{HW} - \underline{h}_{LW}}{2} \sin\left(\frac{2\pi}{T_o}\right) (t + \phi) + \frac{\underline{h}_{HW} + \underline{h}_{LW}}{2} \quad (9)$$

As a consequence of the assumed independence of astronomical tide and wind set up in all aspects, the time shift between them has a uniform probability density function. For symmetry reasons, time shifts of T_o hrs or more are irrelevant, so the probability density function of ϕ becomes (see Figure II-60):

$$\begin{aligned}
p(\phi) &= 0 \quad \text{for } |\phi| > \frac{1}{2}T_o \\
p(\phi) &= \frac{1}{T_o} \quad \text{for } |\phi| \leq \frac{1}{2}T_o
\end{aligned}
\tag{10}$$

Moreover it follows that, ϕ , h_{HW} , D and s_m are stochastically independent of each other.

The wind set up has a duration, which is much larger than the period of the astronomical tide. Therefore the maximum storm surge level z must occur at or very near astronomical high water. For given values of h_{HW} , D and s_m the maximum storm surge level is given by:

$$z_m(\phi|h_{HW}, D, s_m) = h_{HW} + s_m \cos^2\left(\frac{\pi\phi}{D}\right)
\tag{11}$$

Using the relation

$$p(z_m|h_{HW}, D, s_m) = p(\phi|h_{HW}, D, s_m) \left| \frac{\partial z_m}{\partial \phi} \right|^{-1} = p(\phi) \left| \frac{\partial z_m}{\partial \phi} \right|^{-1}
\tag{12}$$

and the expression (10) for $p(\phi)$, the conditional probability density function of z_m can be calculated with the result

$$p(z_m|h_{HW}, D, s_m) = \frac{D}{\pi T_o s_m} \left[\frac{z_m - h_{HW}}{s} - \left(\frac{z_m - h_{HW}}{s} \right)^2 \right]^{\frac{1}{2}}
\tag{13}$$

for z_m in the range:

$$h_{HW} + s_m \cos^2\left(\frac{\pi T_o}{2 D}\right) \leq z_m \leq h_{HW} + s_m
\tag{14}$$

The marginal probability density function of z_m then follows from

$$p(z_m) = \iiint p(z_m|h_{HW}, D, s_m) p(h_{HW}, D, s_m) dh_{HW} dD ds_m
\tag{15}$$

or in view of the independence of h_{HW} , D and s_m

$$p(z_m) = \iiint p(z_m|h_{HW}, D, s_m) p(h_{HW}) p(D) p(s_m) dh_{HW} dD ds_m
\tag{16}$$

Numerical values of $p(z_m)$ have been obtained by substitution of the respective probability density functions into the right hand side of eq. (16). The corresponding cumulative probability distribution has been plotted in Figure II-61 together with the curve published by the Delta committee (1960).

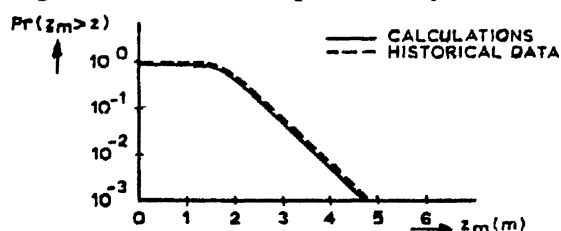


Figure II-61 The comparison of the calculated and the observed exceedance curve of the maximum storm surge level.

The close resemblance of the curves supports the accuracy of the developed model. The model will next be used to calculate the low water level.

II.9.2.3. THE LOW WATER LEVEL

The closing strategy of the barrier greatly influences the basin level. In the design period a closing strategy was assumed that would cause the lowest basin level, as this basin level will yield the largest static load on the barrier. According to this strategy the barrier will be closed at the low water, preceding the first relative storm surge level maximum, which is expected to surpass a certain threshold level (see Figure II-62).

To find the set of low waters at which the barrier will be closed to protect the hinterland against a storm surge, the model, developed in the preceding paragraph, proves valuable.

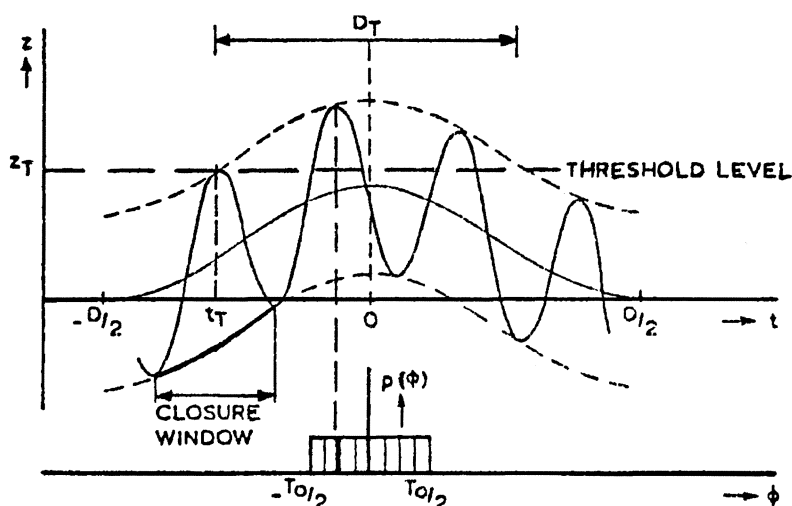


Figure II-62 The set of closure moments for a given threshold level.

Studying the model it is clear, that the earliest possible moment at which the threshold level (z_T) can be surpassed by a storm surge, occurs at time $t = t_T$ such that:

$$z_T = h_{HW} + s_m \cos^2\left(\frac{\pi t_T}{D}\right) \quad (17)$$

For reasons of symmetry the threshold level (z_T) can be exceeded in the interval $-t_T < t < t_T$ only. This interval has the duration of $D_T = 2 t_T$.

The earliest possible closure of the barrier occurs when the high water at t_T just exceeds the threshold level z_T . The barrier is then shut at the preceding low water:

$$t_{close} = t_T - \frac{T_o}{2}$$

The latest closure occurs when the high water at t_T just not reaches z_T . Now the barrier will be closed at the next low water:

$$t_{close} = t_T + \frac{T_o}{2}$$

So for the given closing strategy the closure takes place in the interval:

$$t_T - \frac{T_o}{2} < t_{close} < t_T + \frac{T_o}{2} \quad (18)$$

As this paragraph aims at finding the two dimensional probability function of the basin level and the maximum storm surge level, a relation has to be established between these two parameters.

Figure II-63 The relation between the maximum storm surge level and the low water level at closing.

For given values of ϕ , h_{HW} , s_m and D the maximum storm surge level is calculated by eq. 11. The closing moment for this particular storm surge (see Figure II-63) can be found by straightforward mathematics, which will not be explicated here.

The low water level at which the closing operation starts is

$$z_{LW}(t_{close}, h_{LW}, D, s_m) = h_{LW} + s_m \cos^2\left(\frac{\pi t_{close}}{D}\right) \quad (19)$$

Using the relations (7), (11) and (19), the two dimensional probability density function of maximum storm surge level and low water level can now be evaluated numerically by:

$$p(z_m, z_{LW}) dz_m \cdot dz_{LW} = \int \int \int p(\phi) p(h_{HW}) p(s) p(D) J d\phi dh_{HW} ds dD \quad (20)$$

where J is the Jacobian of the transformation. The result is given in Figure II-64.

Figure II-64 The two dimensional probability density function of maximum storm surge level and low water level at closing.

II.9.2.4. EMPIRICAL EVIDENCE

The integration of the derived two dimensional probability density function of the maximum storm surge level and the low water level with respect to the maximum storm surge level above the threshold level z_T gives the set of low waters at which the barrier will be closed. The probability density function is given by

$$p(z_{LW}) = \int_{z_T}^{\infty} p(z_m, z_{LW}) dz_m \quad (21)$$

The probability density function of z_{LW} at closing can also be found by applying the decision rule as mentioned above on historical data of the period 1957-1976 (17 storms; $z_m \geq \text{NAP} + 2.75 \text{ m}$; $z_T = \text{NAP} + 2.75 \text{ m}$). The result of both methods is given in Figure II-65. The close resemblance of the probability density functions supports the accuracy of the developed model.

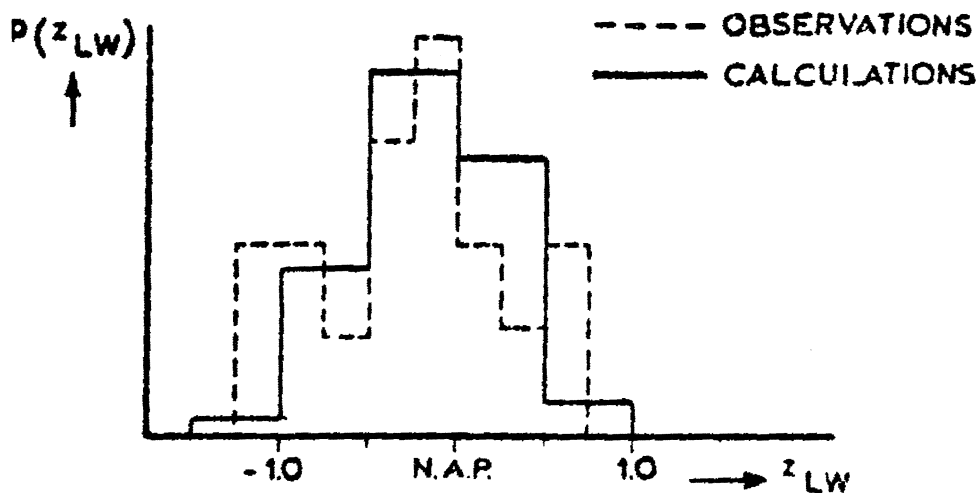


Figure II-65 The probability density function of z_{LW} from observation and model for $z_T = 2.75 \text{ m}$ above NAP

II.9.2.5. THE TRANSFORMATION OF THE LOW WATER LEVELS INTO BASIN LEVELS

In the preceding section the two dimensional probability density function of maximum storm surge level and low water at sea has been determined. However, for the load calculations the basin level at the inward side of the barrier is important. The two dimensional probability density function of maximum storm surge level and basin level can be obtained by transforming the results of eq. 20. The transformation has to take into account five effects that influence the basin level.

1. Reduction of the tidal amplitude in the Oosterschelde due to the resistance of the barrier in opened position.
2. The basin oscillations induced by the sudden closing of the barrier.
3. Wind set down on the Oosterschelde caused by the North Westerly storm.
4. Leakage through the barrier and the sill.
5. wave overtopping of the barrier during the storm surge.

The first three effects influencing the basin level have been incorporated in the model as constants.

The slow filling of the basin by leakage through the barrier and the sill is evaluated for every storm taking into account the time path of the storm surge level starting at the moment of closing until the peak level is reached and the rising basin level.

The wave overtopping is calculated as a function of the storm surge level and the wave height using a simple model.

The result is a realistic approach of the joint probability of occurrence of maximum storm surge level and coinciding basin levels. However, for the load calculation the last two, effects, leakage and wave overtopping, have been discarded for safety reasons, because they raise the basin level and reduce the static load.

II.9.3. THE SURGE LEVELS AND WAVE ENERGY

II.9.3.1. INTRODUCTION

In this chapter the second part of the three dimensional probability density function of hydraulic boundary conditions will be developed, viz. the two dimensional probability density function of maximum storm surge level and wave energy. Due to the complexity of the bar and trough pattern in the mouth of the Oosterschelde and the very restricted available research time it was only possible to use simple models.

First a hypothesis will be formulated on the general relations between wind velocities, the storm surge level and the wave energy on the North Sea and the Oosterschelde. The hypothesis also gives a clue to the typical form of the wave spectrum on the Oosterschelde. Next the part of the hypothesis that relates the wave spectrum near the barrier to the local wind speed, the storm surge level and the wave spectrum on the North Sea is put in a mathematical form. The mathematical model is tested in the hindcast of several storm surges.

Finally the model is expanded with a section that describes the processes on the North Sea. The part that deals with the storm surge level as a result of wind set up and astronomical tide is taken from the preceding chapter. A part is added, which relates the wave energy on the North Sea and the local wind speed at the Oosterschelde to the wind field of the storm. Now concentrating on the maximum storm surge level, the expanded model is tested on historical data. Being in good agreement the last step is made and the two dimensional probability density function of maximum storm surge level and wave energy is evaluated .

II.9.3.2. FOUNDATIONS OF THE MODEL

The projected barrier is situated in the mouth of the Oosterschelde estuary, separated from open sea by a complex of shoals (see Figure II-66).

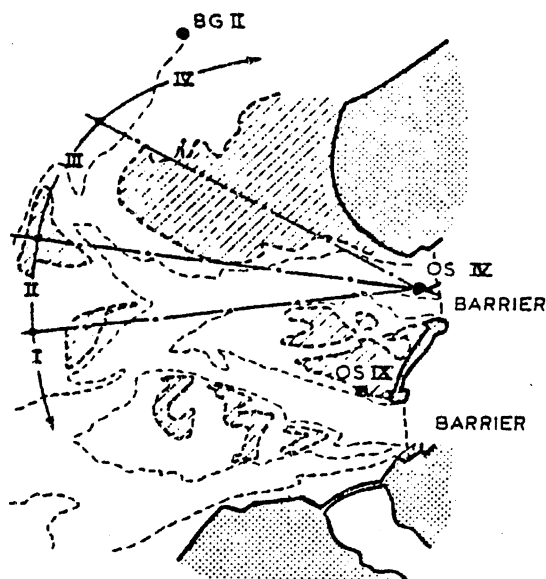


Figure II-66 Sketch of the mouth of the Oosterschelde and the situation of the wave stations BG II, OS IV and OS IX.

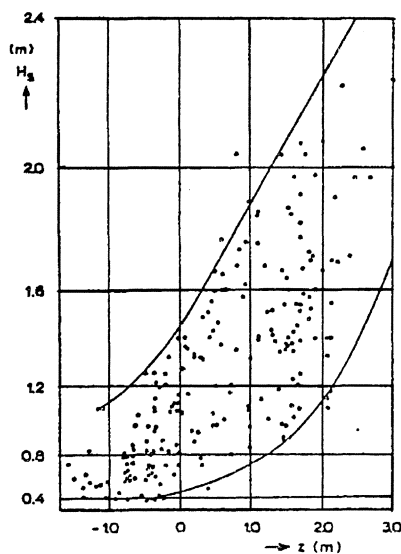


Figure II-67 The relation between the storm surge level and the significant wave height (H_s) at station OS IV.

The idea arises, that wave height near the barrier site during storm surges will be governed by the phenomenon of wave breaking over the shoals. In this case the observed wave height should be a function of the water depth above the shoals. However, if the significant wave heights observed during storm surges are plotted against the water level, the correlation is not very good (see Figure II-67).

Also the local wind speed cannot explain the significant wave height near the barrier site (see Figure II-68).

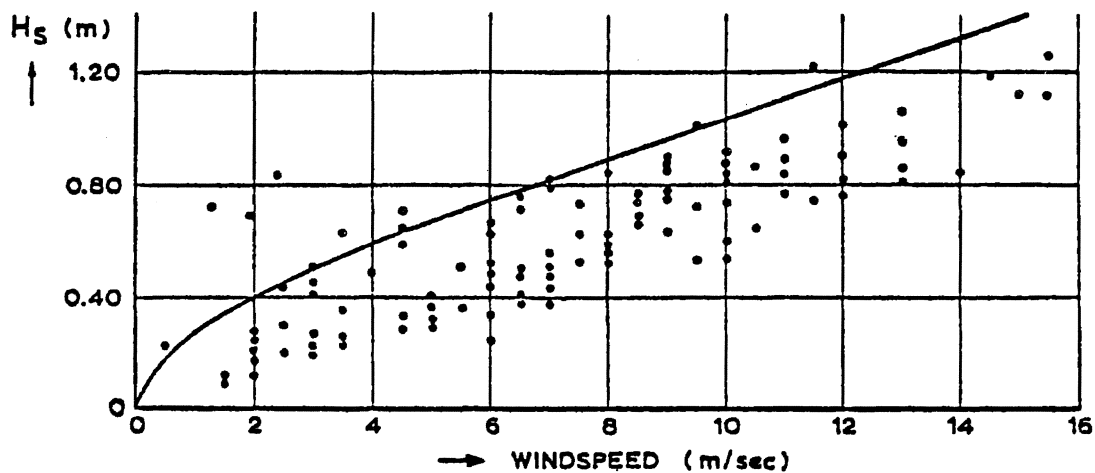


Figure II-68 The relation between local windspeed and significant wave height H_s at location OS IV.

Analyses of wave energy spectra at stations OS IV and OS IX showed, that these were generally double-peaked during storm surges. Taken together, the analyses referred to above suggested the assumption, that the wave energy near the barrier originates from two sources:

1. Wave energy from the wave field in open sea (low frequency) penetrates, after breaking on the shoals, in the mouth of the Oosterschelde.
2. Local wind fields generate wave energy (high frequency) above the shoals.

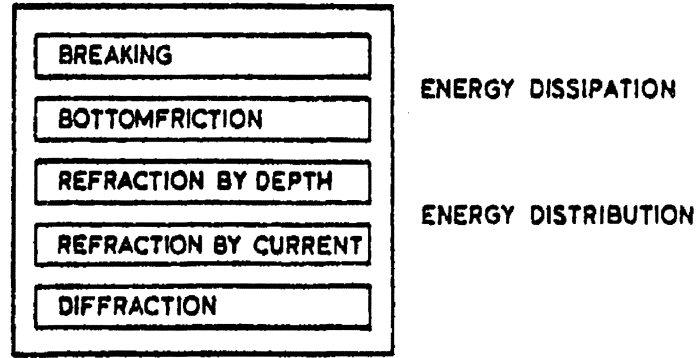
A schematic diagram showing this idea has already been given in Figure II-58.

A central role is played by the wind fields above the North Sea. The wind set up and the wave growth on deep water are both effects of the wind fields of the cyclone. Further there is a loose correlation between the general intensity of the cyclone and the force of the local wind field above the Oosterschelde. The model indicates, that the wave height on the Oosterschelde and the storm surge level should be correlated, as the processes of wind set up and wave growth have roughly the same time lag and the waves have to pass the filter "shoals" that is opened by the water level. The only factor that disturbs the pure correlation seems to be the local wind field. To develop and verify these ideas, a mathematical model has been formulated that calculates from the input data (wave spectrum at sea, the water level in the estuary and the local wind speed) the wave spectrum near the barrier site. The results of these calculation have been checked against measurements of recent storms.

II.9.3.3. THE MATHEMATICAL WAVE MODEL OF THE OOSTERSCHELDE

The above mentioned ideas have been translated into mathematical formulae. For the wind set up the model developed by Weenink (1958) as shown in ch.II.9.2. has been used and for the wave growth the model of Sanders (1976) was employed.

However, for the parts of the model that directly govern the wave height in the estuary, only theories are available, which describe the various sub processes, such as shown in Figure II-69.



Figur II-69 Building blocks of the filter "shoals".

All these processes together form the filter properties of the "shoals", but an overall description is not known. Also the process of wave generation by local wind fields in the presence of broken waves is unclear. After a study of the map of the shoals it was decided to divide the filter in 4 sectors with different properties (see Figure II-66). Every sector is simplified to a schematized bottom profile, that shows only significant changes in depth (see Figure II-70).

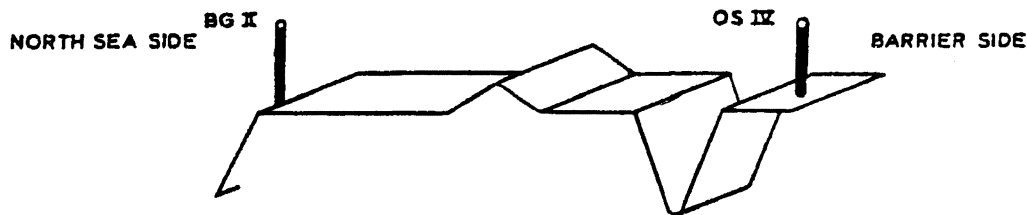


Figure II-70 The schematized bottom profile of sector IV (see Figure II-68).

It is first assumed that the wave energy from the North Sea propagates via the shoals to the barrier without a change of direction. The sector that contains the propagation direction is chosen for the calculation of the energy-loss of the waves. The irregular wave field at sea will be represented by a regular sine wave with an amplitude and period equal to:

$$a = \frac{1}{2} H_{s_{sea}} \quad (22)$$

$$T = T_{z_{sea}} \quad (23)$$

The propagation of this wave through water of changing depth is described by the well known energy balance equation. By including energy dissipation by bottom friction the equation can be written as:

$$\frac{\partial P}{\partial S} + \varepsilon = 0 \quad (24)$$

where P is the energy flux per unit length:

$$P = Enc = \frac{1}{2} \rho g a^2 n c \quad (25)$$

in which:

$$n c = \frac{1}{2} \left(1 + \frac{2 k d}{\sinh(2kd)} \right) \frac{\sigma}{k} \quad (26)$$

$$\sigma = \sqrt{g k \tanh(kd)} \quad (27)$$

For the energy loss in the turbulent boundary layer at the bottom Bretschneider and Reid (1954) proposed

$$\varepsilon = \frac{4 \cdot 10^{-2}}{3 \pi} \rho \left(\frac{\sigma a}{\sin(kd)} \right)^3 \quad (28)$$

Besides by bottom friction, energy loss is also caused by breaking, when the maximum steepness is exceeded. For periodic waves of constant form the criterion of Miche is valid:

$$a_{\max} = \frac{\beta}{k} \tanh(kd) \quad (29)$$

where $\beta = 0.14\pi$.

However if an irregular wave field is schematized to a regular wave as described above, we observed that the coefficient β can be better approximated by 0.093π (v.Marle, 1979).

If at any point the calculated wave amplitude exceeds this breaker criterion, it is assumed to be reduced to the maximum value given by (29).

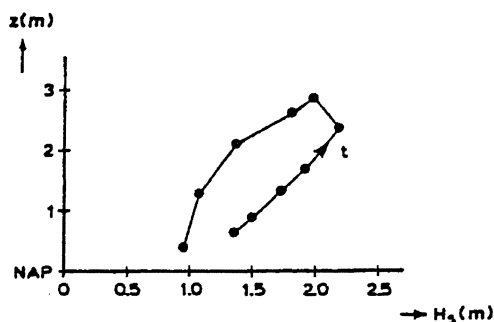


Figure II-71 The significant wave height near the barrier as a function of the storm surge level and time for the April 1973 storm.

Observations show however that the time history of H_s vs. z for any surge shows a hysteresis effect. A typical example during a storm situation has been given in Figure II-71. A possible explanation would be the influence of the tidal current. Using the linear theory Battjes (1977) showed that the refraction of the waves by the tidal current gives an effect which is of the same magnitude. In this paper the complex formalism of refraction by current is modelled by a simple linear relation between the breaker height and the velocity of the current v in the main gully.

$$a \leq a_{\max} (1 + 0.15v) \quad [a] = m; \quad [v] = m/s \quad (31)$$

So far the influence of refraction by depth and diffraction on the energy propagation is neglected. Refraction-diffraction calculations were carried out separately for different water levels and different wave directions. The results of these calculations were incorporated in the simple model in the form of coefficients, partly depending on the water level.

Sector	REFRACTION COEFFICIENT
I	$0.75 + 0.10z$
II	$0.50 + 0.16z$
III	0.90
IV	0.75

N.B. The coefficients maximum value is 1.0.

Now it is possible to calculate for a sector the amount of wave energy, which penetrates from the North Sea via the shoals in the Oosterschelde. As noted before, it appeared from measurements that the wave spectra near the barrier in general show two peaks. Within statistical accuracy the low frequency peak of the Oosterschelde wave spectra is always at the peak frequency of the North Sea wave spectrum. ($f_p \approx 0.1$ Hz). This fact combined with a fit through spectral data led to the following parametrization of the spectral form for the energy penetrating from the North Sea (see Figure II-72).

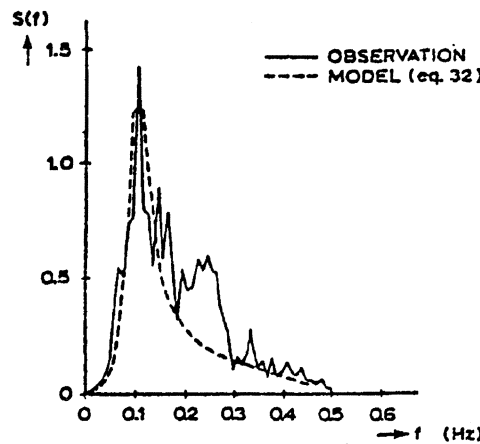


Figure II-72 The spectral form for the energy penetrating from the North Sea.

$$\begin{aligned}
 S(f) &= \gamma f_p^{-6.5} f^4 & \text{for } f < f_p \\
 S(f) &= \gamma f^{-2.5} & \text{for } f \geq f_p
 \end{aligned}
 \tag{32}$$

By equating the calculated wave energy and the spectral area for given f_p , the coefficient γ is solved. The second peak in the wave spectra is strongly correlated with the local wind speed and not due to the non-linear breaking effect. In the calculations so far attention was given only to the energy loss of the waves during their propagation over the shoals. Apparently the energy addition by local wind fields must be taken into account. For simplicity it is assumed that the wave growth process starts with the spectrum calculated above, and that it takes place from the windward edge of the shoals to the barrier site, over a fetch written as F_0 . Further the JONSWAP (1973) growth-curves will be applied to add the local wave generation to the calculated spectrum. From the calculated spectrum the energy density for a frequency f^* is determined. Now a fictitious fetch, that is the fetch that should be necessary to generate an energy density $S(f^*)$ at the prevailing wind speed, is calculated from the JONSWAP growth-curve. The total non-dimensional fetch (F) is found by adding the fetch available after breaking F_0 to the fictitious fetch (see Figure II-73).

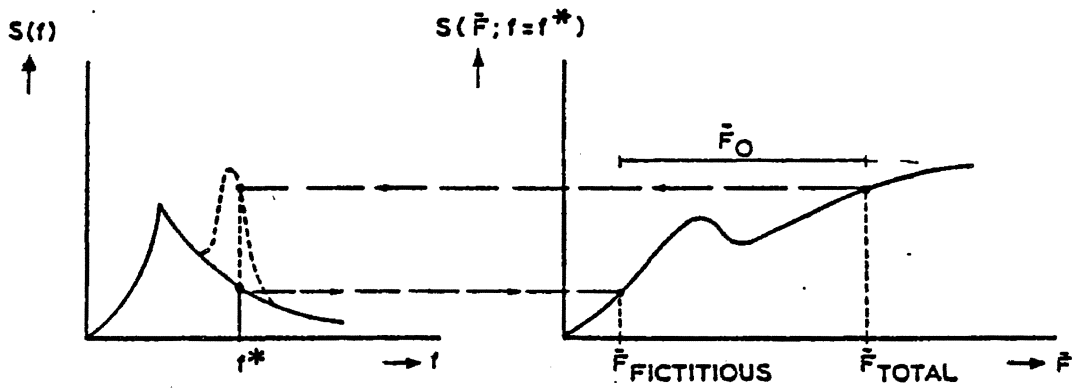


Figure II-73 Calculation of wave spectra by adding local wave generation to waves coming from the North Sea and propagating over the shoals. The figure on the righthand side gives the JONSWAP growth-curve for a given frequency f^* as function of the non-dimensional fetch.

Substituting this total fetch in the JONSWAP growth-curve for a given frequency f^* the total energy density (being the result of penetration and local generation) is evaluated. By repeating this procedure for all frequencies, the high frequency peak of the wave spectrum that is generated by the local windfields, is found.

II.9.3.4. EMPIRICAL EVIDENCE

The simple model described in the preceding paragraph is tested in a hindcast of several recent storms. During these storms hourly observations have been made of wind speed, water level and wave spectrum in the Oosterschelde. Simultaneously the wave spectra at sea (5 miles from the coast) have been measured. Using these data as input, the model predicts the wave spectra in the Oosterschelde reasonably well (see Figures II-74,75). The significant wave height is predicted with an accuracy of 10% .

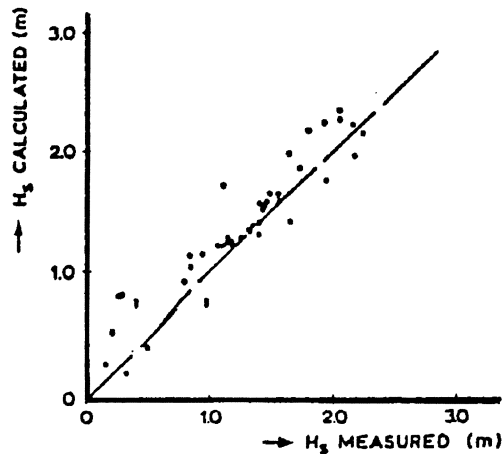


Figure II-74 Comparison of observed and hindcasted significant wave heights at the barrier site (OS IV, OS IX).

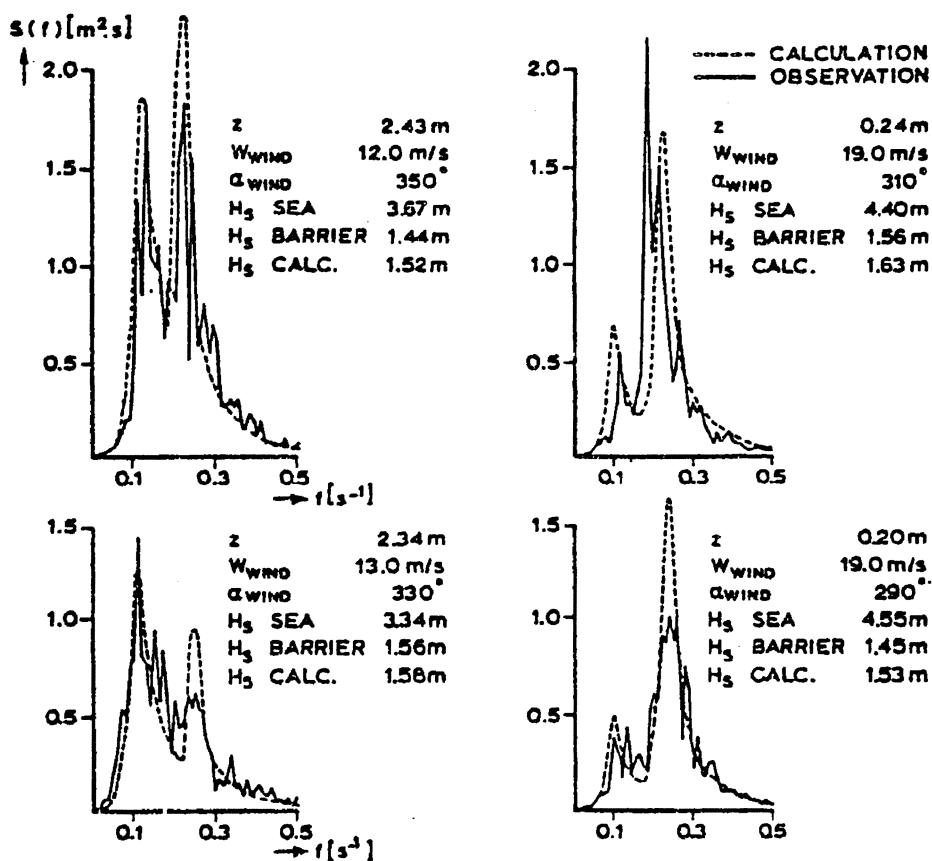


Figure II-75 Comparison of observed and calculated wave spectra at the barrier site.

II.9.3.5. WAVE DIRECTION

The wave load on the barrier depends on the direction of the waves. At the design stage no technique was available to obtain the directional wave spectra. A number of methods have been used to get information about the main wave direction. Calling to mind that the wave energy near the barrier originates from two sources, one can distinguish two main wave directions:

- a) local wind fields generate wave energy (high frequency) above the shoals. The main direction of these waves is the same as the local wind direction.
- b) Wave energy (low frequency) coming from open sea and propagating over the shoals. Here aspects as refraction by depth and current govern the wave directions.

Various visual observations performed during storm situations confirm this hypothesis. However, as the low frequency wave energy is mainly responsible for the wave load on the barrier, all wave energy is reckoned to have the direction of the low frequency part.

Four different methods have been used to get an idea of the main direction and the short crestedness of the low frequency wave energy. With a helicopter flying at varying altitudes visual observations have been made. Further the main direction of the long period wave energy was found by heading a survey vessel to the sea. In addition stereo- and mono-photography have been performed by plane. The photographs were analysed by eye. All these methods were compared in different storms. The results are in good agreement with each other. With these methods the main wave direction is estimated with an accuracy of about 10 degrees.

By visual observation it also appeared that the length of the wave crests near the barrier was about the same as at the open sea. Therefore the same directional distribution of the wave energy was assumed near the barrier. At sea usually a $\cos^2\phi$ distribution is assumed, where ϕ is the angle with the main wave direction.

As only a small amount of storm data were available, an extrapolation of the main wave direction to extreme circumstances was impossible. Therefore a mathematical model (Radder, 1979) was used describing refraction and diffraction. It is based on the parabolic wave equation, derived from the Helmholtz equation using a parabolic approximation. This method described the propagation of regular long crested waves. Although linear wave theory is being used two non-linear effects have been built in:

- a) a non-linear dispersion relation (see eq.27)
- b) the Miche breaking condition (see eq.29).

All other effects are neglected. The results of the model have been compared with the aerial photographs and visual observations in the Oosterschelde. Being in good agreement calculations have been performed for extreme circumstances.

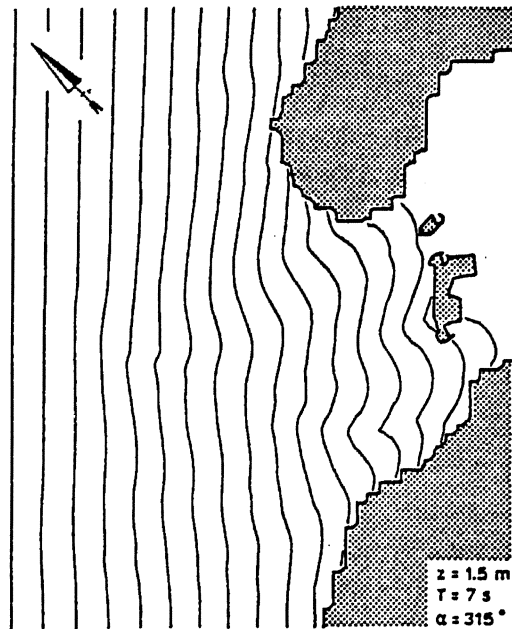


Figure II-76 Wave crests for incoming waves from North West with a wave period of 7 seconds calculated with the refraction-diffraction model of Radder.

An example of a calculation has been given in Figure II-76. It shows the wave crests for incoming waves from North West. The main wave direction is assumed to be perpendicular to the wave crests.

II.9.3.6. THE PROCESSES ON THE NORTH SEA

The wave model described in the previous sections requires the wave conditions on the seaward edge of the Oosterschelde delta, the storm surge level and the local wind speed as input.

As already shown in the introduction to this chapter a general role in the hypothetical relationship between these phenomena is played by the wind fields of the cyclone. Because reliable statistics of total wind fields on the North Sea are difficult to get, a reversed procedure is followed. Using the models from the first chapter, that relate the maximum storm surge level to the wind speed and the astronomical tide, the two dimensional probability density function of maximum storm surge level and the wind speed uninterruptedly exceeded during 9-hours can be approximated. Taking only North Westerly storm directions into account the following formulation is found.

If $\underline{s} = \underline{s}_m$, $\underline{w} = \underline{w}_9$, $\underline{z} = \underline{z}_m$ and $\underline{h} = \underline{h}_{HW}$, then using eq.2, eq.8 can be rewritten as:

$$\underline{z} = \underline{h} + 3.7 * 10^{-2} \frac{w^2}{g} \quad (33)$$

In view of the independence of \underline{h} and \underline{s} the following expression for the probability density function of storm surge level and wind speed may be obtained:

$$p(w,z) = p(h,s) \begin{vmatrix} \frac{\partial h}{\partial w} & \frac{\partial h}{\partial z} \\ \frac{\partial s}{\partial w} & \frac{\partial s}{\partial z} \end{vmatrix} = p(h,s) \left| \frac{\partial s}{\partial w} \right| \quad (34)$$

$$p(w|z) = \frac{p(w,z)}{p(z)} = \frac{p(h) p(s)}{p(z)} \left| \frac{\partial s}{\partial w} \right|$$

If this result is combined with a theory of wave growth on water of limited depth, the two dimensional probability density function of wind speed and storm surge level is transformed into the two dimensional probability density function of maximum storm surge level and significant wave height at the seaward border of the Oosterschelde.

An exact knowledge of the wave height at the seaward border of the Oosterschelde is of minor interest, as the introduction of the approximate breaker criterion for the shoals of the Oosterschelde shows, that nearly all wave fields generated on the North Sea during North Westerly storms will break on the shoals (see Figure II-80). Therefore the wave height at sea will not influence the energy penetrating in the Oosterschelde. The maximum storm surge level is the only parameter governing the penetration.

A very important parameter in the wave load calculation is the spectral peak period of the penetrating wave energy. This peak period, being equal to the peak period of the wave spectrum at the seaward border of the Oosterschelde, is restricted by the limited depth of the Southern part of the North Sea. For North Westerly storms, data as well as the wave growth model of Sanders give a saturation peak period of 11.5 s at the seaward border of the Oosterschelde. In the load calculations this peak period has been held constant as a safe estimate (Mulder and Vrijling 1980). The second source of wave energy near the barrier is related to the local wind speed. To complete the model, the relation between the local wind speed and the wind fields at sea characterised by w_9 must be established. Studies of the wind speed during a storm as a function of time (Rijkoort, 1960) show a result, which can be expressed as:

$$k = 26.8 \left(\frac{w_m}{w_k} - 1 \right)^{0.83} \quad (35)$$

where:

- k = number of hours during which the one hour average wind speed exceeds w_k without interruption (Figure II-77)
- w_m = maximum one hour average wind speed.

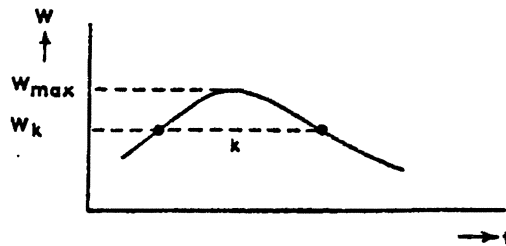


Figure II-77 The windspeed during a storm.

According to Weenink (1958) a time lag τ between the maximum one hour average wind speed and the maximum wind set up in the Southern North Sea amounts to 6 hours on the average. Knowing that the time shift ϕ between the astronomical tide and the wind set up has a uniform probability density function (eq. 10) a conclusion can be drawn concerning the wind speed accompanying the maximum storm surge level (see Figure II-78). The moment of the maximum storm surge level is within $\pm T_o/2$ of the moment of the maximum wind set up or approximately anywhere from the time of maximum wind speed $t=12$ hrs to 12 hrs later, since $T_o/2 \approx \tau \approx 6$ hrs.

As the wind speed is an approximately linear, decreasing function of time over this interval, while ϕ has a uniform probability density, a uniform distribution of wind speeds may be assumed. The maximum

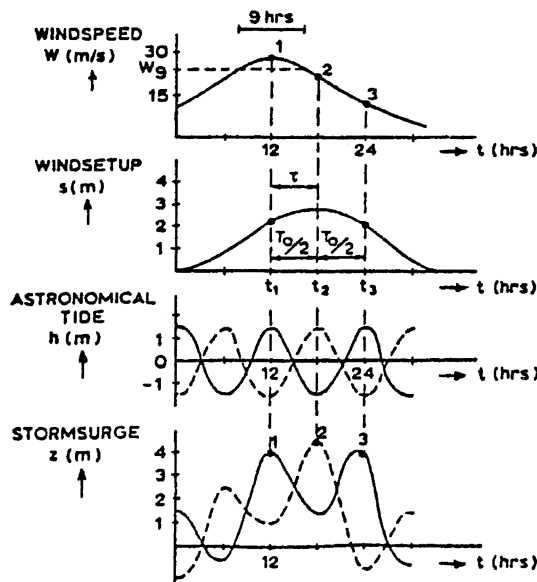


Figure II-78 The relation between the maximum storm surge level and the accompanying windspeed.

and minimum possible wind speeds, for given value of w_o , have to be derived by means of eq. 35, using $k = 9$ hrs and $k = t_3 - t_1 = 24$ hrs respectively, which gives:

$$\begin{aligned} w_{\max} &= 1.27 w_9 \\ w_{\min} &= 0.68 w_9 \end{aligned} \quad (36)$$

so that:

$$\begin{aligned} p(w|w_9) &= 0 \quad \text{for } w < w_{\min} \text{ or } w > w_{\max} \\ p(w|w_9) &= \frac{1}{0.59 w_9} \quad \text{for } w_{\min} \leq w \leq w_{\max} \end{aligned} \quad (37)$$

Having already evaluated the two dimensional conditional probability density function of w_9 and z_m (see eq.34), the conditional probability density function of the maximum storm surge level and the local wind speed coinciding with maximum storm surge level, given a maximum storm surge level, is calculated by:

$$p(w|z_m) = \int_0^{\infty} p(w|w_9) p(w_9|z) dw_9 \quad (38)$$

The local wind speed w accompanying the maximum storm surge level z_m governs the local wave growth at the Oosterschelde.

II.9.3.7. EMPIRICAL EVIDENCE

In the preceding paragraph two conditional probability density functions have been established (eqs 34 and 38). Moreover, combining eq. 34 with the theory of wave growth on water of limited depth a relation between the maximum storm surge level and the significant wave height has been obtained (Figure II-79).

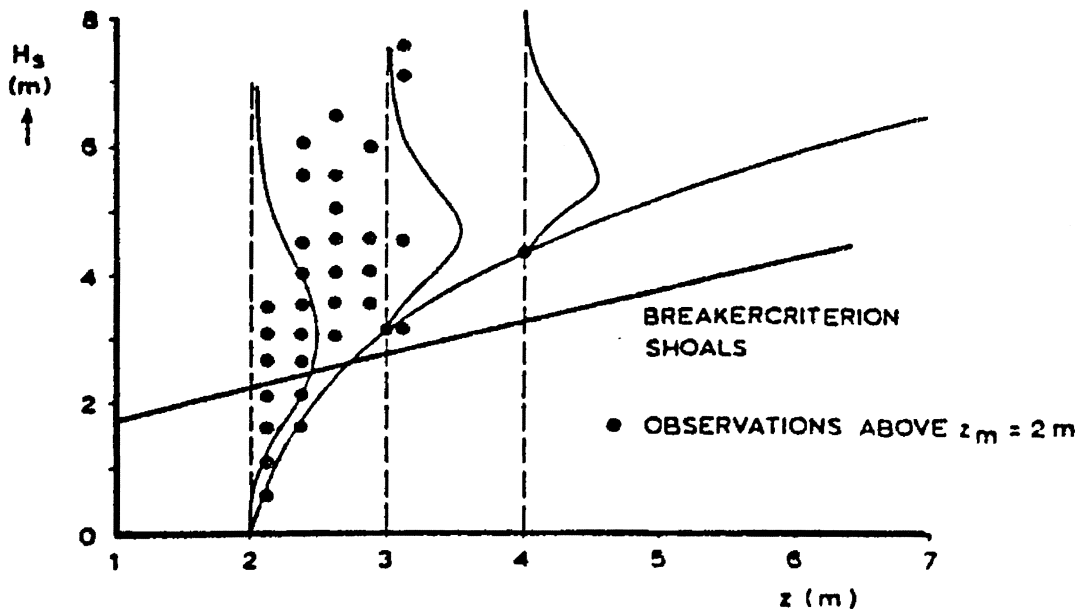


Figure II-79 The relation between the maximum storm surge level and the significant wave height on the seaward edge of the shoals. The conditional probability density function of H_s has been given for $z = 2\text{m}, 3\text{m}$ and 4m .

The historical data are certainly not in contradiction with the theoretical result, but conclusions on the extrapolation cannot be drawn on the basis of this empirical material. The theoretical relation between the maximum storm surge level and the local wind speed (eq.38) is compared with historical data in Figure II-80.

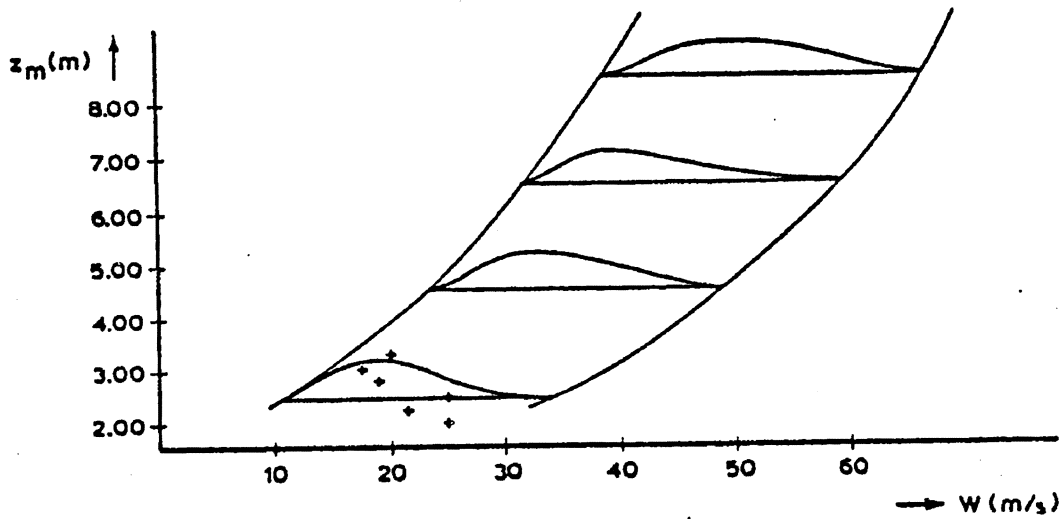


Figure II-80 The relation between the maximum storm surge level and the local wind speed.

Here too agreement is seen between theory and empirical material. The set of data however is far too small to be a reliable base for extrapolation.

II.9.3.8. THE COMPLETED MODEL

In the preceding paragraphs of this chapter two mathematical models have been developed and tested. The first model calculates the wave spectrum near the barrier given the seastate at the North Sea, the storm surge level and the local wind speed. The second model evaluates the joint probability density function of the maximum storm surge level, the seastate at the North Sea and the local wind speed.

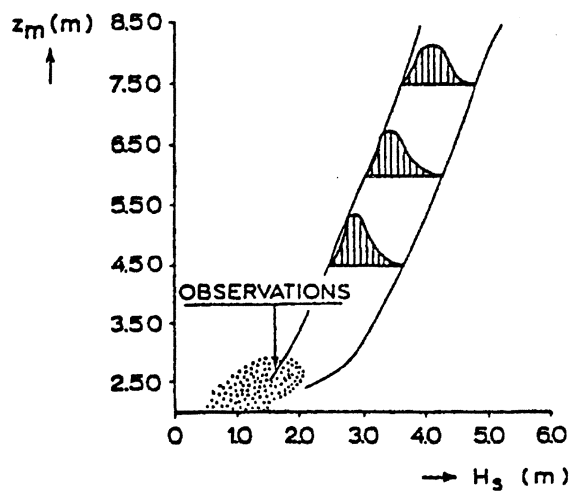


Figure II-81 The relation between the maximum storm surge level and the significant wave height. In the figure the conditional probability density function of H_s for a number of storm surge levels has been given.

As the aim of this paper is the prediction of the future boundary conditions for the barrier, an estimate of the future geometry of the shoals in the mouth of the Oosterschelde (Figure II-66) has to be incorporated in the first model. If it is further realised that the barrier will be maximally loaded during the maximum storm surge level, because the difference between sea level and basin level and the amount of low frequency wave energy penetrating from the North Sea are then both maximal, the models can be joined by introducing the restriction to maximum storm surge levels.

Thus the three dimensional probability density function generated by the second model under the assumption of North Westerly wind direction is used as input for the first model. The result is the conditional probability density function of maximum storm surge level and local wind speed (Figure II-80), where for every combination the wave spectrum near the barrier is known (Figure II-81).

II.9.4. THE THREE DIMENSIONAL PROBABILITY DENSITY FUNCTION OF MAXIMUM STORM SURGE LEVEL, WAVE ENERGY AND BASIN LEVEL.

The aim of this paper was to find the three dimensional probability density function of maximum storm surge level, wave energy and basin level. The result of the work done in ch. II.9.2. is the two dimensional probability function of maximum storm surge level and basin level, written as $p(z_m, b)$. The conditional probability density function of the maximum storm surge level and the local wind speed, where in each point the wave spectrum is known, was evaluated in the third chapter. It is written as $p(w | z_m)$. Now these two functions may be joined to the desired one if the statistical independency of basin level and local wind speed of wave spectrum can be proved.

Starting from the theoretical models it is seen that the basin level shows a very weak correlation with the maximum storm surge level. The local wind speed and the wave spectrum are correlated to the surge level, but there is no obvious reason why any correlation between wave spectra and basin levels should exist. Also, historical data from significant wave heights and low waters show virtually no correlation ($r = 0.17$). Accepting the statistical independency of the basin level and the local wind speed to be a reasonable assumption, the final step can be made, as follows:

$$p(z_m, b, w) = p(z_m, b) \cdot p(w | z_m) \quad (39)$$

where for each combination of (w, z_m) the wave spectrum at the barrier site can be calculated by the method described in ch. II.9.3. . This result has been used as input in the probabilistic load determination for the barrier (see Mulder and Vrijling 1980).

Acknowledgement

The authors are very grateful to Prof. dr. J.A. Battjes for clarifying and stimulating discussions and also to mr. L.A. Langendoen for translating the models into computer codes.

REFERENCES

Battjes, J.A., The influence of currents on waves, Internal Report (1977) (in Dutch).

Bretschneider, C.L. and Reid, R.O., 1954, Changes in wave height due to bottom friction percolation and refraction, US Army Corps of Engineers, BED, Tech. Mem. 45.

Dantzig, D.v., Extrapolation of the frequency curve of the loads at high tide at Hook of Holland by means of selected storms. Delta report, 1960.

Hasselmann, K. et al., Measurements of wind-wave growth and swell decay during the Joint North Sea Wave Project, Deutsche Hydrographische Zeitschrift, Reihe A(8 °) (1973) 12.

Marle, J.G.A. van, The breaker criterion for the mouth of the Oosterschelde, Rijkswaterstaat DDWT-79.031 (in Dutch).

Mulder, Th. and Vrijling, J.K., Probabilistic approach of load calculations, 1980 Proceedings International Symposium on Hydraulic Aspects of Coastal Structures.

Report of the Delta Committee (1960).

Rijkoort, P.J., Statistical Investigation of North Westerly storms, Delta report, 1960.

Sanders, J.W., 1976, A growth-stage scaling model for the wind-driven sea. Deutschen Hydrographische Zeitschrift, Band 29, Heft 4, pl 36.

Schalkwijk, W.F., A contribution to the study of storm surges on the Dutch coast, KNMI, Med. en Verh. B part 1, no.7, 1947.

Weenink, M.P.H., 1958, A theory and method of calculation of wind-effects on sea-levels in a partly enclosed sea, with special application to the southern coast of the North Sea. K.N.M.I., Med. en Verh. No.73.

LIST OF SYMBOLS

$h(t)$	astronomical tide
$s(t)$	wind set up
$z(t)$	water level
$b(t)$	basin level
HW	high water (h_{HW} = astronomical high water)
LW	low water (z_{LW} = low water)
z_m	maximum storm surge level
z_T	threshold water level
w	wind speed
α	wind direction
W_9	hours uninterruptedly exceeded wind speed
H_s	significant wave height
T	wave period
T_p	peak period
f	wave frequency
f_p	peak frequency (= the frequency at which the maximum variance spectral density occurs)
$\hat{S}(f)$	variance spectral density function
k	wave number
d	water depth
v	current velocity

II.10. STRENGTH

II.10.1. Some data

Quantity	type	average	spread
<u>own weight</u>	N	$1.05 * X_{nom}$	$V = 0.07$
<u>separation walls</u>	LN	0.30 Kn/m^2	$V = 0.40$
<u>floor load (inventory/people)</u> office			

II.11. METHODS OF STATISTICAL ANALYSIS

For calculations the relation between quantities is given in mathematical formulations (models). The laws can be physical, chemical, biological, econometric or sociological etc., etc.. Examples of extrapolations which were supported by models of physical laws were given in § II.5. In many cases the knowledge of the (physical) processes is insufficient for a complete description with a mathematical model. The statistical analysis of (model) tests has to offer a solution. Sometimes, the statistical analysis leads to a greater insight into the phenomenon concerned.

The relations are not always apparent from the measurements. Measurements can be widely spread, for example in the case of determination of the coefficient in Chézy's Law. The measured values of the coefficient can deviate greatly from the expected values.

The mathematical relations between physical quantities can't always be clearly indicated. Often no complete mathematical formulation (mathematical model) of the phenomena is known. The relation between the cone resistance in the ground and the increasing depth serves as an example of a partially known mathematical model.

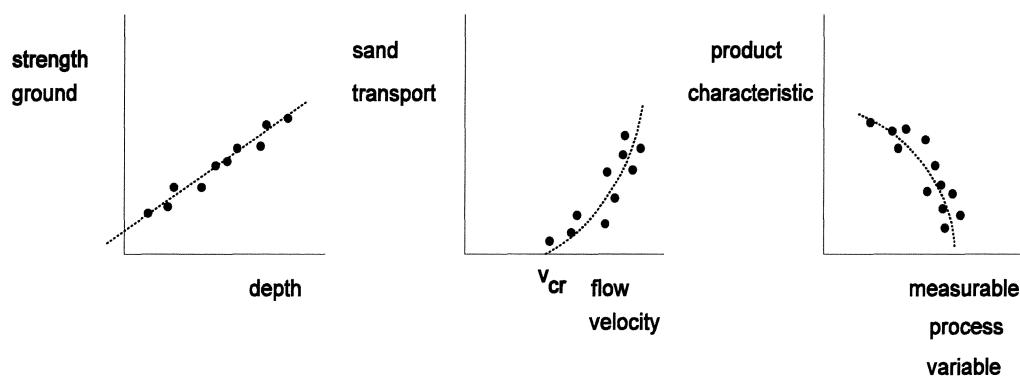


Figure II-82

The mathematical relation can generally be represented by the so-called **THEORETICAL REGRESSION LINE**:

$$y = g(\vec{x}, \vec{\theta})$$

Here y is the dependent variable.
 \vec{x} is the number of independent variables, on which y is dependent: $\vec{x} = X_1, X_2, \dots, X_n$.
 $\vec{\theta} = \theta_1, \theta_2, \theta_3, \dots, \theta_n$ are the parameters of the mathematical relation.

When deriving a relation from observations (a random sample) this relation is known except for the parameters. From measurements one can attempt to find out something about this unknown relation. One *assumes* a relation $g(\vec{x}, \vec{\theta})$ between the dependent variable y and the independent variables X_i and one takes a *random sample*. From the measurements (realisations or separate observations from the sample), the parameters $\vec{\theta}$ of the assumed relation are *estimated*. If a perfect model (i.e. a correct and complete mathematical formulation of the law) were available, the data would satisfy the mathematical formulation exactly. This is almost never the case, if only because the measurement errors have not been included in the model. However, other imperfections can also occur in the model, for example because one (or more) (jointly)determining independent variable(s) X_i has (have) not been recognised, i.e. one (or more) X_i has (have) not been included in the calculation model. Because the model is not (or not completely) known, these imperfections can not be distinguished from measurement errors. To find the parameters (coefficients and possibly powers) of the mathematical model (the **EMPIRICAL REGRESSIONLINE**, empirical because it is deduced from the random sample) one can use different techniques

of analysis, such as linear or non-linear regression analysis, etc.. By correlation analysis the "strength" of a (linear) relation between (normally distributed) random variables (i.e. the extent to which the variance of the one variable can be explained by the variance of the other variable) can be determined. In this course linear regression analysis and correlation analysis (both for only two variables) will be discussed. Non-linear and multi-dimensional regression and correlation analysis are not considered in detail.

II.11.1. REGRESSION ANALYSIS

The term "regression analysis" was introduced by G. Galton (Natural Inheritance, 1889) in a statistical genetics research. He used "regression" to indicate a certain genetic relation between people. The word has been adopted into statistical terminology and it now signifies the statistical method that was used by Galton.

The essence of the regression analysis is that one minimises the deviations of the data from the (assumed) model by an "optimal" selection of the parameters. It is usual to minimise the sum of the squared differences between the observations and the assumed model:

$$var(\underline{\varepsilon}) = \chi^2 = \min_{\vec{\theta} - \hat{\theta}} \sum_{i=1}^N \{y_i - g(\vec{x}, \vec{\theta})\}^2$$

The result is an optimal estimate of the parameters $\vec{\theta}$. This leads to an expression for the empirical regression line.

Applying regression analysis to two variables means considering only one independent variable, \underline{x} , besides the dependent variable, \underline{y} . The assumed relation can be modelled by:

$$\underline{y} = g(\underline{x}, \vec{\theta}) + \underline{\varepsilon}$$

Where $\underline{\varepsilon}$ is the random scatter around the assumed mathematical relation. This scatter is caused by imperfections in the model and measurement errors. The scatter is of no further importance to the mathematical relation.

In regression analysis the nature of x : random or deterministic, and, in the case \underline{x} is a random variable, the type of distribution of \underline{x} , are irrelevant.

The average of $\underline{\varepsilon}$ is defined equal to 0 (zero), so that $\underline{\varepsilon}$ does not contribute towards the expected value of \underline{y} . The chosen denotation distinguishes explicitly between the "moving average" $\mu_{\underline{y}|\underline{x}} = g(\underline{x}, \vec{\theta})$ and the scatter $\underline{\varepsilon}$.

(The notation $\underline{y}|\underline{x}$ indicates that the event \underline{y} occurs on condition that x occurs.)

Regression analysis for two variables (assume x en \underline{y}) considers x an *independent variable* and \underline{y} a *dependent variable* (dependent on x). Selecting which variable should be considered independent and which should be considered dependent *is not without significance!* Different parameters ($\vec{\theta}$) are found for the regression line, depending on that selection. (Remember Figure II-22. The indicated angle α can be measured relative to the x -axis and relative to the y -axis. "Linear Least Squares" can be applied both in the x and in the y direction.)

The following hypotheses underlie regression analysis for two variables:

1. For every value of x , $\underline{\varepsilon}$ (and hence \underline{y}) is *normally distributed*.
2. The expected value (i.e. the average) of \underline{y} , $\mu_{\underline{y}|x}$, is a *known* function of x :

$$\mu_{\underline{y}|x} = g(x, \vec{\theta})$$

in which the *unknown parameters* $\vec{\theta}$ appear. The function $\mu_{\underline{y}|x} = g(x, \vec{\theta})$ is called the *theoretical regression line*, as opposed to the *empirical regression line* which is based on the observations $y = h(x; A, B, \dots, \dots)$.

3. The variance of $\underline{\varepsilon}$, $\text{var}(\underline{\varepsilon} | x)$, is a constant (or is proportional to a given function of x . The latter is left aside here.).
4. The observations are statistically independent.

II.11.1.1. WORKING METHOD FOR LINEAR REGRESSION OF TWO VARIABLES WITH CONSTANT VARIANCE

Given the observations: $\{x_1, y_1\}, \{x_2, y_2\}, \{x_3, y_3\}, \dots, \{x_n, y_n\}$ and assuming the mathematical relation $y = g(x, \vec{\theta})$, to which the scatter $\underline{\varepsilon}$ has been added:

$$\underline{y} = g(x, \vec{\theta}) + \underline{\varepsilon}$$

one can write:

$$\underline{\varepsilon} = \underline{y} - g(x, \vec{\theta})$$

If the assumed regression line is a straight one, the resulting set of equations is solvable using algebra. Assume the linear relation: $\mu_{\underline{y}|x} = \alpha_0 + \alpha_1 \cdot x$, then:

$$\varepsilon_i = y_i - (\alpha_0 + \alpha_1 \cdot x_i)$$

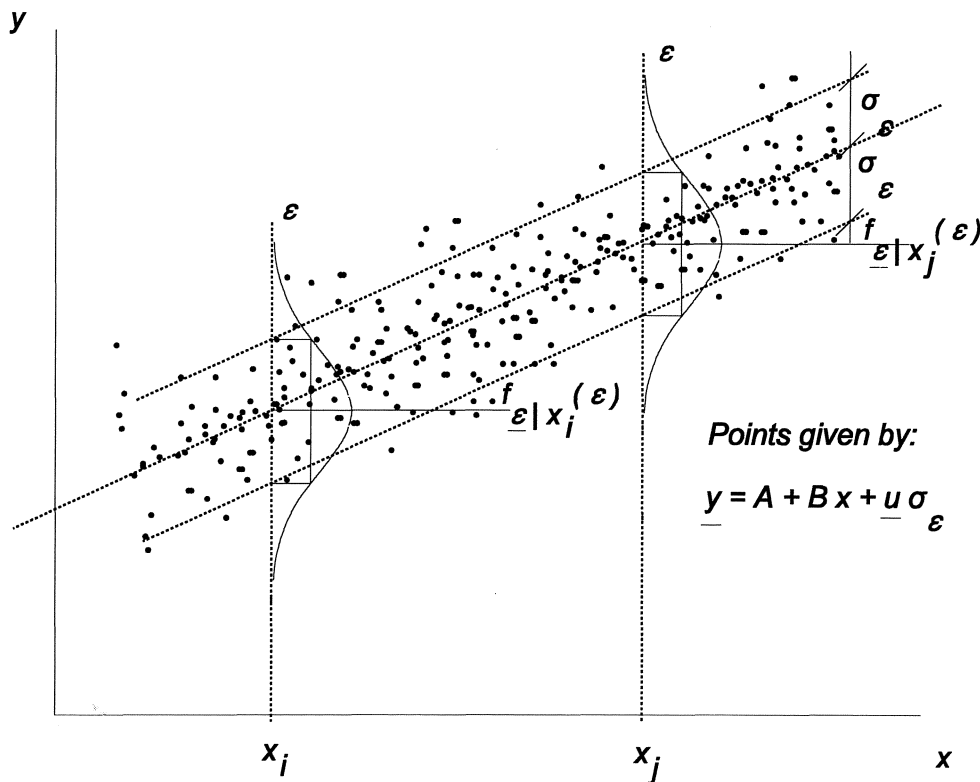


Figure II-83

Wanted are the estimates¹⁾ \underline{A} and \underline{B} of α_0 and α_1 and the estimate s^2 of statistic $\text{var}(\underline{\varepsilon} | x_i)$ so that:

$$\chi^2 = \min_{\hat{\theta}-\hat{\delta}} \sum_{i=1}^N \{y_i - (A + B \cdot x_i)\}^2$$

i.e. minimise the sum of the squares of the deviations of the expected values for the parameters A and B . It is after this that the method of "curve fitting" is named the method of the least squares.

For a minimum the following should apply:

$$\frac{\partial \chi^2}{\partial A} = 0 \quad \text{and} \quad \frac{\partial \chi^2}{\partial B} = 0$$

This leads to two equations with two unknowns.

Assuming the derivatives equal zero gives:

$$\frac{\partial \chi^2}{\partial A} = 0 = 2 \cdot \sum_{i=1}^N \{(y_i - A - B \cdot x_i) \cdot (-1)\} \quad \frac{\partial \chi^2}{\partial B} = 0 = 2 \cdot \sum_{i=1}^N \{(y_i - A - B \cdot x_i) \cdot (-x_i)\}$$

Solving A and B from this gives:

$$A = \frac{1}{N} \sum_{i=1}^N y_i - \frac{B}{N} \sum_{i=1}^N x_i \quad B = \frac{\sum_{i=1}^N x_i \cdot y_i - \frac{1}{N} \sum_{i=1}^N x_i \cdot \sum_{i=1}^N y_i}{\sum_{i=1}^N x_i^2 - \frac{1}{N} \left(\sum_{i=1}^N x_i \right)^2}$$

The scatter of the observations around the empirical regression line is given by the estimator of the variance of $\underline{\varepsilon}$:

$$s_{\varepsilon}^2 = \frac{\sum_{i=1}^N \{y_i - (A + B \cdot x_i)\}^2}{N-2}$$

This way, the *ESTIMATES OF THE PARAMETERS* are "best fit" (or "optimal", see 2nd paragraph of § II.11.1) in as much as they are *NORMALLY DISTRIBUTED*, with the required parameters A and B as *EXPECTED VALUES* and with the *SMALLEST POSSIBLE VARIANCES*.

The estimates $s_{\underline{A}}^2$ and $s_{\underline{B}}^2$ of the variances $\sigma_{\underline{A}}^2$ and $\sigma_{\underline{B}}^2$ of \underline{A} resp. \underline{B} are:

$$s_{\underline{A}}^2 = \frac{\sum_{i=1}^N x_i^2}{N \sum_{i=1}^N x_i^2 - \left(\sum_{i=1}^N x_i \right)^2} \quad s_{\underline{B}}^2 = \frac{N}{N \sum_{i=1}^N x_i^2 - \left(\sum_{i=1}^N x_i \right)^2}$$

II.11.1.2. IMPLICATIONS OF TRANSFORMATIONS

The last paragraph showed that the regression analysis is simple to carry out as long as the relation is linear. Often the considered (physical, econometric, sociological, etc.) relations are not linear. Usually, in those cases, functions which turn into linear functions by axis transformation are used as approximations. For example:

¹⁾ "Estimators" are treated more in depth in § II.12. Note that \underline{A} and \underline{B} are random variables, hence subject to "probability" or "uncertainty". We can not know more about them than follows from the "data".

$$y = A \cdot \exp(B \cdot x) \quad (1)$$

$$y = A \cdot x^B \quad (2)$$

$$y = A + B \cdot \ln(x) \quad (3)$$

Sometimes, people (unjustly!) apply a transformation without considering the background of the phenomenon. The approximation ("fit") takes place *after* transformation. Consider, for example, the given equation (1):

$$\underline{y} = A \cdot \exp(B \cdot x) \cdot \underline{\varepsilon} \quad (\text{and not: } \underline{y} = A \cdot \exp(B \cdot x) + \underline{\varepsilon}.)$$

Transformation gives a linear relation between $\ln(\underline{y})$ and x :

$$\ln(\underline{y}) = \ln(A) + B \cdot x + \ln(\underline{\varepsilon})$$

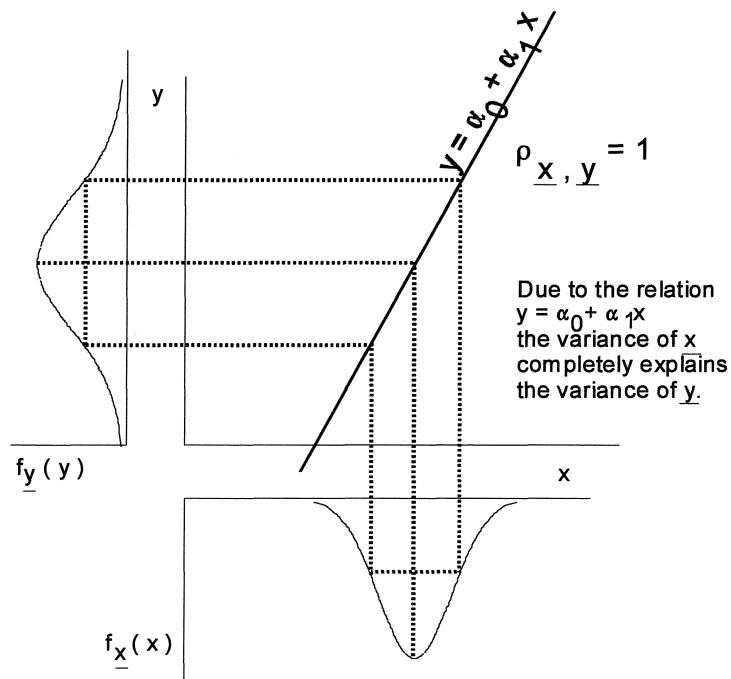
in which $\ln(\underline{\varepsilon})$ is normally distributed with an average of zero, so that $\underline{\varepsilon}$ is assumed to be a *MULTIPLICATIVE ERROR* with a *LOG-NORMAL DISTRIBUTION*.

II.11.2. CORRELATION ANALYSIS

For a correlation analysis two variables (take \underline{x} and \underline{y}) are *both* considered *random variables*. The relation between the variables can be described by a *joint probability density function* of \underline{x} and \underline{y} . *This is NOT possible in regression analysis because the distribution of \underline{x} is not relevant. That distribution is not taken into account.*

The objective of the correlation analysis is finding the statistical dependence (correlation, the extent to which the variance of the one variable can be explained by the variance of the other variable) between the variables.

Correlation between two random variables is defined as: $\rho_{\underline{x}, \underline{y}} = \frac{Cov(\underline{x}, \underline{y})}{\sigma_{\underline{x}} \cdot \sigma_{\underline{y}}}$, with interchangeable \underline{x} and \underline{y} . Hence, it is irrelevant which variable is considered independent of the other. Thus it follows that a correlation matrix is symmetrical.



A correlation analysis can only determine a *statistical* and linear dependence between variables. A *physical relation* between the variables must be determined on *other* grounds.

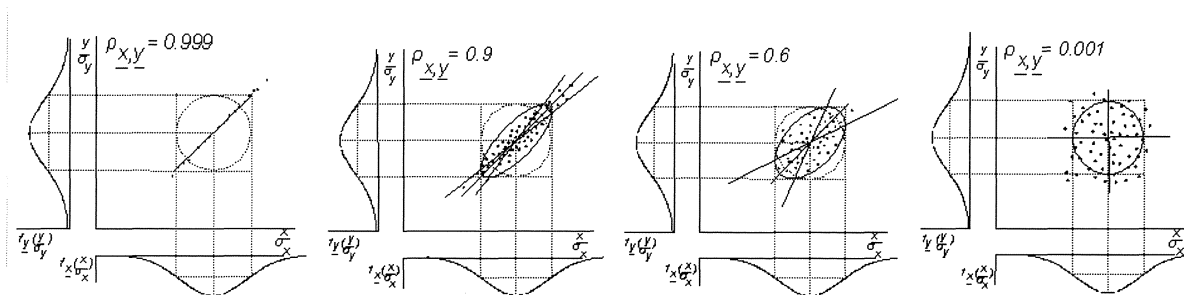


Figure II-85

For an unambiguous interpretation of correlation the relation between the random variables must be **LINEAR**. (See the following paragraph.)

II.11.3. EXPLAINED VARIANCE ¹⁾

The parameter α_1 from Figure II-84 can also be denoted as (see § II.6.):

$$\alpha_1 = \frac{\text{cov}(\underline{x}, \underline{y})}{\text{var}(\underline{x})}$$

Only if a linear relation exists between \underline{x} and \underline{y} can $\frac{\text{cov}(\underline{x}, \underline{y})}{\text{var}(\underline{x})}$ (and the corresponding estimate of statistic B) be interpreted as the gradient of the regression line.

The correlation coefficient $\rho_{\underline{x}, \underline{y}}$ is defined as:

$$\rho_{\underline{x}, \underline{y}} = \frac{\text{cov}(\underline{x}, \underline{y})}{\sqrt{\text{var}(\underline{x}) \cdot \text{var}(\underline{y})}}$$

hence one can also write:

$$\alpha_1 = \rho_{\underline{x}, \underline{y}} \sqrt{\frac{\text{var}(\underline{y})}{\text{var}(\underline{x})}} = \rho_{\underline{x}, \underline{y}} \frac{\sigma_{\underline{y}}}{\sigma_{\underline{x}}}$$

(Compare with Figure II-22.)

From this follows:

$$\alpha_1^2 = \rho_{\underline{x}, \underline{y}}^2 \cdot \frac{\text{var}(\underline{y})}{\text{var}(\underline{x})}$$

The total variance of \underline{y} can be divided in explained variance (from \underline{x}) and the so-called autonomous variance. Calculate $\text{var}\{\underline{y}\}$ from $\text{var}\{\underline{x}\}$ and $\text{var}\{\underline{\varepsilon}\}$. A level II approach for $\underline{y} = \alpha_0 + \alpha_1 \cdot \underline{x} + \underline{\varepsilon}$ (Course CTow4130) gives:

$$\text{var}(\underline{y}) = \alpha_1^2 \cdot \text{var}(\underline{x}) + \text{var}(\underline{\varepsilon})$$

explained + autonomous

$$\text{or:} \quad 1 = \frac{\alpha_1^2 \cdot \text{var}(\underline{x})}{\text{var}(\underline{y})} + \frac{\text{var}(\underline{\varepsilon})}{\text{var}(\underline{y})} \quad \text{or} \quad 1 = \rho_{\underline{x}, \underline{y}}^2 + (1 - \rho_{\underline{x}, \underline{y}}^2)$$

$\rho_{\underline{x}, \underline{y}}^2$ is thus the part of the variance of \underline{y} that (in case of linear dependence) can be explained from the variance of \underline{x} (or the other way around because $\rho_{\underline{x}, \underline{y}} = \rho_{\underline{y}, \underline{x}}$).

Note that replacing the given theoretical quantities ($\alpha_0, \alpha_1, \rho_{\underline{x}, \underline{y}}, \sigma_{\underline{x}}, \sigma_{\underline{y}}$) by the estimates of statistics ($A, B, r_{\underline{x}, \underline{y}}, s_{\underline{x}}, s_{\underline{y}}$) in the preceding paragraph gives a complete analogy.

II.12. ESTIMATES OF STATISTICS

Assume the probability density function of a certain process (e.g. the discharge of a river during high water), $f_{\underline{x}}(x, \theta)$, is known but that the p.d.f. contains an unknown parameter, θ . If data are available, the set x_1, x_2, \dots, x_N serves as a random realisation of the population characterised by that probability

¹⁾ A. Hald, Statistical theory with Engineering applications, Wiley & Sons, Inc., New York, 1952

density function. To estimate the unknown parameter θ , one must calculate the value of a function of the N observations which is suitable for that purpose¹⁾:

$$t = T(x_1, x_2, \dots, x_N)$$

t is called an estimate of θ . The function $T(x_1, x_2, \dots, x_N)$ is called the estimator of θ .

It is assumed that the function $T(x_1, x_2, \dots, x_N)$ does not depend on θ . Based on this assumption, the properties of t may be deduced from the distribution of the random sample.

The main problem concerning the estimation theory is formulating the desired property (/ties) of the estimate(s) of statistic(s), t , and to find (an) estimator(s) $T(x_1, x_2, \dots, x_N)$ with that (those) property (/ties). (Assuming the distribution type is given.)

Desired properties of estimates of statistics are (amongst others and sometimes also subject to circumstances): consistency, efficiency, unbiasedness and robustness.

CONSISTENT ESTIMATE OF STATISTIC

An estimate t of statistic θ is said to be *consistent* if t probably converges towards θ when $N \rightarrow \infty$.

Example:

The average of a random sample is a consistent estimate of the average of a population (on condition that the variance of that population is finite). This follows from the Tchebycheff- inequality which poses that the probability that the average of the random sample differs less than an arbitrary small number ε from the population average, is greater than 1 minus the variance of the population divided by the number of observations times the square of the arbitrary small number ε .

As a formula:

$$P(|\bar{x} - \mu_{\bar{x}}| \leq \varepsilon) > 1 - \frac{\sigma_{\bar{x}}^2}{N \cdot \varepsilon^2}$$

With: \bar{x} = average of the random sample = $\frac{\sum_{i=1}^N x_i}{N}$.

$\mu_{\bar{x}}$ = average of the population.

ε = arbitrary small number.

$\sigma_{\bar{x}}^2$ = variance of the population.

N = number of realisations (observations) in the random sample.

Even if the variance is not finite, the fact that the sample average converges towards the population average, on condition that the population average is finite, can be proven (Khinchine's Theorem).

An example of an inconsistent estimate of the parameter μ , is the random sample average in case of a Cauchy or Lorentz distribution²⁾ of the population. The average of the *RANDOM SAMPLE* can be calculated. The average of the *POPULATION* does not exist because the integral:

$$\frac{1}{\sigma \cdot \pi} \int_{-\infty}^{+\infty} \frac{\xi}{1 + \left(\frac{\xi - \mu}{\sigma}\right)^2} d\xi$$

¹⁾ Choosing "a function suitable for that purpose" means that the *distribution type* is assumed known.

²⁾ Lorentz (Cauchy) distribution:

$$f_{\bar{x}}(\xi) = \frac{1}{\sigma \cdot \pi} \cdot \frac{1}{1 + \left(\frac{\xi - \mu}{\sigma}\right)^2} \Rightarrow F_{\bar{x}}(\xi) = \frac{1}{2} + \frac{1}{\pi} \cdot \arctan \frac{\xi - \mu}{\sigma} \quad -\infty < \xi < +\infty$$

diverges. (In this case the median of the random sample is a consistent estimate of the parameter μ^1 .)

The median of the sample "estimates" the median of the population.

The average of the sample would serve as an estimate of the population average if it existed. Because the population average does not exist, the sample's average is not a consistent estimate.

Both the sample's average and the sample's median are estimates of the parameter μ .

(ASYMPTOTICAL) EFFICIENT ESTIMATE OF STATISTIC

Usually several consistent estimates of a parameter of a distribution exist and some of those can be *asymptotically normally distributed*, which means that (random sample) distributions of these estimates of statistics tend to normal distributions when the number of observations $N \rightarrow \infty$. Comparing the variances of these estimates, the asymptotic normally distributed estimate of statistic is called an *asymptotic efficient estimate of statistic*. The *efficiency* of an estimate of statistic is defined as the ratio between this minimal variance and the variance of the considered asymptotic normally distributed estimate of statistic.

Example:

Consider the average and the median of N observations from a normally distributed population as estimates of the parameter μ of the normal distribution:

$$F_x(\xi) = \frac{1}{\sqrt{2\pi} \cdot \sigma} \cdot \int_{-\infty}^{\xi} e^{-\frac{(\zeta-\mu)^2}{2 \cdot \sigma^2}} d\zeta.$$

1) The median of the population is defined as that value of x for which:

$$\int_{-\infty}^x f_x(\xi) d\xi = 0,5$$

To determine the RANDOM SAMPLE MEDIAN THE OBSERVATIONS ARE PUT IN ORDER OF GREATNESS. The following then applies:

$$x_{\text{mediaan}} = x_i \left(\frac{N+1}{2} \right) \text{ if } N \text{ is odd}$$

$$x_{\text{mediaan}} = \frac{x_i \left(\frac{N}{2} \right) + x_j \left(\frac{N}{2} + 1 \right)}{2} \text{ if } N \text{ is even}$$

One can prove that both estimates are asymptotically normally distributed with averages equal to μ and variances $\frac{\sigma^2}{N}$ (of the sample's average) and $\frac{\sigma^2}{N} \cdot \frac{\pi}{2}$ (of the sample's median). The variance of the random sample average is hence smaller than the variance of the random sample median. The sample average is an efficient estimate of the parameter μ because its standard deviation is smallest. The efficiency of the sample median is $\frac{2}{\pi} \approx 0,64$ which means that the variance of the average of $N = 64$ observations from a normally distributed population equals the variance of the median of $N = 100$ observations.

UNBIASED ESTIMATE OF STATISTIC

An estimate of statistic t_N is said to be an unbiased estimate of the parameter θ if, for every N ,

$$E(t_N) = \theta$$

which means that by drawing random samples, each the size of N , from a given population a random sample of t_N 's is acquired of which the average value is θ .

(NB $E(\varphi)$ denotes the expected value of φ).

Example:

the estimate of the variance of a population:

$$s_u^2 = \frac{\sum_{i=1}^N (x_i - \bar{x})^2}{N-1}$$

is an unbiased estimate.

The central second moment - § II.13.2 :

$$s_b^2 = m_2 = \frac{\sum_{i=1}^N (x_i - \bar{x})^2}{N}$$

is a biased estimate of the variance.

SUFFICIENT ESTIMATE OF STATISTIC

Consider an estimate t_N of θ and the probability density function of the random sample of the estimate:

$f_{t_N}(t_N; \theta)$. If the probability density of the random sample can be denoted as:

$$f_{t_N}(x_1; \theta) \cdot f_{t_N}(x_2; \theta) \cdot \dots \cdot f_{t_N}(x_N; \theta) = f_{t_N}(t_N; \theta) \cdot g(x_1, x_2, \dots, x_N)$$

where $g(x_1, x_2, \dots, x_N)$ does not contain the parameter θ , then t_N is called a *sufficient estimate*. The importance of this definition is, that t_N contains *all information relevant to* θ if t_N is a sufficient estimate.

ROBUST ESTIMATE OF STATISTIC

The term robust was introduced in statistics by G.E.P. Box in 1953. Various definitions are possible but concerning an estimate it signifies: "insensitive to small deviations from the idealised assumption under which the estimate is optimised". "Small" in this description means: concerning large deviations for a small number of observation points. This definition concerns the term "outliers" (points which differ greatly from the general trend). This definition is generally used for statistical procedures.

II.13. ESTIMATING DISTRIBUTION PARAMETERS

In probabilistic design, the distributions of the random variables are assumed to be known. That assumption concerns both the type of the distribution and the corresponding parameters.

The type of distribution should (if at all possible) be selected on grounds of physical or other non- statistical considerations. Often, however, the necessary knowledge is lacking . In those cases, one *chooses* a type and one *estimates* the parameters from a random sample (data from measurements or observations from the population). One subsequently applies a mathematical relation to the given measurement results. Proving the validity of the *hypothesis* that the selected distribution type (which usually - wrongly - is determined on grounds of the same observations as those from which the parameters were estimated!) is *not improbable*, usually (again: wrongly) remains undone.

II.13.1. METHODS FOR THE ESTIMATION OF DISTRIBUTION PARAMETERS

To determine the parameters from observations a number of methods are available. Of these a couple will be treated in the following paragraphs, namely:

- ◆ methods of the moments (§ II.13.2.)
- ◆ (linear) regression (§ II.13.3.). This concerns adjusting points that have been plotted on probability paper "by hand", or calculated adjustment, for example using the method of the least squares. The method of the least squares has already been treated in § II.11.2..
- ◆ method of maximum likelihood (§ II.13.4.).
- ◆ Bayesian parameter estimation (§ II.13.5.).

Because these methods use different estimators

$$t = T(x_1, x_2, \dots, x_N)$$

(see § II.12.) different estimates are found for certain parameters. The parameter(s) of the distribution of the population is (are) estimated on grounds of observations (a random sample). The estimates are (per definition!) not equal to the parameters of the distribution. The random sample contains a limited number of observations and these observations are discrete (have certain defined values) whilst the distribution is often continuous. Not only does this limit the accuracy of the estimate, but it also sometimes leads to the situation where a random sample better satisfies a different distribution than the distribution of the population from which it is taken. Among the tests of the "conformity" of observations with the selected distribution are the χ^2 - test (see § II.13.6) and the Kolmogorov - Smirnov test (K.S. test, § II.13.7).

II.13.2. THE METHOD OF THE MOMENTS

The moments of most distributions can be written as functions of the distribution parameters. The k^{th} central moment of the distribution ($k > 1$) of a population is defined as:

$$\mu_k = E(\underline{x} - \mu)^k = \int_{-\infty}^{+\infty} (\xi - \mu)^k \cdot f_{\underline{x}}(\xi) d\xi \quad \text{with} \quad \mu = \int_{-\infty}^{+\infty} \xi \cdot f_{\underline{x}}(\xi) d\xi = \text{population average}$$

The central moments (the moments "relative to the average") can be determined from (random sample) realisations of observations:

$$m_k = \frac{\sum_{i=1}^N (x_i - \bar{x})^k}{N} \quad \text{with} \quad \bar{x} = \frac{\sum_{j=1}^N x_j}{N} = \text{average of the sample and} \quad k > 1$$

The second central moment that can be calculated from the random sample is, (provided the second moment of the distribution of the population exists) a (biased) estimate of the variance:

$$s_b^2 = m_2 = \frac{\sum_{i=1}^N (x_i - \bar{x})^2}{N}$$

The index b was added to indicate a biased estimate . The unbiased estimate s_u^2 (index u to indicate unbiased estimate), is (see also § II.12):

$$s_u^2 = \frac{N}{N-1} \cdot s_b^2 = \frac{\sum_{i=1}^N (x_i - \bar{x})^2}{N-1}$$

By using the estimates of the moments, calculated from the random sample, as approximations of the moments of the distribution of the population, estimates of the parameters of the distribution can be calculated. Estimation of the parameters of a distribution according to the Method of the Moments assumes:

$$\mu_k \approx m_k$$

(I.e. m_k is selected as an estimation of μ_k)

Example:

For an exponential distribution, the following is given:

$$F_{\underline{x}}(\xi) = 1 - e^{-\frac{\xi - \alpha_0}{\alpha_1}}$$

Differentiation gives:

$$f_{\underline{x}}(\xi) = \frac{1}{\alpha_1} \cdot e^{-\frac{\xi - \alpha_0}{\alpha_1}}$$

Average and higher central moments of an exponential distribution are found simply by partial integration.

The distribution average is:

$$E(\underline{x}) = \mu = \int_{-\infty}^{+\infty} \xi \cdot f_{\underline{x}}(\xi) d\xi = \frac{1}{\alpha_1} \int_{-\infty}^{+\infty} \xi \cdot e^{-\frac{\xi - \alpha_0}{\alpha_1}} d\xi = \alpha_0 + \alpha_1$$

One can state:

$$\mu = \alpha_0 + \alpha_1 \approx A + B = \frac{\sum_{i=1}^N x_i}{N}$$

with which a first relation is made between the parameters α_0 and α_1 , the estimates A and B and the observations x_i .

The variance of the distribution is:

$$E(\underline{x} - \mu)^2 = \sigma^2 = \mu_2 = \int_{-\infty}^{+\infty} (\xi - \mu)^2 \cdot f_{\underline{x}}(\xi) d\xi = \frac{1}{\alpha_1} \int_{-\infty}^{+\infty} (\xi - \alpha_0 - \alpha_1)^2 \cdot e^{-\frac{\xi - \alpha_0}{\alpha_1}} d\xi = \alpha_1^2$$

And:

$$\sigma^2 = \alpha_1^2 \approx m_2 = B^2 = \frac{\sum_{i=1}^N \left(x_i - \frac{\sum_{j=1}^N x_j}{N} \right)^2}{N}$$

This is a second relation between the parameters and the observations.

Solving B gives:

$$\alpha_1 \approx B$$

For A as an estimate of α_0 one finds:

$$\alpha_0 = \mu - \sigma \approx A$$

The skewness of the exponential distribution is calculated as follows:

$$\mu_3 = E(\underline{x} - \mu)^3 = \frac{1}{\alpha_1} \int_{-\infty}^{+\infty} (\xi - \alpha_0 - \alpha_1)^3 \cdot e^{-\frac{\xi - \alpha_0}{\alpha_1}} d\xi = 2\alpha_1^3$$

A distribution with a unimodal or single peak probability density function with a skewness greater than zero slants to the right. The probability density function of the exponential distribution:

$f_{\underline{x}}(\xi) = \frac{1}{\alpha_1} \cdot e^{-\frac{\xi - \alpha_0}{\alpha_1}}$ (and, colloquially: the exponential distribution itself) slants to the right according to this "definition". The third central moment of a symmetrical distribution such as the uniform or the normal distribution equals zero.

The square of the skewness can be standardised by division by the variance to the power three. This standard gives the extent of spreading:

$$\beta_1 = \frac{\mu_3^2}{\mu_2^3}$$

The corresponding estimate is:

$$b_1 = \frac{m_3^2}{m_2^3}$$

often denoted:

for the population: $\sqrt{\beta_1} = \frac{\mu_3}{\mu_2^{\frac{3}{2}}}$ and calculated from the observations: $\sqrt{b_1} = \frac{m_3}{m_2^{\frac{3}{2}}}$

An exponential distribution reads:

$$\beta_1 = \frac{(2 \cdot \alpha_1^3)^2}{(\alpha_1^2)^3} = 4$$

The kurtosis of the exponential distribution is calculated:

$$\mu_4 = E(\underline{x} - \mu)^4 = \frac{1}{\alpha_1} \int_{-\infty}^{+\infty} (\xi - \alpha_0 - \alpha_1)^4 \cdot e^{-\frac{\xi - \alpha_0}{\alpha_1}} d\xi = 9\alpha_1^4$$

The kurtosis can be standardised by division by the square of the variance:

$$\beta_2 = \frac{\mu_4}{\mu_2^2}$$

The standardised kurtosis van of an exponential distribution is:

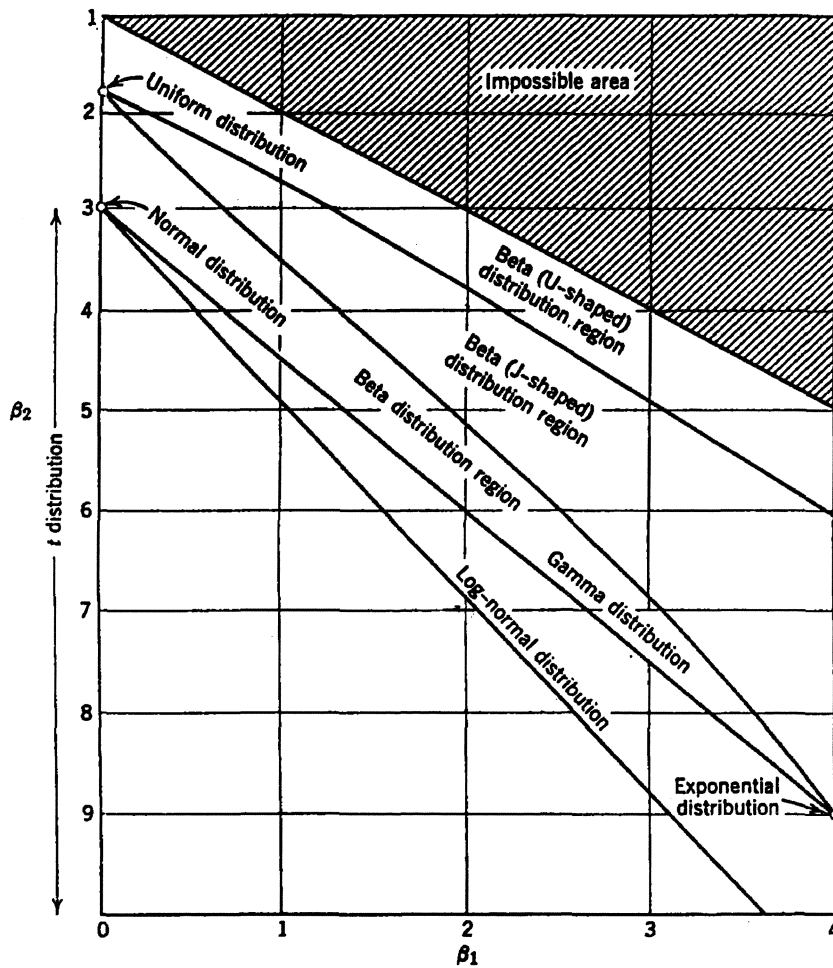
$$\beta_2 = \frac{9\alpha_1^4}{(\alpha_1^2)^2} = 9$$

The standardised kurtosis of a normal distribution is 3. The standardised kurtosis of a uniform distribution is 1.8.

The estimate of the standardised kurtosis is calculated from observations as follows:

$$b_2 = \frac{m_4}{m_2^2}$$

One can consider β_2 a function of β_1 . For various distributions, the relations between β_1 and β_2 have been investigated by Pearson. Figure II-86 is taken from: Hahn, G.J. & Shapiro, S.S., *Statistical Models in Engineering*, Wiley, 1967. In the computer plot (Figure II-87) a + indicates the position of (b_1, b_2) for a data set EXPO1000.DIS with 1000 observations from an exponential distribution. b_1 and b_2 were calculated from this random sample. Based on the large number of observations (1000), one would expect: $b_1 = 4$ and $b_2 = 9$. It transpires: $b_1 \approx 3.6$ and $b_2 \approx 8.6$. On grounds of the computer plot one could believe the observations originate from a gamma distribution or a log-normal distribution. The random sample apparently suggests a different distribution than the distribution of the population from which the observations originate! To compare, the probability density functions and the distribution functions plotted on half-logarithmic paper, both from the 1000 point data set EXPO1000.DIS, are given in Figures II-88 and II-89.



Regions in (β_1, β_2) plane for various distributions. (From Professor E. S. Pearson, University College, London.)

Figure II-86

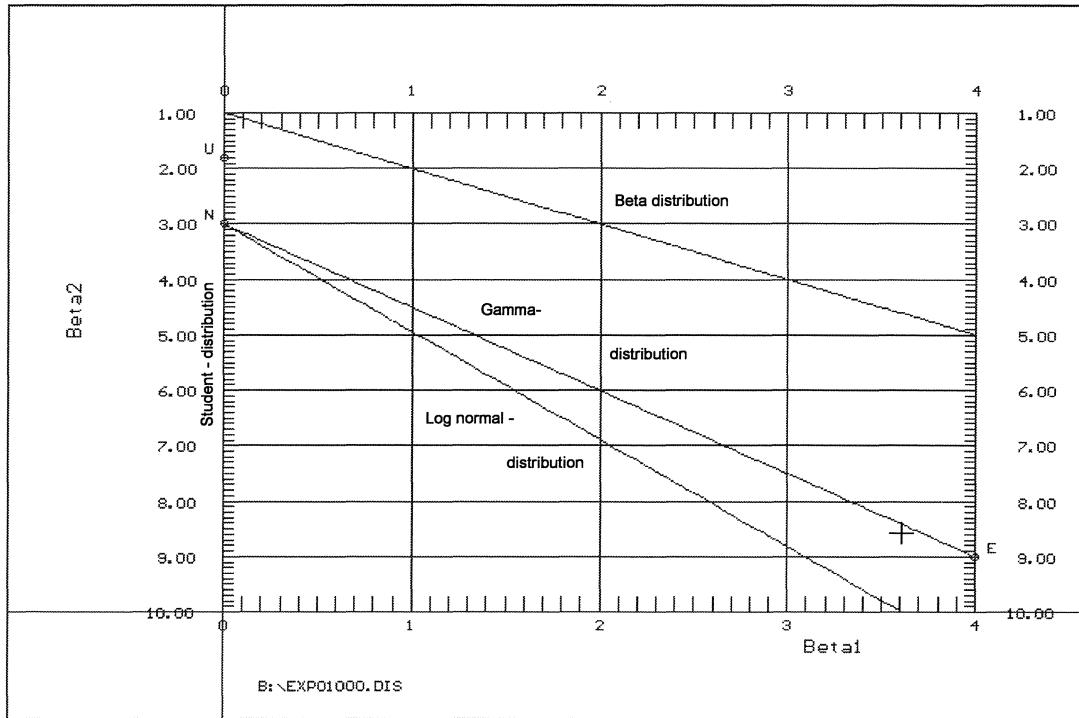


Figure II-87

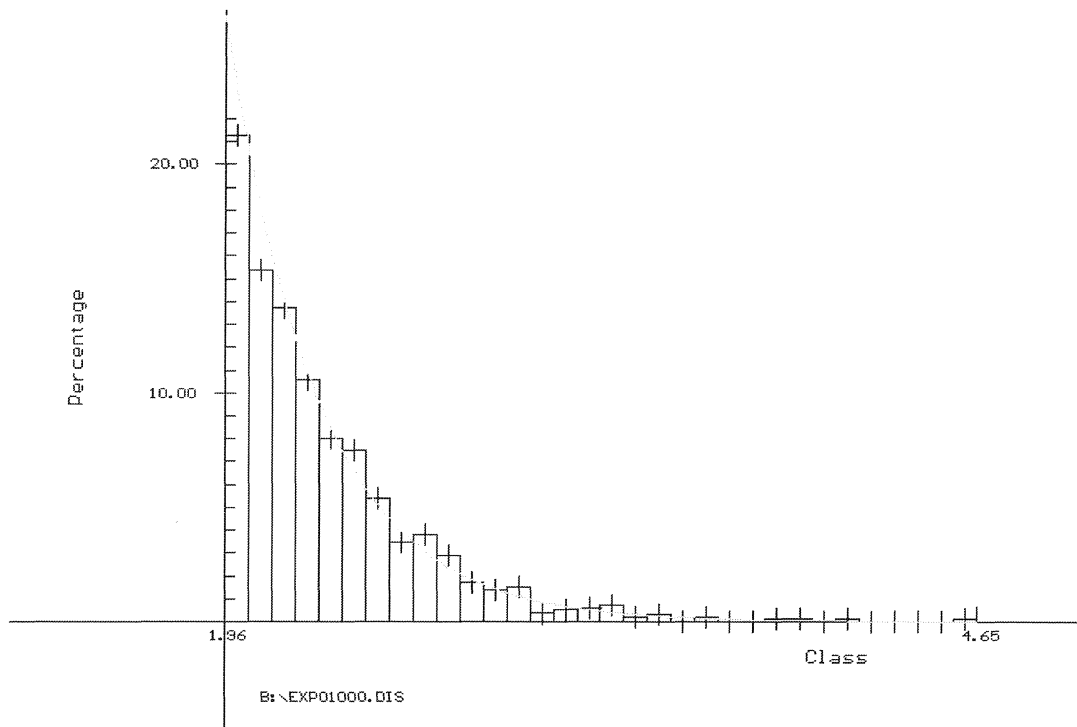


Figure II-88

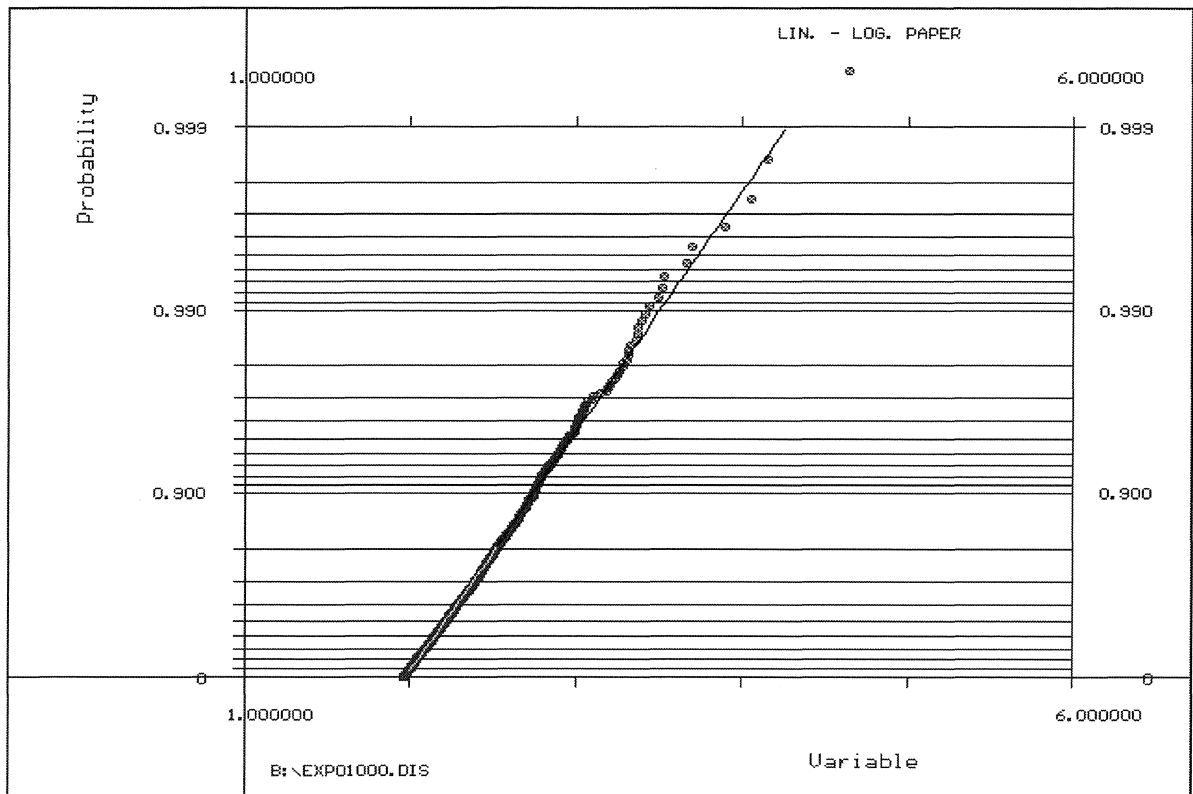


Figure II-89

II.13.3. LINEAR REGRESSION

A second method which is often used for estimating distribution parameters is linear regression. (See § II.11.1. and further.) Using this method to estimate parameters leads to difficulties when only the intercepts are given for the coordinates $x_i, y_i, (x_i$: significant wave heights, yearly maximum river discharges, etc.). To come to coordinates, assumptions have to be made concerning the probability of occurrence of the observations concerned. For this the observations must be organised and, if necessary, transformed.

II.13.3.1. ORGANISATION OF THE OBSERVATION MATERIAL AND TRANSFORMATIONS

To determine the PARAMETERS ¹⁾ of the distribution, observations are first put in order of increasing greatness. These observations in order of greatness are indicated by ${}_N x_i$. Here N represents the number of observations in the considered random sample. These ${}_N x_i$ can be seen as intercepts of coordinates. To the ${}_N x_i$ ordinates, ${}_N y_i$, have to be added. The plot positions of the observations are then characterised by the coordinates (${}_N x_i, {}_N y_i$).

Plot positions have to fulfil the following conditions according to Gumbel ²⁾:

1. it must be possible to plot all observations, therefore ${}_N x_i$ and ${}_N y_i$ (or their transformed forms) must be finite.
2. ${}_N y_i$ must lie between the observed frequencies $\frac{i-1}{N}$ and $\frac{i}{N}$ and be independent of the distribution.
3. The return period of an observation greater than or equal to that of the greatest observation must approach N. (Mutatis mutandis this is valid for observations smaller than or equal to the smallest observation.)
4. The observations must be spread equidistantly over the frequency axis. This means that the difference ${}_N y_i - {}_N y_{i-1}$ is only a function of N, independent of i (and of the distribution, see point 2.)
5. The plot position must have a significance that can be intuitively sensed and it must be easy to calculate.

A couple of plot positions are presented in the following table. Often the selected "significance that can be intuitively sensed" is: $E\left\{{}_N y_i\right\} = \frac{i}{N+1}$: the expected value of the frequency of the ith realisation ³⁾.

¹⁾ **No more than in §II.11. and further**, where the PHYSICAL RELATION had to be established on grounds that were not statistical, is the DISTRIBUTION TYPE derived from the observations here!

²⁾ Gumbel, E.J., Statistics of extremes, Columbia University Press, New York and London, 1958.

³⁾ A further explanation is given in Appendix II-2 (page II-116 and further).

Method	Approximation of the ordinate of the plot position
California	$\frac{i}{N}$
Hazen / Foster	$\frac{i-0.5}{N}$
Gumbel / Weibull	$\frac{i}{N+1}$
Bernard / Bos - Levenbach	$\frac{i-0.3}{N+0.4}$
Blom	$\frac{i-0.375}{N+0.25}$
Tuckey	$\frac{3 \cdot i - 1}{3 \cdot N + 1}$
Gringorten	$\frac{i-0.44}{N+0.12}$

For **LINEAR** regression (grouping the observation points around a straight line) the observations, (x_i) , are plotted as intercepts, and the expected values, (y_i) , as ordinates, if necessary after transformation.

Figure II-89 shows the observations plotted linearly. For the scale of the expected values the transformation: $y_i = -\ln\left(1 - \frac{i}{N+1}\right)$ was selected. This transformation was selected because the observations were taken from an exponential distribution:

$$F_x(\xi) = 1 - e^{-\frac{\xi - \alpha_0}{\alpha_1}}$$

Which can be replaced by:

$$1 - F_x(\xi) = e^{-\frac{\xi - \alpha_0}{\alpha_1}}$$

Calculating the logarithm of both sides of this equation serves as a transformation:

$$\ln\{1 - F_x(\xi)\} = \frac{1}{\alpha_1} \cdot \xi - \frac{\alpha_0}{\alpha_1}$$

Gumbel's choice is used for $F_x(\xi)$:

$$F_x(\xi) \approx \frac{i}{N+1}$$

so the transformation becomes:

$$\ln\left\{1 - \frac{i}{N+1}\right\} = \frac{1}{\alpha_1} \cdot x_i - \frac{\alpha_0}{\alpha_1}$$

Analogously, for other distributions such axis transformations can be found that every (*chosen!*) distribution function can be depicted as a straight line. If the selected distribution is correct, the coordinates formed by the (transformed) observations, (x_i) , and the (transformed) expected values of ordinates of the plot positions, (y_i) , will approximately satisfy a linear relation. In the following table a couple of transformations are named.

Distribution	X- axis	Y- axis
Uniform	Linear	Linear
Normal	Linear	Normally distributed
Log- normal	Logarithmic	Normally distributed
Exponential	Linear	Logarithmic
Gumbel	Linear	Double- logarithmic
Weibull	Logarithmic	Double- logarithmic

- N.B. 1. The "position on a straight line" (if necessary after transformation) does not verify the correctness of the selected distribution. The position of the (x_i, y_i) on a straight line only leads to the conclusion that the **OBSERVATIONS** (coincidentally) **PRESENT IN THE RANDOM SAMPLE** can be modelled well by the selected distribution.
- N.B. 2. A starting point for the regression analysis is that the deviations, e , from the regression line are normally distributed with average value zero and that they are independent. By the organisation ("sorting in order of greatness") of the observations, the successive observations are not independent. (A "next observation" is increasingly greater than its "precedent".) The application of regression analysis for parameter estimation of distributions is, therefore, at least questionable.

II.13.3.2. THE METHOD OF THE LEAST SQUARES

The method of the least squares was treated for linear functions of two variables in § II.11.1.3. For the y_i , plot positions are selected according to one of the rules in the table in § II.13.3., if necessary followed by a transformation to arrive at a linear depiction. The distribution parameters are subsequently estimated by applying the method of the least squares to adjust the distribution, transformed to a straight line, to the random sample.

Various types of probability paper can also be used, a line can be drawn through the points "by visual estimation" ¹⁾, or the line can be calculated using the method of the least squares.

II.13.4. THE METHOD OF MAXIMUM LIKELIHOOD

The Method of Maximum Likelihood does *not* require observations to be sorted according to size. The Method of Maximum Likelihood uses the *random sample likelihood function*. Based on (discrete) (random sample) *observations* conclusions are drawn concerning the parameter(s) of an (assumed known type of) *distribution of the population*.

Assume that the (*population*) *DISTRIBUTION* of a variable x is *KNOWN*, that it has only one parameter, θ , (the case of more parameters will be discussed after this) and that the parameter is also known. The probability of realising one *OBSERVATION* x_1 can be expressed by:

$$P_{\Delta x=0} \left\{ x_1 - \frac{\Delta x_1}{2} < x_1 \leq x_1 + \frac{\Delta x_1}{2} \right\} = f_x(x_1) \cdot dx_1$$

¹⁾ The eye "minimizes" (more or less) the "vertical distances" to the estimated regression line, where the distances of points above the line are considered positive and those of points below the line negative. ("There are approximately as many points equally far "vertically" above the line as below".) "The eye" does not use the least square approach but a "smallest $|y - y_i|$ " approximation! This corresponds to the Chebyshev approach, which determines y such that:

$$\max_{a \leq x \leq b} \{ |y - y_i| \} \text{ minimal}$$

If N INDEPENDENT observations are available, the probability of realising such a random sample is:

$$\begin{aligned}
 & P_{\Delta x_i \rightarrow 0} \left[\left\{ x_1 - \frac{\Delta x_1}{2} < x_1 \leq x_1 + \frac{\Delta x_1}{2} \right\} \cap \{ \dots \} \cap \left\{ x_N - \frac{\Delta x_N}{2} < x_N \leq x_N + \frac{\Delta x_N}{2} \right\} \right] \\
 &= f_{\underline{x}}(x_1, x_2, \dots, x_N | \theta) \cdot dx_1 \cdot dx_2 \cdot \dots \cdot dx_N \\
 &= f_{\underline{x}}(x_1 | \theta) \cdot dx \cdot f_{\underline{x}}(x_2 | \theta) \cdot dx \cdot \dots \cdot f_{\underline{x}}(x_N | \theta) \cdot dx \\
 &= \prod_{i=1}^N f_{\underline{x}}(x_i | \theta) \cdot dx
 \end{aligned}$$

From this follows:
$$f_{\underline{x}}(x_1, x_2, \dots, x_N | \theta) = \prod_{i=1}^N f_{\underline{x}}(x_i | \theta)$$

The other way round, if the observations x_1, x_2, \dots, x_N are a random sample from a distribution (of a known type) of which the parameter, θ , is *not* known, the equation above can be considered a function of θ alone. The random sample likelihood function is defined as:

$$L(\theta | x_1, x_2, \dots, x_N) = \prod_{i=1}^N f_{\underline{x}}(x_i | \theta)$$

This equation reads from left to right: the (relative) probability of occurrence of a certain random sample, x_1, x_2, \dots, x_N , as a function of a (given) parameter θ , or reversed, (read from right to left) the (relative) probability of a value of θ occurring, given that certain random sample. (The probability of θ given the observations $x_{1\dots N}$ equals the probability of observations $x_{1\dots N}$ given θ). This interpretation is attractive because it suggests that the value of θ for which the random sample is (relatively, i.e. compared with other random samples) more probable, is also the value of θ which (relative to other values of θ) is more probable. Hence, one has to find the value of the estimate of θ , for which the likelihood function is maximum: *The maximum likelihood estimate of θ is the value t for which the likelihood function $L(\theta)$ assumes a maximum.*

Example:

Assume an exponential distribution:

$$F_{\underline{x}}(x) = 1 - e^{-\frac{x}{\theta}}$$

The probability density function is:

$$f_{\underline{x}}(x) = \frac{1}{\theta} \cdot e^{-\frac{x}{\theta}}$$

The joint probability density function of N independent observations in a random sample, from which the estimate B of α_1 is determined, is:

$$f_{\underline{x}}(x_1, x_2, \dots, x_N | t) = \prod_{i=1}^N \frac{1}{\theta} \cdot e^{-\frac{x_i}{t}}$$

De likelihood function for the estimate t of θ is:

$$L(t | x_1, x_2, \dots, x_N) = \prod_{i=1}^N \frac{1}{t} \cdot e^{-\frac{x_i}{t}} = \frac{1}{t^N} \cdot e^{-\frac{\sum_{i=1}^N x_i}{t}}$$

This likelihood function has a maximum at:

$$t = \frac{\sum_{i=1}^N x_i}{N} \quad \text{as follows simply from } \frac{dL}{dt} = 0.$$

Concerning the determination of the maximum of a function "many paths lead to Rome". If the likelihood function is at least monotonous, a method which is often used for the determination of estimates according to the Method of Maximum Likelihood is calculating the maximum of the logarithm¹⁾.

An example for the abovementioned exponential distribution:
The likelihood function for a estimate B is:

$$L(t | x_1, x_2, \dots, x_N) = \frac{1}{t^N} e^{-\frac{\sum_{i=1}^N x_i}{t}}$$

Its logarithm is:

$$\ln(L) = -N \cdot \ln(t) - \frac{\sum_{i=1}^N x_i}{t}$$

Its derivative is:

$$\frac{d \ln(L)}{dt} = -\frac{N}{t} + \frac{\sum_{i=1}^N x_i}{t^2}$$

Assuming this equal to zero and solving t gives:

$$t = \frac{\sum_{i=1}^N x_i}{N}$$

The preceding theory can easily be extended to cases where the probability distribution contains more (assume M) parameters:

$$L(\theta_1, \theta_2, \dots, \theta_M | x_1, x_2, \dots, x_N) = \prod_{i=1}^N f_{\underline{x}}(x_i | \theta_1, \theta_2, \dots, \theta_M)$$

or, equally:

$$\ln(L) = \ln \left(\prod_{i=1}^N f_{\underline{x}}(x_i | \theta_1, \theta_2, \dots, \theta_M) \right) = \sum_{i=1}^N \ln(f_{\underline{x}}(x_i | \theta_1, \theta_2, \dots, \theta_M))$$

Solving a set of equations is typical for the determination of the maximum:

$$\sum_{i=1}^N \frac{\partial}{\partial \theta_j} \ln(f_{\underline{x}}(x_i | \theta_1, \theta_2, \dots, \theta_M)) = 0 \quad \text{with } j = 1, 2, \dots, M$$

E.g.:

$$F_{\underline{x}}(\xi) = 1 - e^{-\frac{\xi - \alpha_0}{\alpha_1}}$$

The probability density function is:

$$f_{\underline{x}}(\xi) = \frac{1}{\alpha_1} \cdot e^{-\frac{\xi - \alpha_0}{\alpha_1}}$$

¹⁾ As a result of the monotony of the likelihood function and the one to one relation between the likelihood function and its logarithm, these have a maximum for the same value of the estimate of the parameter.

The likelihood function is:

$$L(A, B | x_1, x_2, \dots, x_N) = \frac{1}{B^N} e^{-\frac{\sum_{i=1}^N x_i}{B}} \quad \text{with } A \leq x_1, B > 0.$$

The likelihood function of A has a maximum at:

$$(t =) A = x_1 \quad (\text{bordermaximum})$$

The most probable curve found is the line - - - - - in Figure II-90. Imagine the curve I-I-I-I-I or the curve II-II-II-II-II in Figure II-90 is the p.d.f. of the population. On grounds of the RANDOM SAMPLE these curves are considered less likely. Values of α_0 , the parameter of the distribution for which A is an estimate, larger than x_1 are ruled out because the random sample contains smaller values. x_1 could not be a realisation from the population if x_1 was smaller than α_0 .

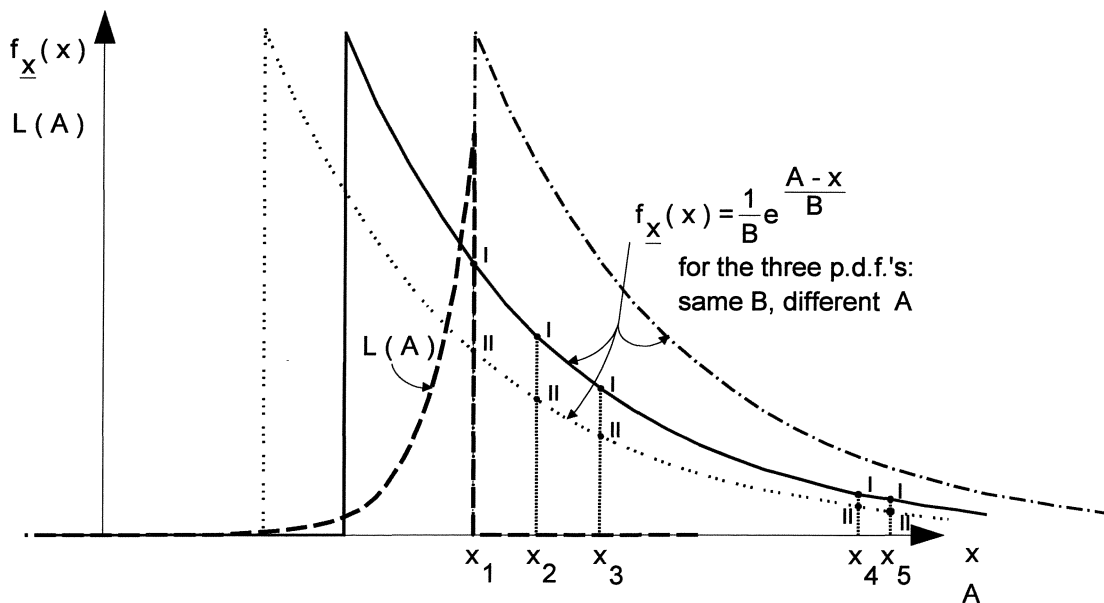


Figure II-90

If the likelihood function:

$$L(\theta_1, \theta_2, \dots, \theta_M | x_1, x_2, \dots, x_N) = \prod_{i=1}^N f_{x_i}(x_i | \theta_1, \theta_2, \dots, \theta_M)$$

is solved numerically, the numbers often become too small (underflow condition). The logarithmical transformation again offers a solution.

II.13.5. BAYESIAN PARAMETER ESTIMATION

The Bayesian parameter estimation is based on a so-called a priori distribution of the parameter θ . (A priori (Lat.): beforehand.) This a priori distribution indicates what is known at the moment that data are not yet available. The determination of it thus takes place on subjective grounds.

According to a prescribed procedure this a priori distribution is combined with the objective statistical data (observations) and thus turns into a so-called a posteriori distribution. (A posteriori (Lat.): afterwards.) Adjusting the a priori distribution on grounds of the observations leads to the a posteriori distribution.

Bayes' theorem is central in the Bayesian analysis:

$$P(A|B) = \frac{P(B|A) \cdot P(A)}{P(B)}$$

(See Lecture notes CTow30, Vrijling, J.K. and Vrouwenvelder, A.C.W.M., Probabilistic Design, Fac. Of Civil Engineering, TU Delft, 1984 (in Dutch)).

This theorem indicates how the probability of event A is adjusted under the influence of fact B. For the statistical processing of data, a hypothesis concerning a statistical parameter (e.g.: the average is between 10 and 11) is used for event A and the observations (realised statistical data) is used for B. Rewritten with new symbols (H = hypothesis, W = Observations), Bayes' Theorem reads:

$$P(H|W) = \frac{P(W|H) \cdot P(H)}{P(W)}$$

with:

$P(H|W)$ = probability that the considered hypothesis is right in view of the available data (a posteriori probability).

$P(W|H)$ = probability of observing the statistical data (observations) assuming that hypothesis H is valid. This corresponds to the likelihood function introduced earlier.

$P(H)$ = the a priori probability that the hypothesis is right. This probability has to be estimated in advance (a priori). This is the vulnerable point of the analysis.

$P(W)$ = a quantity which is not easy to interpret. In practice, however, it is a standardisation constant which makes the integration of the likelihood function from $-\infty$ to $+\infty$ equal 1 (and hence signifies a probability density).

In a formula:

$$f_{\theta}(t|x_1, x_2, \dots, x_N) = C \cdot \prod_{i=1}^N f_x(x_i, x_2, \dots, x_N | t) \cdot f_{\theta}(t)$$

The distribution type can also be determined using this Bayesian technique. The hypothesis is that the observations originate from certain distributions $V(j)$.

$$f_{\theta}(V_j|x_1, x_2, \dots, x_N) = C \cdot \prod_{i=1}^N f_x(x_1, x_2, \dots, x_N | V_j) \cdot f_{\theta}(V_j)$$

Of the various SELECTED distributions, V_j , the parameters of a certain data set are determined first. Subsequently, the most likely distribution for a DIFFERENT DATA SET from the same population is determined.

When using a computer to process these procedures, one should be aware of over- and underflow problems. In most cases it is recommended to take the logarithm both left and right.

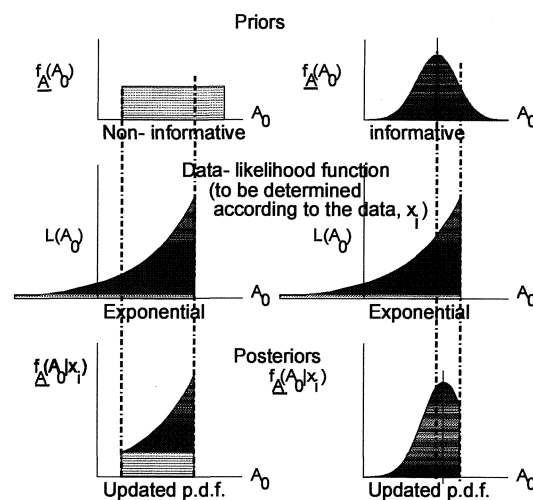


Figure II-91

II.13.6. χ^2 -TEST

The χ^2 -test determines the maximum difference between the (assumed) probability density function and the histogram that can be drawn up from the observations. If the observations are sorted in k classes with width Δx , the i^{th} interval will contain n_i observations out of a total of N observations. The expected value of the number of observations in the i^{th} interval is:

$$N \cdot p_i = N \cdot f_x(x_i) \cdot dx$$

The test quantity is the difference between the realised number of observations n_i and the expected value of the number of observations in that class, where the probability density function, $f_x(x_i)$, is assumed.

The used test quantity is:

$$D = \sum_{i=1}^k \frac{(n_i - N \cdot p_i)^2}{N \cdot p_i}$$

wit D = test quantity, with a χ^2 -distribution.

A result of the dependency, created by sorting into classes and the fact that r parameters of the probability density function $f_x(x)$ are estimated from the observations, is that the number of degrees of freedom equals $k - r - 1$.

Using a table for the χ^2 -distribution one can determine the maximum value of D for which the zero-hypothesis with a certain reliability won't be rejected:

$$P(D \leq \chi_{\alpha, k-r-1}^2) = 1 - \alpha$$

A disadvantage of the χ^2 -test is that the observations have to be classified. The number of classes can influence the result of the test. This limitation may not be neglected when applying the χ^2 -test.

II.13.7. KOLMOGOROV-SMIRNOV TEST

In literature a number of test can be found which do not reject the correctness of a hypothesis with a certain reliability. This does NOT mean that the hypothesis is correct with that certain reliability!

The Kolmogorov-Smirnov test (or K.S.- test) is applicable to observations from given distributions which have not been classified. The "test statistic" is the maximum deviation from a point, (x_i, y_i) , of the given distribution. This test gives an indication of the "join" (of the *CHOSEN* distribution) with the observations surrounding the *MODAL VALUE* of the *POPULATION* if the approximation (type AND estimated parameters) of the population distribution is correct. For extrapolations the *TAILS* of the distribution are of importance.

If the N observations x_i ($i = 1, 2, \dots, N$) are mentioned, then $S_N(x)$ is the function which gives the part of the population with observations smaller than the given value x . This function is constant between successive (i.e.: sorted in order of size) x_i s and it increases with a constant $\frac{1}{N}$ with every x_i (see Figure II.92).

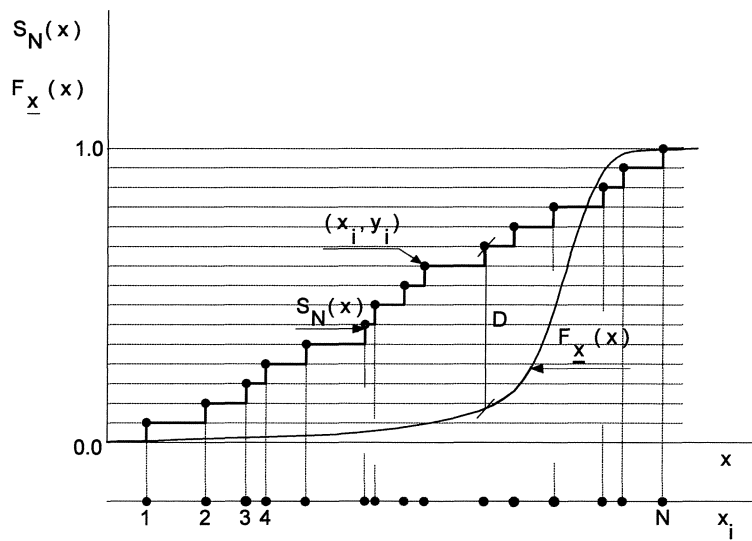


Figure II-92

The test quantity selected is the distance D (see Figure II-92):

$$D = \max_{i=1}^N \left| S_N(x) - F_x(x) \right| = \max_{i=1}^N \left| y_i - F_x(x_i) \right| \quad \text{with } y_i = \frac{i}{N}$$

The DISTRIBUTION may *not* be deduced from the GIVEN OBSERVATIONS .

The test is that:

$D < \frac{\alpha}{\sqrt{N}}$ for $N > 5$.	$\alpha = 1.23$	Reliability threshold
	$\alpha = 1.36$	10%
	$\alpha = 1.63$	5%
		1%

If the distribution is estimated from the observations, a correction seems necessary for the number of estimated parameters M :

$$D < \frac{\alpha}{\sqrt{N+M}}$$

However, no theory concerning this matter is known.

II.14. LOADS

For the final design (of a port or a hydraulic structure) one (or more) reliability function(s) is (/are) regarded to determine the probability of failure:

$$\underline{Z} = \underline{R} - \underline{S}$$

In an early design stage it is often useful to have a probability distribution or an exceedance frequency curve of the loads at one's disposal. The strength \underline{R} is then replaced in the formula by a constant S_0 :

$$\underline{Z} = S_0 - \underline{S}$$

A level II- or level III- calculation is then used to determine the probability that a load is greater than the constant S_0 . By varying S_0 , an exceedance frequency curve of the considered load is obtained. To introduce the reliability (or the probability of failure) of the structure in calculations, a mathematical model based on the calculated points, $(S_0, P_f(S_0))$, must be given.

Various versions of the structure to be designed, or parts of it, can be "confronted" with the found load exceedance curves, aimed at weighing up the probabilities of failure of several variants.

Often calculating the load is a problem in its own right. The load on the Oosterschelde storm surge barrier serves as an example. The barrier closes off a basin with a more or less fixed water level from the sea.

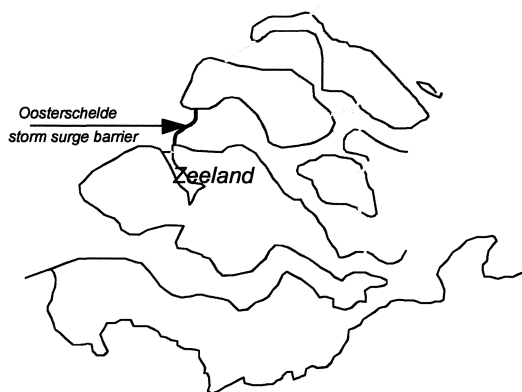


Figure II-93

Given:

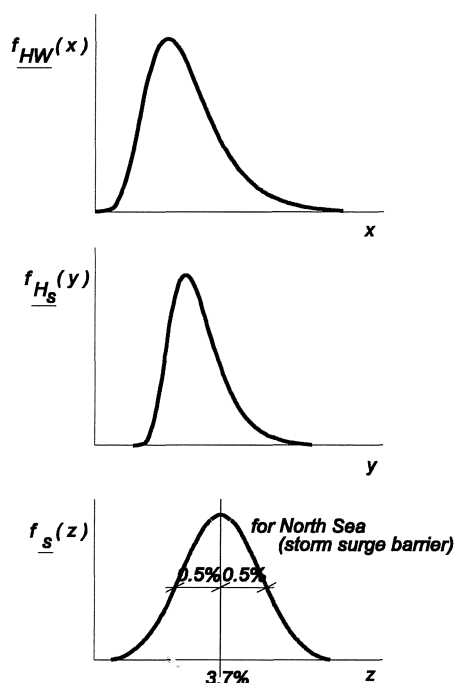


Figure II-94

1. the probability density function of the High Water levels on sea. (For the Oosterschelde barrier this follows from the exceedance frequency curve of the storm surge levels on the North Sea.)
2. The probability density function of the (significant) wave heights. (This follows from the long term exceedance frequency curve of the wave heights.)
3. For both the wave run up and the loads (forces, resonances) it is necessary to know a probability density function of the periods. In the past, little attention was paid to the influence of the periods of the waves, but from modern research it appears that periods are very important. The probability density function of the periods is often difficult to determine.

A certain wave height corresponds to a whole range of periods, as could be seen earlier (see for example Figure II-42). In young swell high waves are often long, short waves are often low. In swell low waves can have very long periods. An alternative to the probability density function of the wave period is the probability density function of the wave steepness:

$$\underline{s}_p = \frac{H_s}{L_p} \quad \text{with} \quad \underline{L}_p = \frac{g \cdot T_p^2}{2 \cdot \pi}$$

Experience shows that the wave steepness is independent of the wave height. The conditional probability density function of the wave period can be calculated from the probability density function of the wave steepness. Thus, the probability density function of the wave period can be acquired by multiplication with the probability density of the wave height. If necessary, the wave directions also have to be taken into account.

Forces on a structure can be divided into static and dynamic forces. Of the first kind, the head force needs to be mentioned. To determine (dynamic) wave forces on a structure, linear wave theory is often applied.

The first load to be taken into account is the head force, K_{head} (see Figure II-95), which should be considered a function of the difference between the outer and the inside water levels:

$$\underline{K}_{head} = g(\underline{HW}, \underline{BW})$$

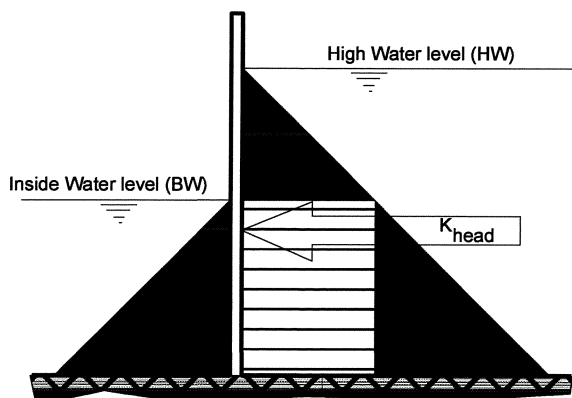


Figure II-95

For the wave load on very stiff structures, such as lock doors, another procedure should be followed than that for the (static) "head load". The gates in the Oosterschelde barrier react quasi-statically to wave load. Because waves have a spectrum, the wave force on the structure is calculated for a number of frequencies. Wave forces are a function of $\underline{H}_s, \underline{T}_p$ and the water level \underline{HW} :

$$\underline{K}_{significant\ wave} = \underline{K}_s = h(\underline{H}_s, \underline{T}_p, \underline{HW})$$

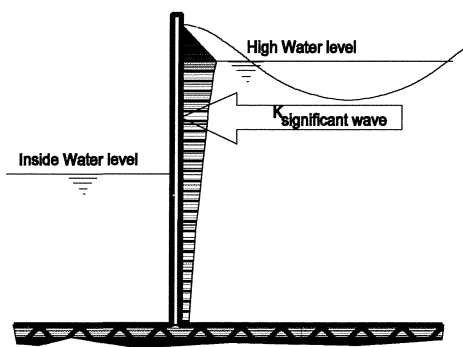


Figure II-96

Load by high low frequency wave
with one high outside water level (and fixed inside water level)

The load is standardised with the wave amplitude, $\eta(f) = \frac{1}{2} \cdot H(f)$. The transfer function (standardised load as a function of the frequency) becomes:

$$R_{K\eta}(f) = \frac{K_{significant\ wave}}{\frac{1}{2} \cdot H(f)}$$

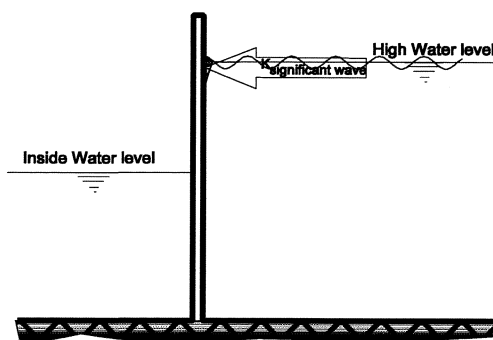
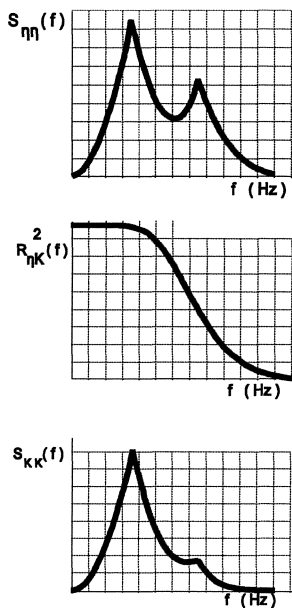


Figure II-97

Load by low high frequency wave

The forces or load spectrum $S_{KK}(f)$ is found by multiplying the wave spectrum $S_{\eta\eta}(f)$ by the square of the transfer function $R_{K\eta}$:

$$S_{\eta\eta}(f) * R_{K\eta}^2(f) = S_{KK}(f)$$



Wave (amplitude) spectrum (square of the wave amplitude per frequency band).

The surface of the spectrum is called m_0 .

The significant wave height (with a Rayleigh distribution of the wave heights - see § II.3) is : $H_s = 4\sqrt{m_0}$ (See lecture notes CTWA5316, b78, Wind waves, as mentioned earlier.)

Square of the transfer function. The sketched transfer function is characteristic for a structure which reacts quasi-statically. The structure is so stiff and inert that it does not react dynamically to the wave load.

Load or force spectrum. The load spectrum shows that, in this case, a second (higher frequency) peak in the wave spectrum doesn't or hardly does "affect" the force spectrum.

Figure II-98

Due to the linear theory the forces are also Rayleigh distributed. The significant force can be calculated according to $K_s = 2\sqrt{m_0}$, but now m_0 is the surface of the force spectrum.

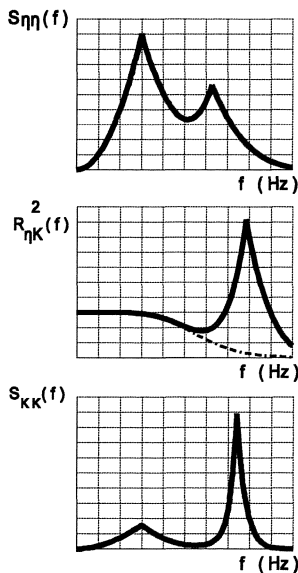


Figure II-99

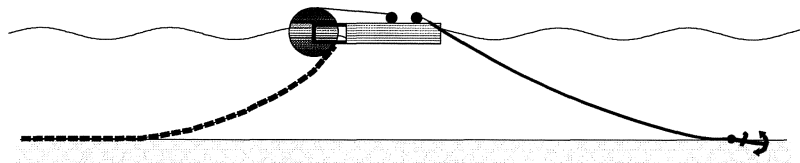


Figure II-100

When determining the transfer function of structures which react dynamically to wave load (in a laboratory where a model of the structure can be tested: the linear theory no longer holds then) the structure may appear to be hit in its eigen frequency. The forces (and mutatis mutandis the displacements) then increase greatly. For the mat laying ship The Cardium (used for the realisation of the Oosterschelde storm surge barrier) the MARIN institute in Wageningen determined that the coil, onto which the concrete mats had been rolled, would be driven by waves with periods of approximately 8 seconds. The mass of the coil (including the mat) was 9000 metric tonnes and it was thought that this mass would be too inert to be brought into motion by waves. The period of the swell on the North Sea, however, is 8 to 10 seconds and when this swell reached The Cardium the coil did have to be connected more stiffly with the ship!

For structures that react dynamically the following also holds:

$$S_{\eta\eta}(f) * R_{\eta K}^2(f) = S_{KK}(f)$$

Note that structures that react quasi-statically to wave loads, such as lock doors, gates of barrages or other defence structures etc., can sometimes start to vibrate due to current forces (oscillation with large amplitude: in the order of metres!).

Often, wave spectra (from measurements) can be better approximated by power functions than by standard spectra (Neumann, Pierson- Moscovitz or JONSWAP). Hand books state that for the right flank side of the spectrum (the high- frequency area): $S_{\eta\eta} \propto f^{-6}$ (\propto = directly proportional to). This is the so-called equilibrium range of O. Philipps. For Karwar $S_{\eta\eta} \propto f^{-3.5}$ and for the Oosterschelde $S_{\eta\eta} \propto f^{-2.5}$ were found. Standard spectra often don't "fit" and a "second top" can not be modelled by standard spectra either. By approximating the measurements with power functions, however, a second top can be easily be included by superposition.

From the following, the method to determine the extents of the forces is known. Furthermore, it is known that the forces caused by wave loads are Rayleigh distributed:

$$F_{\underline{K}}(F) = 1 - e^{-2\left(\frac{F}{K_s}\right)^2}$$

The distribution of the forces which occur due to the N highest waves, which are Rayleigh distributed, is:

$$F_E(F) = \left\{ 1 - e^{-2\left(\frac{F}{K_s}\right)^2} \right\}^N \approx e^{-N \cdot e^{-2\left(\frac{F}{K_s}\right)^2}}$$

The equation

$$\underline{Z} = S_0 - \underline{S}$$

given at the beginning of this paragraph, can be replaced by:

$$\underline{Z} = S_0 - \underline{K}_{head} - \underline{K}_s * \underline{M}$$

in which M has the distribution of the N highest waves.

In "PROBABILISTIC LOAD DETERMINATION", Th. Mulder and J.K. Vrijling's contribution to the SYMPOSIUM ON HYDRAULIC ASPECTS OF COASTAL STRUCTURES, held in 1980, the probabilistic approach to hydraulic loads on the Oosterschelde storm surge barrier is treated in detail. This article is reproduced in full on the following pages.

II.15. PROBABILISTIC DETERMINATION OF THE LOAD FOR THE OOSTERSCHELDE STORM SURGE BARRIER

The following article, with the title Probabilistic Load Determination, written by Mulder, Th. and Vrijling, J.K., is taken from a contribution towards the Symposium on Hydraulic Aspects of Coastal Structures (1980).

SUMMARY

This paper deals with a probabilistic approach of the hydraulic loading conditions of the Oosterschelde storm surge barrier. The joint probability density function of the hydraulic boundary conditions (storm surge level, wave energy and water level at the Oosterschelde-basin) is used as input. By introducing linear spectral transfer functions between the load and the hydraulic parameters, this density function can be transformed into the two-dimensional probability density function of wave and static loads, from which the probability distribution of the total hydraulic load can be derived by integration.

The transfer functions needed were determined with the aid of a mathematical model, which has been checked by a series of hydraulic model tests.

By applying a probabilistic load determination as indicated above, the total horizontal load at the storm surge barrier was reduced by approximately 40%, as compared to the rather pessimistic outcome of a deterministic load determination, in which all unfavourable and unlikely effects are assumed to coincide. The probabilistic load determination has also been used in a probabilistic approach of the behaviour of the storm surge barrier, in which the structural properties were treated as random variables, in addition to the loads. In this way a risk analysis has been executed to find the failure probabilities of several parts of the barrier, which have to be in balance.

II.15.1. INTRODUCTION

After the storm flood disaster of February 1st. 1953, The Netherlands Delta Committee stipulated that primary sea-retaining structures have to provide full protection against storm surge levels with an excess frequency of 2.5×10^{-4} times per year. In the case of conventional defences, such as dikes, an extreme water level may be used as a design criterion, because overtopping is considered to be the most important threat to dikes. In the preliminary design stage of the Oosterschelde storm surge barrier, a design storm surge level was chosen in accordance with the report of the Delta Committee. This surge level was combined with a maximum extrapolated single wave and a low estimate of the inside water level to determine the hydraulic load (deterministic approach).

In fact this approach is unsuitable for a storm surge barrier. The structure consists of concrete piers, steel gates, a sill, a bed protection and a foundation. These components have to be designed on the basis of load combinations, which will give the most dangerous threat to the structural stability. These load combinations originate from waves and a difference in water level across the barrier. They are therefore only partially depending on the seawater level. Thus, in the case of the storm surge barrier, the hydraulic load has to be chosen as the "potential threat". Since the design method used is a quasi-probabilistic one, this means that a design hydraulic load was chosen with a probability of exceedance of 2.5×10^{-4} per year.

In order to be able to determine this design load for the various structural parts of the barrier, a method for a probabilistic load determination has been developed.

II.15.2. HYDRAULIC BOUNDARY CONDITIONS

The basic parameters in the determination of the hydraulic load at the storm surge barrier are:

- z_m = maximum storm surge level at sea
 w = wind speed
 b = basin level at the Oosterschelde

In the paper "Hydraulic Boundary Conditions" the joint probability density function of these parameters $p_{z_m, b, w}(z_m, b, w)$ is discussed.

This joint probability density function (p.d.f.) has been used as input for the calculation of the probability distribution of the hydraulic load on the storm surge barrier.

II.15.3. TRANSFER FUNCTIONS

To transfer the hydraulic parameters into the hydraulic loads, the static loads and the wave loads have to be written as functions of the parameters:

Static load:

$$S = G(z_m, b, geometry) \quad (1)$$

Wave load spectrum:

$$S_w = H(z_m, w, geometry) \quad (2)$$

In the case of the static load this function can be easily determined from the hydrostatic pressure distribution on both sides of the barrier and potential flow pattern in the sill around the base of the pier.

The transfer from waves to wave loads has been done with the aid of a spectral method. To allow the application of such a method the transition from waves to wave loads has to be a linear system. In the case of the storm surge barrier this criterion was fulfilled, as has been proved by model tests. This will be shown in the sections 3.2 - 3.4.

For the storm surge barrier the transfer functions have been determined with the aid of a mathematical model, as will be discussed in the next section.

II.15.3.1. MATHEMATICAL MODEL

In the mathematical model an incoming wave field with elevation η_i is considered as a stochastic process in (x,y,t). The two-dimensional energy density spectrum of η_i is $S_{\eta_i}(f, \theta)$. This spectrum is defined as follows:

$$S_{\eta_i}(f) = \int S_{\eta_i}(f, \theta) d\theta \quad (3)$$

$$D(\theta; f) = \frac{S_{\eta_i}(f, \theta)}{S_{\eta_i}(f)} \quad (4)$$

in which $D(\theta; f)$ is a directional spectrum, giving the relative energy density for the directions in case of a fixed f . For the storm surge barrier the following function has been assumed (see [1])

$$D(\theta; f) = 2 \cdot \cos^2(\theta - \bar{\theta}) \quad \text{for } |\theta - \bar{\theta}| < \frac{\pi}{2} \text{ and } 0 < f < \infty \quad (5)$$

in which θ = angle between the mean direction of wave propagation and the axis perpendicular to the barrier.

The energy density spectrum $S_w(f)$ of the wave load $W(t)$ at the structure can be determined as (see [1]):

$$S_w(f) = \int_{-\pi}^{\pi} O^2(f) r^2(f, \theta) S_{\eta_i}(f, \theta) d\theta \quad (6)$$

in which:

$O(f)$ = the wave load (o-top) per unit of incoming wave amplitude, as a function of the frequency f . The waves are assumed to be long crested and perpendicular to the structure.
 k = wave number.
 $r(f, \theta)$ = the ratio of the total wave load of a structure of length $2l$ for oblique wave attack (approach angle θ) of the total wave load for a perpendicular approach of the waves:

$$r(f, \theta) = \frac{\sin(kl \sin\theta)}{kl \sin\theta} \quad (7)$$

Assuming a relatively narrow wave load spectrum $S_w(f)$, and a Rayleigh- distribution of the individual wave load peaks, the traditional parameters W_s (significant wave load) and T_w (mean wave load period) can be obtained by the following relations.

$$W_s = 2\sqrt{m_0} \quad (8)$$

$$T_w = \sqrt{\frac{m_0}{m_2}} \quad (9)$$

$$m_n = \int_0^{\infty} f^n S_w(f) df \quad (10)$$

Function $O(f)$ is determined numerically by calculating per wave frequency (wave period) the wave load per unit of wave amplitude a_i ($= H_i/2$).

The basis of this calculation is the following wave pressure distribution according to a linear wave theory, for partially reflected waves against a vertical wall:

- between the upper side of the sill and the sea water level ($0 < z < d$):

$$p(x, z, t) = \rho g a \frac{\cosh(kz)}{\cosh(kd)} \sqrt{1 + \alpha^2 + 2\alpha \cos(kx)} \sin(\omega t + \varphi) \quad (11)$$

with the boundary pressures:

$p_d(x, t)$ for $z=d$;

$p_0(x, t)$ for $z=0$.

- above the sea water level ($z > d$):

$$p(x, z, t) = p_d(x, t) - \rho g(z - d) \quad (12)$$

- in the sill ($z < 0$):

$$p(x, z, t) = p_0(x, t) e^{-kz} \quad (13)$$

in which:

k = wave number

α = reflection coefficient

ω = angular frequency

t = time

$$\varphi = \text{phase shift} = \arctan\left(\frac{1 - \alpha}{1 + \alpha} \tan(kx)\right)$$

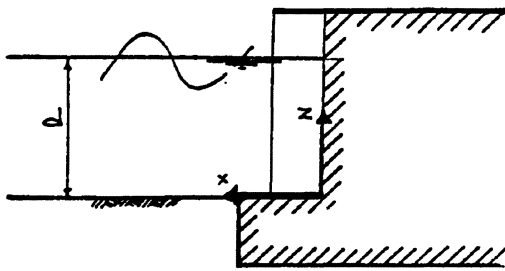
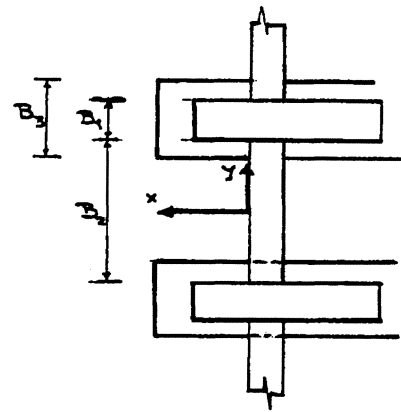


Figure II-101 Cross section.



Top view.

By integration of the pressure distribution over the height of the structure the wave load at a vertical plane j with a width B_j can be determined:

$$W_j = \int p(x_j, z, t) B_j dz \quad (14)$$

By doing this for the various vertical planes of the barrier, like the gate, the front of the pier wall and the front of the pier footing, the total load due to a regular wave at the barrier can be found:

$$W(t) = \sum_{j=1}^{\infty} W_j(t) \quad (15)$$

The maximum of this wave load function $W(t)$ divided by the incoming wave amplitude gives us the transfer value for the wave period considered.

II.15.3.2. DESCRIPTION OF MODEL FACILITIES

The hydraulic model tests have been executed in two 100 m long wind-wave flumes of the Delft Hydraulic Laboratory.

Investigations with perpendicular wave attack were executed in the 2 m wide wind-wave flume, and investigations with oblique wave attack in the 8 m wide wind-wave flume (see Figures II-106 and II-107). The irregular waves applied in the investigations were generated by programmable wave boards, driven by hydraulic actuators and commanded by analogue signals.

Wave conditions characterized by the spectral shape and wave height distribution, may be generated by a proper adjustment of the input filter function and amplification. The wave form is further adjusted to the natural shape by wind.

The wave pattern has been measured by resistance type wave height metres. The tests with perpendicular wave attack were carried out using a model scale 1:60, with dummy sections at both sides of the measuring sections, to close the flume entirely.

The total forces are measured by strain gauges attached on a dynamometer frame. The model section is hanging free from dummy sections and the bottom.

II.15.3.3. SERIES OF TESTS

In the first place, tests with regular waves have been executed in the 2 m wide wind wave flume. A great number of H,T- combinations have been tested varying the following parameters:

- sea water level
- basin level Oosterschelde
- water depth

In this way it was possible to check the linearity of the transfer from waves into wave loads and to determine the reflection coefficient as a function of the above mentioned parameters (incl. the wave

period). The reflection coefficients have been determined from wave height measurements in a "standing" wave in front of the structure. From a linear wave theory the reflection coefficient will be:

$$\alpha = \frac{H_{\max} - H_{\min}}{H_{\max} + H_{\min}} \quad (16)$$

in which H_{\max} and H_{\min} are respectively the wave height in a anti node and in a node of the "standing" wave. Secondly, tests with irregular waves have been performed to check the transfer functions determined by the mathematical model. The same parameters have been varied as in the regular tests.

The influence of an oblique wave attack has been tested in the 8 m wide wind-wave flume approach with angles of 30° and 45°.

The incoming wave spectrum $S_{\eta}(f)$, needed for the determination of a transfer function, has been derived from the measured wave spectrum $S_{\eta m}(f)$ using the following relation:

$$S_{\eta}(f) = \frac{S_{\eta m}(f)}{[1 + \alpha(f)]^2} \quad (17)$$

in which $\alpha(f)$ is the reflection coefficient as a function of the wave frequency f determined from the tests with regular waves (see [4]).

II.15.3.4. RESULTS

The results of the hydraulic model tests were given as:

- wave forces per unit of wave amplitude for several wave frequencies and amplitudes (check on linearity).
- reflection coefficients as function of the wave frequency
- transfer functions
- cumulative frequency distributions of wave load peaks

Some typical results are shown respectively in Figures II-108, II-109, II-110 and II-111.

In general it could be concluded, that

- the transfer value "wave load per unit of wave height" is almost independent of the wave height: in other words, the wave load is almost linearly dependent on the wave height.
- The measured and calculated transfer functions are in good agreement, except that:
 - the transfer functions derived from measurements in the shallower locations show oscillations, in contrast to the calculated transfer functions. No satisfactory explanation has been found for this phenomenon. (See Figure II-110).
 - In approximately 10% of the cases the measured transfer functions exceed the calculated ones. So the mathematical model is not giving the mean of the test results, but a rather conservative result.
 - In the case of high sea water levels, the results of the model tests for frequencies greater than 0.11 Hz give significantly greater transfer values than one would expect from the calculation (no explanation has been found for this difference).
- The distribution of the wave load peaks follows the Rayleigh distribution quite well. (See Figure II-111.)
- The reflection coefficient is a function of the sea water level, the level of the sea bottom and the wave frequency. In general the reflection coefficient decreases for:
 - increasing wave frequency
 - increasing sea water level
 - increasing water depth
 (in case of frequencies lower than 0.15 Hz)

Summarizing it can be concluded, that the model tests support the mathematical model. Consequently this model has been used in the probabilistic load determination.

II.15.4. PROBABILISTIC LOAD DETERMINATION

II.15.4.1. GENERAL

Starting from the joint p.d.f. of the boundary conditions, the joint p.d.f. of the static load (S) and the significant wave load (W_s) - being the characteristic value of a wave load spectrum - can be found.

Secondly, the joint p.d.f. of the static load and the wave load peaks can be determined using the distribution of the individual wave load peaks, given a wave load spectrum.

Finally, the probability of exceedance of the total load can be determined.

These three steps will be described in detail in section 4.2. In view of a clear and brief notation this is done analytically. However, due to the absence of an analytical description of the wave spectra in case of the Oosterschelde storm surge barrier the determination of the load distribution has been done numerically. An impression of such a numerical transfer is given in section 4.3.

II.15.4.2. THE DESCRIPTION OF THE METHOD (see [6])

Since the basin level was found to be virtually statistically independent of the wind speed, the joint probability density function of the boundary conditions can be written as:

$$p_{z_m, b, w}(z_m, b, w) = p_b(b | z_m) \cdot p_w(w | z_m) \cdot p_{z_m}(z_m) \quad (18)$$

Using the equations (1) and (2) the conditional p.d.f.s of the static load S and the significant wave load W_s can be determined from the conditional p.d.f. $p_b(b | z_m)$ and $p_w(w | z_m)$.

$$p_w(w | z_m) = p_{W_s}(W_s | z_m) \frac{\partial W_s}{\partial w} \quad (19)$$

$$p_b(b | z_m) = p_S(S | z_m) \frac{\partial S}{\partial b} \quad (20)$$

Using (19) and (20), equation (18) can be transferred in

$$p_{z_m, b, w}(z_m, b, w) = p_{W_s}(W_s | z_m) \cdot p_S(S | z_m) \cdot p_{z_m}(z_m) \cdot \frac{\partial W_s}{\partial w} \cdot \frac{\partial S}{\partial b} \quad (21)$$

so:

$$p_{W_s, S}(W_s, S) = p_{z_m, b, w}(z_m, b, w) \cdot \frac{1}{\frac{\partial W_s}{\partial w} \cdot \frac{\partial S}{\partial b}} \cdot dz_m \quad (22)$$

Secondly, it is now possible to transfer $p_{W_s, S}(W_s, S)$ in a joint p.d.f. of the static load and the wave load peaks W , as follows:

$$p_{W, S}(W, S) = \int_{W_s} p_{W_s, S}(W_s, S) \cdot \frac{\partial Pr_i}{\partial W} \cdot dW_s \quad (23)$$

in which Pr_i represents a probability distribution, which depends on the limit state considered. In the following, three kinds of limit state are discussed.

1. In cases, where all wave load peaks are in principle important, the Rayleigh distribution will be used:

$$Pr_1 = Pr(W > W | W_s) = e^{-2 \left(\frac{W}{W_s} \right)^2} \quad (24)$$

In case of the storm surge barrier this distribution has been used for the increasing deformations of the subsoil (see Kooman e.a. [12]).

2. If, however a model is considered in which a one time exceedance of the load leads to a collapse, than the probability distribution of the wave loads, which are exceeded at least once, has to be used. Starting from N independent wave load peaks within the duration of a sea state, according to the binomial distribution the probability, that none of the wave load peaks will exceed a level W, equals

$$\{1 - Pr(\underline{W} > W | W_s)\}^N$$

The probability Pr_2 that W is exceeded at least once, equals

$$Pr_2 = 1 - \{1 - Pr(\underline{W} > W | W_s)\}^N \quad (25)$$

In case of the storm surge barrier this probability distribution has been used in the structural design of the pier, the beams and the gate.

3. Finally, we can also look at another model, where collapse only occurs, when a load level is exceeded several times (in case of failure of an element of the barrier due to fatigue). Based on the binomial distribution we find for the probability Pr_3 that a load peak exceeds a given level W at least m times, out of N.

$$= 1 - \left[\sum_{h=0}^{h=m-1} \frac{N!}{h!(N-h)!} \cdot Pr(\underline{W} > W | W_s)^h \cdot \{1 - Pr(\underline{W} > W | W_s)\}^{N-h} \right] \quad (26)$$

To arrive at a probability distribution of a total load T for a specific limit state, based on the joint p.d.f. of the wave load peaks and the static load, it has to be known in which ratio the wave load and the static load contribute to this limit state.

In general this can be defined as follows:

$$\underline{T} = \beta \underline{S} + \gamma \underline{W} \quad (27)$$

Now the probability of exceedance of a specified total load $Pr\{\underline{T} > T\}$ can be determined per limit state by integrating the bidimensional probability density function $p_{\underline{W},\underline{S}}(W,S)$ over the area for which $\beta S + \gamma W > T$.

$$Pr(\underline{T} > T) = \int_{\beta S + \gamma W > T} p_{\underline{W},\underline{S}}(W,S) dW dS \quad (28)$$

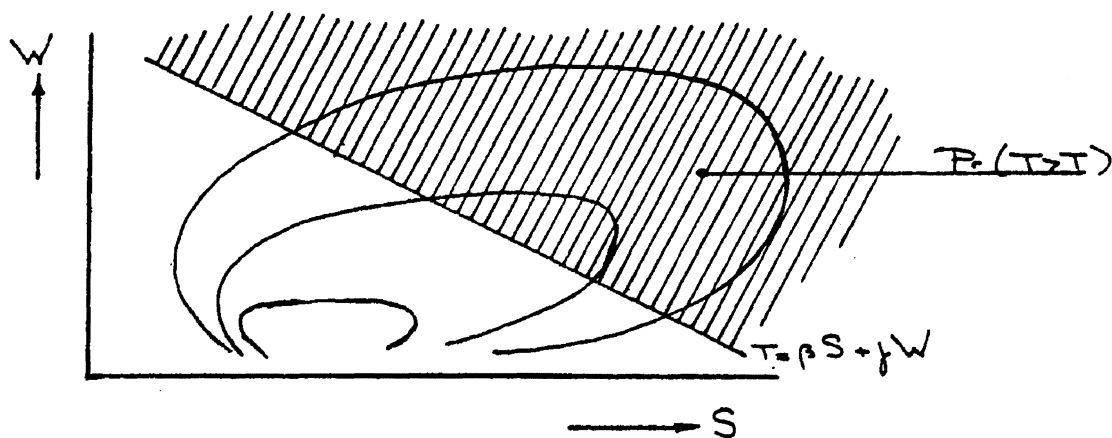


Figure II-102

II.15.4.3. NUMERICAL TRANSFER (see [6])

Since a description of the complete numerical transfer will be too extensive, only one transfer will be described, which is typical for the entire method. For this purpose the transfer from the joint p.d.f. of the basin level and the sea water level to the p.d.f. of the static load is chosen.

From the p.d.f. of the sea water level the probability of occurrence per class Δz can be determined as follows:

$$Pr\{z_{mi} - \frac{\Delta z}{2} < z_m < z_{mi} + \frac{\Delta z}{2}\} = \int_{z_{mi} - \frac{\Delta z}{2}}^{z_{mi} + \frac{\Delta z}{2}} p_{z_m}(z_m) dz_m$$

In the same way for the basin level can be calculated:

$$Pr\{b_j - \frac{\Delta b}{2} < b < b_j + \frac{\Delta b}{2} | z_m\} = \int_{b_j - \frac{\Delta b}{2}}^{b_j + \frac{\Delta b}{2}} p_b(b | z_m) db$$

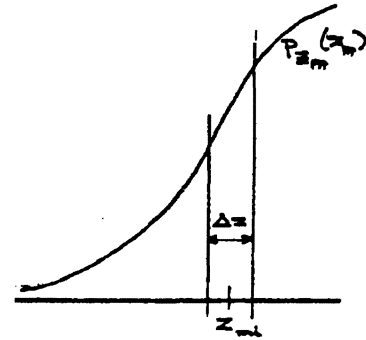


Figure II-103

The joint probability of occurrence $Pr\{z_{mi}, b_j\}$ of the basin level class and the sea water class z_{mi} will be:

$$Pr\{z_{mi}, b_j\} = Pr\{z_{mi} - \frac{\Delta z}{2} < z_m < z_{mi} + \frac{\Delta z}{2}\} * Pr\{b_j - \frac{\Delta b}{2} < b < b_j + \frac{\Delta b}{2} | z_m\}$$

For a given geometry the static load S_{ij} for a sea water level z_{mi} and basin level b_j can be determined.

Per definition the probability of occurrence of this static load equals the joint probability of occurrence:

$$Pr\{S = S_{ij}\} = Pr\{z_{mi}, b_j\}$$

By dividing the complete static load range in classes S_{ij} with class middle S_i it is possible to group all the static loads S_{ij} ($i = 1, 2, \dots, I$ and $j = 1, 2, \dots, J$).

By adding the probabilities of occurrence of the static loads S_{ij} which belong to a static load class S_i , the probability of occurrence of S_i can be found:

$$Pr\{S_i - \frac{\Delta S}{2} < S < S_i + \frac{\Delta S}{2}\} = \sum_{i=1}^I \sum_{j=1}^J Pr\{S = S_{ij}\} * Y_{ij}$$

in which $Y_{ij} = 1$ for those combinations ij , satisfying:

$$S_i - \frac{\Delta S}{2} < S_{ij} < S_i + \frac{\Delta S}{2}$$

$Y_{ij} = 0$ for the other combinations i, j .

In this way a histogram of the static load is found.

II.15.5. THE RELIABILITY OF THE METHOD

II.15.5.1. THE DESCRIPTION OF THE ANALYSES

The probabilistic load determination as described in the previous paragraph, is based on the statistical descriptions of the hydraulic boundary conditions. After the transfer from boundary conditions into loads and executing the statistical compilations, the probability distribution of the hydraulic load was found. In this method the statistical descriptions of the hydraulic boundary conditions, the assumptions with regard to the determination of wave spectra and some assumptions in the method itself, have not been varied. Therefore the result of the method will be a probability distribution with deterministic parameters. In reality the parameters of the probability distribution will have a stochastic character.

A study has been executed concerning this stochastic character. This has been done by means of a so called "mean value first order second moment method" [5].

This method is based on the following assumptions:

- The probability distribution Pr can be described as a function of the parameters x_i determining this distribution. These parameters are considered to be stochastic variables.

$$Pr = f(x_1, x_2, \dots, x_i, \dots, x_n)$$

- The parameters x_i have Gaussian distributions with means μ_{xi} , and a standard deviations σ_{xi}
- A linear approximation of $f(x_1, x_2, \dots, x_n)$ is obtained by expanding the relationship in a Taylor series in a point x^* and retaining the first two terms.

$$Pr = f(x_1^*, x_2^*, \dots, x_n^*) + \sum_{i=1}^n (x_i - x_i^*) \frac{\partial f(x_i^*)}{\partial x_i}$$

- The function $f(x_1, x_2, \dots, x_n)$ is linearized at the mean $\underline{m} = (m_1, m_2, \dots, m_n)$, so $\underline{x}^* = \underline{m}$.

These assumptions justify the following conclusions with regard to Pr :

1. Pr has a Gaussian distribution
2. The distribution properties are:

$$\mu_{Pr} = f(\underline{m})$$
$$\sigma_{Pr} = \sqrt{\sum_{i=1}^n \left(\frac{\Delta f(\underline{m})}{\Delta x_i} \sigma_{xi} \right)^2}$$

As an example in this paper, the reliability of the probability distribution of the total hydraulic load normal to be barrier in case of 4 piers, namely R3, R19, H9 and H15 will be discussed.

The following parameters x_i have been considered:

1. the frequency of exceedance curve of storm surge levels;
2. the probability distributions of basin levels;
3. transfer functions with regard to:
 - a. static load above the sill;
 - b. static load in the sill;
 - c. wave load above the sill;
 - d. wave load in the sill.
4. the duration of a storm surge level;
5. wave spectrum;
6. the p.d.f. of wave spectra per storm surge level class.

For the parameters on which 5 and 6 have been based, reference is made to Vrijling and Bruinsma [9].

An overview of the values $\frac{\Delta f(m)}{\Delta x_i} \sigma_{x_i}$ for the various piers is given in Table 1.

parameters	R 19		R 3		H 15		H 9	
	kN	%	kN	%	kN	%	kN	%
1	4250	26.7	3420	24.0	3070	30.3	3620	35.2
2	2272	7.6	1480	4.5	1423	6.5	1779	8.5
3a,b	2146	6.8	1610	5.3	1498	7.2	1644	7.2
3c,d	2870	12.1	2616	14.0	1915	11.8	1879	9.5
4	229	-	203	-	149	-	150	-
5,6	5636	47.0	5045	52.2	3709	44.2	3842	39.6
	8240	100.0	6987	100.0	5580	100.0	6106	100.0

Table 1.

II.15.5.2. RESULTS

The results of the analyses, being the mean μ_{Pr} , the standard deviation σ_{Pr} and the contribution of each parameter to the standard deviation (in percentages), are given in Table 1.

Comparing the results of this study with the probability distribution with deterministic parameters used in the design, it became clear that the deterministic distributions give approximately 7% higher load values than the "mean" distribution curve of the stochastic approach. This has been caused by the fact that the by "engineering judgement" chosen constants were rather pessimistic mainly for the parameters:

- wave load above sill (see section II.15.3.3);
- schematized relation H - T (see [9]);
- foreshore (see [9]).

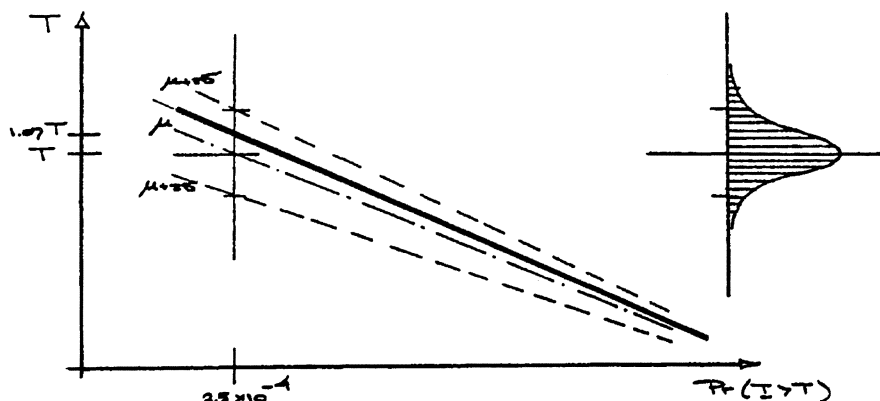


Figure II-104

Also it can be seen that the probability distribution curve with an excess frequency of 2.3% ($\mu_{Pr} + 2\sigma_{Pr}$) exceeds the curve calculated with deterministic parameters only in a minor way. This exceedance has been embodied in a partial safety coefficient γ_{s3} (according to ISO standard 2394). This coefficient is intended to allow possible adverse modification of the load effects, due to incorrect design assumptions and constructional discrepancies.

II.15.6. THE APPLICATIONS IN THE DESIGN PROCESS

The probability distributions of the total hydraulic load have been applied in two ways, depending on the design method used. To be able to discuss the applications a brief review of the existing design methods is given first.

II.15.6.1. THE DESIGN METHOD

The element "load greater than strength" is one of the most fundamental criteria in a design process. To ensure the fulfilment of this criterion a safety margin is introduced between the expected load and the strength pursued.

In principle there are three philosophies regarding the way of introducing a safety margin in the design:

1. the deterministic design method
2. the quasi-probabilistic method
3. the (semi-) probabilistic method

ad. 1.

In the case of a deterministic method, "safe" values are chosen for the basic variables causing the load. Usually the mean values of the strength parameters are used to determine the strength. The safety margin is guaranteed by a safety-coefficient based on engineering experience.

ad. 2.

The basis of the quasi probabilistic design method is that the parameters used in the structural design are not specified constants, but stochastic variables, whose exact magnitudes are not known with certainty in the design state and in case of the hydraulic parameters, not even after construction. Because the use of these stochastic elements is not practical for the normal design activities due to the lack of statistical information and of computer programs for mass production, the concept "characteristic value" has been introduced in the structural design. The safety margin will be guaranteed by partial safety coefficients.

ad. 3.

The most advanced design method is the (semi-) probabilistic method. In this method all basic variables are specified by probability density functions. With the help of theoretical models the p.d.f.'s of the strength and of the load can be derived. These two p.d.f.'s form the basis in determining the failure probability of the mechanism. By checking this failure probability against the allowable failure probability of the total system, one can determine whether or not the safety is sufficient.

II.15.6.2. THE APPLICATION OF THE LOAD DISTRIBUTION

In case of the storm surge barrier two design methods have been used, the quasi-probabilistic and the semi probabilistic one. In both of the methods the probability distribution of the hydraulic loads has been used.

II.15.6.2.1. QUASI- PROBABILISTIC DESIGN METHOD

In this method, which is the most practical one, a load with a certain excess frequency is chosen from the load distribution.

In the case of the storm surge barrier the design criterion is that the barrier has to withstand - with a certain safety margin - a potential threat with an excess frequency of $2.5 \cdot 10^{-4}$ /year. Considering the task of the barrier it will be obvious that this potential threat is based on the natural boundary conditions, mainly waves and water level differences, which manifest themselves in the hydraulic load. For that reason the design loading has been defined as the total hydraulic load with an excess frequency of $2.5 \cdot 10^{-4}$ times/year.

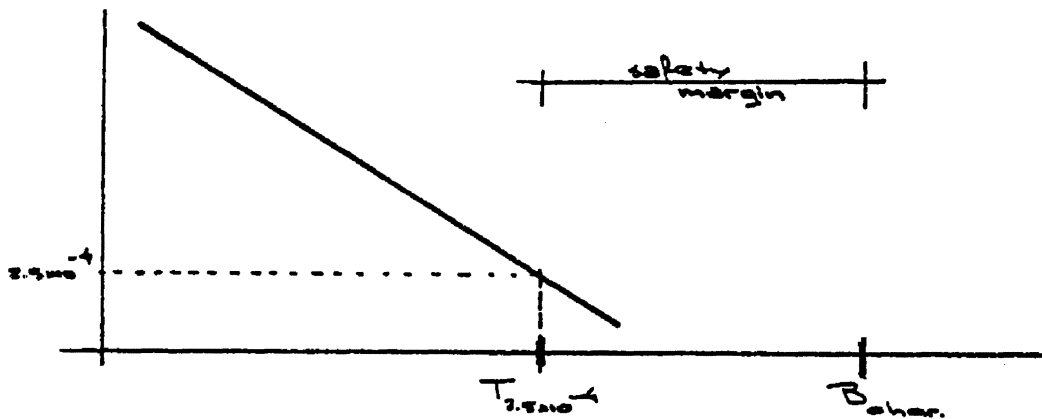


Figure II-105

This hydraulic load derived from the probability distribution has been used as an extreme load, being a characteristic load multiplied by a safety coefficient of overloading. This extreme load is used in combination with a characteristic strength and the partial safety coefficients needed. So, in terms of design methods, a quasi-probabilistic design method has been applied.

II.15.6.2.2. SEMI- PROBABILISTIC DESIGN METHOD

Simultaneously with the "everyday" design activities a risk analysis of the storm surge barrier has been executed. A first step in this risk analyses was to make an overview of all possible causes and circumstances which may lead to a mal-functioning of the storm surge barrier and from that to the inundation of several parts of SW- Netherlands.

Subsequently, the causal connection between the elements have been determined, which has been done with the aid of so called fault trees (and event trees). An ever returning element in the fault tree is the state "Load greater than strength". This plays a very important role in every part of the barrier. A state in which the external load at the structure equals the loading capacity of the structure is called a limit state. Consequently, a structure has a number of limit states equal to the number of failure mechanisms.

A last step in the risk analyses is to determine as exactly as possible the probabilities of all the elements in a fault tree, in order to determine the probability of mal-functioning of the barrier. This overall mal-functioning probability has to fulfil an acceptable level.

To be able to determine the probability of failure of a limit state of a structural part of the barrier a semi-probabilistic design method has been applied. In this method it is possible to use the full statistical description of the hydraulic load in combination with strength parameters as stochastic variables.

For those cases when:

the transfer functions from the hydraulic parameters to the hydraulic load are available in an analytical form

and:

the theoretical models are available to determine the loading capacity of the structure from the strength parameters,

the semi-probabilistic design method can be done fully analytically. A so called "advanced first order second moment method" can be used in that case (see 5). In the design of the storm surge barrier this has been applied to:

- the main cross section of the floor slab;
- the overall stability of the piers;
- the main girders of the gate.

II.15.7. CONCLUSIONS

- A probabilistic load determination as discussed in this paper allows a more realistic hydraulic design load, to be used in the prevailing design methods, than the conventional deterministic methods. It avoids a too pessimistic load determination. In the case of the most heavily loaded pier this has resulted in the figures as mentioned in the table below.

	deterministic approach	probabilistic approach
storm surge level	NAP + 5.50 m	$Pr(z_m > z_m) = e^{-2.3 \frac{z_m - 2.94}{0.696}}$
wave spectrum	height = 10 m; period = 12 s	$P_{S_{\eta_i}}(S_{\eta_i} z_m)$
basin level	NAP - 1.70 m	$P_b(b z_m)$
total hor. force	T = 173 MN	$Pr(T > 100 MN) = 2.5 * 10^{-4}$

- A reliability analysis of the probabilistic method shows that a probability distribution curve with an excess frequency of 2.3% ($\mu_{Pr} + 2 \sigma_{Pr}$) exceeds the curve derived from constant p.d.f.'s of the parameters only in a minor way.
- The applications of a semi-probabilistic design method provides a quantitative insight into the influence of the stochastic uncertainty of the basic parameters. It thus forms an important tool in assigning priorities in study or quality control to specific parameters of theoretical models. It contributes moreover to an overall risk analysis of the system by providing the probability of failure of each element of the system.

ACKNOWLEDGEMENTS

The authors wish to express their thanks to Dr. Ir. J.A. Battjes for his valuable comments during the preparation of the manuscript.

REFERENCES

1. Battjes, J.A.; The effect of the oblique wave attack and short crestedness on the wave load (Dutch), 1978.
2. Betlehem, J.G., Does, R.J.M.M., and Helmers, R.; Report of a statistical investigation with regard to a probabilistic load determination (Dutch), 1978.
3. Does, v.d. , Bijl, de, Mazijk, A. van and Thabet, R.A.H.: Stability of the top layer of the sill. Symposium on Hydraulic aspects of coastal structures, Rotterdam , 1980.
4. Ishida, A.; Transformation of power spectra of wind generated waves caused by reflection. Coastal engineering in Japan, Vol. 15, 1972.
5. Flint, A.R. and Baker, M.J.; Rationalisation of safety and service ability factors in structural codes. CIRIA report 63, 1976.
6. Mulder, Th.; Probabilistic load determination in case of storm surge barrier Oosterschelde. Deltadienst DDTW 79.009 (Dutch).
7. Mulder, Th.; The reliability of the probability distribution of the hydraulic load. Deltadienst DDWT 78.276 (Dutch).
8. Mulder, Th.; The transfer functions of the hydraulic load perpendicular to the storm surge barrier. Deltadienst DDWT 79.325 (Dutch).
9. Vrijling, J.K. and Bruinsma, J.; Hydraulic Boundary Conditions. Symposium on Hydraulic aspects of coastal structures, Rotterdam, 1980.
10. Probabilistic calculations. T.N.O.- IBBC report B-78-30 (Dutch).
11. Risk analyses of the storm surge barrier. T.N.O.-IBBC report B-79-494 (Dutch).

LIST OF SYMBOLS

α_i	amplitude of a regular wave
B_j	width of a structure element
B_{char}	characteristic strength
b	basin level Oosterschelde
d	water depth (till still water line)
$D(\cdot)$	directional spectrum
f	wave frequency
$G(\cdot)$	function (static load)
H_{max}	wave height in an anti node of a standing wave
H_{min}	wave height in a node of standing wave
H_s	significant wave height
h	binomial coefficient
k	wave number
l	dimension of the structure
m	number of load exceedances
m_0	area of wave load spectrum
m_2	second moment of wave load spectrum
m_n	n-th moment of wave load spectrum
N	number of wave loads
$O(f)$	transfer function
Pr	probability of exceedance
p	probability density
$p(x,z,t)$	wave pressure
$r(\cdot)$	correction factor (oblique wave attack)
S	static load
$S_{ni}(f)$	spectral density of incoming waves
$S_w(f)$	spectral density of wave loads
t	time

T_p	peak period of waves
T_w	mean wave load period
T	total load
w	wind velocity during 1 hour
W	wave load
W_s	significant wave load
x	coordinate
x_i	basic variable hydraulic load
x_i^*	x_i in design point
y	coordinate
z	accounting factor
z	coordinate
z_m	maximum storm surge level
$\alpha, \alpha(f)$	reflection coefficient
β	contribution factor (static load)
γ	contribution factor (wave load)
φ	phase shift
ϱ	approach angle of waves
θ	mean approach angle of waves
μ_{Pr}	mean of $Pr(\underline{T} > T)$
μ_{x_i}	mean of x_i
σ_{Pr}	standard deviation of $P(\underline{T} > T)$
σ_{x_i}	standard deviation of x_i
ω	angular frequency
ρ	specific density of water
η_i	elevation

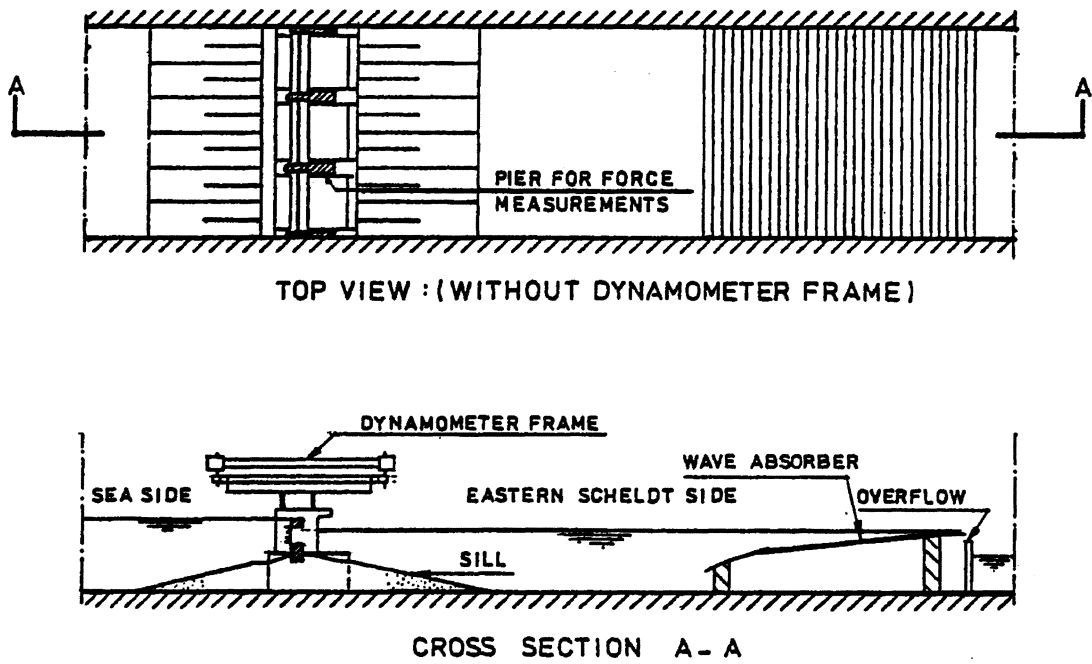


Figure II-106: Model set-up in the 2 meters wide wind-wave flume

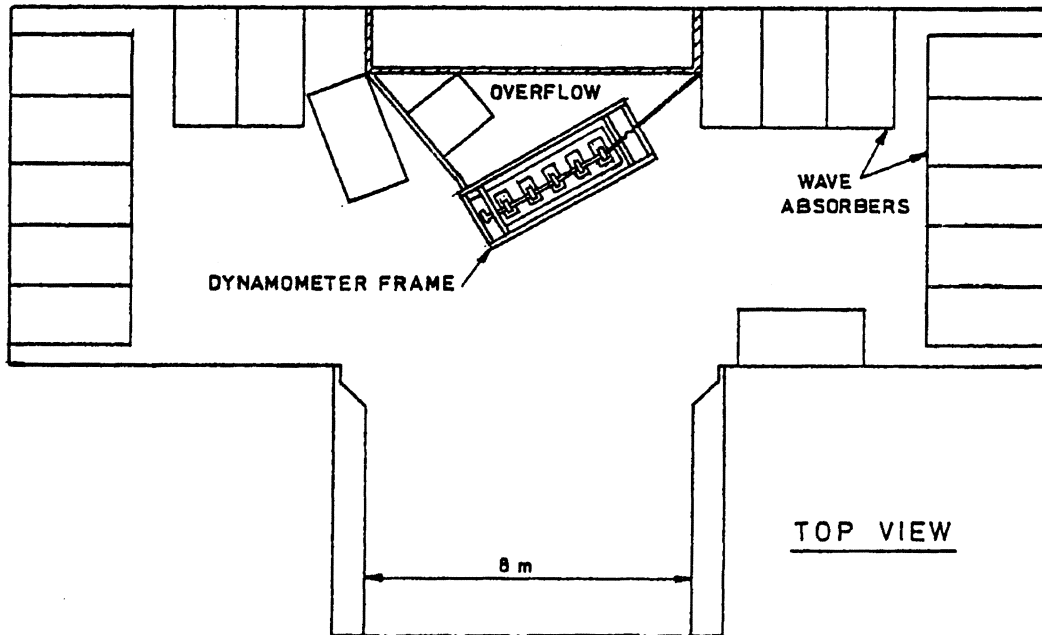


Figure II-107: Model set-up in the 8 meters wide wind-wave flume

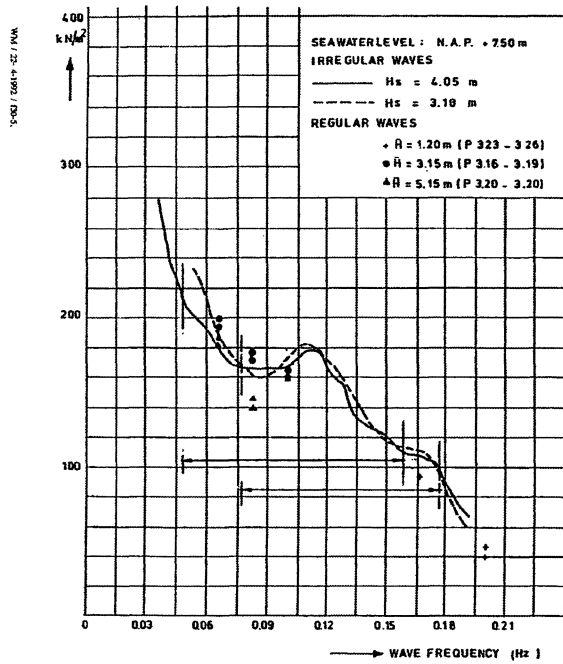


Figure 108: Wave forces per unit of wave amplitude in comparison with a continuous transfer

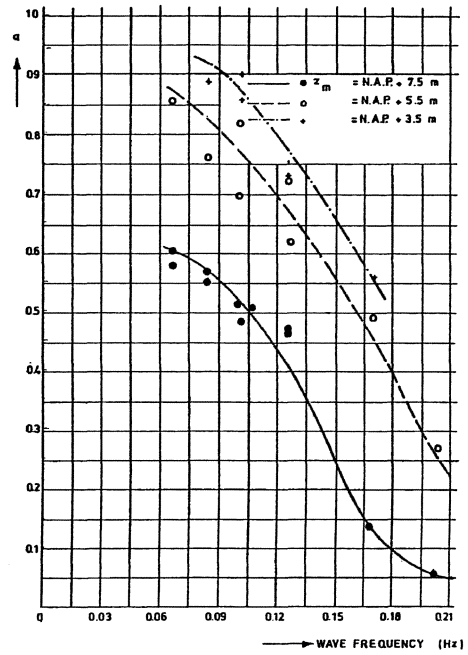


Figure II-109: Reflection coefficient

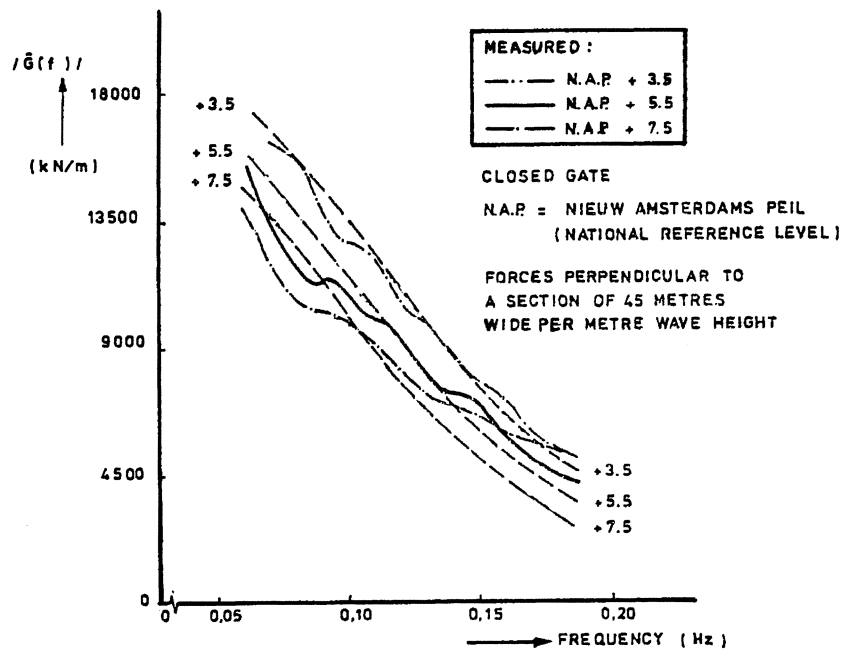


Figure II-110: Comparison of calculated and measured transfer functions for different water levels at the sea side

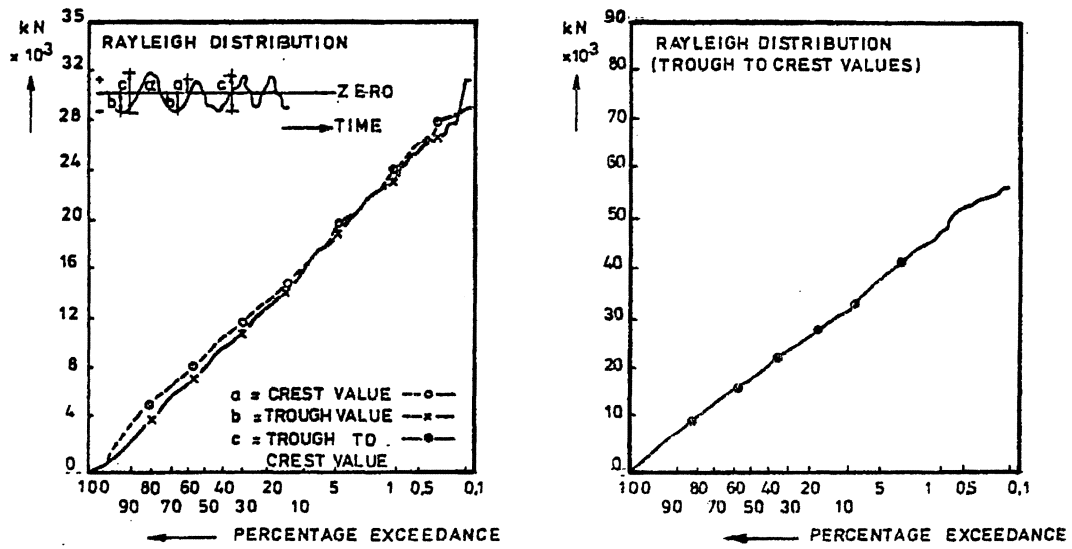


Figure II-111: Cumulative frequency distributions of total force perpendicular to structures' center-line

APPENDIX II-1 COMPARISON OF GUMBEL DISTRIBUTION WITH WEIBULL DISTRIBUTION

Wave data Karwar JUNE2JULY WAVE DATA. (291 observations)

↓	Hs	Tz	Tp	Hs	Tz	Tp	Hs	Tz	Tp	Hs	Tz	Tp	Hs	Tz	Tp
1.94	7.54	10.5	2.49	7.54	11.1	2.08	7.84	11.1	1.76	7.44	11.1	2.37	6.0	8.3	
1.95	7.52	10.5	2.87	7.54	10.5	2.05	7.2	11.1	1.72	7.12	10.5	2.21	6.08	8.6	
1.9	7.35	15.3	3.18	7.53	12.5	2.1	7.31	11.1	1.82	7.34	10.5	2.23	6.47	10.0	
1.81	7.32	10.5	2.8	7.31	11.7	2.25	7.78	11.1	1.73	6.98	10.5	2.27	6.87	10.5	
1.95	7.39	10.5	2.91	7.69	11.7	2.24	6.2	11.7	1.69	6.97	11.1	2.29	6.31	10.5	
1.85	6.97	10.5	2.76	7.36	11.7	2.44	6.37	11.7	1.69	6.97	10.5	2.27	6.29	10.5	
1.8	7.03	10.5	2.78	7.74	12.5	2.56	6.28	11.7	1.69	7.02	10.5	2.4	6.07	11.1	
1.8	7.11	10.5	2.4	7.6	12.5	2.32	6.42	11.7	1.84	7.46	10.5	2.58	5.98	11.1	
1.84	7.67	10.5	2.56	7.65	11.7	2.31	7.03	11.7	1.76	6.76	10.5	2.52	6.39	11.1	
1.68	7.3	10.5	2.66	7.49	11.1	2.2	6.57	11.7	1.73	7.01	11.1	2.5	6.46	10.5	
1.62	7.38	10.5	2.63	7.58	12.5	2.43	7.25	11.7	1.76	7.13	11.1	2.37	6.3	11.1	
1.65	7.38	11.1	2.66	7.68	11.7	2.24	7.14	11.1	1.91	6.59	11.7	2.29	6.35	11.1	
1.64	6.76	11.1	2.79	7.5	11.7	2.22	6.89	11.1	1.77	6.73	11.1	2.47	6.07	11.1	
1.69	7.11	11.1	2.59	7.02	12.5	2.57	6.44	11.7	1.81	7.22	11.1	2.7	6.36	10.5	
1.65	6.94	10.5	2.8	7.14	11.7	2.62	6.55	10.5	1.77	7.71	11.1	2.76	7.42	13.3	
1.63	6.55	11.1	2.85	6.92	11.7	2.43	7.3	11.7	1.72	7.54	11.1	2.85	7.42	13.3	
1.66	6.35	10.0	2.5	6.88	11.7	2.51	7.42	11.7	1.71	7.4	11.1	2.59	7.4	12.5	
1.73	6.76	10.5	2.79	7.5	11.7	2.57	7.8	11.7	1.85	7.13	11.1	2.72	7.52	12.5	
1.78	6.4	10.5	2.59	7.02	12.5	2.38	7.53	12.5	2.02	7.39	11.1	2.71	7.64	12.5	
1.63	6.3	9.5	2.8	7.14	11.7	2.45	7.74	11.7	1.85	7.25	11.1	2.37	7.45	11.1	
1.55	7.0	9.5	2.85	6.92	11.7	2.24	7.6	12.5	1.72	7.24	11.7	2.49	7.66	12.5	
1.63	7.34	11.1	2.5	6.88	11.7	2.15	7.38	11.7	1.86	7.52	11.7	2.52	7.71	12.5	
1.62	7.21	11.1	2.62	7.57	11.1	2.27	7.33	11.7	1.85	7.8	11.7	2.31	7.64	12.5	
1.72	6.65	11.1	2.56	7.54	11.7	2.06	7.28	12.5	1.81	7.99	11.1	2.32	7.57	12.5	
1.71	7.55	11.7	2.19	7.86	11.7	2.06	7.5	10.5	1.86	6.99	11.7	2.38	7.69	12.5	
1.72	7.4	11.7	2.13	7.22	11.1	2.09	6.91	11.1	1.85	6.64	11.1	2.38	7.62	12.5	
1.82	7.65	11.7	2.25	7.71	11.7	2.27	7.61	12.5	1.92	6.82	11.1	2.4	7.78	12.5	
1.67	7.48	10.5	2.24	7.05	11.7	2.34	7.77	11.7	1.9	6.36	11.1	2.44	7.39	11.7	
1.73	7.33	10.5	2.24	7.16	11.7	2.25	7.61	11.7	1.98	6.55	11.1	2.18	6.93	12.5	
1.7	6.75	11.1	2.23	7.18	11.7	2.03	7.54	11.1	2.05	6.57	11.7	2.44	7.39	12.5	
1.71	6.82	10.5	2.12	7.19	11.1	1.99	7.58	11.1	2.27	7.32	11.1	2.43	7.62	13.3	
1.69	6.81	11.1	2.1	7.58	11.1	1.84	7.68	11.1	2.45	6.39	11.1	2.36	7.9	12.5	
1.7	6.94	10.0	2.02	7.26	11.1	1.66	6.99	11.1	2.3	6.87	11.7	2.41	7.71	12.5	
1.74	6.12	11.1	2.07	7.65	11.1	1.68	7.52	11.1	2.13	6.63	10.5	2.5	7.37	12.5	
1.89	6.54	10.5	2.02	7.43	11.1	1.77	7.22	11.1	1.95	6.45	11.1	2.21	7.69	12.5	
1.83	6.28	10.0	2.05	7.53	11.1	1.78	6.32	10.5	2.04	6.76	11.1	2.25	7.46	12.5	
1.93	6.34	10.5	1.94	7.21	11.1	1.78	6.6	11.7	1.89	6.67	11.1	2.54	7.45	11.1	
2.12	6.61	18.1	1.94	7.21	11.1	1.92	7.15	11.1	1.87	6.64	11.1	2.55	7.68	11.1	
2.18	6.06	16.6	2.27	7.5	11.1	1.97	6.68	11.1	1.83	6.28	11.1	2.53	7.41	11.1	
2.15	6.36	10.5	2.06	7.53	11.1	1.83	6.73	11.1	2.15	5.44	10.0	2.51	6.96	12.5	
2.24	6.45	10.5	2.09	7.32	11.1	2.06	7.16	11.1	2.2	5.78	11.1	2.83	7.66	11.7	
2.23	6.56	10.5	2.0	7.32	10.5	1.98	7.45	11.7	2.08	6.44	11.7	2.67	7.89	10.5	
2.19	6.4	9.0	1.74	6.93	10.5	1.76	7.16	11.7	1.94	6.5	9.0	2.7	8.07	12.5	
2.12	6.88	10.0	1.83	6.97	10.5	1.76	7.4	11.1	2.18	6.66	11.1	2.74	7.88	12.5	
2.24	6.86	10.5	1.92	6.52	10.5	1.76	7.44	11.1	2.17	6.05	11.1	2.66	8.14	11.7	
2.24	6.92	10.5	1.92	7.07	11.1	2.06	7.16	11.1	2.31	5.77	11.7	2.37	8.34	11.7	
2.16	7.04	10.5	1.92	7.14	10.5	1.98	7.45	11.7	2.27	6.37	8.6	2.46	8.33	11.1	
2.4	7.66	10.5	2.16	7.4	11.1	1.76	7.16	11.7	2.18	6.12	9.0	2.46	8.33	11.1	
2.46	6.65	10.5	2.08	7.62	11.1	1.76	7.4	11.1	2.35	5.94	10.5	2.46	8.33	11.1	
2.29	7.74	11.1	1.71	6.46	11.1	1.75	5.81	10.5	1.86	6.4	10.0	1.97	6.48	10.0	
2.48	7.81	12.5	1.68	6.14	11.1	1.67	5.67	10.0	1.74	6.13	10.5	1.75	6.32	10.0	
2.33	7.67	11.7	1.65	6.17	10.5	1.75	6.19	10.0	1.74	6.21	10.5	1.7	6.08	11.1	
2.17	8.17	11.7	1.79	6.05	11.1	1.71	5.61	10.5	1.71	6.24	9.0	1.76	6.34	10.5	
1.81	7.32	11.7	1.77	5.93	10.5	1.74	5.85	8.6	1.83	6.38	10.0	1.79	6.14	10.0	
2.07	7.87	11.7	1.82	5.94	10.5	1.74	5.94	9.0	1.81	6.25	9.5	1.84	6.07	10.5	
1.81	7.32	11.7	1.68	5.9	10.5	1.71	5.66	10.0	1.8	5.89	10.0	1.84	6.34	9.5	
1.79	7.17	17.7	1.63	5.86	10.5	1.7	5.83	10.5	1.91	6.26	10.0	1.98	6.22	10.0	
1.78	6.99	10.0	1.83	5.84	10.5	1.78	6.22	10.0	1.81	5.84	10.0	2.02	6.36	10.0	
1.82	6.86	11.7													

2.16 7.4 11.1 = Start of July

The wave heights, H_s , plotted against $\frac{i}{N+1}$ (see § II.13.3.1.), are given in Figure II-38. The approximation with a Weibull distribution given there:

$$F_{H_s}(H) = 1 - e^{-\left(\frac{H-1.5}{0.675}\right)^{1.866}}$$

was determined using the Method of the Linear Least Squares (see § II.13.3.2.).

A measure for the spread around the "fit": $s = \sqrt{\frac{\sum_{i=1}^{291} (F_{H_s}(H) - y_i)^2}{291 - 2}}$.

For the above mentioned "Weibull fit" this is: $s = 0.048$.

A different measure often used for the spread around the "fit" is the correlation coefficient, r . Here: $r = 0.959$

The fit of the Gumbel distribution:

$$F_{H_s}(H) = \exp\left(-e^{-\frac{H-1.941}{0.284}}\right)$$

given in § II.3. (top of page II - 11) is also calculated using the method of the Linear Least Squares. A figure, analogue to II-38 is presented opposite.

For the spread around the fit for the Gumbel distribution $s = 0.045$ is found. The correlation coefficient for this Gumbel distribution is: $r = 0.952$.

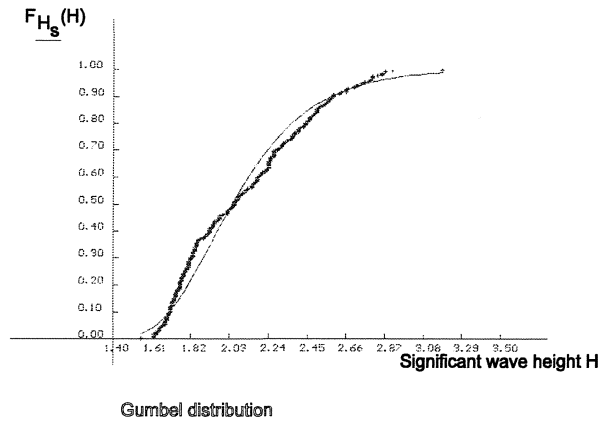


Figure II-112

Both approaches are displayed in Figure II-113:

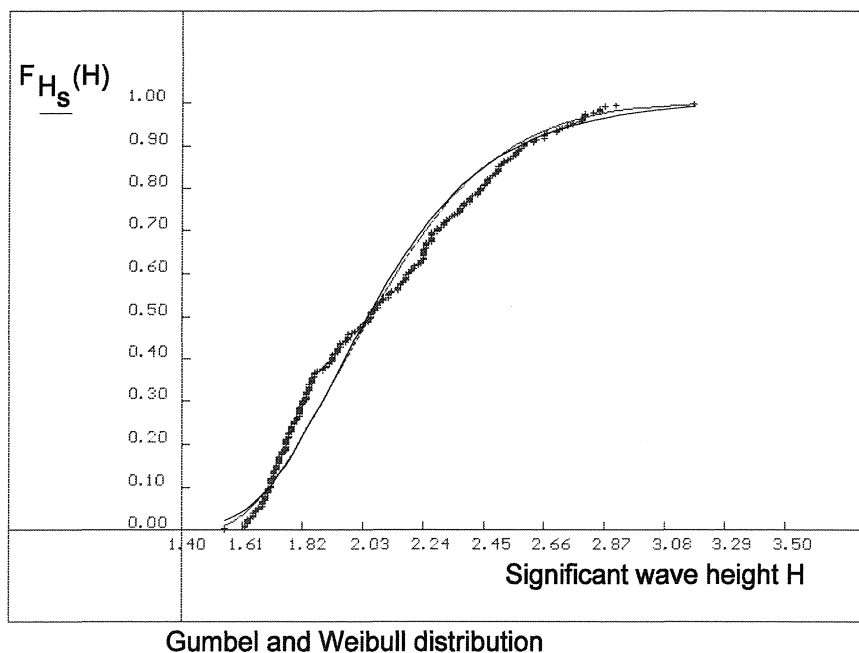


Figure II-113

Based on this figure, neither of the distributions can be selected "at a glance". The distributions, "fitted" on the data, the values of which lie between 1.55 m (lowest measured H_s) and 3.18 m (greatest measured H_s) (practically) coincide.

If one wishes to extrapolate to wave heights with small probabilities of occurrence, it is of great importance which distribution is selected. This is clearly reflected when both distributions are plotted on "Gumbel paper":

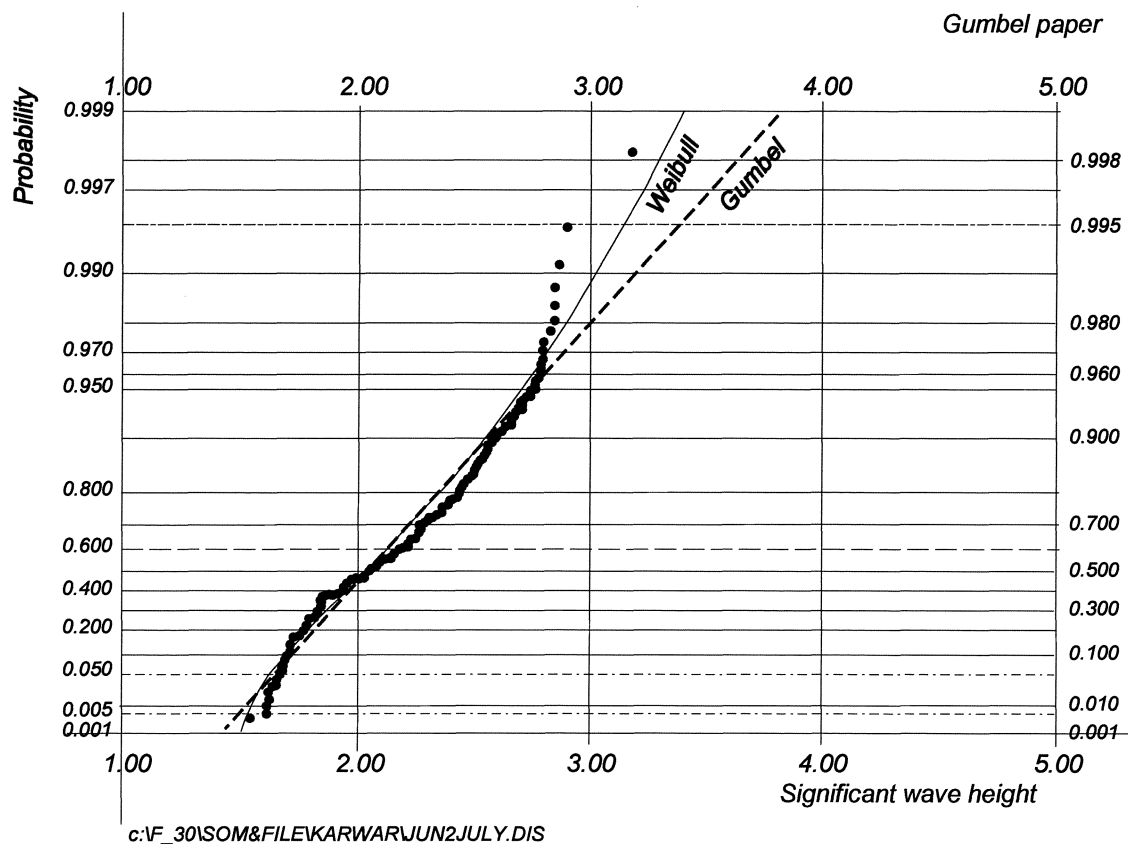


Figure II-114

The approximations are still a good fit for the point "mass", but for the extrapolations beyond the observations area, the distributions vary widely.

A probability of 0.999 that H_s stays smaller than a certain H (i.e.: $P\{H_s \leq H\} = 0.999$) gives, by approximation with a Gumbel distribution:

$$0.999 = \exp\left(-e^{-\frac{H-1.941}{0.284}}\right)$$

a wave height of $H = 3.90$.

Approximation by a Weibull distribution:

$$0.999 = 1 - e^{-\left(\frac{H-1.5}{0.675}\right)^{1.866}}$$

gives a wave height $H = 3.40$.

With an equal probability of exceedance, ($P\{H_s > H\} = 10^{-3}$), H , is 0.5m higher extrapolated according to the Gumbel distribution, than would have been the case if it had been extrapolated according to the Weibull distribution.

APPENDIX II-2 ORDINATES WITH DATA SETS OF OBSERVATIONS

To determine the ordinates of the "plot positions" of the observations, arranged in order of greatness, the following methodology can be used:

The intercepts, sorted in order of greatness, Nx_i , of N observations which constitute a random sample of a certain distribution, each have a probability density function. For a uniform distribution, the probability density functions for $N = 10$, $f_{Nx_i}(\xi)$, of $Nx_1, Nx_2, \dots, Nx_{10}$ are shown in Figure II-115 (bottom figure, plotted downward).

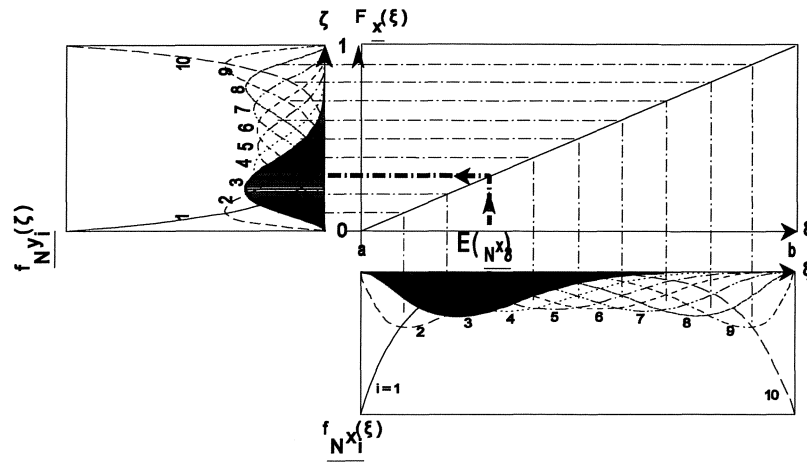


Figure II-115

The reasoning which leads to the probability density function of the i^{th} observation in a random sample consisting of N observations, sorted from the smallest to the largest value, is an analogy of the reasoning behind the derivation of the binomial distribution:

1. Assume that the p.d.f. of the i^{th} observation in a random sample, consisting of N observations placed in order of greatness, equals $f_{Nx_i}(\xi)$.
2. $i - 1$ observations have smaller values and $N - i$ observations have values which are greater than the i^{th} observation. In a random sample of N observations there are $\frac{N!}{(i-1)!(N-i)!}$ different possible results.
3. The probability of observations smaller than or at most equal to the i^{th} observation is: $(1^e \leq \xi_i \cap 2^e \leq \xi_i \cap \dots \cap (i-1)^e \leq \xi_i)$. This equals: $[F_X(\xi)]^{i-1}$. (N.B. the observations are presumed INDEPENDENT, because placing the observations in order of greatness is not necessary to establish the NUMBER (the probability of) observations smaller than or at least equal to the i^{th} observation.)
4. The probability of observations greater than the i^{th} occurring observation is: $((i+1)^e > \xi_i \cap (i+2)^e > \xi_i \cap \dots \cap N^e > \xi_i)$. This equals: $[1 - F_X(\xi)]^{N-i}$.
5. The probability of an observation occurring in the interval $\xi_i - \Delta \xi < \xi_i < \xi_i + \Delta \xi$ is, according to the definition of the p.d.f.,: $f_X(\xi)$.
6. The probability density function of the i^{th} observation in a random sample of N observations, arranged in order from smallest to greatest is thus:

$$f_{Nx_i}(\xi) = \frac{N!}{(i-1)!(N-i)!} \cdot F_X(\xi)^{i-1} \cdot \{1 - F_X(\xi)\}^{N-i} \cdot f_X(\xi)$$

The vertical axis in Figure II-115 is used for the (cumulative) (probability) distribution function, $F_{\underline{x}}(\xi)$. This $F_{\underline{x}}(\xi)$ can be interpreted as a new variable, ζ . For $f_{\underline{x}}(\xi)$ we can write: $d(F_{\underline{x}}(\xi))$. The last cited equation then turns into:

$$f_{\underline{Y}}(\zeta) = \frac{N!}{(i-1)! \cdot (N-i)!} \cdot \zeta^{i-1} \cdot \{1-\zeta\}^{N-i} \cdot d\zeta$$

Here, \underline{Y} is the ordinate (y- value) of the plot position of the i^{th} draw. The expected value is:

$$E\{\underline{Y}\} = \mu_{\underline{Y}} = \frac{N!}{(i-1)! \cdot (N-i)!} \cdot \int_0^1 \zeta \cdot \zeta^{i-1} \cdot (1-\zeta)^{N-i} d\zeta = \frac{i}{N+1}$$

So, is this also the probability of non-exceedance of the expected value of the i^{th} draw? The answer is: generally, no. Let us first consider the exceptional case in which it is.

The $f_{\underline{N}^{x_i}}(\xi)$ are plotted in the lower part of Figure II-115 for a uniform distribution, for which:

$$f_{\underline{N}^{x_i}}(\xi) = \frac{N!}{(i-1)! \cdot (N-i)!} \cdot \left(\frac{\xi-a}{b-a}\right)^{i-1} \cdot \left(1 - \frac{\xi-a}{b-a}\right)^{N-i} \cdot \frac{1}{b-a}$$

The vertical axis of Figure II-115 shows the (cumulative) (probability) distribution function. This can be used to transform the probability density, $f_{\underline{N}^{x_i}}(\xi)$, into the probability density of the frequency of non-exceedance

of the i^{th} draw, i.e. to transform $f_{\underline{N}^{x_i}}(\xi)$ into $f_{\underline{N}^{y_i}}(\eta)$, as follows:

$$f_{\underline{N}^{y_i}}(\eta) = \frac{d F_{\underline{N}^{y_i}}(\eta)}{d\eta} = \frac{d F_{\underline{N}^{x_i}}(\xi)}{d\xi} \cdot \left| \frac{d\xi}{d\eta} \right| = \left[f_{\underline{N}^{x_i}}(\xi) \cdot \left| \frac{d\xi}{d\eta} \right| \right]_{\xi = \psi(\eta)}$$

of:

$$f_{\underline{N}^{y_i}}(\eta) = f_{\underline{N}^{x_i}}\{\psi(\eta)\} \cdot \left| \frac{d\xi}{d\eta} \right|$$

For a uniform distribution:

$$F_{\underline{X}}(\xi) = \eta = \frac{\xi-a}{b-a} \text{ for } a < \xi \leq b \text{ and } 0 \text{ elsewhere.}$$

Leading to:

$$\xi = \eta(b-a) + a$$

$$\frac{d\xi}{d\eta} = b-a$$

Substituted in $f_{\underline{N}^{y_i}}(\eta)$ this gives:

$$\begin{aligned} f_{\underline{N}^{y_i}}(\eta) &= \frac{N!}{(i-1)! \cdot (N-i)!} \cdot \left\{ \frac{\eta(b-a) + a - a}{b-a} \right\}^{i-1} \cdot \left\{ 1 - \frac{\eta(b-a) + a - a}{b-a} \right\}^{N-i} \cdot \frac{1}{b-a} \cdot (b-a) = \\ &= \frac{N!}{(i-1)! \cdot (N-i)!} \cdot \eta^{i-1} \cdot (1-\eta)^{N-i}. \end{aligned}$$

These probability density functions are plotted in Figure II-115 on the left side.

The expected value (the average), $\mu_{\underline{u}}$, of the random variable \underline{u} is found from:

$$\mu_{\underline{u}} = \int_{-\infty}^{\infty} v \cdot f_{\underline{u}}(v) dv$$

For the expected value of the i^{th} realisation of the random variable \underline{x} in a random sample of N realisations from a distribution which is uniform in $[a,b)$ this gives:

$$E\left\{\underline{N}x_i\right\} = \underline{\mu}_{\underline{N}x_i} = \frac{N!}{(i-1)! \cdot (N-i)!} \cdot \int_a^b \xi \cdot \left(\frac{\xi-a}{b-a}\right)^{i-1} \cdot \left(1 - \frac{\xi-a}{b-a}\right)^{N-i} \cdot \frac{1}{b-a} d\xi = \frac{i \cdot (b-a)}{N+1}$$

Analogously, for the expected value of the **FREQUENCY** of the i^{th} realisation of the random variable \underline{x} in a random sample of N realisations from a distribution which is uniform in $[a,b)$:

$$E\left\{\underline{N}y_i\right\} = \underline{\mu}_{\underline{N}y_i} = \frac{N!}{(i-1)! \cdot (N-i)!} \cdot \int_0^1 \eta \cdot \eta^{i-1} \cdot (1-\eta)^{N-i} d\eta = \frac{i}{N+1}$$

For a uniform distribution, $f_{\underline{N}x_i}(\xi)$ turns into $f_{\underline{N}y_i}(\eta)$ via a linear transformation, because the (cumulative) (probability) distribution function is linear in that case. Only then: the transformed expected value of $f_{\underline{N}x_i}(\xi)$, $E\left\{\underline{N}x_i\right\} = \underline{\mu}_{\underline{N}x_i}$, is the expected value of the frequency $E\left\{\underline{N}y_i\right\} = \underline{\mu}_{\underline{N}y_i}$. This is checked for the Gumbel distribution. (see Figure II-116.)

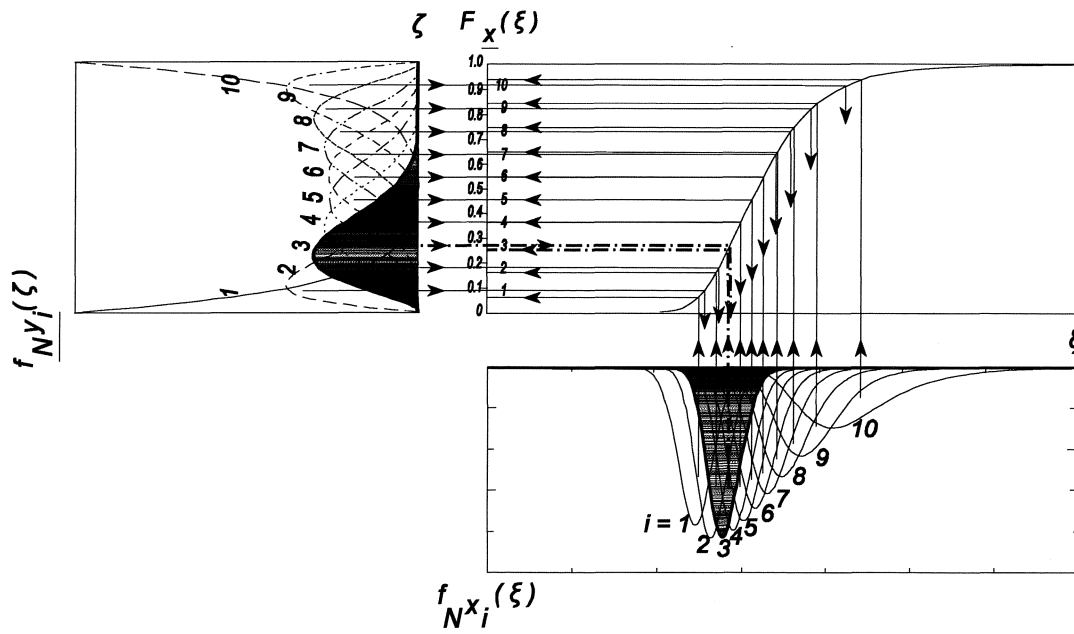


Figure II-116

The figure shows, that the expected value of the frequency of the i^{th} realisation does not equal the transformed expected value of the i^{th} realisation. The figure is based on a random sample, consisting of $N = 10$ realisations. The probability density functions $f_{\underline{N}x_i}(\xi)$ and $f_{\underline{N}y_i}(\eta)$ for $i = 3$ are hatched. The transformations of the expected values are indicated by dash-dot-lines.

The expected value of $\underline{N}x_i$ for a Gumbel distribution can't always be calculated analytically. The expected value of $\underline{N}y_i$ is derived from the fact that $\underline{N}y_i$ is located between 0 and 1 and that the expected value has a uniform distribution there. In that case:

$$E\left\{\frac{\underline{N}y_i}{N}\right\} = \mu_{\underline{N}y_i} = \frac{N!}{(i-1)! \cdot (N-i)!} \cdot \int_0^1 \eta \cdot \eta^{i-1} \cdot (1-\eta)^{N-i} d\eta = \frac{i}{N+1}$$

automatically follows. See for yourself, that the probability density function of the i^{th} realisation from a Gumbel distribution turns into a probability density function of the i^{th} realisation from a uniform distribution in $[0,1)$.

Analogously, the variance of $\underline{N}y_i$ is found:

$$\begin{aligned} \text{VAR}\left\{\frac{\underline{N}y_i}{N}\right\} &= \frac{N!}{(i-1)! \cdot (N-i)!} \cdot \int_0^1 F_{\underline{x}}(\xi)^{i+1} \cdot \{1 - F_{\underline{x}}(\xi)\}^{N-i} \cdot d F_{\underline{x}}(\xi) + \\ &\quad - \left\{ \frac{N!}{(i-1)! \cdot (N-i)!} \cdot \int_0^1 F_{\underline{x}}(\xi)^i \cdot \{1 - F_{\underline{x}}(\xi)\}^{N-i} \cdot d F_{\underline{x}}(\xi) \right\}^2 = \frac{i \cdot (i+1)}{(N+1) \cdot (N+2)} - \frac{i^2}{(N+1)^2} \end{aligned}$$

In order to calculate the integrals used in this appendix, a basic understanding of Beta functions is useful. (See Abramowitz ¹⁾ page 258):

The Beta function, $B(z,w)$, is defined as follows:

$$B(z,w) = \int_0^1 t^{z-1} \cdot (1-t)^{w-1} dt = \frac{\Gamma(z) \cdot \Gamma(w)}{\Gamma(z+w)}$$

For whole values of the argument of the Gamma function:

$$\Gamma(n) = (n-1)!$$

For the integral: $\int_0^1 F_{\underline{x}}(\xi)^i \cdot \{1 - F_{\underline{x}}(\xi)\}^{N-i} \cdot d F_{\underline{x}}(\xi)$ this means:

$$\int_0^1 F_{\underline{x}}(\xi)^i \cdot \{1 - F_{\underline{x}}(\xi)\}^{N-i} \cdot d F_{\underline{x}}(\xi) = B(i+1, N-i+1) = \frac{\Gamma(i+1) \cdot \Gamma(N-i+1)}{\Gamma(N+2)} = \frac{i! \cdot (N-i)!}{(N+1)!}$$

hence:

$$E\left\{F_{\underline{N}x_i}(\xi)\right\} = \frac{N!}{(i-1)! \cdot (N-i)!} \cdot \frac{i! \cdot (N-i)!}{(N+1)!} = \frac{i}{N+1}.$$

¹⁾ Handbook of Mathematical Functions, M. Abramowitz and I.A. Stegun (eds.), Dover Publications, Inc., New York

APPENDIX II-3 COMPARISON OF LINEAR REGRESSION (METHOD OF LEAST LINEAR SQUARES) WITH THE METHOD OF THE MOMENTS

An exponential distribution is used as an example:

$$F_{\underline{x}}(x) = 1 - e^{-\frac{x-A}{B}}$$

Transformation leads to the linear equation:

$$\ln(1 - F_{\underline{x}}(x)) = -\frac{1}{B} \cdot x + \frac{A}{B}$$

The observations, x , are arranged from smallest to greatest. Assume there are N observations. Intercepts are found by assigning a number of ranking, i , to the observations. To every observation placed in order,

x_i , an ordinate is added according to: $y_i = \ln\left(1 - \frac{i}{N+1}\right) = \ln\left(\frac{N+1-i}{N+1}\right)$. On grounds of the coordinates

(x_i, y_i) and using the method of the least linear squares, the parameters A and B are estimated by:

$$\ln\left(1 - \frac{i}{N+1}\right) = -\frac{1}{B} \cdot x_i + \frac{A}{B}$$

As $0 < \frac{i}{N+1} < 1$; $0 < \frac{N+1-i}{N+1} < 1$ too; so $\ln\left(\frac{N+1-i}{N+1}\right) < 0$. The parameter B thus has a positive value.

The gradient $-\frac{1}{B}$ can be estimated by:

$$\text{tga} = -\frac{1}{B} = \frac{\text{cov}(x,y)}{s_x^2} \quad \text{or} \quad B = -\frac{s_x^2}{\text{cov}(x,y)} = -\frac{s_x^2}{r_{x,y} \cdot s_x \cdot s_y} = -\frac{s_x}{r_{x,y} \cdot s_y} \quad (\text{see page II - 18})$$

The parameter can also be estimated as the second moment of the observations x :

$$B_m = s_x \quad (\text{see page II - 78})$$

Still: $B_m \leq B$.

PROOF:

$$B_m \leq B$$

or: $s_x \leq -\frac{s_x}{r_{x,y} \cdot s_y}$ or: $1 \leq -\frac{1}{r_{x,y} \cdot s_y}$

$y = \ln\left(\frac{N+1-i}{N+1}\right) = -\frac{1}{B} \cdot x_i + \frac{A}{B}$, so y is a decreasing function of x , from which is known that: $-1 \leq r_{x,y} < 0$
 $s_y < 1$ thus remains to be proven.

The p.d.f. of $y = \ln z$ with $z = U(z; \frac{1}{N+1}, \frac{N}{N+1})$. (z uniformly distributed in $[\frac{1}{N+1}, \frac{N}{N+1})$)

Assume $\frac{1}{N+1} = \varepsilon$, then $\frac{N}{N+1} = 1 - \varepsilon$. If $N \rightarrow \infty$ then $\varepsilon \downarrow 0$.

The expected value of y is: $E(y) = \lim_{\varepsilon \downarrow 0} \left\{ \int_{\varepsilon}^{1-\varepsilon} \ln z \, dz \right\} \downarrow -1$ (approaches from the top to -1).

The variance is $\lim_{\varepsilon \downarrow 0} \left\{ \int_{\varepsilon}^{1-\varepsilon} (\ln z)^2 \, dz \right\} - (E(y))^2 \uparrow +1$ (approaches from below to +1).

This leads to $s_y < 1$ for finite N .

III. PROBABILISTIC CALCULATIONS

III.1. COMPARISON OF PROBABILISTIC CALCULATIONS AT LEVELS II AND III

In the table below some aspects of different types of calculations are compared:

	Full integration	Monte Carlo	Level II
Many stochastic variables	-	0	0
Accuracy	0	+/-	0
Calculation time	:: (Number of integration steps) ^{Number of variables}	:: $1/P_f$	moderate
Discontinuous reliability function	0	0	-
Discontinuous derivative $f'_x(x)$	0	0	-
Insight in α_i^2	+/-	+/-	0
Correlation within reliability function	0	0	-/0
More than one reliability function	0	0	-
Reliability function consisting of more than one reliability function	0	0	-

- = awkward to treat with this method

P_f = failure probability

+ = this method is quite adequate for this purpose

:: = proportional to

0 = method is (practically) insensitive for this aspect

III.2. THE WEIGHTED SENSITIVITY ANALYSIS AT LEVEL III

The problem space (X- space) is divided in two parts by the failure function (failure boundary). The problem space consists of:

- a failure domain, in which $Z \leq 0$ and
- a safe domain, in which $Z > 0$.

(See lecture notes CTOW4130 / CUR- manual number 190¹⁾)

The Design Point (DP), i.e. the point X_1, X_2, \dots, X_N satisfying the failure function $Z(X_1^*, X_2^*, \dots, X_N^*) = 0$ and for which the probability density of the reliability function, Z , is maximum, is a by-product in a level II-calculation. In the DP the contributions to the variance of the reliability function, α_i^2 , equal the squares of the coefficients of correlation between X_i en Z , X_i taken as the values in the DP. The α_i are called sensitivity factors²⁾.

The fraction of the variance of Z that originates from a stochastic basic variable X_i equals:

$$\alpha_i^2 = \left(\frac{\frac{\partial Z}{\partial X_i} \cdot \sigma_{X_i}}{\sigma_Z} \right)^2$$

¹⁾ CUR- publication 190, Probabilities in Civil Engineering, part 1: probabilistic design in theory (in Dutch: "Kansen in de Civiele Techniek, deel 1: probabilistisch ontwerpen in theorie"), March 1997, CUR Foundation, Gouda, The Netherlands, ISBN 90 - 376 - 0102 - 2.

²⁾ Madsen, H.O., S. Krenk, N.C. Lind, Methods of Structural Safety, Prentice-Hall, Inc., Englewood Cliffs, 1986, ISBN 0 - 13 - 579475 - 7.

The derivative of the reliability function Z ¹⁾ can be written as: $\frac{\partial Z}{\partial X_i} = \frac{cov(X_i, Z)}{\sigma_{X_i}^2}$

From this: $\frac{\partial Z}{\partial X_i} \cdot \sigma_{X_i} = \frac{cov(X_i, Z)}{\sigma_{X_i}}$

This substituted in the expression for α_i^2 and taking the square root leads to:

$$\alpha_i = \rho_{X_i, Z} = \frac{cov(X_i, Z)}{\sigma_{X_i} \cdot \sigma_Z}$$

Contributions to the variance in level III- calculations can be established by calculating $cov(X_i, Z)$, $\sigma_{X_i}^2$

and σ_Z^2 and from those: $\alpha_i^2 = \frac{cov^2(X_i, Z)}{\sigma_{X_i}^2 \cdot \sigma_Z^2}$. This procedure provides approximations of the α_i^2 that are

(roughly) comparable with those found in a mean value approach.

A calculation of the sensitivity factors is possible once the DP is known. The DP can be approximated by Monte Carlo- simulation as will be shown in section III.3.2.

III.3. TRANSFORMATION TO STANDARD- NORMALLY DISTRIBUTED VARIABLES

If the distribution of a variable, X_i , is given by $F_{X_i}(X_i)$ then X_i can be transformed to a standard- normally distributed variable, U_i , by $U_i = \Phi^{-1}(F_{X_i}(X_i))$, provided the probability density function of X_i is differentiable. NB $\Phi^{-1}(\cdot)$ represents the standard normal distribution. The space to which the X- space is transformed by $U_i = \Phi^{-1}(F_{X_i}(X_i))$ is called the U-space.

In the DP the sensitivity factors can be calculated and so it is possible to get an impression of the influence of the variables on the probability of failure. The Hasofer Lind- reliability index, β , is defined as the distance from the origin to the (transformed) DP in the U-space. The relationship between the values of the standard normally distributed variables, U_i , in the DP and the reliability index, β , is given by:

$$U_i^* = \alpha_i \cdot \beta$$

The values of the basic variables, X_i , can be calculated from the standard- normally distributed variables, U_i , by the transformation:

$$X_i = F_{X_i}^{-1}(\Phi(U_i))$$

III.3.1 THE DESIGN POINT IN AN INTEGRATION PROCEDURE

The DP in a level III calculation using integration can be found by registering the probability density of all points in which $Z \leq 0$ provided the variables are independent. In such a point, $(\xi_1, \xi_2, \dots, \xi_N)$ the probability density is:

$$f_Z(\zeta_i) \cdot d\zeta_i = \prod_{i=1}^N f_{X_i}(\xi_i) \cdot d\xi_i,$$

in which $f_{X_i}(\xi_i) \cdot d\xi_i$ is the probability density function of the basic variable X_i for the value ξ_i . It is simple to keep count of this product while integrating over the failure domain. The integration is commonly performed on a grid. The grid point at which the failure function is (approximately) zero and $f_Z(\zeta_i) \cdot d\zeta_i$ is maximum is (an approximation of) the DP. The approximation is better as the integration grid is finer.

¹⁾ Compare: $B = \frac{cov(x, y)}{var(x)}$ in section II.11.3, now stated for a function in more than two stochastic variables.

III.3.2. THE DESIGN POINT IN MONTE CARLO SIMULATIONS

In a simple Monte Carlo-simulation ¹⁾ the values of the variables, X_i , are generated from their distributions and substituted in the reliability function, Z . The resulting Z is called a “failure” if it is smaller than or equal to zero. An estimate of the probability of failure is calculated by dividing the number of failures by the total number of simulations, the approximation being better as the number of simulations is increased. If combinations of values of X_i for which $Z \leq 0$ are close together, it is likely that in that neighbourhood the probability density of the combinations is high. If symmetric probability densities like normal probability densities are considered, such clusters will be found near to the expected values of the variables, see Figure II-21, in which the normal joint probability density of two variables is sketched. The maximum probability density in Figure II-21 is at $(x = \mu_x, y = \mu_y)$.

In the following it is assumed that the reliability function is described by independent normally distributed variables. If the variables are not normally distributed and/or they are not independent a transformation has to be performed first.

As an example the “classical problem” of the weight hanging from a circle-cylindrical steel bar ²⁾ can be taken. The reliability function is:

$$Z = \sigma - \frac{4 \cdot F}{\pi \cdot d^2}$$

in which σ = tensile strength of the bar, mean $\mu_\sigma = 290 \text{ N/mm}^2$, standard deviation $\sigma_\sigma = 25 \text{ N/mm}^2$
 F = weight deterministic, 100000 N
 d = diameter of the bar mean $\mu_d = 30 \text{ mm}$, standard deviation $\sigma_d = 3 \text{ mm}$

The reliability function can be expressed in standard-normal variables, U_i , as follows:

$$Z = \mu_\sigma + \sigma_\sigma \cdot U_1 - \frac{4 \cdot F}{\pi \cdot (\mu_d + \sigma_d \cdot U_2)^2}$$

The failure boundary, a characteristic point in the failure domain derived from the simulations (indicated as C) and the DP are sketched in Figure III-1. The axes have been scaled in such a way that the standard deviation of σ on the vertical axis is equal in length as the standard deviation of d on the horizontal axis. By this the contours of equal reliability are transformed to circles and the connecting line between the DP and the (scaled) centre of the joint probability density, $\left(\frac{\mu_d}{\sigma_d}, \frac{\mu_\sigma}{\sigma_\sigma} \right)$, is perpendicular to the (transformed) failure function. The origin of the axes is translated to $\left(\frac{\mu_d}{\sigma_d}, \frac{\mu_\sigma}{\sigma_\sigma} \right)$

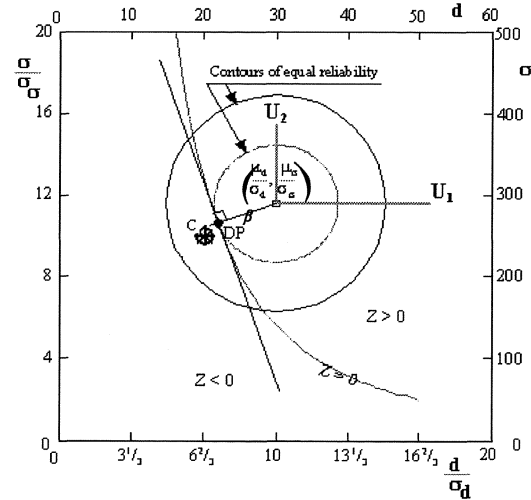


Figure III-1

By scaling and translation the failure function is expressed in standard normally distributed variables U_1 and U_2 . The distance from the origin to the failure function is the Hasofer Lind- reliability index, β .

¹⁾ In literature several Monte Carlo- procedures are mentioned. (See among others CUR- publication 190.) Here, i. e. in these lecture notes, the most simple method of calculation is used: the straight forward method of simulation.

²⁾ Rationalisation of safety and serviceability factors in structural codes, Hallam, M.G., N.I. Heaf and I.R. Wooton, CIRIA Report 63, London, 1977

Travelling from the point C in the failure domain in the direction of the centre of the joint probability density (the point $\left(\frac{\mu_d}{\sigma_d}, \frac{\mu_\sigma}{\sigma_\sigma} \right)$ in the transformed space or the point $(0, 0)$ in the U- space) the probability density increases. If the failure domain is not convex ¹⁾ it is possible that the calculated point C is not in the failure domain. This can complicate the calculation of the DP. These complications will not be dealt with here.

If the reliability function is not sharply curved in the neighbourhood of the DP in the U- space, a good approximation of the DP is given by the intersection of the connection of the point C in Figure III-1 and the mean of the joint probability density (the origin in the U-space) with the failure boundary. Once the (approximation of the) DP is established, the derivatives of the reliability function can be calculated and from them the sensitivity factors, α_i .

A straight line that contains the origin in the U- space can be written in vector notation as:

$$\begin{aligned} U_1 &= b_1 \\ \vdots &= \lambda \star \vdots \\ U_n &= b_n \end{aligned}$$

if the parameter λ is properly chosen.

The vector on the left hand side with elements U_1 through U_n can be seen as the coordinate of the DP in U- space. The elements b_1 through b_n of the vector on the right hand side can be determined in more than one way. For example the following methods can be applied:

- the method “centre of gravity”,
- the method “angles”,
- the method “nearest to the mean”

These methods will be explained in the following sections.

Starting point for all methods are simulations for which $Z < 0$. These simulations are called realisations. The number of simulations has to be large enough, so that at least one realisation occurs.

III.3.2.1. METHOD “CENTRE OF GRAVITY”

The coordinate of the centre of gravity (CG in Figure III-2) of the realisations is connected with the origin in the U-space. The connecting line intersects the failure boundary at DP^* , being an approximation of the “real” DP.

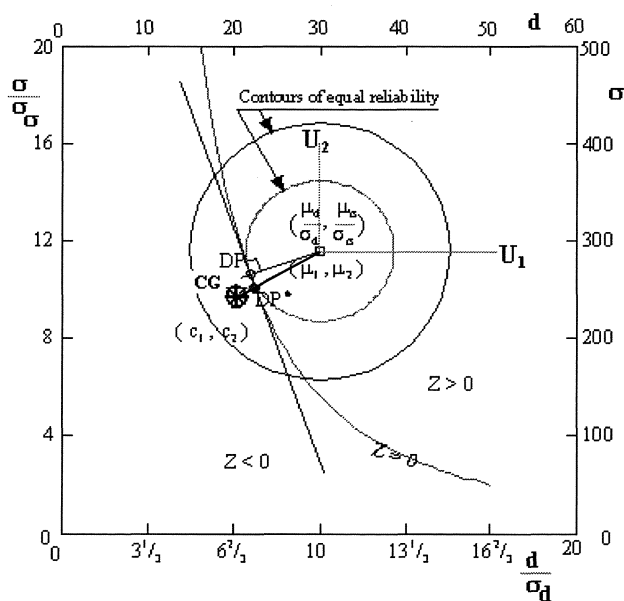


Figure III-2

¹⁾ A domain is convex if the connection of any two points in that domain is inside the domain. In the chosen example of the weight hanging from a bar the failure domain is concave. It does not complicate the calculation of the DP in this case as the failure function is not sharply curved in the neighbourhood of the DP.

If (c_1, \dots, c_n) is the coordinate of the afore mentioned centre of gravity, the elements of vector b can be

written as: $b_i = \frac{c_i}{c_1}$ for $i \in 1, 2, \dots, n$

in which: n = number of basic variables

$$c_i = \frac{1}{M} \cdot \sum_{j=1}^M U_{j,i}$$

= value of the i^{th} element in the coordinate vector of the centre of gravity of the realisations for which $Z \leq 0$.

M = number of realisations (number of simulations for which $Z \leq 0$).

A flow diagram for the approximation of the DP by the method “centre of gravity” applied to the example of the weight hung from a bar, could be as follows:

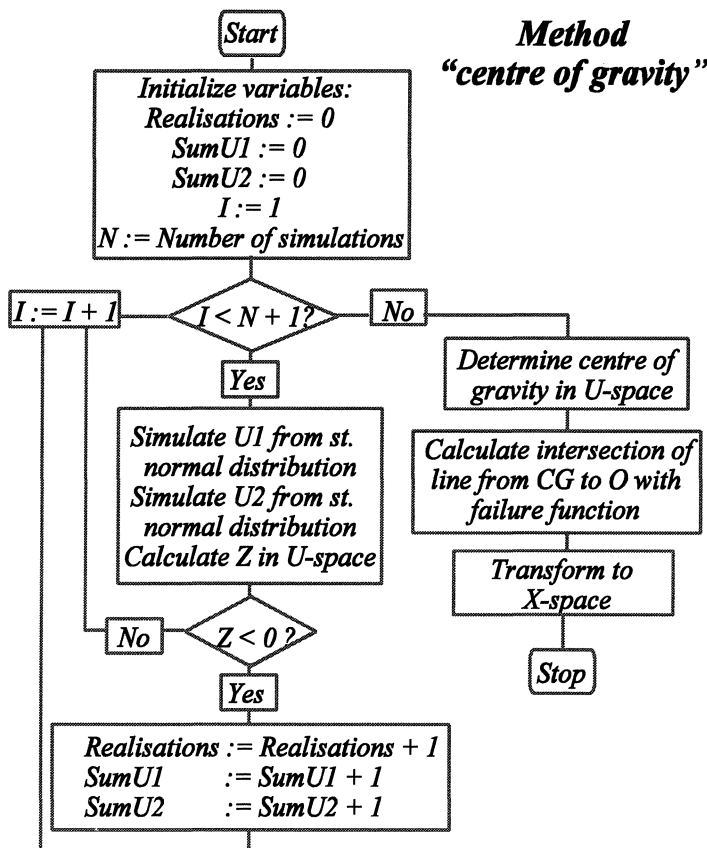


Figure III-2a

Computer programmes for the example are given in MathCad7.3 and in Turbo Pascal (Version 4 or higher) in section III.3.2.5.

III.3.2.2. METHOD “ANGLES”

This approximation differs from the former one. Only part of the information is considered, namely only the part regarding the *direction* and *not* the part regarding the *length* of the vector. Again (if necessary) basic variables, X_i , are transformed to standard-normally distributed variables, U_i . Each set of U_i , for which $Z \leq 0$, can be identified by $(n - 1)$ angles with the coordinate axes and one distance from the origin, n being the number of basic variables. If the angles of the directions of the realisations are taken as a sample, the mean of this sample can be considered as an approximation of the angle between the direction in which the DP has to be found and the coordinate axes.

The direction can be characterised by the angle $\varphi_{j,1,i}$ for transformed realisations $U_{j,i}$ and $U_{j,1}$ in the j^{th} simulation. i is the serial number of the stochastic variable considered in the reliability function concerned. It is mentioned that:

$$\begin{aligned} U_1 &= b_1 \\ \vdots &= \lambda^* \vdots \\ U_n &= b_n \end{aligned}$$

The vector on the left hand side (elements U_1 through U_n) is the approximation of the coordinate of the DP. The elements b_1 through b_n of the vector on the right hand side are calculated as follows:

The angle $\varphi_{j,1,i}$ is (by definition) in the interval $[0, 2\pi)$. If $Z \leq 0$ in the j^{th} simulation, then the angle $\varphi_{j,1,i}$ is:

$$\begin{aligned} \text{If } U_{j,i} > 0 \text{ and } U_{j,1} > 0 \text{ then } \varphi_{j,1,i} &= \arctan\left(\frac{U_{j,i}}{U_{j,1}}\right) \\ \text{If } U_{j,i} < 0 \text{ then } \varphi_{j,1,i} &= \pi + \arctan\left(\frac{U_{j,i}}{U_{j,1}}\right) \\ \text{If } U_{j,i} < 0 \text{ and } U_{j,1} > 0 \text{ then } \varphi_{j,1,i} &= 2 * \pi + \arctan\left(\frac{U_{j,i}}{U_{j,1}}\right) \end{aligned}$$

The mean of j angles can be expressed as: $M_{1(\varphi_{j,1,i})} = \frac{1}{j} \{ (j-1) \cdot M_{1(\varphi_{j-1,1,i})} + \varphi_{j,1,i} \}$.

For the first simulation in which $Z \leq 0$ (the first realisation) is: $M_{1(\varphi_{1,1,i})} = \varphi_{1,1,i}$.

In every successive realisation (every new simulation in which $Z \leq 0$) the values of the elements of the vector have to be adapted:

$$b_i = \tan(M_{1(\varphi_{j,1,i})}) \text{ with } i \in 2, 3, \dots, n, \quad j \in 1, 2, \dots, M$$

M is the number of realisations (number of simulations in which $Z \leq 0$).

NB Recurrent relationships for higher moments can be derived analogous to this formulation.

The slopes, b_i , are derived from the mean angle $M_{1(\varphi_{j,1,i})}$ by calculating $b_i = \tan(M_{1(\varphi_{j,1,i})})$.

The tangent is not defined for $0,5 \cdot \pi \pm n \cdot \pi$. As an angle is nearer to these values, the sensitivity of the tangent for (small) changes in the angle increases. If the angle of the vector of mean values of U is near $0,5 \cdot \pi \pm n \cdot \pi$, the spreading in the calculated slope increases. The answers will be less reliable.

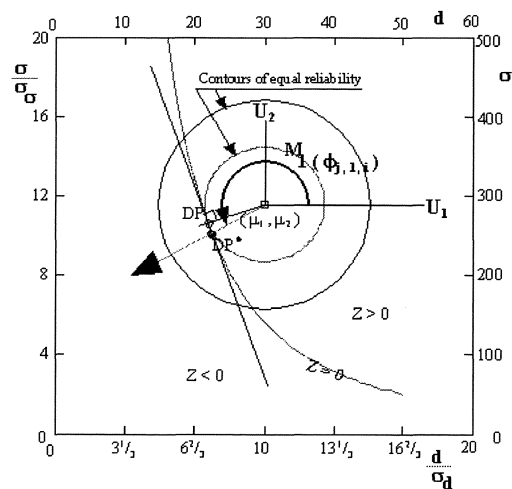


Figure III-3

Flow diagram for the example:

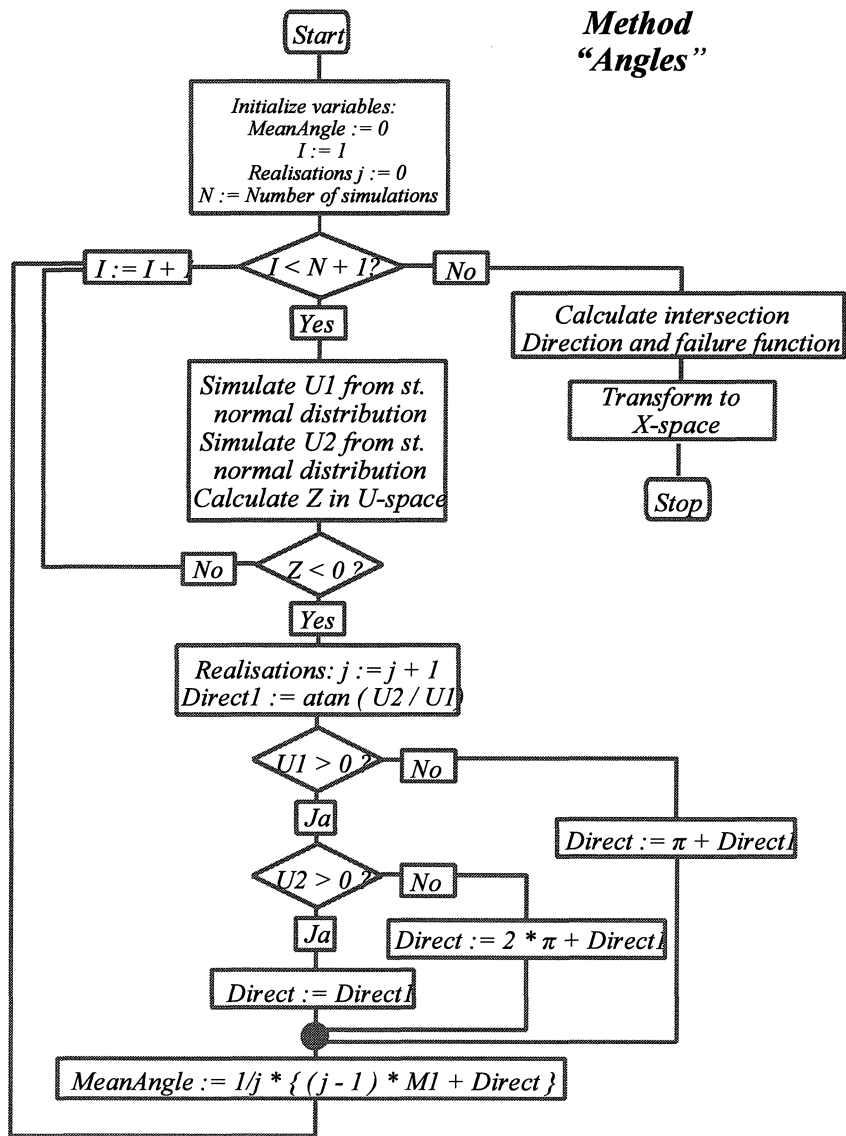


Figure III-3a

III.3.2.3. METHOD “NEAREST TO THE MEAN”

The starting point in the former two methods was the centre of gravity of the points simulated in the failure domain or of the direction of that centre of gravity, both measured from the origin in the U-space. The realisation nearest to the origin in the U-space can be considered as another starting point. Analogous to the method “centre of gravity” a vector of b_i can be calculated.

Suppose the coordinates of the realisation nearest to the origin in the U-space are $(p_1, p_2, \dots, p_i, \dots, p_n)$, then the vector $(b_1, b_2, \dots, b_i, \dots, b_n)$ can be calculated:

$$b_i = \frac{p_i}{p_1} \quad \text{for } i \in 1, 2, \dots, n$$

with: n = number of basic variables

$p_i = U_{j,i}$ for the simulation of $Z(U_{j,i}, \dots, U_{j,n}) \leq 0 \quad j \in 1, 2, 3, \dots, M$ for which

$$\sqrt{\sum_{i=1}^N U_{j,i}^2} \text{ is minimum. See Figure III-4.}$$

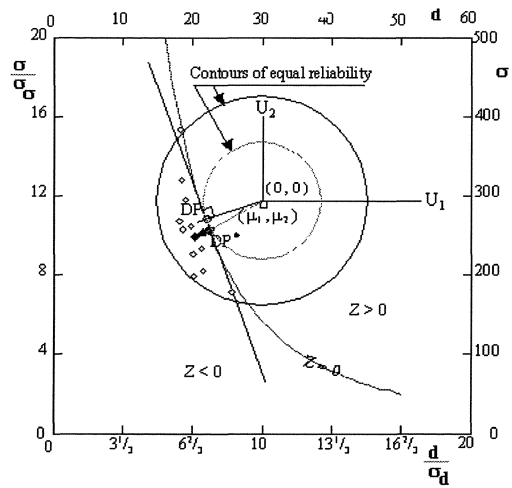


Figure III-4

Flow diagram for the example of the weight on the bar:

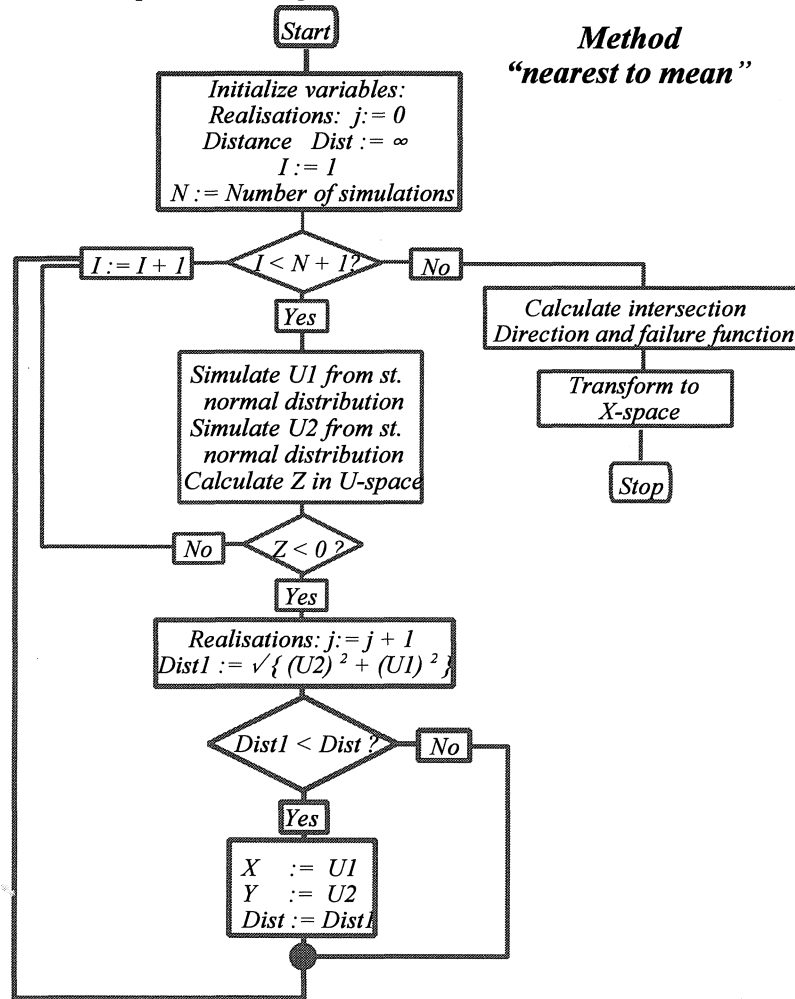


Figure III-4a

III.3.2.4. COMPARISON OF THE RESULTS FOR THE CHOSEN EXAMPLE

In the example of the weight hung from a circle-cylindrical bar and data as given on page III-3 the following results are obtained by the Turbo Pascal programs given in section III.3.2.5. For better comparison these Turbo Pascal programmes were combined, so that randomly generated values for U_1 (transform of tensile stress in the bar) and U_2 (transform of diameter of the bar) could be used in all three methods. As a consequence there was only one failure probability calculated for all three methods.

If 10000 simulations are calculated

DESIGN POINT VALUES:	d	σ	failure frequency
<i>Method "centre of gravity"</i>	21.94	264.62	$2.05 \cdot 10^{-3}$
<i>Method "angles"</i>	21.94	264.54	$(2.05 \cdot 10^{-3})$, same simulations used as in method "centre of gravity")
<i>Method "nearest to mean"</i>	20.96	289.94	

If 100 000 simulations were calculated, the results could be:

DESIGN POINT VALUES:	d	σ	failure frequency
<i>Method "centre of gravity"</i>	21.81	267.72	$2.32 \cdot 10^{-3}$
<i>Method "angles"</i>	21.81	267.64	$(2.32 \cdot 10^{-3})$, same simulations used as in method "centre of gravity")
<i>Method "nearest to mean"</i>	21.01	288.51	

If 1 000 000 simulations were calculated, the results could be:

DESIGN POINT VALUES:	d	σ	failure frequency
<i>Method "centre of gravity"</i>	21.09	266.93	$2.230 \cdot 10^{-3}$
<i>Method "angles"</i>	21.87	266.27	$(2.230 \cdot 10^{-3})$, same simulations used as in method "centre of gravity")
<i>Method "nearest to mean"</i>	20.90	289.60	

For comparison:

Design point values:	d	σ	failure probability
LEVEL II- METHOD	21.85	266.82	$2.039 \cdot 10^{-3}$

NB. De failure probability calculated by the level II- method is smaller than the one calculated by any Monte Carlo (level III-) method. This is caused by the linearisation of the reliability function if the level II- method is applied.

The DPs found agree well with the one found by using the level II-method. The DP found by the method "nearest to the mean" differs most from the one calculated by the level II- method and can be regarded as least accurate. The lever II-method is assumed to provide the "exact" DP. The DPs found by the other methods are approximately equally accurate.

III.3.2.5. PROGRAMS IN MATHCAD7.3 AND IN TURBO PASCAL (version 4.0 or higher).

Program for the method "centre of gravity" in Mathcad7.3

Method Centre of gravity	ORIGIN=1	N := 10000 simulations			
Problem of the wire: $Z = \sigma - \frac{4 \cdot F}{\pi \cdot d^2}$	Z in standard-normally distributed variables: $Z = \mu_\sigma + \sigma_\sigma \cdot U_1 - \frac{4 \cdot F}{\pi \cdot (\mu_d + \sigma_d \cdot U_2)^2}$				
Variable	μ	σ	V	[]	
tensile stress	$\mu_\sigma := 290$	$\sigma_\sigma := 25$	$\frac{1}{11.6}$	$\frac{N}{\text{mm}^2}$	A 266 MHz PENTIUM processor can perform 10 ⁶ simulations in ca. 12 minutes. For N = 10000 simulations the calculation time is ca. 7.2 s.
load	F := 10 ⁵	-	-	N	
diameter	$\mu_d := 30$	$\sigma_d := 3$	$\frac{1}{10}$	$\frac{\text{mm}^2}{10}$	

```

M :=
  NZsm0 ← 0
  TotU1 ← 0
  TotU2 ← 0
  for i ∈ 1..N
    U1 ← qnorm(rnd(1), 0, 1)
    U2 ← qnorm(rnd(1), 0, 1)
    Z ← μσ + σσ · U1 - 4·F / (π · (μd + σd · U2)²)
    NZsm0 ← NZsm0 + 1 if Z < 0
    TotU1 ← TotU1 + U1 if Z < 0
    TotU2 ← TotU2 + U2 if Z < 0
  G1 ← NZsm0
  G2 ← TotU1
  G3 ← TotU2
  G
  
```

Initialising variables

N simulations

Generate U1 and U2 from standard-normal distribution

Calculate Z

If Z < 0 a "failure case" is added to the total of calculated "failure cases". The abscissae and ordinates of the "failure cases" are added in case of a "failure case".

Vector contains 3 elements: Number of "failure cases"
Sum of the abscissae
Sum of the ordinates

Total of "failure cases": M₁ = 25 from 10000 simulations

Abscissa of the centre of gravity in U-space: $U_{1Z} := \frac{M_2}{M_1}$ Ordinate of the centre of gravity in U-space: $U_{2Z} := \frac{M_3}{M_1}$

Intersection of the line between the centre of gravity and the origin with the failure function:

abscissa in U-space: $U_1 := -1$ (starting value) $U_1 := \text{root} \left[\mu_\sigma + \sigma_\sigma \cdot U_1 - \frac{4 \cdot 10^5}{\pi \cdot \left(\mu_d + \sigma_d \cdot \frac{U_{2Z}}{U_{1Z}} \cdot U_1 \right)^2}, U_1 \right]$ $U_1 = -0.901$

Ordinate in U-space: $U_2 := \frac{U_{2Z}}{U_{1Z}} \cdot U_1$ $U_2 = -2.728$

Intersection in X-space (approximation of DP):

$X_I := U_1 \cdot \sigma_\sigma + \mu_\sigma$ $X_I = 267.487$

$Y_I := U_2 \cdot \sigma_d + \mu_d$ $Y_I = 21.817$

Check: (X_I, Y_I) on failure boundary: $X_I - \frac{4 \cdot F}{\pi \cdot Y_I^2} = -4.164 \cdot 10^{-8}$ Approximately zero

Program for the method "angles" in Mathcad7.3

Method "angles"

ORIGIN=1

N := 10000 simulations

Problem of the wire: $Z = \sigma - \frac{4 \cdot F}{\pi \cdot d^2}$ Z in standard-normally distributed variables: $Z = \mu_\sigma + \sigma_\sigma \cdot U_1 - \frac{4 \cdot F}{\pi \cdot (\mu_d + \sigma_d \cdot U_2)^2}$

Variable	μ	σ	V	[]
tensile stress	$\mu_\sigma := 290$	$\sigma_\sigma := 25$	$\frac{1}{11.6}$	$\frac{N}{mm^2}$
load	$F := 10^5$	-	-	N
diameter	$\mu_d := 30$	$\sigma_d := 3$	$\frac{1}{10}$	mm^2

Mathcad program Explanation

```

M := j ← 0                               Initializing variables
M1 ← 0
for i ∈ 1..N                               N simulations
    U1 ← qnorm(rnd(1), 0, 1)              Generate U1 and U2 from standard-normal distribution
    U2 ← qnorm(rnd(1), 0, 1)
    Z ← μσ + σσ · U1 -  $\frac{4 \cdot 10^5}{\pi \cdot (\mu_d + \sigma_d \cdot U_2)^2}$       Calculate Z
    if Z < 0                                If Z < 0 .....
        j ← j + 1                            a "failure case" is added to the total of failure cases
        Richt1 ← atan( $\frac{U_2}{U_1}$ )                Calculate the angle of the direction to the point with the
                                                U1-axis
        if U1 > 0                            The angle is calculated in the first or in the fourth
            Richt ← Richt1 if U2 > 0        quadrant. In the first quadrant the angle is positive, in the
            Richt ← 2 · π + Richt1 if U2 < 0 fourth quadrant the angle is negative. From this the
                                                following IF-statements result.
        Richt ← π + Richt1 if U1 < 0
        M1 ←  $\frac{1}{j} \cdot [(j-1) \cdot M_1 + Richt]$       Calculate the mean of all angles associated with "failure
                                                cases".
    G1 ← j                                    Vector contains 2 elements: The number of "failure cases"
    G2 ← M1                                The expected value of the
                                                angle with the U1-axis
G

```

Number of "failure cases" M₁ = 25

Intersection of the mean direction in which Z < 0 with the failure function in U-space

$$U_1 := -1 \quad U_1 := \text{root} \left[\mu_\sigma + \sigma_\sigma \cdot U_1 - \frac{4 \cdot 10^5}{\pi \cdot (\mu_d + \sigma_d \cdot \tan(M_2) \cdot U_1)^2}, U_1 \right] \quad U_1 = -0.905$$

$$U_2 := \tan(M_2) \cdot U_1 \quad U_2 = -2.726$$

Idem in X-space

$$X := \mu_\sigma + \sigma_\sigma \cdot U_1 \quad X = 267.369 \quad Y := \mu_d + \sigma_d \cdot U_2 \quad Y = 21.822$$

Check: $X - \frac{4 \cdot F}{\pi \cdot Y^2} = -2.682 \cdot 10^{-8}$ which is approximately zero.

Program for the method "nearest to the mean" in Mathcad7.3

Method "nearest to mean"

ORIGIN := 1 N := 10000 simulations

Problem of the wire: $Z = \sigma - \frac{4 \cdot F}{\pi \cdot d^2}$ Z in standard-normally distributed variables: $Z = \mu_\sigma + \sigma_\sigma \cdot U_1 - \frac{4 \cdot F}{\pi \cdot (\mu_d + \sigma_d \cdot U_2)^2}$

Variable	μ	σ	V	[]
tensile stress	$\mu_\sigma := 290$	$\sigma_\sigma := 25$	1/11.6	N / mm ²
load	$F := 10^5$	-	-	N
diameter	$\mu_d := 30$	$\sigma_d := 3$	1/10	mm ²

Mathcad program Explanation

```

M := j ← 0
Dist ← 1020
for i ∈ 1.. N
    U1 ← qnorm (rnd(1), 0, 1)
    U2 ← qnorm (rnd(1), 0, 1)
    Z ← μσ + σσ · U1 -  $\frac{4 \cdot F}{\pi \cdot (\mu_d + \sigma_d \cdot U_2)^2}$ 
    if Z < 0
        j ← j + 1
        Di ← √(U12 + U22)
        if Di < Dist
            X ← U1
            Y ← U2
            Dist ← Di
G1 ← j
G2 ← Dist
G3 ← X
G4 ← Y
G
    
```

Explanation

- Initialise variables
- N simulations
- Generate U₁ and U₂ from standard-normal distribution
- Calculate Z in U-space
- If Z < 0
 - o one "case of failure" is added to the total of failure cases
 - o the distance to the origin is calculated
 - If this distance is smaller than those calculated so far :
 - o "Update" the abscissa
 - o "Update" the ordinate
 - o Replace the "old" calculated distance by the new one
- Vector contains:
 - o the number of "cases of failure"
 - o the distance of the failure case that in this run is calculated nearest to the origin
 - o the abscissa of the "failure case" in U-space
 - o the ordinate of the "failure case" in U-space

Abscissa of the point in U-space: $U_{1D} := M_3$ Ordinate of the point in U-space: $U_{2D} := M_4$ Distance: $M_2 = 2.901$

In X-space:

$X_D := \mu_\sigma + \sigma_\sigma \cdot M_3$ $X_D = 267.258$ $Y_D := \mu_d + \sigma_d \cdot M_4$ $Y_D = 21.737$ Failures: $M_1 = 25$

Intersection of the line from the calculated point to the origin and the failure boundary:

Abscissa of the intersection in U-space: $U_1 := -1$ (starting value) $U_1 := \text{root} \left[\mu_\sigma + \sigma_\sigma \cdot U_1 - \frac{4 \cdot F}{\pi \cdot \left(\mu_d + \sigma_d \cdot \frac{U_{2D}}{U_{1D}} \cdot U_1 \right)^2}, U_1 \right]$
 $U_1 = -0.901$
 Ordinate of the intersection in U-space: $U_2 := \frac{U_{2D}}{U_{1D}} \cdot U_1$ $U_2 = -2.727$

Intersection in X-space (approximation of the Design Point):

$X_{DP} := U_1 \cdot \sigma_\sigma + \mu_\sigma$ $X_{DP} = 267.479$ $Y_{DP} := U_2 \cdot \sigma_d + \mu_d$ $Y_{DP} = 21.818$

Check: $Z = \sigma - \frac{4 \cdot F}{\pi \cdot d^2}$ $X_{DP} - \frac{4 \cdot F}{\pi \cdot Y_{DP}^2} = -4.044 \cdot 10^{-8}$ (Approximately zero)

Program for the method "centre of gravity" in Turbo Pascal:

```
PROGRAM CGRAVITY;
USES CRT;
CONST
  N = 1000000;
VAR
  NuZsmaller0, i          : LONGINT;
  U1, U2, TotU1, TotU2, muSigma, Func, Deriv,
  sigmaSigma, mud, sigmad, FLoad, Help,
  X1, X2, U1Z, U2Z, U10, U11, U12, Z : EXTENDED;
BEGIN
  ClrScr;
  RANDOMIZE; NuZsmaller0 := 0; TotU1 := 0; TotU2 := 0;
  muSigma := 290; sigmaSigma := 25; mud := 30; sigmad := 3; FLoad := 1e5;
  FOR i := 1 TO N DO
  BEGIN
    GOTOXY(36,12); WriteLn(i);
    X1 := Random; X2 := Random;
    U1 := SQRT ( - 2 * ln ( X1 )) * cos ( 2 * pi * X2 );
    U2 := SQRT ( - 2 * ln ( X1 )) * sin ( 2 * pi * X2 );
    Z := muSigma + sigmaSigma * U1 - 4 * FLoad / pi / SQR ( mud + sigmad * U2 );
    IF Z < 0 THEN
    BEGIN
      NuZsmaller0 := NuZsmaller0 + 1; TotU1 := TotU1 + U1; TotU2 := TotU2 + U2
    END
    ELSE { DO NOTHING }
  END;
  U1Z := TotU1 / NuZsmaller0; U2Z := TotU2 / NuZsmaller0;
  ClrScr;
  WriteLn('Number Z < 0: ',NuZsmaller0:6);
  WriteLn('Prob Z < 0: ',NuZsmaller0/N:16);
  U10 := -1; U12 := 10;
  WHILE abs ( U12 - U10 ) > 1e-10 DO
  BEGIN
    Help := mud + sigmad * U2Z / U1Z * U10;
    Func := muSigma + sigmaSigma * U10 - 4 * FLoad / pi / SQR ( Help );
    Deriv := sigmaSigma +
      4 * 2 * FLoad * sigmad * U2Z / U1Z /
      pi / Help / Help / Help;
    U11 := U10 - Func / Deriv;
    IF abs ( U11 - U10 ) < 1e-10 THEN U12 := U10 ELSE U10 := U11
  END;
  WriteLn('Xint:      ',U11*sigmaSigma+muSigma:16);
  WriteLn('Yint:      ',U2Z/U1Z*U11*sigmad+mud:16);
  GOTOXY(27,12); Write('To continue, hit <RETURN> '); ReadLn
END.
```

OUTPUT:

```
Number Z < 0: 2196
Prob Z < 0: 2.1960000E-0003
Xint: 2.6693140E+0002
Yint: 2.1840131E+0001
```

With this Turbo Pascal program adjacent results were calculated in 44 s. Compare this with the 12 minutes calculation time for the Mathcad program!

Program for the method "angles" in Turbo Pascal:

```
PROGRAM ANGLES;
USES CRT;
CONST
  N = 1000000;
VAR
  NuZsmaller0, i                : LONGINT;
  U1, U2, U10, U11, U12, Deriv,
  ResAngle, ResAngle1, Help, Func,
  MeanAngle, muSigma, sigmaSigma,
  mud, sigmad, FLoad, X1, X2, Z : EXTENDED;
BEGIN
  ClrScr;
  RANDOMIZE; NuZsmaller0 := 0; MeanAngle := 0;
  muSigma := 290; sigmaSigma := 25; mud := 30; sigmad := 3; FLoad := 1e5;
  FOR i := 1 TO N DO
  BEGIN
    GOTOXY(36,12); WriteLn(i);
    X1 := Random; X2 := Random;
    U1 := SQRT ( - 2 * ln ( X1 )) * cos ( 2 * pi * X2 );
    U2 := SQRT ( - 2 * ln ( X1 )) * sin ( 2 * pi * X2 );
    Z := muSigma + sigmaSigma * U1 - 4 * FLoad / pi / SQR ( mud + sigmad * U2 );
    IF Z < 0 THEN
    BEGIN
      NuZsmaller0 := NuZsmaller0 + 1; ResAngle1 := ArcTan(U2/U1);
      IF U1 > 0 THEN
      BEGIN
        IF U2 > 0 THEN ResAngle := ResAngle1 ELSE ResAngle := 2 * pi + ResAngle1
      END ELSE
        ResAngle := pi + ResAngle1;
      MeanAngle := ( ( NuZsmaller0 - 1 ) * MeanAngle + ResAngle ) / NuZsmaller0
    END ELSE { DO NOTHING }
  END;
  ClrScr;
  WriteLn('Number Z < 0: ',NuZsmaller0:6);
  WriteLn('Prob Z < 0: ',NuZsmaller0/N:16);
  WriteLn('MeanAngle:      ',MeanAngle:16);
  U10 := -1; U12 := 10;
  WHILE abs ( U12 - U10 ) > 1e-10 DO
  BEGIN
    Help := mud + sigmad * sin ( MeanAngle ) / cos ( MeanAngle ) * U10;
    Func := muSigma + sigmaSigma * U10 - 4 * FLoad / pi / SQR ( Help );
    Deriv:= sigmaSigma +
      4 * 2 * FLoad * sigmad * sin ( MeanAngle ) / cos ( MeanAngle ) /
      pi / Help / Help / Help;
    U11 := U10 - Func / Deriv;
    IF abs ( U11 - U10 ) < 1e-10 THEN U12 := U10 ELSE U10 := U11
  END;
  WriteLn('Xint:          ',muSigma + sigmaSigma * U10:16);
  WriteLn('Yint:          ',mud + sigmad * U10 * sin ( MeanAngle ) / cos ( MeanAngle ) :16);
  GOTOXY(27,12); Write('To continue, hit <RETURN> '); Readln
END.
```

OUTPUT:

```
Number Z < 0: 2196
Prob Z < 0: 2.1960000E-0003
Xint:      2.6683549E+0002
Yint:      2.1844055E+0001
```

Program for the method "nearest to the mean" in Turbo Pascal:

```
PROGRAM Distance;
USES CRT;
CONST
  N = 1000000;
VAR
  NuZsmaller0, i                : LONGINT;
  U1, U2, Distance, Dist,
  muSigma, sigmaSigma, X, Y,
  mud, sigmad, FLoad, X1, X2, Z : EXTENDED;
BEGIN
  ClrScr;
  RANDOMIZE; NuZsmaller0 := 0; Distance := 1e20;
  muSigma := 290; sigmaSigma := 25; mud := 30; sigmad := 3; FLoad := 1e5;
  FOR i := 1 TO N DO
  BEGIN
    GOTOXY(36,12); WriteLn(i);
    X1 := Random; X2 := Random;
    U1 := SQRT ( - 2 * ln ( X1 ) ) * cos ( 2 * pi * X2 );
    U2 := SQRT ( - 2 * ln ( X1 ) ) * sin ( 2 * pi * X2 );
    Z := muSigma + sigmaSigma * U1 - 4 * FLoad / pi / SQR ( mud + sigmad * U2 );
    IF Z < 0 THEN
    BEGIN
      NuZsmaller0 := NuZsmaller0 + 1; Dist := SQRT ( SQR ( U1 ) + SQR ( U2 ) );
      IF Dist < Distance THEN
      BEGIN
        X := U1;
        Y := U2;
        Distance := Dist;
      END ELSE { NOTHING }
    END ELSE { DO NOTHING }
  END;
  ClrScr;
  WriteLn('Number Z < 0: ',NuZsmaller0:6);
  WriteLn('Prob Z < 0: ',NuZsmaller0/N:16);
  WriteLn('X: ',muSigma + sigmaSigma * X:16);
  WriteLn('Y: ',mud + sigmad * Y:16);
  GOTOXY(27,12); Write('To continue, hit <RETURN> '); ReadLn
END.
```

OUTPUT:

```
Number Z < 0: 2181
Prob Z < 0: 2.1810000E-0003
Xint:      2.6547600E+0002
Yint:      2.1896883E+0001
```

III.4. BOUNDARY CONDITIONS AS A FUNCTION OF TWO PHENOMENA

III.4.1. EXTREME HIGH WATER LEVELS

Extreme high water levels are caused by wind set up (in a lake; at sea the tide is also involved), by high discharges (in a river, resulting in an increasing river level, or in a lake, resulting in an increasing basin level) or by a combination of both.

Along the North Sea Coast high water levels are mainly caused by superposition of the tide (high tide) and wind set up. Besides that, shower gusts and oscillations can be of influence. Before construction of the storm surge barrier, high water levels in the Oosterschelde basin were determined by, besides the tide, wind set up on the North Sea. No large rivers discharge into the Oosterschelde basin. Since the realisation of the barrier, the water level in the basin during high water levels in the North Sea is influenced greatly by the use of the storm surge barrier.

The extremely high river water levels inside the flood plane are determined by the high water discharges caused by melting snow in spring (Rhine) or caused by rain fall in the flow area of the river (Rhine or Meuse).

When calculating the high water levels in a lower river area (e.g. for the benefit of the Storm surge barrier in the Nieuwe Waterweg or for the strengthening of dykes in the western part of the Alblasserwaard) both wind set up at sea (storm surges) and high river discharges, as well as a combination of both should be taken into account.



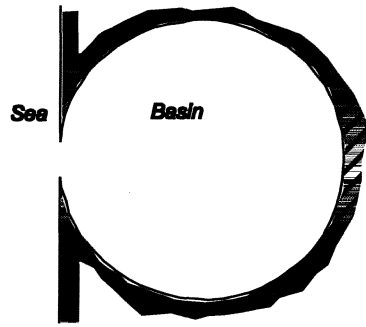
Figure III-5

To gain an insight into the factors that cause a high water level at a certain measuring post and into how these factors are manifested in the high water level exceedance frequency curve, some schematisations are introduced. The influences of the sea and a high river discharge on the high water level in a basin (a schematisation of a lower river area) are first considered separately. Subsequently, a possible simultaneous occurrence of a storm surge and a high river discharge is analysed. The effect of a storm surge barrier is examined.

III.4.2. STORM SURGE LEVELS

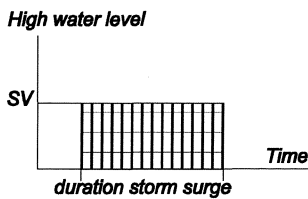
In the Netherlands a storm surge is understood to mean a high water level as a consequence of tide (high tide) and wind set up (caused by a "storm"), which exceeds a certain threshold level. The threshold level is defined as the water level that is exceeded on average 0.5 times per year. Hence, on average, a storm surge occurs once every two years.

Let us consider a basin is open connection with the sea. In that basin storm surges may occur. A schematisation of the Oosterschelde basin (which serves as an example) is shown in Figure III-6 on the right side.



Figure

III-6



To simplify, we assume the wind set up so great, that the influence of the tide can be neglected. Furthermore, the high water level is assumed constant during the storm which causes the wind set up. The duration of the storm surge is assumed such that the maximum water level is attained everywhere in the basin in the considered storm.

Figure III-7

The probability density function, the probability distribution and the exceedance frequency curve of the high water level in the basin all have (practically) the same shape as those of the storm surge at sea. The high water level in the basin "follows" the storm surge level at sea: $h_{basin} = h_{sea}$, provided that the estuary is wide and deep enough relative to the length of the basin and that the bed slope multiplied by the basin length is not too great, relative to the height of the storm surge level.

Note, that (in civil engineering) the probability *exceedance curve* (and NOT the probability distribution) is usually presented with the high water levels as ordinates and the logarithm of the probabilities of *exceedance* as intercepts, as is the case in the opposite figure. In the presentations of probability density and probability distribution the storm surge level is plotted on the axis of the intercepts. The probability exceedance curve plots the storm surge level on the axis of the ordinates. (Compare the bold points in the opposite figures.)

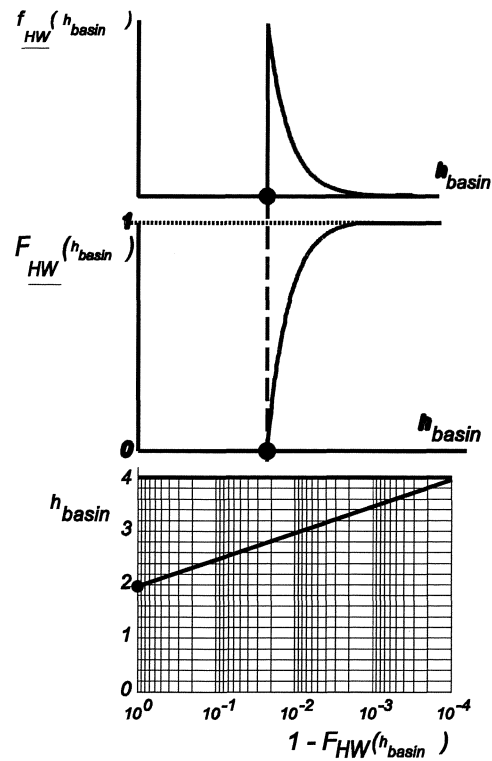


Figure III-8

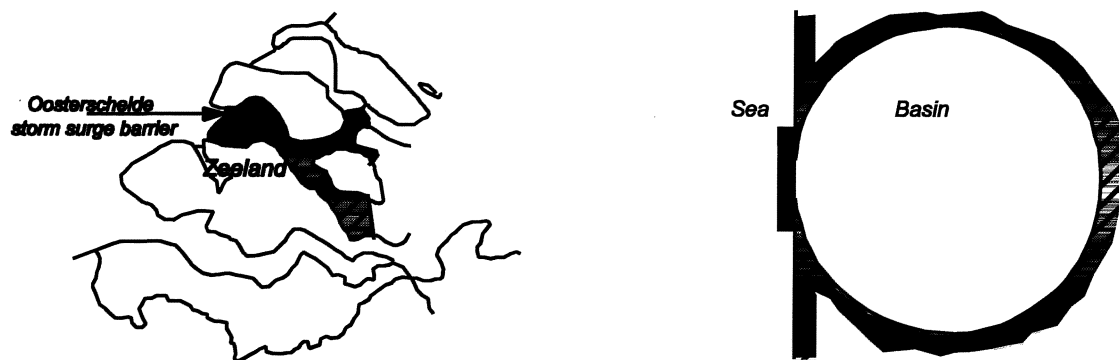


Figure III-9

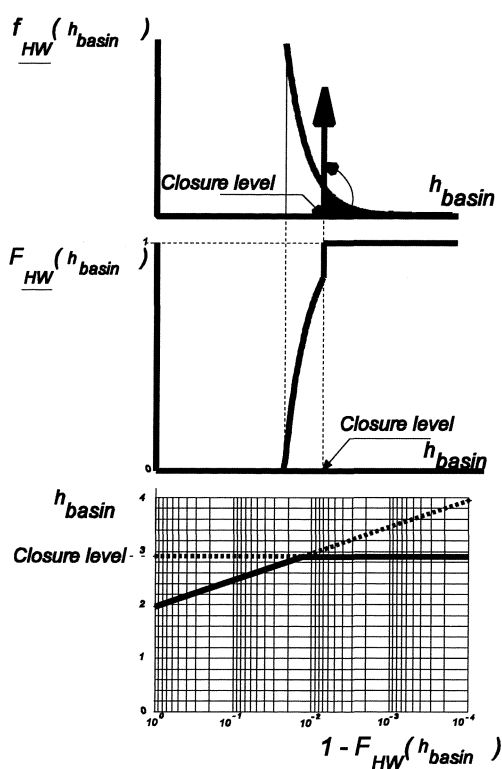


Figure III-10

In the case of closure of a defence:

$$h_{basin} = h_{sea} \quad \text{if } h_{basin} \leq \text{Closure level}$$

$$h_{basin} = \text{Closure level} \quad \text{for all other (higher) water levels at sea.}$$

N.B. The defence must be closed gradually to avoid translation waves in the basin.

If, for whatever reason, the high water levels in the basin are considered too high, the basin can be closed off, as has been done on several sites in the Netherlands as part of the Delta works. The high water levels' threat to the land needn't be resolved by raising all protection works surrounding the basin. The length of the sea dykes to be maintained decreases by closing off the basin (coast line shortening). The dykes along the closed off basin can be lower than would be necessary without closing off.

When a movable defence is in use, the storm surges at sea can be kept out of the basin by shutting the defence at a certain water level (the *closure level*). In that case, all storm surge levels at sea, higher than the closure level are "censored". (For censored distributions, see § II.5.) The probability density function, the probability distribution and the probability exceedance curve of the high water levels in the basin are as is illustrated opposite.

III.4.3. RIVER DISCHARGES

The second case is a situation in which a river flows into a basin (e.g. the Haringvliet). The following also applies to big rivers that flow through the basin formed by their "winter bed" or estuary.

SCHEMATISATION OF THE BASIN LEVEL OF AN OPEN BASIN WITH A FIXED OUTSIDE WATER LEVEL:

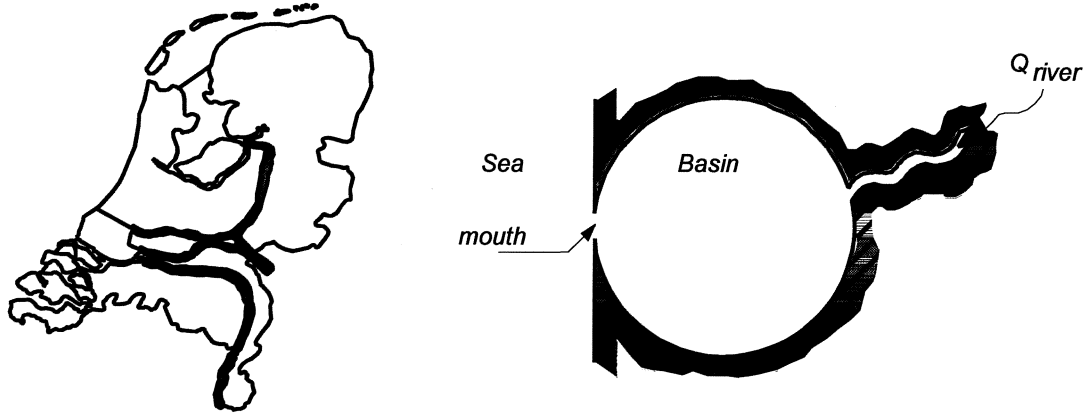


Figure III-11

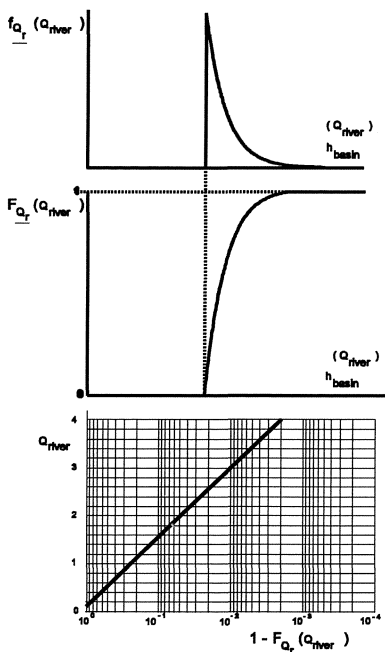


Figure III-13

For the sake of simplicity, the water level outside the estuary (at sea) is assumed a fixed level. (Instead of at sea one can imagine at a - fixed - lake water level.) Water level increases are measured relative to this level. The variation of the water level in the basin is a result of flood waves in the river.

Assume that the flood wave lasts a "time unit" (e.g. 5 days), regardless of the size of the discharge wave:

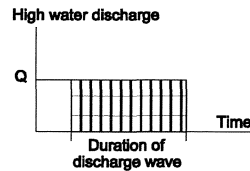


Figure III-12

The high water levels in the basin follow from the river's high water discharges. (Compare § II.5.) The river discharges (as well as the storm surge levels) can be assumed distributed exponentially. The probability distribution of the river discharges to the basin and the river discharge exceedance frequency curve can be shown as in Figure III-13. In formula:

$$F_{Q_r}(Q_{river}) = 1 - e^{-\frac{Q_{river} - \alpha}{\beta}}$$

Furthermore, assume a stationary situation, so that all river discharges are transported via the mouth of the basin. Also assume that the flow section of the mouth of the basin doesn't change much due to the water level rise (storage) in the basin, as a result of river discharge. In the equation:

$$Q_{mouth} = \mu A_{mouth} \sqrt{2g \Delta h_{basin}}$$

in which $Q_{\text{mouth}} = \text{discharge via the mouth of the basin } (= Q_{\text{river}})$

$\mu = \text{discharge coefficient}$

$A_{\text{mouth}} = \text{surface of the flow profile of the basin mouth}$

$g = \text{acceleration due to gravity}$

$\Delta h_{\text{basin}} = \text{water level rise in the basin as a result of the river discharge, also high water level } h_{\text{basin}} \text{ in the basin,}$

μ and A_{mouth} are assumed constants, so that $\Delta h_{\text{basin}} = h_{\text{basin}} = \left(\frac{Q_{\text{river}}}{\mu \cdot A_{\text{mouth}}} \right)^2 \cdot \frac{1}{2 \cdot g} \therefore Q_{\text{river}}^2$ (water level rise in the basin is proportional to the square of the river discharge).

SCHEMATISATION OF AN OPEN BASIN WITH VARIABLE OUTSIDE WATER LEVEL:

If (as is usually assumed) the river discharges are independent¹⁾ of the high outside water levels (storm surge levels), the water levels at sea may be added to the water level (rise) as a result of river discharges. The water level in the basin can then be described with (see: bottom of page III - 5 and bottom of page III - 6):

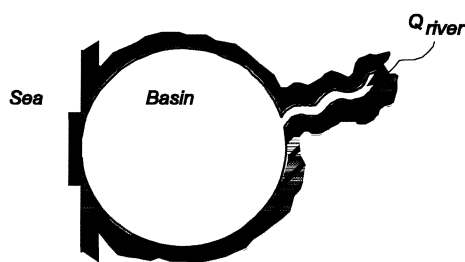
$$h_{\text{basin}} = h_{\text{sea}} + \left(\frac{Q_{\text{river}}}{\mu \cdot A_{\text{mouth}}} \right)^2 \cdot \frac{1}{2 \cdot g}$$

CLOSING THE DEFENCE:

The defence is closed at the closure level s , for which (apparently):

$$s = h_{\text{basin}} = h_{\text{sea}} + \left(\frac{Q_{\text{river}}}{\mu \cdot A_{\text{mouth}}} \right)^2 \cdot \frac{1}{2 \cdot g}$$

FILLING THE BASIN WITH A CLOSED DEFENCE:



Closing the defence prevents the flow of river water from the basin. After closing the defence, the water level in the basin will rise because the total river discharge now has to be stored in the basin. The corresponding equation which describes this is:

$$\Delta h_{\text{basin}} = \frac{Q_{\text{river}}}{B_{\text{basin}}} \Delta t$$

Figure III-14

- $\Delta h_{\text{basin}} = \text{water level rise in the basin}$
- $Q_{\text{river}} = \text{river discharge}$
- $B_{\text{basin}} = \text{storage surface of the basin}$
- $\Delta t = \text{duration of the discharge wave.}$

WATER LEVEL IN THE BASIN JUST BEFORE THE REOPENING OF THE DEFENCE:

Just before the reopening of the defence, the basin water level, h_{basin} , can be modelled with:

$$h_{\text{basin}} = s + \frac{Q_{\text{river}} \cdot \Delta t}{B}$$

Calculating the exceedance frequency curve of the basin water level is not a simple task.

¹⁾ Van der Made demonstrated that the wind set up in the North Sea and the Rhine discharges are not totally independent (See footnote on page II - 19.)

III.4.4. EQUAL LEVEL CURVES

For every one of the previously described situations for a basin (tide without and with a defence and river discharge with and without a defence) equal level curves can be determined. Equal level curves¹⁾ are displayed in a line nomogram, indicating which high water levels are *equally* high as a result of storm surge levels at sea and/or as a result of high river discharge and/or as a result of combinations of both.

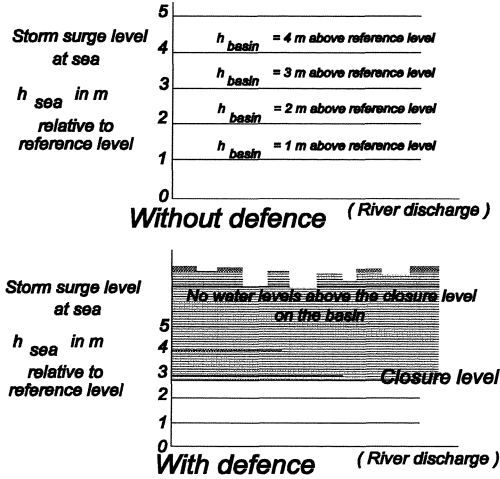


Figure III-15

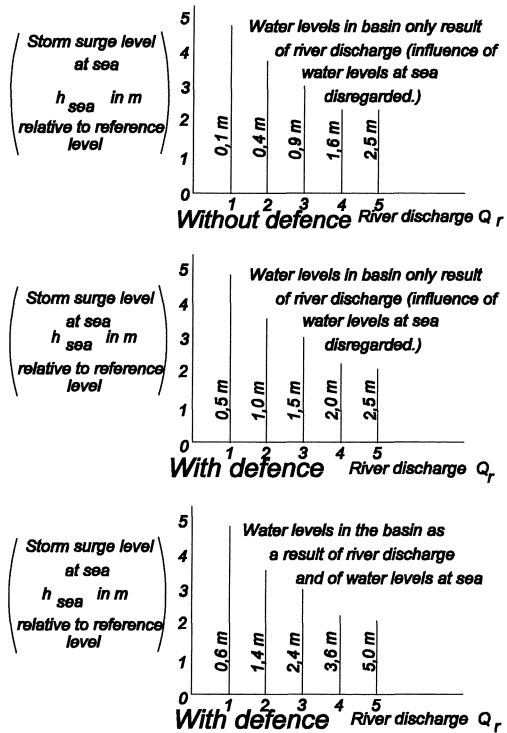


Figure III-16

In case no river flows into the basin the high water level in the basin is determined by the water level at sea. The river discharge has no influence.

In Figure III-15, in which Q_r the river discharge, is selected as intercept and the storm surge level at sea, h_{sea} , as an ordinate, a coordinate defines a point of an equal level curve, that is, the line of equal high water level in the basin. The equal level curves for a basin *without* river discharge run parallel to the axis on which the discharge (or the water level as a result of it) is plotted.

Closure of the water defence rules out water levels higher than the closure level (in principle). (In principle, because the defence can collapse. This subject will be re-opened later.)

In case the river discharge is solely of influence on the high water level and the water level at sea is constant, the equal level curves run parallel to the axis on which the storm surge levels are marked. The water levels in the basin increase quadratically with the discharge.

Closure of the defence (still assuming a constant outside water level) gives equal level curves which are also parallel to the axis on which the storm surge levels are marked, only now the water levels in the basin increase linearly with the discharge.

A closed defence where initially the outside water level did vary (combination of opened and closed defence) corresponds to the equal level curves in the top of Figure III-16, moved over a distance

$$\frac{Q_{river} \cdot \Delta t}{B_{basin}}$$

¹⁾ Instead of the term "equal level curves" the term "*bearing line*" is sometimes used, INCORRECTLY. A bearing line gives a relation (borne) between water levels and different water level gauges with a permanent river discharge.

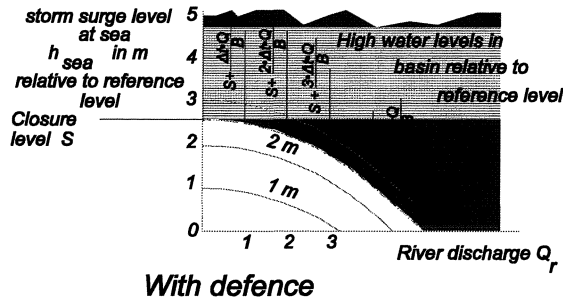
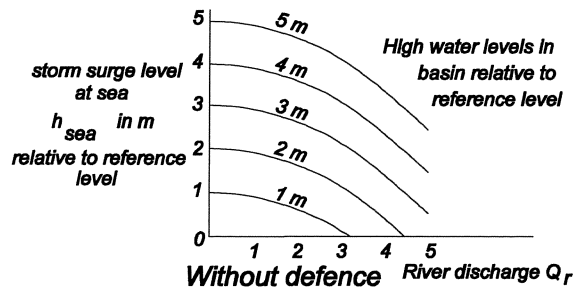


Figure III-17

There are areas where both the water levels at sea and the river discharges influence the water level. In this so-called transitory area (in the Netherlands: the part of the river area to the east of the line Schoonhoven - Werkendam and west of the line Jaarsveld - Gorinchem) every rise of the sea water level is increased by a water level rise as a result of the river discharge. The result is that the lines of equal basin water level, h_{basin} , go down to the right due to the raising influence of the discharge, Q_{river} (Figure III-17, above), because for the equal level curves:

$$h_{basin} = h_{sea} + \frac{1}{2 \cdot g} \cdot \left(\frac{Q_{river}}{\mu \cdot A_{mouth}} \right)^2 = constant$$

By closing the defence at a certain closure level (in Figure III-17 Reference level + 2.60 m was chosen) the equal level curves (of course) keep the same gradient below the closure level. The equal level curves above the closure level have the characteristics of curves of "only river discharge influence", since the sea's influence is eliminated by the defence.

In practice, the equal level curves aren't calculated using a discharge formula and/or a basin approach, but using a tide model, such as DUFLOW.

III.4.5. EQUAL LEVEL CURVES IN THE "GUIDELINES LOWER RIVERS"

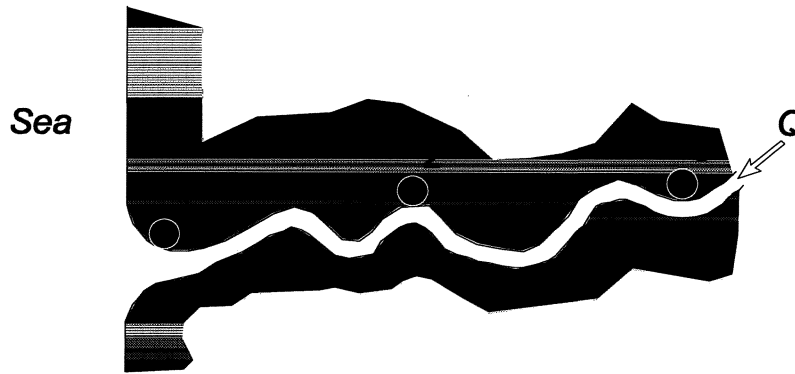


Figure III-18

For three selected stations along a river: one at the estuary mouth, where the high water levels are solely determined by the storm surge levels at sea, one in the "tidal area" (lower river), where both storm surge levels and high water discharge waves determine the high water levels and one where the influence of the storm surges is no longer noticeable (upper river) and the high water levels are determined only by high river discharges, the shapes of the equal level curves are globally as illustrated in Figure III-19. As a simplification, the curves in the middle figure have been drawn as straight lines. Theoretically, these should be parabolas, but on the next page the cases of Streefkerk and Jaarsveld are seen to differ in reality. The probability density functions of storm surge levels and of river discharges are also given.

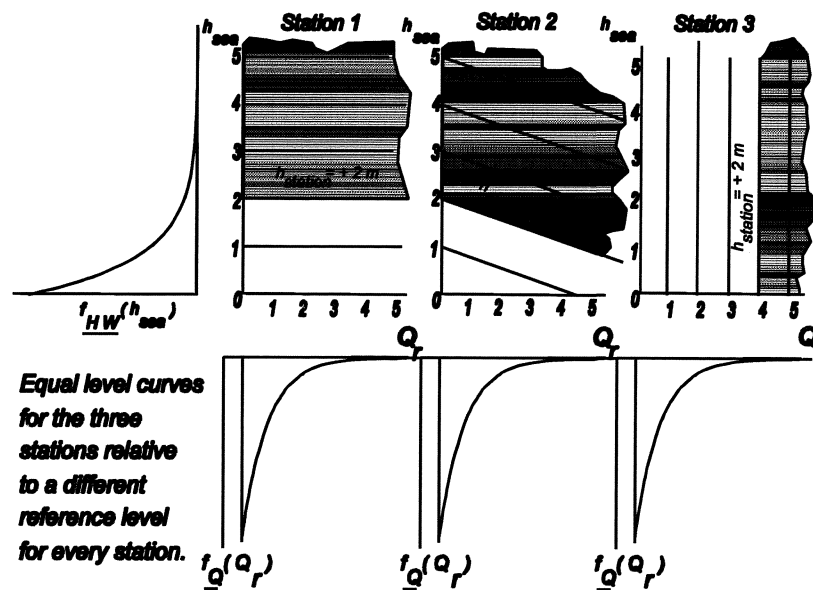
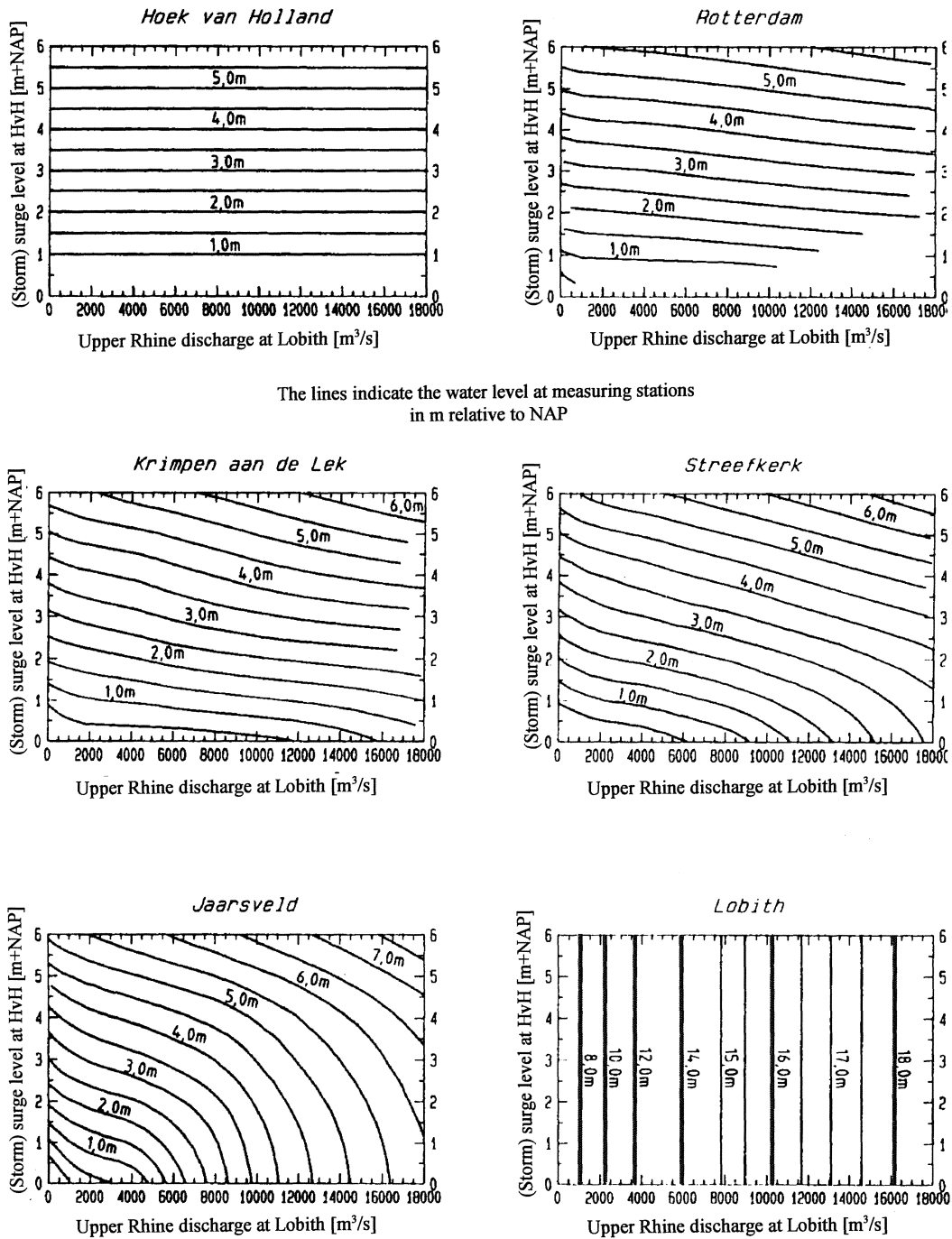


Figure III-19

In the preceding paragraphs drastic simplifications were introduced. The most striking simplifications are the assumption of a constant basin surface at all basin water levels and the assumption of the constant duration of a storm surge situation and a flood wave. Only the height of the storm surge level and the amount of discharge were considered (random) variables. Contrary to the impression given above, the equal level curves (particularly in the transitory area) won't be straight in reality. A couple of equal level curves published in the Guide to the design of river dykes, part 2, lower river area, (in Dutch, "Leidraad voor het ontwerpen

van rivierdijken, deel 2, benedenrivierengebied”), Technical Advisory Committee on Water Defences, the Hague, September 1989, published by Waltman, Delft, are shown below.

Equal level curves Nieuwe Waterweg - Nieuwe Maas - Lek



The lines indicate the water level at measuring stations in m relative to NAP

Figure III-20

III.4.6. PROBABILITY DENSITY OF THE HIGH WATER LEVELS IN THE BASIN

In Figure III-19, which shows the equal level curves for three stations along a river, the hatched areas indicate where the basin water level is "reference level + 2 m and higher". Integration of the joint probability density functions of storm surge levels and high river discharges over these areas in the direction perpendicular to the equal level curves gives the exceedance probability of the high water level considered. The exceedance probability, $P\{h > h_{basin}\}$, the probability distribution $F_h(h_{basin})$ and the probability density function $f_h(h_{basin})$ of high water levels in the basin can be determined this way.

The figure below illustrates the procedure for determining the histogram (probability density function) of the high water levels in a lower river area, where, at a certain moment, the defence structure in the river estuary is closed.

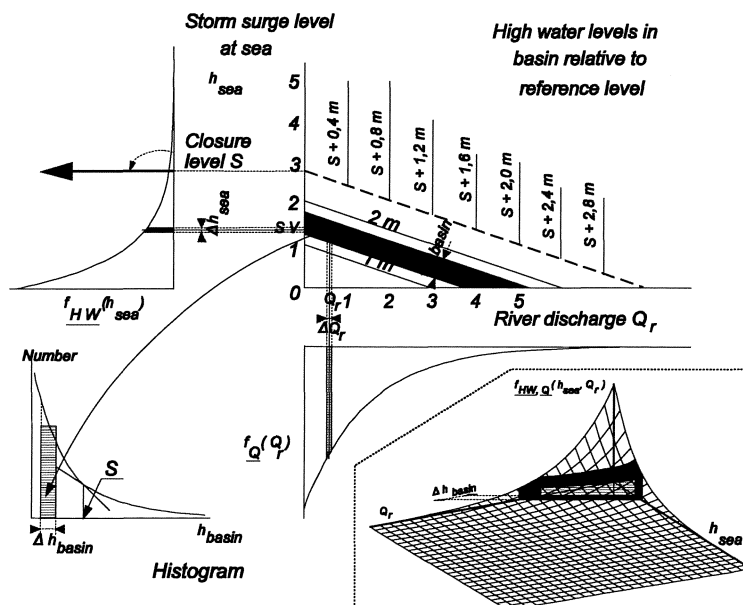


Figure III-21

For every combination of h_{sea} and $Q_{r(iver)}$, the basin water level has to be calculated. For an opened defence structure:

$$h_{basin} = h_{sea} + \frac{1}{2 \cdot g} \cdot \left(\frac{Q_r}{\mu \cdot A_{mouth}} \right)^2$$

If, however, the defence structure is closed and the outside water level exceeds the closure level, the following formula for the closed defence applies:

$$h_{basin} = s + \frac{Q_r \cdot \Delta t}{B}$$

With this function definition the probabilities $p_h(h_{basin})$ along the h_{basin} axis are classified. Hence a probability density function (see page II - 5) of the basin water level is determined.

$$P\{h = h_{basin}\} = p_h(h_{basin}) \Delta h_{basin} = \sum_{h_{basin} - \frac{\Delta h_{basin}}{2} < h_{basin}(h_{sea}, Q_r) \leq h_{basin} + \frac{\Delta h_{basin}}{2}} f_{HW}(h_{sea}) f_Q(Q_r) \Delta h_{sea} \Delta Q_r$$

The figure in the bottom right corner of Figure III-21 shows the part below the joint probability density function of storm surge levels and discharges, which is representative in the histogram (bottom left, that is the probability density function of the basin water level) for the considered interval Δh_{basin} (here about 1.5 m above chart datum) of high water levels in the basin.

III.4.7. FAILURE OF THE WATER DEFENCE

The purpose of the defence structure is reducing the probability of exceedance of a certain basin water level to a determined (small) value (e.g. 10^{-4}).

Assume, for simplicity's sake, that only sea water levels are of influence. (There is no river discharge into the basin.) If the water level at sea becomes too high the defence can collapse. In the figure below this is expressed in the equal level curves which regain a meaning above a certain level. The corresponding probability density function is sketched next to the equal level curves.

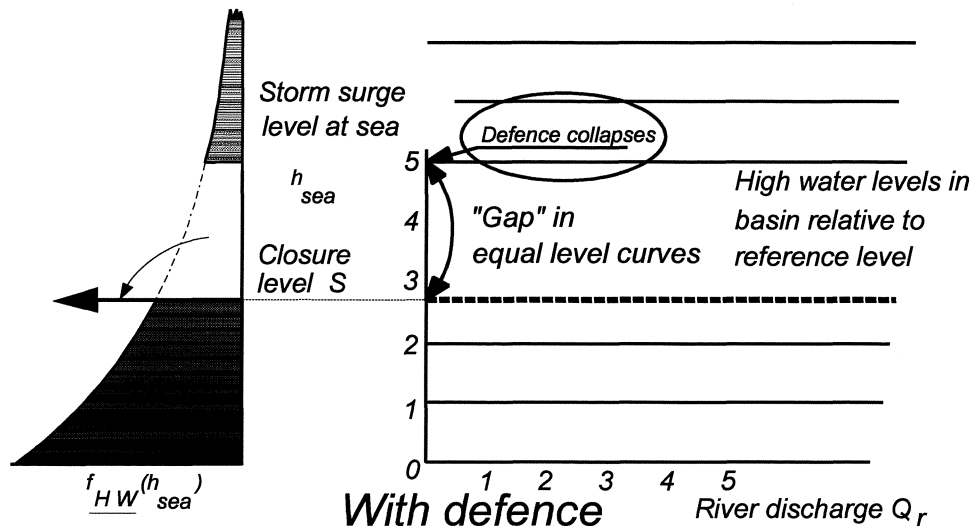


Figure III-22

To calculate the probability that a certain water level in the basin is exceeded in one year, "failure of the defence" has to be involved. Firstly, there is a probability (assume: p), that the defence structure is not closed (e.g. due to human failure or to a defective operation mechanism). The probability of closure of the defence is then $(1 - p)$. For that, the set of equal level curves given at the beginning of this section is valid. The "surface below the probability density function" now isn't 1 (as is usual), but $(1 - p)$. The probability of occurrence of a certain high water level in a year, which is calculated using the lines, has to be increased by the probability of that high water level if the defence is not closed.

III.4.8. COINCIDING LOADS

In the previous sections it was assumed that, in the case of high water levels caused by tide, wind set up and high river discharges, these three elements occur together simultaneously and for the same period of time. A discharge wave, however, lasts approximately 3 weeks, a storm (wind set up) for example 36 hours and the tide (in the Netherlands) lasts 12 hours and 25 minutes. The combination of these three high water level determining factors ¹⁾, is what is of importance, for example in the lower rivers area: the water level that is assumed constant during 5 days (the "top" of the 20 day lasting flood wave), on top of which the highest 10 (5 days discharge wave "contains" 10 tides) storm surge levels are superposed. (This leaves the problem of § II.2.: If 10 realisations are drawn from the storm surge levels, what is the probability density function of the highest of these 10 realisations?)

¹⁾ Turkstra, C.J. and H.O. Madsen, Load combinations in codified structural design, Journal of Engineering, Structural Division, ASCE, Volume 106, nr. St. 12, December 1980.

Figure III-23 could, for example, relate to the loads on a (part of a) structure near Sliedrecht.

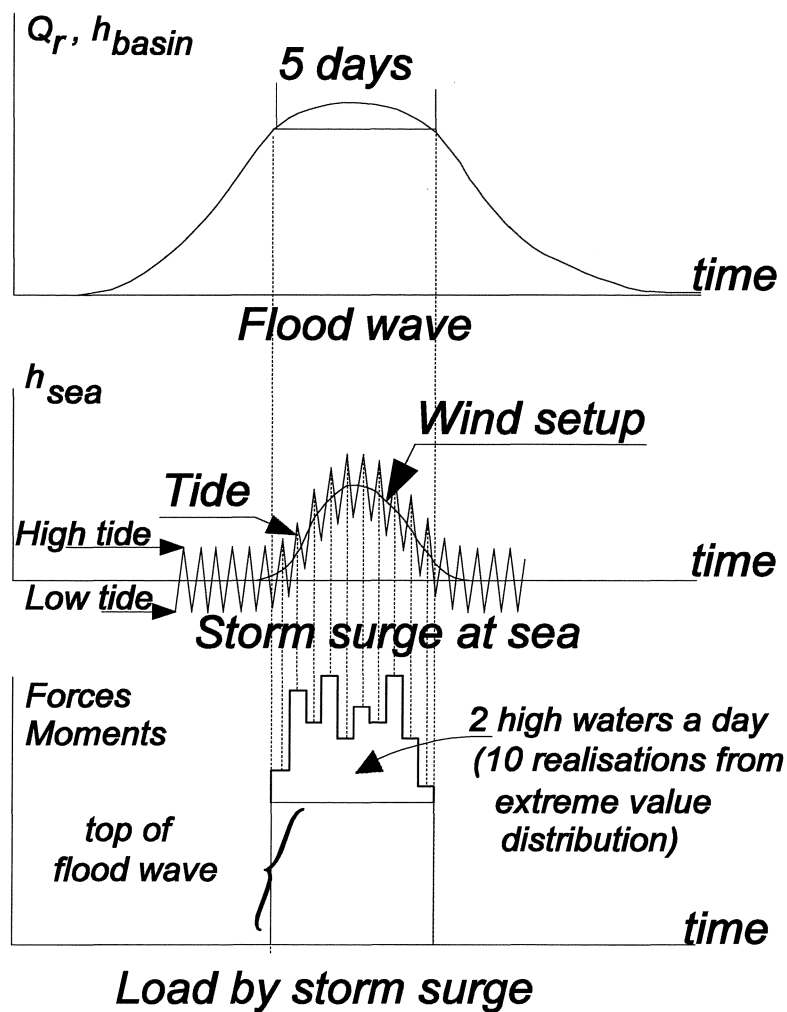


Figure III-27

The problem for the Storm surge barrier in the Nieuwe Waterweg is different than in the lower rivers area. This defence structure is closed in the case of extreme storm surges ($1 - F_{HW}(s) \leq 0.1$ in a year). Such extreme storm surges won't coincide with the yearly maxima of the discharge. That is why, in this case, the probability density function of the yearly maxima of the outside water level ($f_E(h_{sea})$) was combined with the probability density function of the momentary values of the river discharges ($f_Q(Q_r)$). The water levels caused by high outside water levels and those caused by river discharges had to be calculated separately. From that the load as a result of the head difference over the defence could be calculated.

IV. FAILURE MODES IN A CROSS SECTION

IV.1. FAILURE MODES

Systems are designed to satisfy civil engineering needs. A system usually consists of a number of structures.

Structures are designed and constructed to fulfil one or several needs. A structure *fails* or *collapses* when this(these) function(s) can no longer be carried out.

The way a structure collapses or fails is called a *failure mode*.

A failure mode occurs when a *limit state* is exceeded, i.e. when the load exceeds the strength.

To assess to what extent the occurrence of a failure mode leads to the failure of a certain structure and whether the failure of the structure leads to the failure of the system, risk analytical methods have been developed which are summarised by the name "trees". In the lecture series b3, Probabilistic design, fault and event trees were introduced and explained. Fault trees are particularly suitable for the illustration of cause and consequence chains which lead to an (unwanted top-)event if one cause has only two consequences which can be clearly distinguished (yes or no, positive or negative, right or wrong, failure or non-failure, etc.). Only the negative consequences (no, wrong, etc.) are included in the fault tree. To illustrate consequences which can't be as clearly distinguished, a cause- consequence chart is more suitable.

To efficiently present chains of modes, which (could) lead to failure of a system in a fault tree, a function analysis of the considered system is necessary. Which loss of function is selected as the top event must be well defined. For the safety evaluation of water defences this is usually clear. The unwanted top event can usually be described as follows: The water is no longer kept out. For a breakwater around a port the function is: providing calm water to facilitate the loading and unloading of ships.

The general structure of a fault tree is presented in Figure IV-1. Different aspects which are relevant for the analysis, are also indicated.

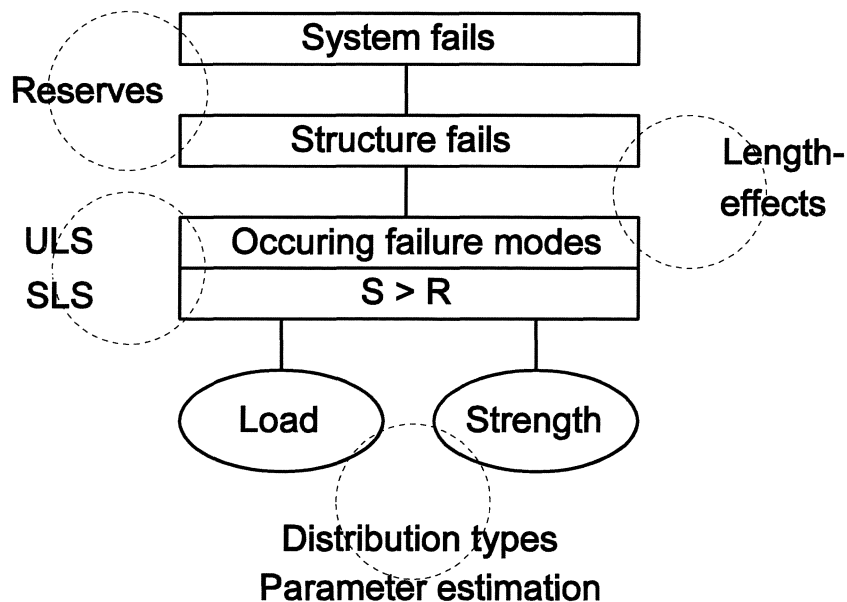


Figure IV-1

The sea defence system of the town Whitstable before 1980 serves as an example. Whitstable is located near the Thames estuary, namely on the south bank of the Thames, to the north east of Canterbury. The town itself lies below the sea defence system and below the (assumed impermeable) North Downs (hills). The sea defence system consisted of the following elements (see Figure IV-2):

1. a new sea wall in the east (crest amply above average sea level).
2. a port terrain in the middle. This port terrain is (before 1980 and still: anno 1996 !) closed off during high water levels by placing sandbags.
3. an old, low, unstable sea wall in the west. (In the course of a number of years this wall was improved. The renovation had not yet been totally completed in 1994.)
4. an oyster warehouse, built in the western old sea wall.
5. a couple of land partitions to the south and the west of Whitstable. In the west these land partitions are linked to the dyke along the southern bank of the Thames.

People feared the town would be flooded due to failure of the sea defence system.

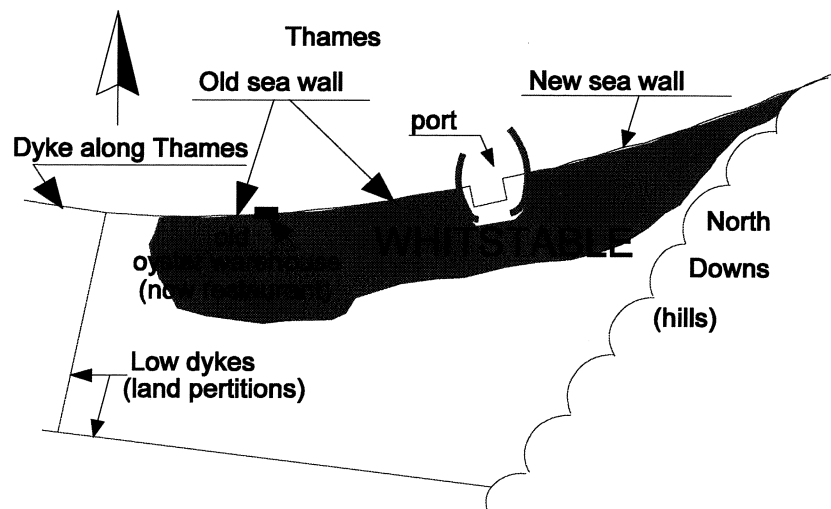


Figure IV-2

A fault tree (see Figure IV-3) indicates how the most unwanted reaction of the system (flooding of Whitstable) can arise.

The five structures mentioned in the example's description can be distinguished in the fault tree in Figure IV-3. Note that every mode is considered characteristic for a certain cross section (structure or section: land partitions, old sea wall, oyster warehouse, port terrain, new sea wall). Several modes can be relevant to one cross section (e.g.: "OLD SEAWALL IS INUNDATED" and "OLD SEAWALL COLLAPSES").

Every cross section is expected to concern a whole (stretch of a) structure. "Failure" is considered "in a cross section" ("per section" or "per structure"). If, for example, the water level in a cross section is higher than the defending height, the structure is considered failing over the entire length. Analogous circumstances lead to the collapse of the old sea wall and of the oyster warehouse. The approach is characteristic for the analysis of a *serial system* (here the serial system is: the succession of individual structures).

A closed system of water defences doesn't usually consist of a single defence structure, which, in turn, doesn't usually consist of one section. This is a serious complication because it makes it virtually impossible to calculate the probability of collapse of a vaguely realistic system of water defence structures. In literature, a number of upper and lower limit approximations for simple serial systems can be found, which can be worked out numerically. Until now, however, the knowledge to calculate these limits for more realistic systems of water defence structures is lacking. We will come back to this subject in the following chapter V. LENGTH- EFFECTS.

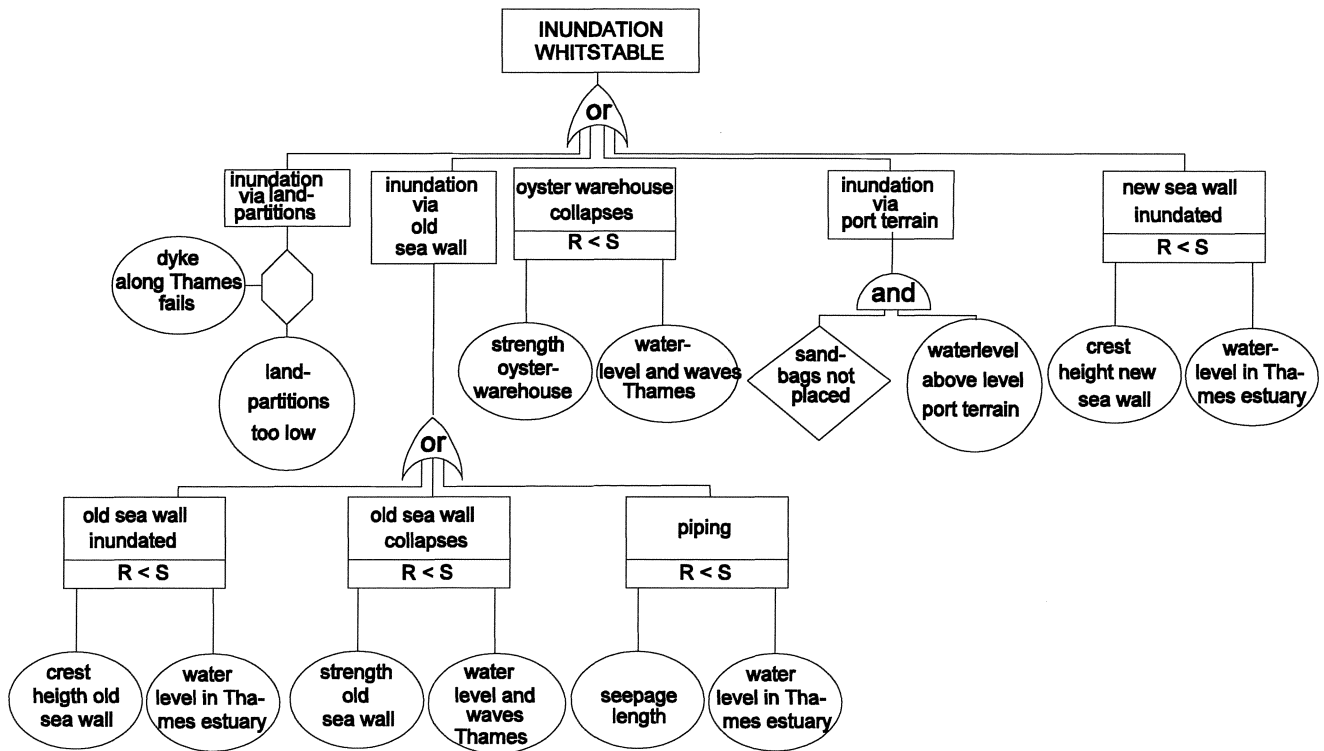


Figure IV-3

A regularly voiced objection against the fault tree analysis is that it is a *technical* analysis, whilst, to a great extent, human intervention (or the lack of it) determines the reliability of a system. However, in the fault tree depicted above, the aspect of "human intervention" is also included. If the water level exceeds the level of the port terrain, a temporary defence made of sandbags is to be created. This temporary defence structure fails if the water level exceeds the level of the port terrain and the sandbags aren't placed by the responsible organisation. (This could be analysed further: sandbags not in place, sandbags not in good state, people to place sandbags absent , etc..)

IV.2. EXAMPLES

FAILURE MODES FOR WATER DEFENCES

A closed system to defend a dyke ring against the water is sketched in Figure IV-4. The system consists of several types of defence structures besides dykes (and dams). The defences, which make up a defence system, could be:

- ◆ dykes and dams
- ◆ dunes
- ◆ other structures
- ◆ natural high grounds.

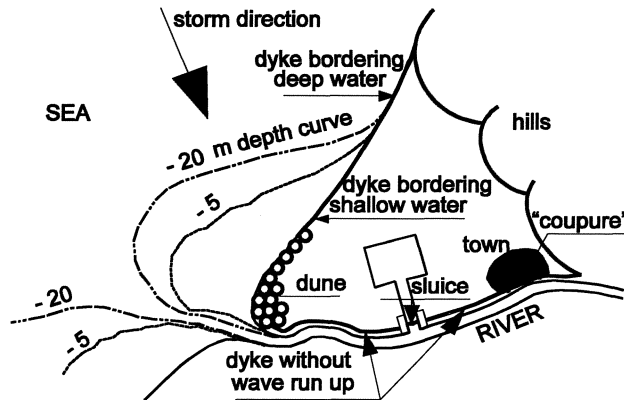


Figure IV-4

Sometimes, dependent on the "load", different courses can be distinguished for one type of defence (e.g. a dyke). (Compare Figure IV-4.) That way a dyke bordering deep water could be considered part of one course, whilst a dyke bordering shallow water could be attributed to a second course. In the fault tree in Figure IV-5 one can recognise the serial system of six construction elements. A fault tree for "Inundation of the dyke ring of Figure IV-4" can be drawn up just like in Figure IV-5. Note that the failure modes are considered per structure (characterised by a cross section).

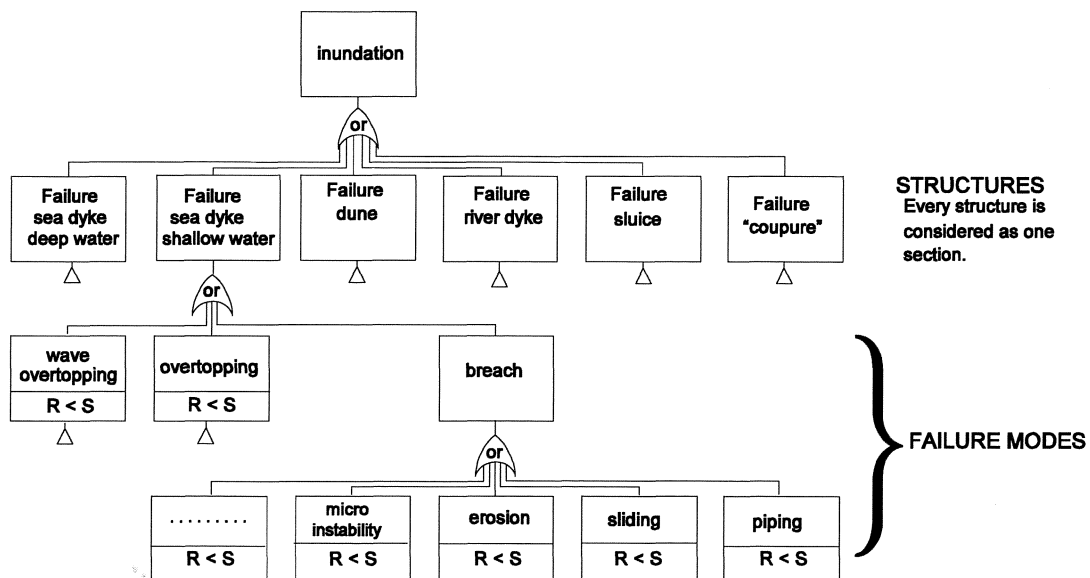


Figure IV-5

In the fault tree, besides technical causes of failure, human mistakes or insufficiencies can also be included. For certain defences such as sluices and coupures¹⁾, these can be important components of the total probability of failure of the defence system. (Many managers of water defences "forbid" coupures in their dyke ring.)

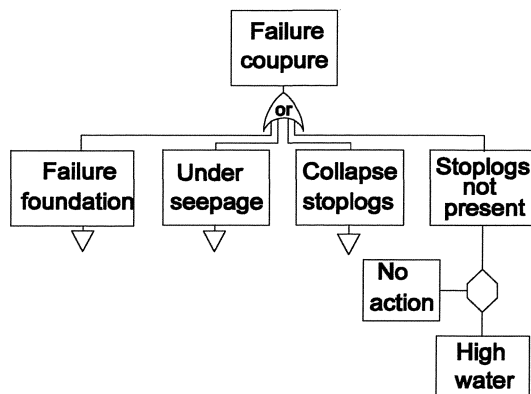


Figure IV-6

For every section, characterised by one cross-section, a probability of failure can be calculated by determining the probabilities of all relevant failure modes for that cross-section according to level II or level III calculations. An upper limit of the probability of failure of the system of water defences is acquired by adding the probabilities of failure of all sections. The greatest failure probability serves as a lower limit of the probability of failure for the system.

The upper limit of the failure probability can be established because several failure modes can be determined by the same (common) parameters. Sections can be correlated because, for example, the storm surge level burdens all of them.

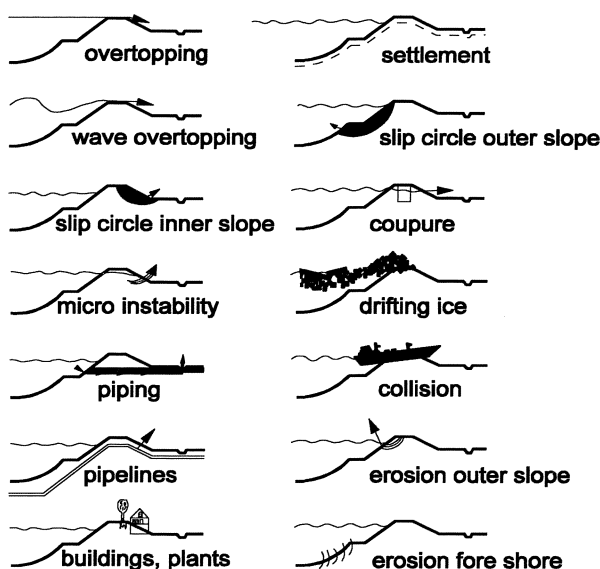


Figure IV-7

A certain dependence of the sections, caused by the load, was pointed out earlier (bottom of page IV - 2). Several failure modes in one cross-section are not totally independent either. A limited number of parts of a dyke ensure the defending function and the stability of the core, the revetment and the subsoil.

¹⁾ A coupure is a cut through the water defense which allows the passage of a (rail) road. In case of high water levels the gap is barricaded with large beams called stoplogs.

If one part is insufficiently strong, it raises the probability of failure for more than one failure mode. Care must be taken of each of these parts during the design phase. In practice, if the various parts of a dyke have been carefully and well designed, measures will have been taken to reduce the probability of occurrence of the failure modes. A relation scheme for parts and modes is given in Figure IV-8.

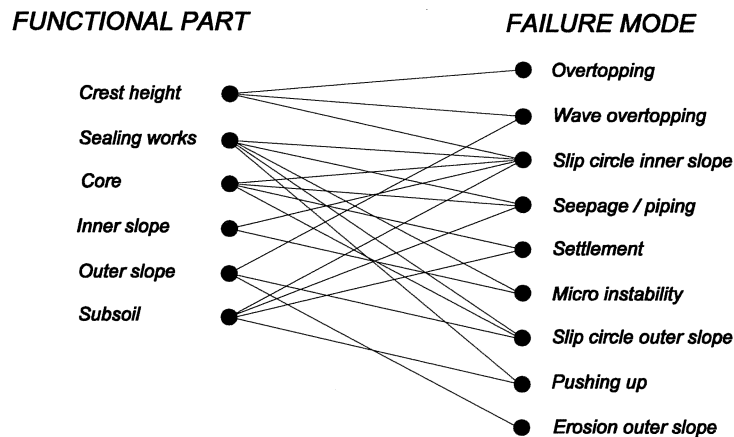


Figure IV-8

The dependence of failure modes in one cross-section due to a certain load, which is involved in more than one mode, and the coherence of functional parts and failure modes is still the subject of research.

Recognising the relation between functional parts and failure modes also has a significance in the design practice. The function of a dyke does not have to be limited to defending against water. Traditionally, dykes were used to connect settlements, attributing the function of traffic road to the dyke. Due to its location along the water, the dyke can also fulfil a leisure function (sport fishing, ramp for pleasure craft, etc.). In the evaluation of safety against flooding the unwanted top event can be described as : The water can no longer be kept out. Inundation, dyke breach, insufficient dune profile, lock door collapses, etc., are alternatives (different descriptions) of this event. This does not mean that the analyses of other functions can't be presented with the use of fault trees.

Some examples of the liberty a designer has when objects (in Figure IV-7: houses) appear in the dyke, are sketched below. The dyke has a function as a "landscape or cultural historical element". Note how different parts of the "classical" dyke profile are replaced by alternative structures, which limit the probability of occurrence of various failure modes.

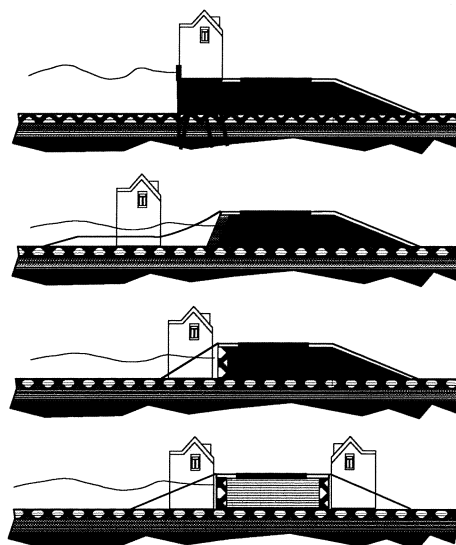


Figure IV-9

EXAMPLE OF SEVERAL FAILURE MODES IN ONE CROSS SECTION: A DUNE SECTION

To illustrate several failure modes in one cross section of a water defence, a dune section is considered. The fundamental lower, respectively upper, limit for the probability of collapse of the section, which can be interpreted as a serial system¹⁾ of N modes is:

$$\text{MAX}_{i=1}^N P_{b_i} \leq P_{b \text{ section}} \leq \sum_{i=1}^N P_{b_i}$$

in which: N = number of modes according to which the section can collapse
 P_{b_i} = probability of collapse in case of collapse according to failure mode i
 $P_{b \text{ section}}$ = total probability of collapse of the section

The lower limit is valid if there is one mode that includes all the others. The upper limit is applicable if all modes exclude each other. "Including" and "excluding" can be indicated in Venn diagrams (in Figure V-4 indicated for 3 events. Ω is the total failure probability space, which, thus, also includes "no failure".):

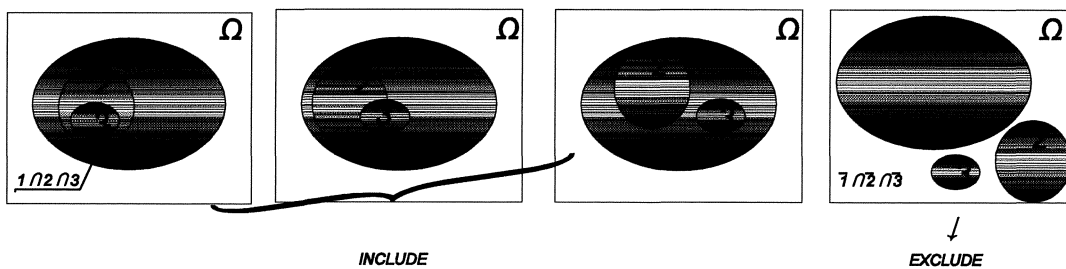


Figure IV-10

Of all the failure modes for a dune *EROSION, WAVE OVERTOPPING AND OVERTOPPING* satisfy the demands for the lower limit. The mode *DUNE EROSION* includes the other two, because in case of overtopping or inundation a breach will certainly follow as a result of dune erosion (and/or has followed). The Dune Erosion Guidelines see to this by requiring the dune crest to be at least 2.50 m above the design water level, or higher if wave circumstances call for it.

There is less dependence between the failure modes "sliding" and "seepage". The high water level is also of importance to these modes, but so are the steepness of the inner slope and, for example, the absence of rabbit burrows. These are two aspects that don't influence dune erosion. The Dune Erosion Guidelines aim to keep the probability of failure for these modes small by requiring certain values for the minimum crest width after erosion (3 m), the maximum gradient of the inner slope ($\arctan(1/2)$) and the minimum width at storm surge level (10 m; see Figure V-11).

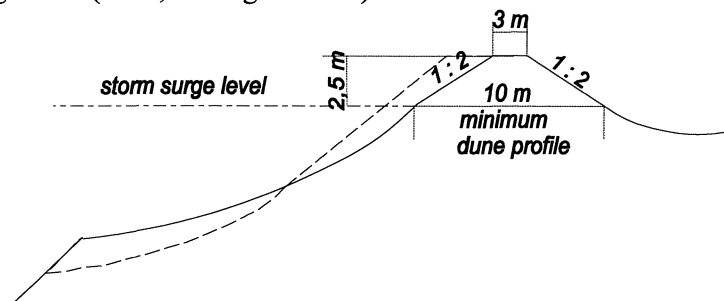


Figure IV-11

¹⁾ The dune section is required to collapse either according to the first failure mode or the second failure mode or ... or according to the Nth mode. This is characteristic for a serial system.

A formal check on the probability of collapse for these modes is not required by the Dune Erosion Guidelines. Such a check is only demanded for *dune erosion*. The probability of failure according to that mode must be smaller than or at most equal to 10^{-5} .

A practical result of a probabilistic check on a dune section could be:

Dune section	
Failure mode	Associated failure probability
1. dune erosion	10^{-5} in a year
2. wave overtopping	10^{-6} in a year
3. overtopping	$5 \cdot 10^{-8}$ in a year
4. sliding	10^{-7} in a year (fictitious)
5. seepage	10^{-7} in a year (fictitious)
TOTAL: $1.125 \cdot 10^{-5}$ in a year	

The elementary limits of the probability of collapse of this dune section are:

$$\underset{i=1}{\overset{5}{MAX}} P_{b_i} \leq P_{b \text{ section}} \leq \sum_{i=1}^5 P_{b_i}$$

Inserting numerical values from the table above:

$$10^{-5} \leq P_{b \text{ section}} \leq 1.125 \cdot 10^{-5}$$

Using the previously mentioned considerations concerning the first three failure modes, the upper limit can be reduced to:

$$P_{b \text{ section}} \leq \left\{ \underset{i=1}{\overset{3}{MAX}} P_{b_i} \right\} + P_{b_4} + P_{b_5} = 10^{-5} + 10^{-7} + 10^{-7} = 1.02 \cdot 10^{-5}$$

The elementary limits of the probability of collapse of this dune section become:

$$10^{-5} \leq P_{b \text{ section}} \leq 1.02 \cdot 10^{-5}$$

By taking correlation between the failure modes into account the upper limit can be decreased further. However, the limits are already so close to each other that, considering the inaccuracy of the mathematical models, a further refinement based on statistical techniques (taking into account correlation) is futile.

The probability of collapse due to dune erosion appears to be dominating for the safety of a dune section, provided the probabilities of failure according to the modes wave overtopping and overtopping are smaller. The probabilities of collapse due to the modes sliding and seepage should be *FAR* smaller than the first mentioned failure probability so as not to endanger the total safety of the section.

This example is based on the assumption that a stretch of dune can be characterised entirely by one single cross section. This assumption is incorrect, considering the erratic course (both lengthwise and in time!) of the cross section of the dunes. The course should really be divided into a number of independent sections, each with its own cross section (and at a certain point in time). The probabilities of failure of all sections should be combined. The Dune Erosion Guidelines resolved this issue by applying the lower limit approximation only for the weakest section.

EXAMPLES OF FAILURE MODES FOR BREAKWATERS

A breakwater can be constructed for various purposes:

- ◆ the breaking of waves. (lower waves behind the breakwater)
- ◆ catching (diversion) of sand transport .
- ◆ guiding the current. (limiting the cross current for navigation)
- ◆ visual guidance. (marking the navigation channel between shallow areas)
- ◆ foundation of port lights.
- ◆ offering a berth ("outer harbour". Beware of settlements! Pipe lines settle along with the breakwater!)

Sometimes the following aspects need to be taken into account:

- ◆ recreation.
- ◆ realisation as a prestige object (developing countries).

In many places in the world it is usual to create a (relatively) calm loading and unloading facility for sea vessels by constructing breakwaters in seawardly direction (see sixth point above), as is the case in Figure IV-12.

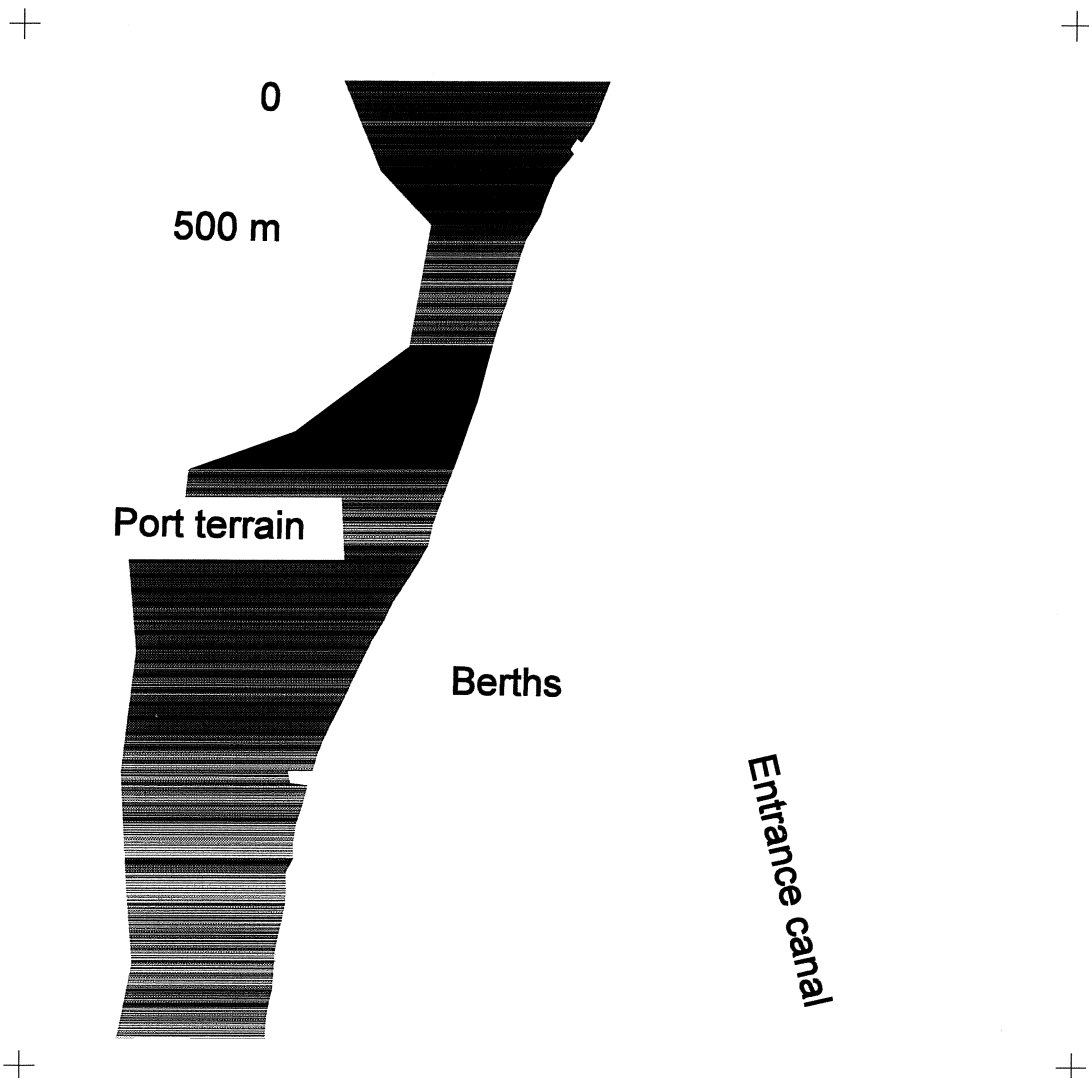


Figure IV-12

In this case, the aim of the breakwater is to limit the duration of high waves occurring in the port basin. Basically three phenomena contribute towards the generation of waves in a port basin:

- ◆ diffraction and refraction of waves which enter the basin via the harbour mouth
- ◆ wave transmission through the breakwater and wave overtopping over the breakwater
- ◆ wave generation in the port basin (ships waves and wind waves).

Below, the fault tree for the breakwater is given; underneath the top event one sees all of the failure modes previously mentioned, except for wave generation in the port basin. (A breakwater can't do much about this.)

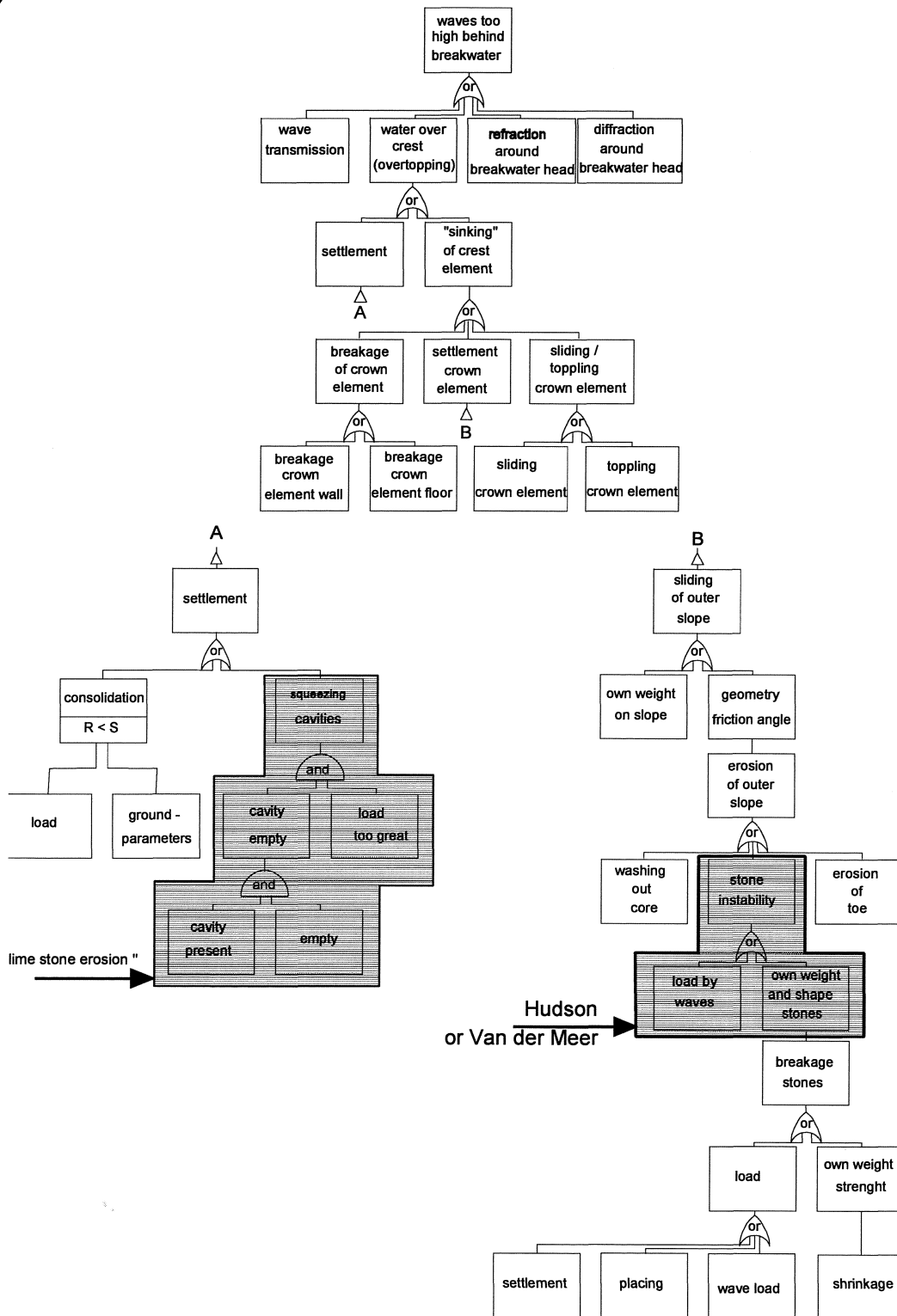


Figure IV-13

As for water defence structures, various failure modes which can lead to the unwanted top event, can be distinguished for breakwaters. However, the relations between the modes and the functional parts are not so clear. In practice, this leads to a disproportionally large emphasis on the stability of the revetment, whilst a mode such as "wave overtopping" is underexposed. This last mode is actually the central issue. Again, it has to be clear what is to be selected as the top event. One defines "failure" as not (no longer) fulfilling the main function. In this case, the top event is defined as: "disturbance (significant wave height H_s) too great behind the breakwater".

A TRADITIONAL BREAKWATER can consist of tout venant (unsorted, usually small sized stones from a quarry) dumped on the seabed, covered with heavier stones, armour units and a toe construction and completed with a crest (or crown element), as is illustrated below:

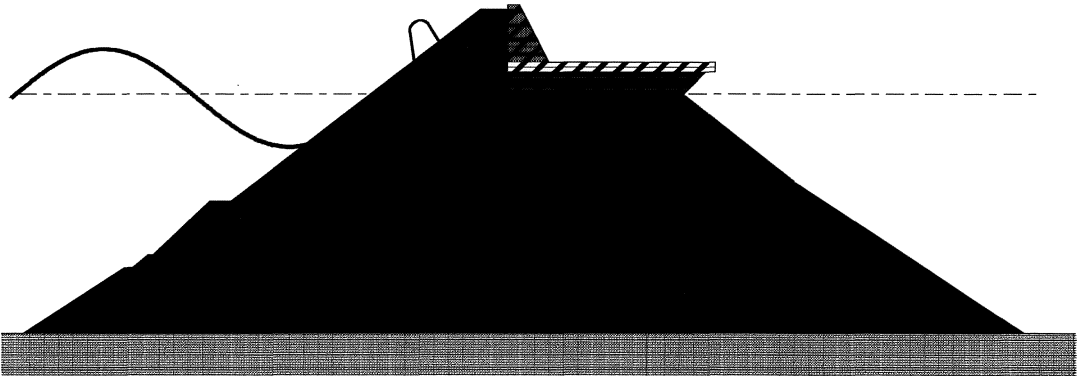


Figure IV-14

A summary of failure modes of such a breakwater is given in Figures IV-15a to IV-15j.

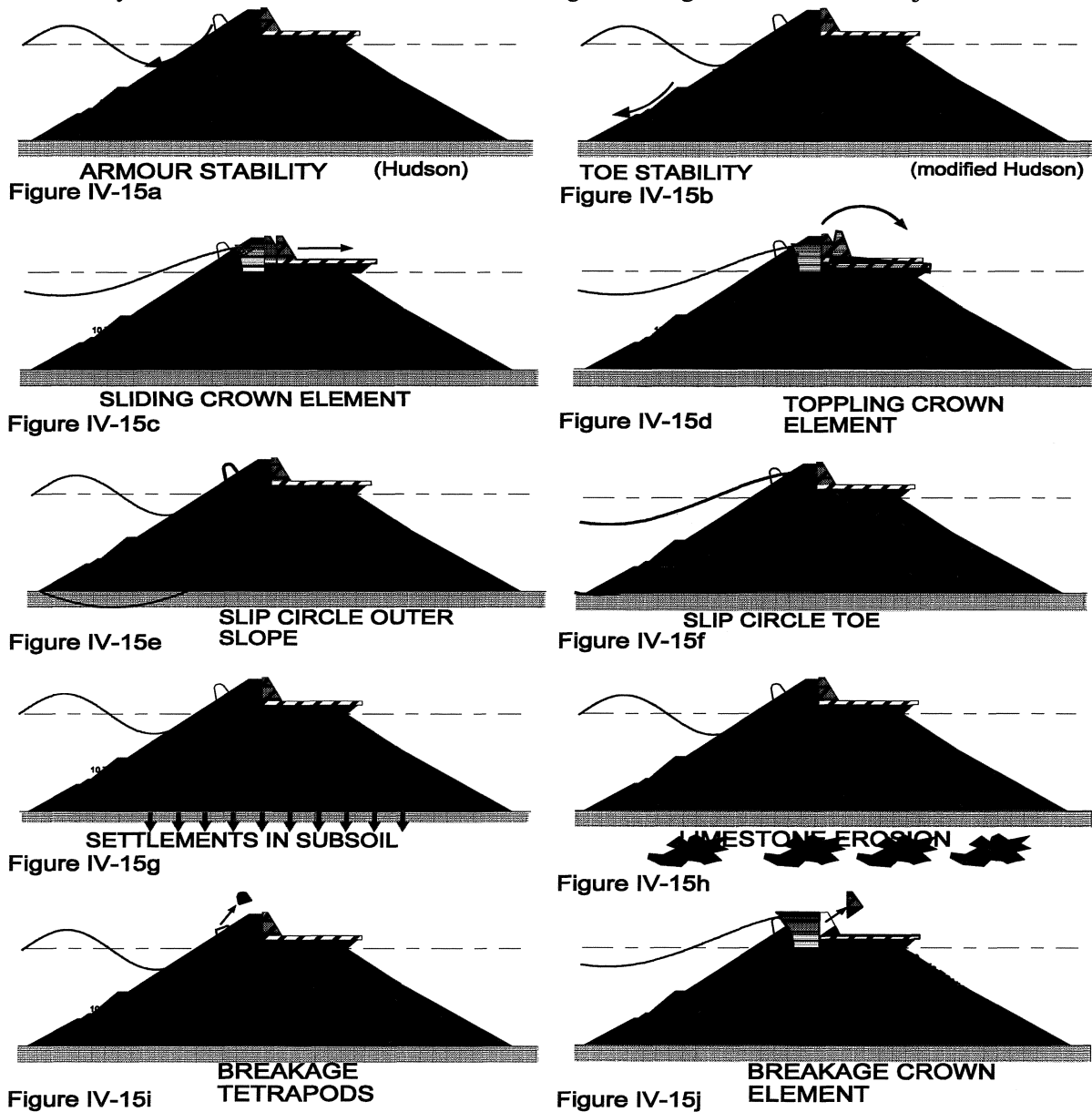


Figure IV-15

The mathematical models of several modes are unknown. The squeezing of subterranean cavities in an area with signs of limestone erosion (Arzew) is an example of such a mode. Many applied formulas (Hudson or, more recent: Van der Meer) concern the displacement of the armour units (stones in the outer stone layer). One could call this failure mode "erosion of the outer slope". The mode is found "halfway down the fault tree". Hence, it only models a part of the top event.

EXAMPLE OF AN ULTIMATE LIMIT STATE MODE IN A CROSS SECTION

The stability of the armour layer is an example of a U.L.S.. The armour layer must remain stable during extreme (design) wave loads. The probability of loss of stability can be determined with an Approximate Full Distribution Approach (level II calculation) or with a level III calculation (Monte Carlo simulation or Riemann integration). (See Lecture notes b3, Probabilistic Design).

The stability of the armour layer can be modelled with Hudson's formula: ¹⁾

$$G = \frac{\rho_s \cdot g \cdot H_s^3}{K_D \cdot \left(\frac{\rho_s - \rho_w}{\rho_w} \right)^3 \cdot \cotan \alpha}$$

in which: H_s = significant (design) wave height [m]

G = weight of block [N]

ρ_s = mass density of the armour stone [kg/m³]

ρ_w = mass density of (sea) water [kg/m³]

g = acceleration as a result of gravity [m/s²]

K_D = stability coefficient []

α = outer slope angle [°]

This formulation of the weight of the block is not directly useful as a reliability function in an approximate full distribution approach. In such a reliability function the variables may not be independent of each other. (The variables must be so-called basic variables.) As: $G = \rho_s \cdot g \cdot v \cdot A^3$, G contains the variable ρ_s which also appears on the right side of Hudson's formula²⁾

From the above mathematical modelling the following reliability function can be deduced:

$$G = \rho_s \cdot g \cdot v \cdot A^3 = \frac{\rho_s \cdot g \cdot H_s^3}{K_D \cdot \left(\frac{\rho_s - \rho_w}{\rho_w} \right)^3 \cdot \cotan \alpha}$$

from which:

$$\underline{Z} = \left(\frac{\rho_s - \rho_w}{\rho_w} \right) \cdot \underline{A} \cdot \sqrt[3]{\underline{K}_D \cdot \underline{v} \cdot \underline{n} - \underline{H}_s}$$

with $n = \cotan \alpha$.

¹⁾ Shore Protection Manual, Coastal Engineering Research Center, U.S. Army Corps of Engineers, U.S.A., 1984, from now on referred to as SPM.

²⁾ N.B. v is a shape factor, which expresses the ratio between the stone size A and the nominal diameter

D_{n50} . The nominal diameter for quarry stone is defined as: $D_{n50} = \sqrt[3]{\frac{W_{50}}{\rho_s \cdot g}}$, in which W_{50} is the

median stone weight, that is the weight given by the 50% point of the weight distribution. For a sphere with the same weight $G = \rho_s \cdot g \cdot \frac{\pi \cdot A^3}{6}$, so that $v = \frac{\pi}{6} \approx 0.52$ if A is the diameter of the

spheres. This way the relation is made between concrete elements (tetrapods etc.) and a characteristic dimension of the element. (See SPM, chapter 7)

An example considers the calculation of dimension A of the armour units of the "root" of a breakwater in Karwar, using an Approximate Full Distribution Approach. (N.B. For the "head" of a breakwater different formulas apply.)

The variables: $\underline{\rho_s}$, $\underline{\rho_w}$, \underline{A} , $\underline{K_D}$, and \underline{n} are assumed normally distributed.

For the variable v the deterministic value 0 can be chosen ($v = 1$ means that the nominal stone diameter, D_{n50} , is selected as the dimension A .)

The rock to be used is expected to have a mass density of 2650 kg/m^3 , with a standard deviation of 50 kg/m^3 .

The mass density of (sea) water is assumed to be 025 kg/m^3 on average, with a standard deviation of 20 kg/m^3 .

The expected value of the nominal diameter, $\mu_{D_{n50}}$, is determined in such a way that the "beta-value" is around .65 ("probability of failure" of approximately 5%, a "prevailing value" for the design of breakwaters). The standard deviation of the nominal diameter is estimated at 0. m.

K_D is the so-called stability coefficient, which is assumed 4.0 for non-breaking waves. (In this case, a "breaking wave" means that the wave breaks against the breakwater as a result of the increasingly shallow foreshore in front of the breakwater. It doesn't describe the type of breaking as a result of the slope of the breakwater itself.) The mentioned value $K_D = 4.0$ is considered an average. The standard deviation of K_D is assumed 0.8.

The breakwater is designed with slopes of the cross section of 1:2, so that, on average: $n = 2.0$. The assumed standard deviation is 0.

For the conditional distribution for the significant wave heights (long-term wave height distribution, see §II.3., text accompanying Figure II-3) during hurricanes, the Fréchet distribution (Figure II-52) is available:

$$F_{\underline{H_s} | cyclone}(H) = e^{-\left(\frac{H}{2.498}\right)^{3.388}}$$

The probability of a hurricane in one year is 0.5, so that:

$$F_{\underline{H_s}}(H) = 1 - \left\{ 1 - e^{-\left(\frac{H}{2.498}\right)^{3.388}} \right\} * 0.5$$

For an Approximate Full Distribution Approach this distribution has to be replaced by an approximative normal distribution. (See lecture notes b3, chapter 3.)

The Manual on the use of rock ...²⁾ recommends using H_{10} , which is³⁾ the average of the highest 10% of the waves, rather than the significant wave height (H_s) as a design wave. If the waves in the wind field are distributed according to a Rayleigh distribution: $H_{10} \approx 1.27 \cdot H_s$.

¹⁾ Manual on the use of rock in coastal and shoreline engineering, CIRIA Special Publication 83 / CUR Report 154, London / Gouda, 1991, hereafter referred to as: Manual on the use of rock ...

²⁾ Manual on the use of rock ... : § 5.1.3.2. Armour layers

³⁾ SPM § 3.2. EXAMPLE PROBLEM 1

Appendix II-1 made it plausible that the (selected) type of distribution greatly influences the numerical result of the probability of failure according to a certain failure mode. The (selected) Fréchet distribution of the yearly maxima for hurricanes has no theoretical base. The Fréchet distribution, just like the least squares method, is "fitted" around data that have a certain spread around the "fit".

To model both effects (with possibly different distributions and spreads around the selected distribution) a normally distributed variable, fH_s , is added. In practice, there are two "prevailing" methods for such an additive:

- ◆ addition to H_s (Normal distribution: $N(fH_s; 0, \sigma_{fH_s})$): dummy variable fH_s , average 0, standard deviation σ_{fH_s}).
- ◆ multiplication factor for H_s (Normal distribution: $N(fH_s; 1, \frac{\sigma_{fH_s}}{\sigma_{H_s}})$): dummy variable fH_s , average 1, standard deviation $\frac{\sigma_{fH_s}}{\sigma_{H_s}}$).

In the first case:

$$F_{fH_s}(fH_s) = \frac{1}{\sigma_{fH_s} \cdot \sqrt{2 \cdot \pi}} \int_{-\infty}^{fH_s} e^{-\frac{h^2}{2 \cdot \sigma_{fH_s}^2}} dh$$

In the second case:

$$F_{fH_s}(fH_s) = \frac{1}{\left(\frac{\sigma_{fH_s}}{\sigma_{H_s}}\right) \cdot \sqrt{2 \cdot \pi}} \int_{-\infty}^{fH_s} e^{-\frac{1}{2} \cdot \left(\frac{h-1}{\frac{\sigma_{fH_s}}{\sigma_{H_s}}}\right)^2} dh$$

The numerical differences (see lecture notes b3, Probabilistic design, pages 2-27 and 2-28: z as the sum of x and y and z as a product of x and y; in this case, for x: read H_s and for y: read fH_s) as a result of applying these models are generally negligible. A conditional probability density of fH_s is assumed along (the expected value of) the long term wave height distribution. This is illustrated schematically for an exponential distribution of the long term distribution of significant wave heights, in Figure IV-16.

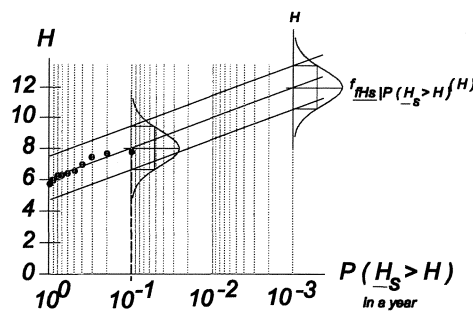


Figure IV-16

Here the first method is chosen: adding fH_s to H_s .

The spectra for the breakwater in Karwar were not determined in Karwar, but many miles further to the north. A separate study with the programme package HISWA concluded that, at the breakwater to be designed, $H_{s0} = -0.5 + 1.38 \cdot H_{10} - 0.08 \cdot H_{10}^2$ could be assumed as the design wave.

Based on the measured values, the reliability function is to be altered as follows:

1. $H_{10} := 1.27 \cdot (H_s + fH_s)$
2. $H_{s0} := -0.5 + 1.38 \cdot H_{10} - 0.08 \cdot H_{10}^2$
3. $Z := \frac{\rho_s - \rho_w}{\rho_w} \cdot A \cdot \sqrt[3]{K_D \cdot n} - H_{s0}$

The distribution types, the parameters of the distributions and the initial values (averages) of an approximate full distribution approach are given in the table below:

Random variable X_i	Distribution type	Parameter A	Parameter B	Parameter C	Initial value	Unit
$\underline{\rho}_s$	Normal	2650	50	0.00	2650	kg/m ³
$\underline{\rho}_w$	Normal	1025	20	0.00	1025	kg/m ³
\underline{A}	Normal	1.50..0.05..2.00	0.1	0.00	1.50..0.05..2.00	m
\underline{K}_D	Normal	4.0	0.8	0.00	4.0	-
\underline{n}	Normal	2.0	0.1	0.00	1.500	-
\underline{H}_s ¹⁾	Fréchet	0.5	2.498	3.388	1.6117	m
\underline{fH}_s	Normal	0.000	0,5	0.00	0.000	m

The parameters A and B in the normal distribution concern respectively the average and the standard deviation.

For the expected value of the stone dimension, with a probability of $P\{Z < 0\} = 5\%$:

$$\underline{\mu}_A = \underline{\mu}_{D_{n50}} \approx 1.6 \text{ m. ("Exactly" 1.62 m.)}$$

is found.

The design point values and the contributions of the variances of the variables to the variance of the reliability function ("the α_i^2 ") then become:

Variable X_i	Value at the design point : X_i^*	Share of the variance α_i^2
ρ_s	2642 kg/m ³	0.8%
ρ_w	1028 kg/m ³	0.9%
A	1.589 m	3.5%
K_D	3.721 -	4.5%
n	2.00 -	0.0%
H_s	4.54 m	87.6%
fH_s	0.136 m	2.7%

¹⁾ The parameters A, B and C in the Fréchet distribution are defined in the following:

$$F_{H_s}(H) = 1 - \left\{ 1 - e^{-\left(\frac{H}{B}\right)^{-C}} \right\} * A \text{ with } A = 0.5, B = 2.498 \text{ en } C = 3.388.$$

The greatest advantages of Hudson's formula are the simplicity and the diversity of armour unit shapes for which K_D - values have been determined. However, the formula also has many disadvantages such as:

- ◆ possible scale effects as a result of the small model scale on which most tests were carried out.
- ◆ only regular waves were used for the tests.
- ◆ the wave period, the storm duration (or, see § II.8.: the wave steepness) can't be taken into account explicitly
- ◆ no description of the level of damages
- ◆ only applicable for permeable cores and for waves that don't overtop the breakwater.

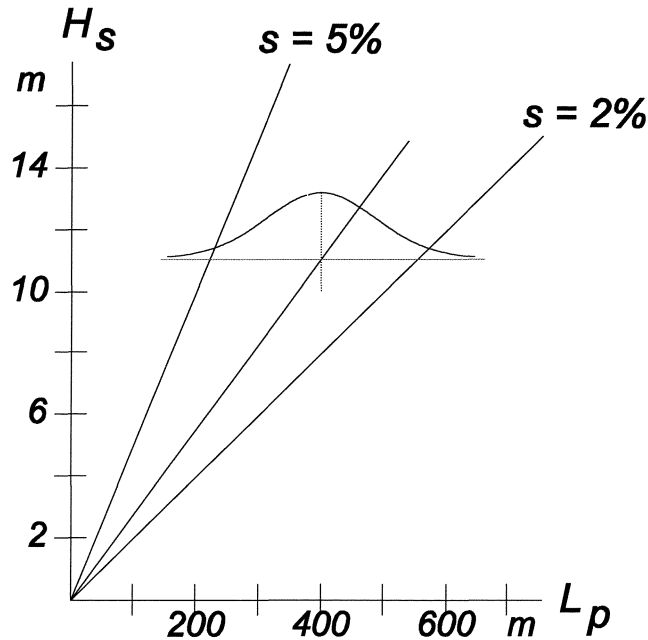


Figure IV-17

The Van der Meer formulas ¹⁾ partially resolve the abovementioned shortcomings. Two types of waves are distinguished, namely plunging and surging waves, dependent on the surf similarity parameter $\xi = \frac{\tan \alpha}{\sqrt{\frac{H}{L}}}$.

The formulas are sketched in Figure IV-5 for two different levels of damages.

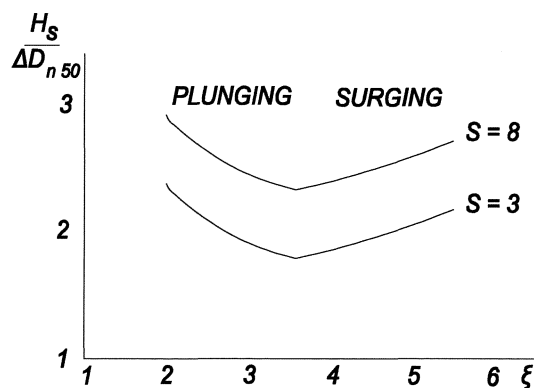


Figure IV-18

¹⁾ Rock Slopes and Gravel Beaches under Wave Attack, J.W. van der Meer, Dissertation, Delft, 1988

For a breakwater in deep water (no breaking waves on the foreshore in front of the breakwater) ¹⁾:
 For plunging waves:

$$\frac{H_s}{\Delta \cdot D_{n50}} = 6.2 \cdot P^{0.18} \cdot \left(\frac{S_d}{\sqrt{N}} \right)^{0.2} \cdot \xi_m^{-0.5}$$

For surging waves:

$$\frac{H_s}{\Delta \cdot D_{n50}} = 1.0 \cdot P^{-0.13} \cdot \left(\frac{S_d}{\sqrt{N}} \right)^{0.2} \cdot \sqrt{\cot \alpha} \cdot \xi_m^P$$

The transition between both formulas can be calculated for the critical value of ξ_m :

$$\xi_{mc} = \left[6.2 \cdot P^{0.31} \cdot \sqrt{\tan \alpha} \right] \left(\frac{1}{P+0.5} \right)$$

In the above formulas:

H_s = significant wave height = average of the highest one third of the waves in a wind field

$$\Delta = \frac{\rho_s - \rho_w}{\rho_w}$$

ρ_s = mass density of stone in the armour layer

ρ_w = mass density of (sea) water

$$D_{n50} = \text{nominal stone diameter} = \sqrt[3]{\frac{W_{50}}{\rho_s}}$$

W_{50} = median weight of a stone in the armour layer, given by the 50 percent value of the weight distribution

P = porosity parameter $P = 0$ for a breakwater with impermeable core

$P = 0.3$ for a somewhat permeable core

$P = 0.5$ for a permeable core

$P = 0.6$ for a homogeneous breakwater

S_d = level of damages $S_d = 2$ for the beginning of damages

$S_d = 5$ for moderate damages

$S_d = 8$ for serious damage

$S_d = 2$: filter layer visible

N = number of waves during a storm (Maximum $N = 7500$)

α = slope angle

$$\xi_m = \text{surf similarity parameter} = \frac{\tan \alpha}{\sqrt{\frac{2 \cdot \pi \cdot H_s}{g \cdot T_m^2}}}$$

T_m = average wave period

$$s_p = \text{wave steepness} = \frac{H_s}{L_p}$$

$$L_p = \text{wave length (in deep water)} = \frac{g \cdot T_p^2}{2 \cdot \pi}$$

g = acceleration as a result of gravity

T_p = period with which energy density in the spectrum is maximum

ξ_{mc} = critical surf similarity

¹⁾ Rock Slopes and Gravel Beaches under Wave Attack, J.W. van der Meer, Dissertation, Delft, 1988
 en: Manual on the Use of Rock ... § 5.1.3.2 Armour layers

Analogous to assumptions for breakwater design according to the Hudson formula, the following distribution types, distribution parameters and initial values (averages) for an Approximate Full Distribution Approach can be selected for breakwater design according to the Van der Meer formulas:

Random variable	Distribution type	Parameter A	Parameter B	Parameter C	Initial value	Unit
ρ_s	Normal	2650	50	0.00	2650	kg/m ³
ρ_w	Normal	1025	20	0.00	1025	kg/m ³
A	Normal	1.62	0.1	0.00	1.776	m
S_d ¹⁾	Normal	3.0 .. 0.05 .. 4.0	0.02	0.0	3.0 .. 0.05 .. 4.0	-
n	Normal	2.0	0.1	0.00	1.500	-
H_s ²⁾	Fréchet	0.5	2.498	3.388	3.2121	m
fH_s	Normal	0.000	0.5	0.00	0.000	m
P	Normal	0.45	0.05	0.00	0.45	-
s_p ³⁾	Normal	2.82	0.724	0.00	2.82	-

The parameters A and B for the normal distribution concern respectively the average and the standard deviation.

The following constants are used: $N = 7500$ (max. number of waves)
 $g = 9.82 \text{ m/s}^2$

The reliability function can be derived as follows:

$$Z = \Delta * D_{n50} - DELTA_D$$

In this $DELTA_D$ has to be determined with the Van der Meer formula for plunging waves (surging waves don't occur in this calculation), hence:

$$Z = \frac{\rho_s - \rho_w}{\rho_w} \cdot D_{n50} - \frac{H_{s0}}{N_{stab}}$$

¹⁾ $S_d = 2$ à 4 (The beginning of damages in the Van der Meer formulas) corresponds to $K_D = 4$ for non breaking waves and $K_D = 3.5$ for breaking waves ("no damages" in the Hudson formula). With $K_D = 4$ the expected stone dimension $\mu_{D_{n50}} = 1.62 \text{ m}$ was found using the Hudson formula This dimension is also chosen here. The level of damages is determined by try and error with an assumed probability of $P\{Z < 0\} = 5 \%$.

²⁾ This was also the starting point for the calculation of the stone stability according to Hudson's formula (page IV-12/14). The same probability distribution is used in this case.

³⁾ The distribution of the wave steepness is taken from § II.8., page II - 36, Figure II-54.

in this $N_{stab} = \frac{6.2 \cdot P^{0.18} \cdot \left(\frac{S_d}{\sqrt{N}}\right)^{0.2}}{\sqrt{\xi_m}}$, so:

$$Z = \frac{\rho_s - \rho_w}{\rho_w} \cdot D_{n50} - \frac{H_{s0} \cdot \sqrt{\xi_m}}{6.2 \cdot P^{0.18} \cdot \left(\frac{S_d}{\sqrt{N}}\right)^{0.2}} \quad \text{mits } \xi_m \leq \left(\frac{6.2 \cdot P^{0.31}}{\sqrt{n}}\right)^{\left(\frac{1}{P+0.5}\right)}$$

(N.B. N is the number of waves, n is the cotangent of the slope gradient.)

Now $\xi_m = \frac{\tan \alpha}{\sqrt{s_m}} = \frac{1}{n \cdot \sqrt{\frac{H_{s0}}{L_m}}} = \frac{1}{n \cdot \sqrt{\frac{H_{s0} \cdot 2 \cdot \pi}{g \cdot T_m^2}}}$, so that:

$$Z = \frac{\rho_s - \rho_w}{\rho_w} \cdot D_{n50} - \frac{H_{s0} \cdot \sqrt{\frac{1}{n \cdot \sqrt{\frac{H_{s0} \cdot 2 \cdot \pi}{g \cdot T_m^2}}}}}{6.2 \cdot P^{0.18} \cdot \left(\frac{S_d}{\sqrt{N}}\right)^{0.2}}$$

The following relation between the peak period and the average period is assumed: ¹⁾

$$T_m = \frac{T_p}{1.35}$$

so:

$$Z = \frac{\rho_s - \rho_w}{\rho_w} \cdot D_{n50} - \frac{H_{s0} \cdot \sqrt{\frac{T_p}{1.35 \cdot n \cdot \sqrt{\frac{H_{s0} \cdot 2 \cdot \pi}{g}}}}}{6.2 \cdot P^{0.18} \cdot \left(\frac{S_d}{\sqrt{N}}\right)^{0.2}}$$

For the determination of the design wave height, the significant wave height on the breakwater spot has to be taken into account again:

$$H_{s0} = -0.5 + 1.38 \cdot H_s - 0.08 \cdot H_s^2. \quad (\text{N.B. now it is not necessary to take } H_{10} \text{ into account.})$$

¹⁾ De relation: $\frac{T_p}{T_m} = 1.35$ is determined as an average over many spectra. An order of magnitude

is taken from page II-29, Figure II-37-1-a, where from $T_p = 10.5$ and $T_m = 8.4$, $T_p = 1.25 T_m$ is found. The spectrum of the wave steepness depicted next to it, Figure II-37-2-a, measured the next day, is a different realization.

With a probability $P\{Z < 0\} = 5\%$ (equal to the value in the calculation with Hudson's formula) the expected value S_d is found: $\mu_{S_d} \approx 2.5$. This means practically "no damage" ($S_d = 2 \text{ a } 4$ for "no damage").

With the input data presented in the table on page IV-16 the following design point values and the following contributions of the variables' variances to the variance of the reliability function ("the α_i^2 ") are found (still assuming $P\{Z < 0\} = 5\%$)

Variable X_i	Value in design point: X_i^*	Share in the variance α_i^2
ρ_s	2644.78 kg/m ³	0.4%
ρ_w	1027.15 kg/m ³	0.4%
A	1.599 m	1.7%
S_d	2.5 -	0.0%
n	2.0 -	0.0%
H_s	4.666 m	92.6%
fH_s	0.35 m	2.7%
P	0.447 -	0.2%
s_p	2.653 -	2.0%

These results can be compared with those in the table at the bottom of page IV - 16.

A failure probability (in one year) of 5% (as is presumed for both the design according to the Hudson formula and the design according to Van der Meer's formulas) seems rather high. Considering the "lifetime" of a breakwater is in the order of 20 years, the probability of failure of a breakwater in its life can be calculated as follows:

$$P_{f20yr} = 1 - \overline{P_{f1yr}}^{20} = 1 - (1 - 0.05)^{20} \approx 1 - 0.36 \approx 0.64$$

The probability of failure can be calculated exactly by using the table at the top of page IV-16 with $\mu_{S_d} = 2.5$ as the average of S_d and by opting for the special distribution of H_s :

$$F_{H_s}(H) = \left[1 - \left\{ 1 - e^{-\left(\frac{H}{2.498}\right)^{-3.388}} \right\} * 0.5 \right]^{20}$$

With these data, a probability of failure ($P\{Z < 0\}$) of 58.5% is found. This is a little different from the 64% found earlier.

Maybe it is economical to construct breakwaters with such a high failure probability. This should be subject to further investigation.

RELIABILITY FUNCTION "HUDSON"

FUNCTION Z(X: ARY): EXTENDED;

VAR

Rho_a, {mass density stone}
Rho_w, {mass density water}
D, {stone dimension}
k_d, {damage factor}
N_talud, {cotangent slope angle}
H_sign, {significant wave height on measurement location}
H_so, {significant wave height near wave breaker}
fHs {uncertainty modelling H_s}

: EXTENDED;

BEGIN

Rho_a:=X[1]; Rho_w:=X[2]; D:=X[3]; k_d:=X[4];
N_talud:=X[5]; H_sign:=X[6]; fHs:=X[7];
H_so := ,27 * (H_sign + fHs);
H_so:=-0.5 + .38 * H_so - 0.08 * SQR(H_so);
Z:=(Rho_a - Rho_w) * D * Power((k_d*N_talud),/3) / Rho_w - H_so;

END;

RELIABILITY FUNCTION "VAN DER MEER"

Function Z(X : ARY):EXTENDED;

{ wave climate height and period }

{ break water stability Karwar }

VAR

H_s, fHs, H_so, S_p, L_p, T_p, N_talud, S, P, Delta_D, rho_a, rho_w, Delta, D : EXTENDED;

PROCEDURE Exchange;

BEGIN

H_s := X[1];

S_p := X[2];

N_talud := X[3];

S := X[4];

rho_a := X[5];

rho_w := X[6];

P := X[7];

D := X[8];

fHs := X[9]

END;

PROCEDURE Riprap(Hs, Tz, N_talud, P, S: EXTENDED;

VAR Delta_D: EXTENDED);

CONST

{ start of damages S=2 ; moderate damages S=5 ; failure S=8 }

N = 7500; { number of waves }

{ impermeable core P=0.; permeable core P=0.5 ;

homogeneous core P=0.6 }

g = 9.82;

VAR

L_z, ksi_z, ksi_criterium, N_stab: EXTENDED;

BEGIN

L_z := g * SQR(Tz)/(2*pi);

ksi_z := (N_talud) / SQR(Tz);

ksi_criterium := Power(6.2*Power(P,0.3)/SQR(Tz),/(P+0.5));

IF ksi_z < ksi_criterium THEN

N_stab := 6.2 * Power(P,0.8)*Power(S/SQR(N),0.2)/SQR(ksi_z)

ELSE

N_stab := Power(P,-0.3)*Power(S/SQR(N),0.2)*SQR(N_talud)*Power(ksi_z,P);

Delta_D := Hs / N_stab

END; {OF PROCEDURE RIPRAP}

BEGIN

Exchange;

H_s := H_s + fHs;

L_p := 0.0 * H_s/S_p;

T_p := SQR(L_p/.56);

H_so := -0.5 + .38* H_s - 0.08 * SQR(H_s); { see hindcast study DHL }

Riprap(H_so, T_p/.35, N_talud, P, S, Delta_D);

Delta := rho_a/rho_w -;

Z := Delta * D - Delta_D

END;

EXAMPLE OF A SERVICEABILITY LIMIT STATE MODE : CALM POSITION OF SHIPS IN AN OUTER PORT

WAVE TRANQUILLITY IN THE PORT BASIN

For rapid and safe handling of goods in a port basin a certain degree of calm is required. This calm can be disturbed by three causes (compare page IV - 11):

- a. by waves which enter via the harbour mouth. This is a combined effect of refraction and diffraction. Calculation programmes are based on the assumption of monochromatic waves.
- b. by transmission of energy or by wave overtopping. A part of the wave energy that hits the breakwater will enter the port basin through the breakwater. Transmission can be limited by a good design and good realisation. Waves which overtop the breakwater, also transmit energy into the port basin. The permissible wave overtopping has to be established in (physical) model tests. (N.B. in these tests disturbance in the port due to overtopping can't be separated from disturbance by transmission.)
- c. by waves which are generated in the port basin by wind and/or vessel movements. Usually these causes don't contribute much to the disturbance. The wind's fetch over the port basin is generally too limited to generate waves of any significance and the velocity of the ships in the basin is usually too small, also leading to the generation of little wave overtopping.

The effects (consequences) of the various causes will first be treated separately and consequently combined. The design of the naval port in Karwar (Figure IV-19), on the west coast of India, is selected as an example. For comparison some data are presented concerning the port in Ennore, which is located on the east coast of India (Figure IV-20 = Figure IV-12).

AIM OF THE CALCULATION

Aim of the calculation is to check the assumption that the significant wave height in certain points of the port basin are not exceeded more than a certain amount of time.

The "check up" is based on a certain port and breakwater layout, whereby the cross section of the breakwater (which determines the permeability and the wave overtopping) is also considered fixed. I.e.: the design is fixed and the probability of a certain (still considered permissible) significant wave height, which is exceeded too often with this design, is to be ascertained. If the probability is considered too great, the design needs to be adjusted.

BOUNDARY CONDITIONS

The "certain (still considered permissible) significant wave height" and the maximum allowed duration in the port are established. For different points in the basin these can be different wave heights and a different duration can correspond to every point.

For freight shipping (port of Ennore), for example, the following situations are accepted for **NO MORE THAN 5 days a year**:

- for the handling of coal (points A and B in Figure IV-20) a H_s greater than 0.5 m,
- for the turning circle (point G in Figure IV-20) a H_s greater than 0.9 m and
- for the rest (points C, D and E in Figure IV-20) a H_s greater than 0.6 m.

For the handling of arms smaller permissible wave heights apply. For the landing stage near the points J and K in Figure IV-19 the requirements for the significant wave height in the port are:

- during 95% of the time (247 days a year) it may not exceed 0.2 m,
- during 4% of the time (15 days a year) it may be in the range 0.2 to 0.3 m and
- during 1% of the time (4 days a year) it is allowed to exceed 0.3 m.

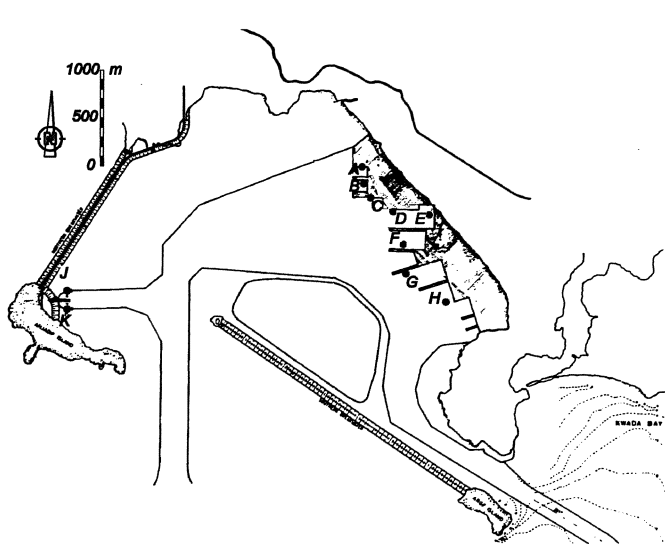


Figure IV-19

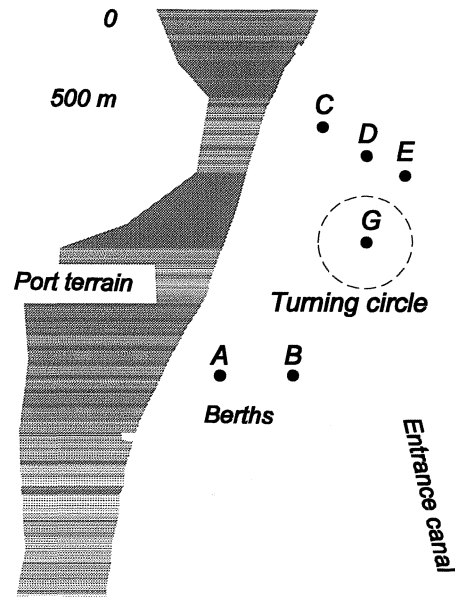


Figure IV-20

That's all, as far as the data connected to the "strength side" of the design is concerned. For the "load" the wave boundary conditions have to be taken into account. Along the Indian coast (both for the Arabian Gulf (port of Karwar) and for the Gulf of Bengalen (port of Ennore)) the wave climate can be summarised in two different wave spectra: one for the southwestern monsoon and one for the northeastern monsoon. For the port of Karwar, the data presented on page II - 29 are assumed. The various measured spectra (of which two are given on page II - 29: one measured during the southwestern monsoon and one during the northeastern monsoon) were averaged, as were the directions of wave incidence. For the southwestern monsoon, this resulted in the schematised spectrum in the top left corner of Figure IV-21 with the corresponding directions spread as sketched below. For the northeastern monsoon these data are presented in Figure IV-21 top right and bottom right.

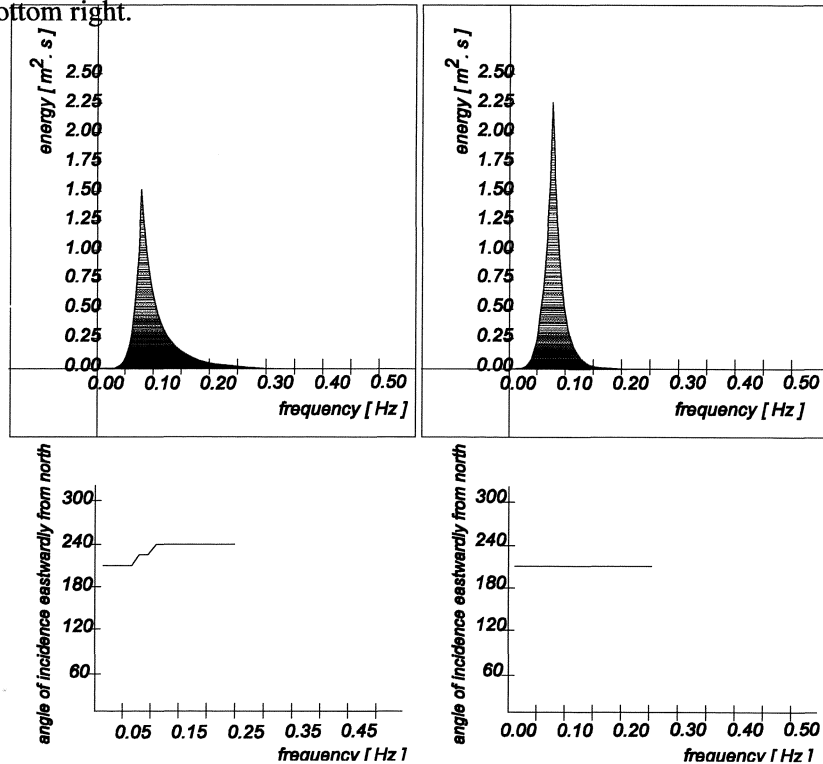


Figure IV-21

CALCULATING REFRACTION/DIFFRACTION

To calculate refraction and diffraction different programmes are in use. DIFFRAC, DIFHA, HISWA and PHAROS are amongst them. These programmes require the following input:

- wave parameters (period, height and angle of incidence relative to the harbour mouth)
- shape (and, to calculate refraction also the depth) of the port basin
- reflection coefficients (amount of energy reflected by the basin edges).

The output consists of the wave height in various locations in the port basin as a fraction, K_a , of the incoming wave. The selected locations in the port basin are points A to K in Figure IV-19.

The enlargement factor K_a is:

$$K_a(f) = \frac{H_{\text{refraction/diffraction}}(f)}{H_{\text{incoming}}(f)}$$

with: $H_{\text{refraction/diffraction}}(f)$ = the refracted/diffracted wave height in metres
 $H_{\text{incoming}}(f)$ = the height of the incoming wave in metres
 $K_a(f)$ = enlargement factor for the wave height

Enlargement factors are calculated for many wave periods, from 2.5 s to 40 s. Thereby the corresponding directions of incidence are taken into account. Some calculated values of K_a are given in the table below:

Period/Direction	8s	8s	8s	10s	10s	10s	12s	12s	12s	20s	20s	20s
Location in port basin	210°	225°	240°	210°	225°	240°	210°	225°	240°	210°	225°	240°
A	0.023	0.293	0.151	0.034	0.230	0.129	0.198	0.200	0.099	0.367	0.192	0.123
B	0.190	0.284	0.177	0.073	0.168	0.026	0.128	0.135	0.086	0.053	0.135	0.079
C	0.214	0.246	0.154	0.071	0.168	0.080	0.141	0.146	0.105	0.164	0.177	0.156
D	0.058	0.062	0.091	0.055	0.072	0.031	0.082	0.163	0.064	0.097	0.235	0.110
E	0.161	0.284	0.253	0.043	0.043	0.037	0.015	0.019	0.068	0.040	0.040	0.105
F	0.291	0.260	0.283	0.074	0.102	0.035	0.044	0.140	0.071	0.061	0.032	0.051
G	0.037	0.074	0.077	0.015	0.051	0.043	0.002	0.021	0.058	0.110	0.100	0.024
H	0.034	0.020	0.059	0.062	0.061	0.050	0.054	0.032	0.036	0.059	0.022	0.012

Enlargement factors K_a in various locations in the port basin for different directions of incidence.

The calculation results greatly fluctuate. This is not the result of errors in the calculation. In nature, such fluctuations are found too, judging by the results of prototype measurements in the port of Visakhapatnam¹⁾ in which the square of the enlargement factor is given:

¹⁾ Gadre, M.R. and C.N. Kanetkar, Wave transmission in the Visakhapatnam Outer Harbour, Central Water and Power Research Station, Pune, India.

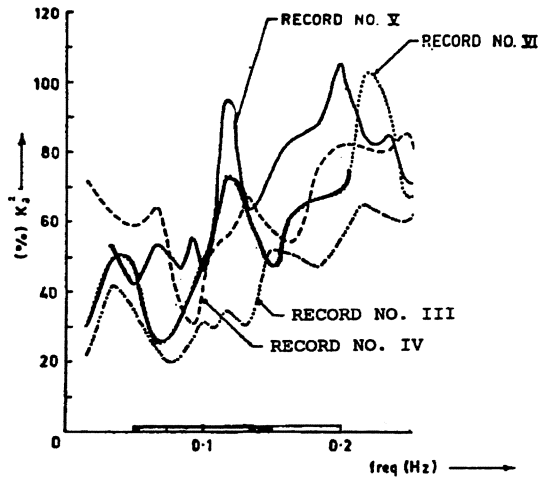


Figure IV-22

The energies per frequency band of the (average) energy density spectrum (average of many measured spectra such as on page II - 29) are multiplied by *THE SQUARE OF* the calculated enlargement factor K_a . From that, (taking into account the angle of incidence of in the incoming wave) the energy density spectrum of the waves in the considered location in the port basin during the considered monsoon period follows. Both the spectrum of the incoming wave and that of the wave in the considered location in the port basin can be characterised by their respective significant wave heights. The ratio between these significant wave heights is an enlargement factor calculated on grounds of the (average) spectra, but now for the significant wave. This enlargement factor is indicated by $K_{a_{H_s}}$. The calculation according to the above method is known as "enlargement factor calculated with spectral analysis". The calculation scheme is given in the figure below.

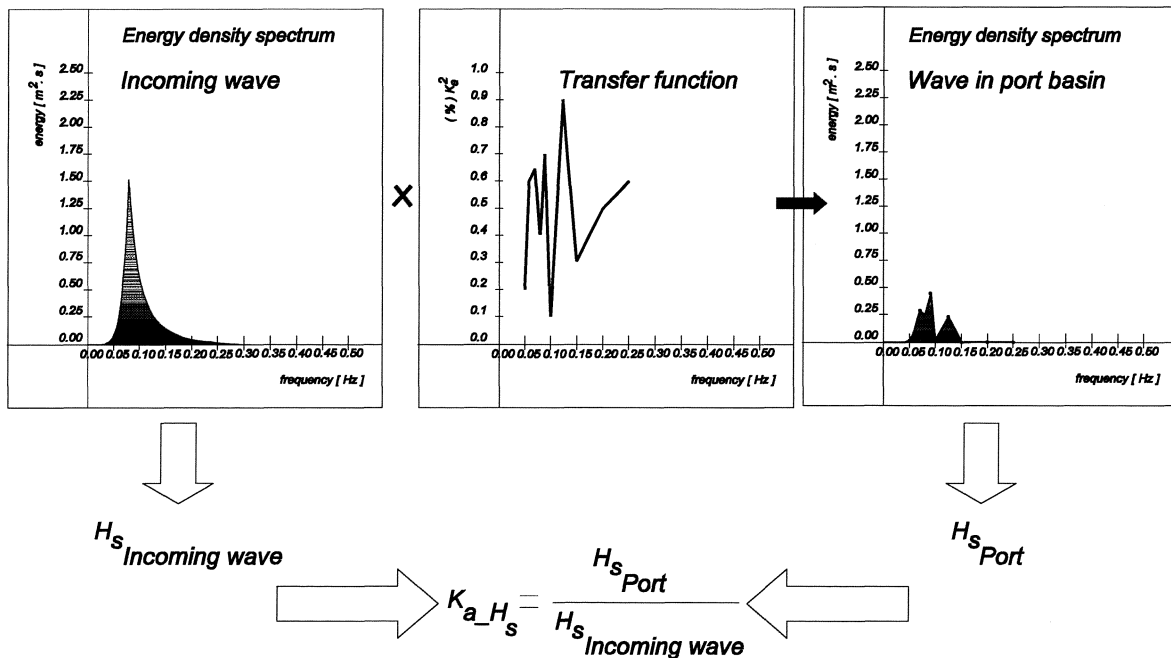


Figure IV-23

Taking into account the correct directions, incoming wave heights, periods and depths and averaging the H_{a,H_s} - values gives the following results for the southwestern monsoon period:

Considered location	$\overline{K_{a,H_s}}$
A	0,03
B	0,03
C	0.04
D	0.05
E	0.07
F	0.06
G	0.08
H	0.02
J	0.04
K	0.03

CALCULATING TRANSMISSION AND OVERTOPPING

When waves hit a breakwater a part of the wave energy is either reflected or dissipated in warmth and sound, or is transmitted, or a part of the wave overtops the breakwater. How the energy of the incoming wave is divided in reflection, dissipation, transmission and overtopping depends on:

- the parameters of the incoming wave (period, height and water depth)
- the type of breakwater (rough or smooth, permeable or impermeable)
- the geometry of the structure (slope, height of the crest relative to the water surface, width of the crest)

The number of parameters which describe the influence of overtopping and transmission are thus very large.

In model tests, one can't separate the influence of overtopping and of transmission on the wave height in the port basin. (By placing partitions in the harbour mouth one can eliminate refraction and diffraction influences.) Many laboratory tests have been carried out, but they usually involved monochromatic waves.

Powell and Allsop¹⁾ investigated transmission/ overtopping for rubble mound breakwaters and for irregular waves. The results are given in Figure IV-24.

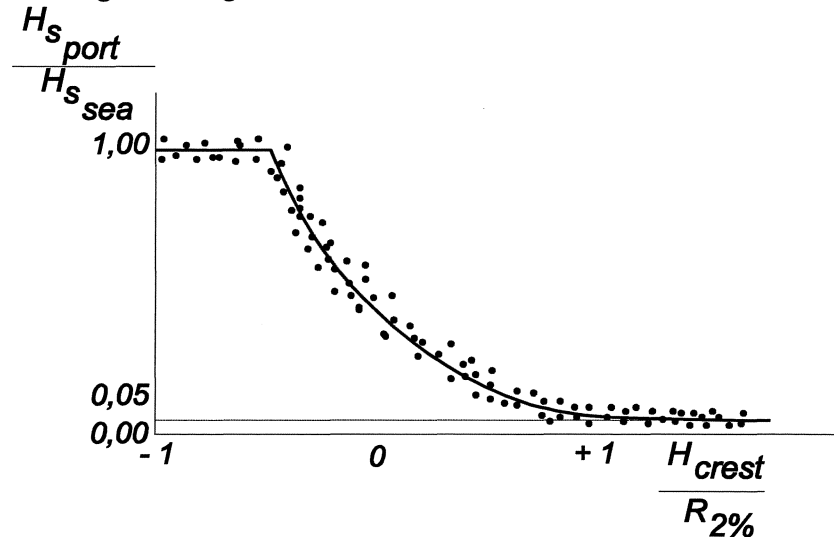


Figure IV-24

Here: $H_{s_{port}}$ = the significant wave height in the port basin, caused by transmission/ wave overtopping.
 $H_{s_{sea}}$ = the significant wave height of the incoming wave.
 H_{crest} = the crest height of the breakwater, relative to the still water level.
 $R_{2\%}$ = the height of the wave run-up which is exceeded by 2% of the wave run-ups.

With these data the mathematical model for the significant wave height as a result of (relative) overtopping/transmission is:

$$\frac{H_{s_{port}}}{H_{s_{sea}}} = 0.05 + 0.12 \cdot \left(\frac{H_{crest}}{R_{2\%}} - 1 \right)^2 \quad \text{provided } -0.5 \leq \frac{H_{crest}}{R_{2\%}} \leq +1$$

The horizontal right part of the graph indicates that there is always a minimum of 5% transmission/overtopping of the energy of the incoming wave, independent of the height of the crest of the breakwater.

¹⁾ Powell, K.A. and N.W.H. Allsop, Low-crest breakwaters, hydraulics performance and stability, Report SR 57, Hydraulics Research, Wallingford, July 1985.

For the mathematical modelling of the wave run-up, $R_{2\%}$, physical model research carried out by Delft Hydraulics Laboratory¹⁾ is used. The results of the research are presented as a bent straight line in Figure IV-25.

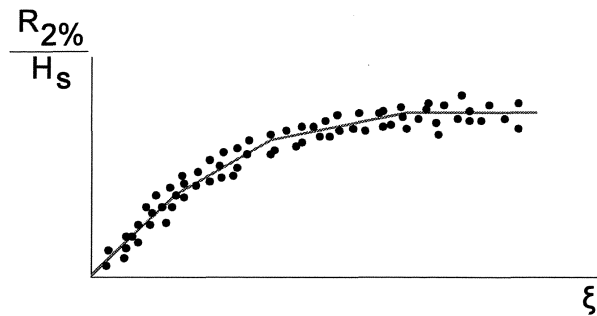


Figure IV-25

With: ξ = the breaker parameter, equal to $\frac{\tan \alpha}{\sqrt{s}}$.
 H_s = the significant wave height of the incoming wave.
 α = the slope gradient of the breakwater on the sea side.
 s = wave steepness of the incoming wave.

The other parameters are as defined before.

With the results in Figures IV-24 and IV-25 a level II- calculation can be carried out. By varying the crest height a fraction of the exceedance time of a certain significant wave height in the port basin can be established. Three crest heights (7, 8 and 9 m above C.D. = Chart Datum) with a standard deviation of 0.2 m have been considered. The selected still water level was C.D. + 1.0 m with a standard deviation of 0.1 m. The results of the level II calculations are listed in the following table:

$H_{s_{port}}$		0.1 m	0.2 m	0.3 m	0.4 m	0.5 m
month / crest height						
June	7m	$4.0 \cdot 10^{-1}$	$5.7 \cdot 10^{-2}$	$2.3 \cdot 10^{-2}$	$1.1 \cdot 10^{-2}$	$5.3 \cdot 10^{-3}$
	8m	$4.0 \cdot 10^{-1}$	$2.8 \cdot 10^{-2}$	$1.0 \cdot 10^{-2}$	$4.5 \cdot 10^{-3}$	$2.1 \cdot 10^{-3}$
	9m	$4.0 \cdot 10^{-1}$	$1.5 \cdot 10^{-2}$	$4.7 \cdot 10^{-3}$	$1.9 \cdot 10^{-3}$	$8.9 \cdot 10^{-4}$
July	7m	$5.5 \cdot 10^{-1}$	$2.5 \cdot 10^{-2}$	$5.6 \cdot 10^{-3}$	$1.6 \cdot 10^{-3}$	$5.3 \cdot 10^{-4}$
	8m	$5.5 \cdot 10^{-1}$	$8.0 \cdot 10^{-3}$	$1.5 \cdot 10^{-3}$	$4.0 \cdot 10^{-4}$	$1.2 \cdot 10^{-4}$
	9m	$5.5 \cdot 10^{-1}$	$2.8 \cdot 10^{-3}$	$4.3 \cdot 10^{-4}$	$1.0 \cdot 10^{-4}$	$2.9 \cdot 10^{-5}$
August	7m	$2.2 \cdot 10^{-1}$	$1.2 \cdot 10^{-2}$	$3.5 \cdot 10^{-3}$	$1.2 \cdot 10^{-3}$	$4.9 \cdot 10^{-4}$
	8m	$2.2 \cdot 10^{-1}$	$4.8 \cdot 10^{-3}$	$1.2 \cdot 10^{-3}$	$3.8 \cdot 10^{-4}$	$1.4 \cdot 10^{-4}$
	9m	$2.2 \cdot 10^{-1}$	$2.0 \cdot 10^{-3}$	$4.1 \cdot 10^{-4}$	$1.2 \cdot 10^{-4}$	$4.3 \cdot 10^{-5}$
September	7m	$2.6 \cdot 10^{-2}$	$1.5 \cdot 10^{-4}$	$1.9 \cdot 10^{-5}$	$3.5 \cdot 10^{-6}$	$7.4 \cdot 10^{-7}$
	8m	$2.6 \cdot 10^{-2}$	$3.1 \cdot 10^{-5}$	$3.1 \cdot 10^{-6}$	$5.0 \cdot 10^{-7}$	$9.8 \cdot 10^{-8}$
	9m	$2.6 \cdot 10^{-2}$	$3.4 \cdot 10^{-6}$	$5.5 \cdot 10^{-7}$	$7.8 \cdot 10^{-8}$	$1.4 \cdot 10^{-8}$

¹⁾ Golf run-up on statically stable rockfill slopes under wave attack, slopes of loosely dumped materials report on model investigations, M1983 part III, (in Dutch: Golfoploop op statisch stabiele strotsteen taluds onder golfaanval, taluds van los gestorte materialen) Delft Hydraulics Laboratory/ Rijkswaterstaat DWW, The Netherlands, June 1988.

WAVE GENERATION IN LOCAL WIND FIELD

If a storm blows in the longitudinal direction of the port (east southeastern or west northwestern storm in Karwar, in the port of Ennore wind waves generated in the port don't need to be taken into account) wind waves of some significance can be generated. Calculations based on the JONSWAP spectrum and with the following parameter values:

- fetch = 4000 m
- wind velocity = 10 m/s

were considered representative for storms from the west, which occur approximately 10 days a year. The results of these calculations are:

- significant wave height: 0.34 m
- peak period: 2.1 s

During the months December and January only less high and slightly longer waves occur. A significant wave height of 0.2 m will be taken into account with (wherever necessary) a wave period of 3 s.

COMBINATION OF EFFECTS

Due to the occurring phase differences, it is not correct, to simply add the energies (or the squares of the wave heights) of the different significant waves. By doing this regardlessly (and by taking the square root of the sum of the squares), an upper limit for the significant wave which is exceeded a certain percentage of time (number of days a year) is acquired. The following table gives the results of level II calculations for a crest height of C.D. + 8 m. An enlargement factor, K_a , of 0.07 has been used. (See the table on page IV - 28.) This value is considered representative for the points A to H in Figure IV-20.

months	$\overline{H}_{s_{port_total}}$	percentage exceedance
June	0.20 m	23
	0.30 m	5.5
	0.50 m	0.7
July	0.20 m	24
	0.30 m	2.6
	0.50 m	0.4
August	0.20 m	9
	0.30 m	1.2
	0.50 m	0.1
September	0.20 m	1
	0.30 m	0.4
	0.50 m	0.0

From the previous table, the following table was derived. The latter gives the calculated total number of days that a certain significant wave height on the north side (points A to H in Figure IV-20) of the port of Karwar is exceeded, as well as the maximum number of days during which the considered significant wave height was allowed to be exceeded.

$\overline{H}_{s_{port_total}}$	Number of days a year exceedance	Assumed number of days of exceedance in a year
0.20 m	17	18
0.30 m	3	4
0.50 m	0	1

THE BERM BREAKWATER

A more recently applied type of breakwater is the BERMBREAKWATER. Its core consists of tout venant. The core is covered by a cap made of coarser stones, however, not so coarse that no transport (profile change of the cap) could take place. The breakwater cap is constructed with the natural slope angle. Subsequently, the waves will bring about an equilibrium profile, as happens for dunes. The fine tout venant in the core reduces the height of the incoming waves.

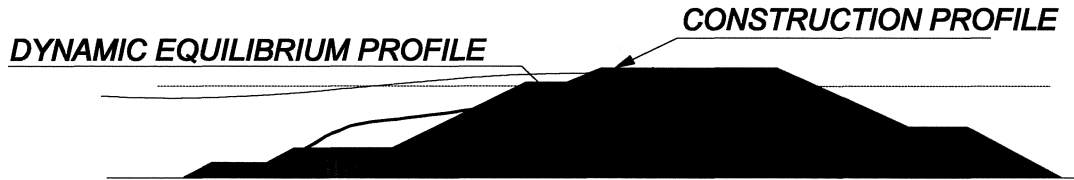


Figure IV-26

If the core becomes too low or too high as a result of settlements or other causes, waves will penetrate into the coarser stones in the cap. A fault tree for "wave behind the breakwater too high as a result of transmission and/or overtopping" is given on the next page. However, more modes are possible:

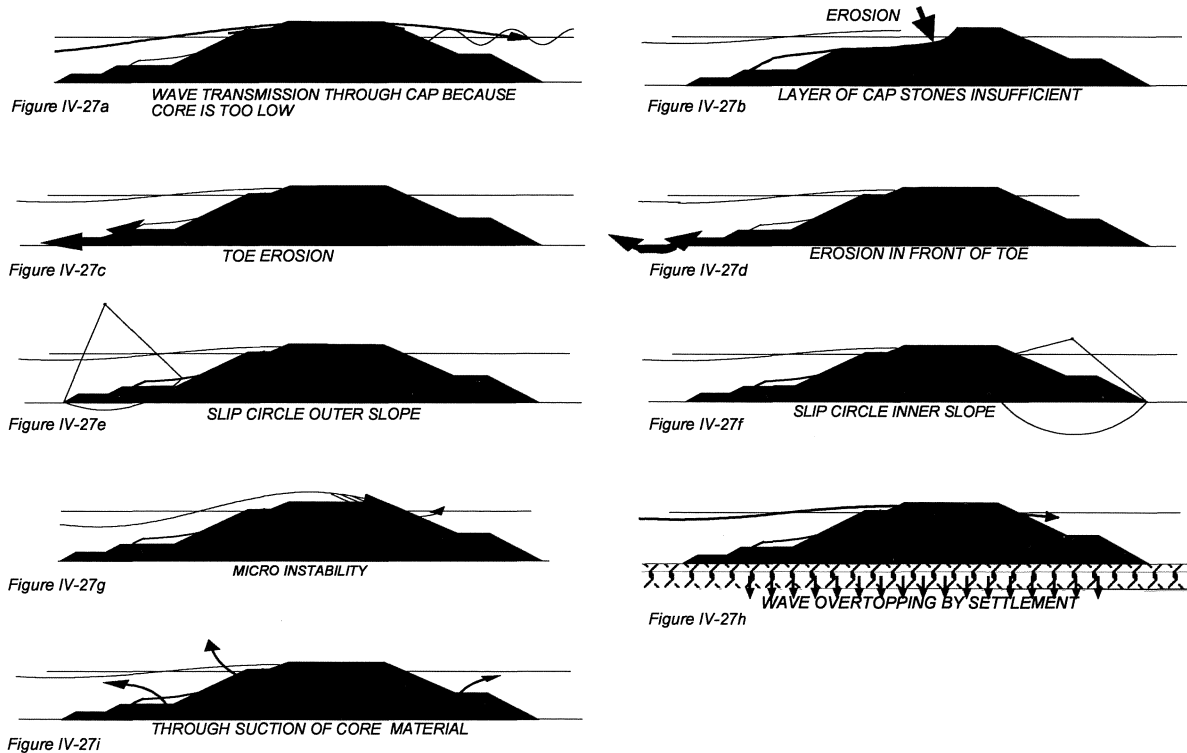


Figure IV-27

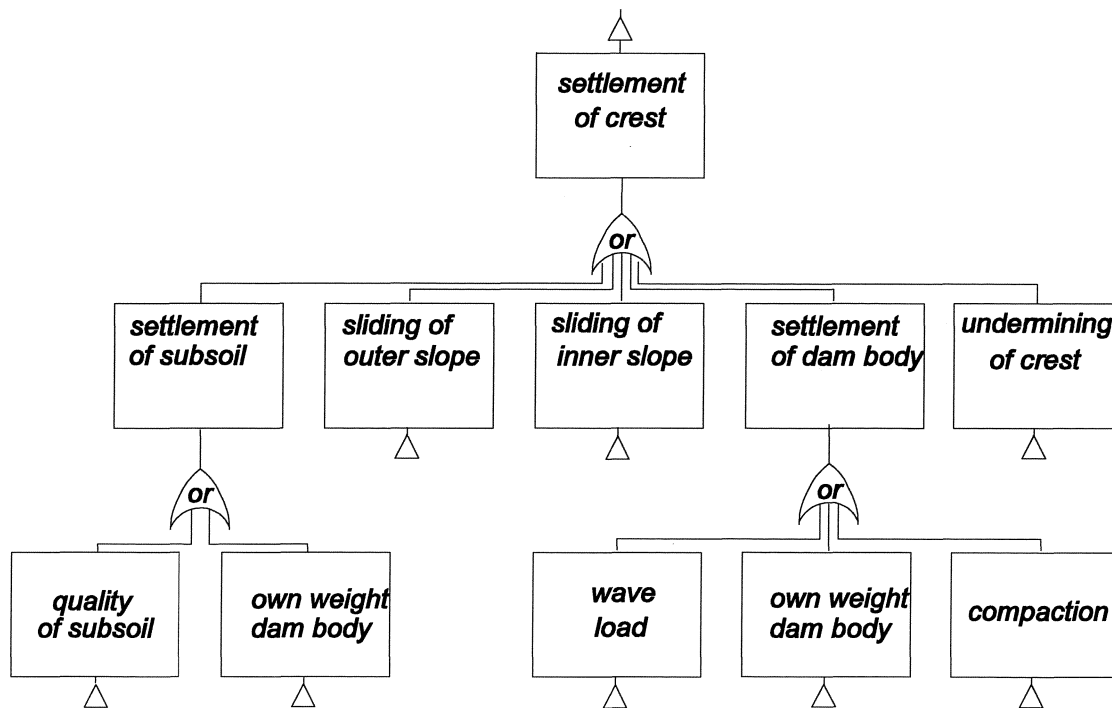


Figure IV-28

A danger with berm breakwaters is that the equilibrium profile in a cross-section doesn't lead to a minimal weight of the rock in the outer layer. After all, a dune is also stable.

With light stones and not totally perpendicular wave incidence, longshore transport can occur. In the following article¹⁾ the evaluation of the longshore transport is discussed.

¹⁾ Vrijling, J.K., E.S.P. Smit, P.F. de Swart, Berm breakwater design - the longshore transport case: a probabilistic approach, Coastal structures and breakwaters, Thomas Telford, London, 1991.

by

prof. drs. ir. J.K. Vrijling, Delft University of Technology, Stevinweg 1, 2600 GA Delft, the Netherlands,
ir. E.S.P. Smit, HASKONING, Royal Dutch Consulting Engineers and Architects, Barbarossastraat 35,
P.O. Box 151, 6500 AD Nijmegen, the Netherlands and
ir. P.F. de Swart, Civil Engineering Division, Rijkswaterstaat, P.O. Box 20000, 3502 LA Utrecht, the Netherlands.

SYNOPSIS

In the last decade a renewed interest has been shown for the berm breakwater concept. In the design of a berm breakwater many limit states have to be checked: stability of the armour layer in both cross and longshore directions, compliance of the secondary layers with filter rules, stability of the toe under wave attack, geotechnical stability, overtopping, etc. In this paper attention will be focussed on the stability of the outer armour. Special attention is given to the longshore transport case. It will be shown that only a probabilistic approach provides an insight into the sensitivity of the associated failure mechanism.

THE DYNAMICALLY STABLE ARMOUR LAYER

1. The design of the armour of a berm breakwater was brought on a more scientific footing by Van der Meer (ref.1), who developed a computational model to predict the cross-sectional profile of the armour layer after the reshaping process. The variables governing the reshaping process and the final profile are:

- size of the armour units, D_{n50} [m],
- relative mass density of armour stone
in water, Δ [-],
- significant wave height, H_s [m],
- average wave period, T_z [s],
- number of waves, N [-],
- angle of wave attack, θ [degr.],
- water depth in front of the structure, h [m].

2. A rough indication of the stability of the armour rock is given by the ratio $H_o = H_s / \Delta D_{n50}$. According to Van der Meer this ratio should lie in the range of 3 - 6 for berm breakwaters. It should be noted, however, that in two-dimensional flume tests structures with higher H_o ratios can be perfectly stable under wave attack after the reshaping process has taken place. Sand dunes, where this ratio exceeds the value of 300, provide an example. In such cases the longshore transport of material quickly gains in importance.

Two-dimensional model tests on berm breakwaters confirm this hypothesis. It is very difficult to destroy a model berm breakwater by incoming waves, unless the structure is overtopped. Overtopping waves can easily damage the back slope of the breakwater. Consequently, an erosion process may start that quickly causes a breach in the breakwater.

LONGSHORE TRANSPORT OF THE ARMOUR LAYER

3. The reshaping process of the cross-section thus places no obvious upper limit on the H_o ratio. However, for high values of this ratio a considerable longshore transport will take place when the waves attack under an angle. In cases where the amount of material available on the weather side is insufficient the breakwater will collapse.

4. The longshore transport case is not well researched for berm breakwaters. Burcharth and Frigaard (ref.2) made a first contribution. On the basis of Burcharth's data and data gained in tests performed by Van der Meer on a berm breakwater design of the authors, a model of the following form is proposed to predict the longshore transport after the reshaping process has taken place:

$$\begin{aligned}
 S &= A (H_o T_o - B)^C && \text{for } H_o T_o > B \\
 S &= 0 && \text{for } 0 \leq H_o T_o \leq B
 \end{aligned}
 \tag{1}$$

where: S = longshore transport rate of primary armour material [stones/wave]
 $T_o = T_p \sqrt{g/D_{n50}}$ [-]
 T_p = spectral peak period [s]
 g = acceleration due to gravity [m/s²]
A, B, C = 4.8*10⁻⁵, 100.0, 2.0 (empirical constants)

A plot of the proposed function and the data points is given in Figure IV-29. It is clear that the theoretical understanding should be improved and that the number of data points could be increased considerably.

5. The uncertainty reflected by the difference between the data points and the function can be modelled by varying the constants A and B (Figures IV-30 and IV-31) by 50% and 20% respectively. If these numbers are interpreted as variation coefficients the standard deviation of the transport at any value of $H_o T_o$ can be calculated by means of the error propagation law. For $H_o T_o = 245$ the mean value of S is 1.009 stones/wave and the standard deviation amounts to 0.57 stones/wave. The limited number of data points prohibits a more thorough statistical analysis.

THE WAVE CLIMATE

6. For the wave climate a typical monsoon climate is adopted. During three months the South-westerly monsoon is blowing, causing a wave field with an average H_s of approximately 2.0 m.

During the other months of the year the sea is very calm and the breakwater is not damaged during this period.

7. The three-hourly observations of the monsoon wave climate are modelled by the following Gumbel distribution (Figure IV-32 = Figure II-112):

$$F_{H_s}(x) = e^{-e^{-\frac{x-A}{B}}}
 \tag{2}$$

where: A = 1.941 and B = 0.284

The deep water wave steepness H_s/L_p defined on the spectral peak period is independent of the wave height and also modelled by a Gumbel distribution (Figure IV-33) with parameter values of A = 0.01 and B = 0.00167.

On the basis of a visual comparison the significant wave height can be equally well described by a Weibull distribution (Figure IV-34):

$$F_{H_s}(x) = 1 - e^{-\left(\frac{x-A}{B}\right)^C}
 \tag{3}$$

where: A = 1.50, B = 0.675 and C = 1.866

8. Every year during the monsoon the coast is assumed to be hit by one hurricane. The significant wave height during the hurricane that lasts 24 hours is modelled by a Fréchet distribution (Figure IV-35):

$$F_{H_s}(x) = e^{-\left(\frac{x-A}{B}\right)^{-C}}
 \tag{4}$$

where: A = 0.00, B = 2.498 and C = 3.388

The wave steepness H_s/L_p follows a Normal distribution with $\mu = 0.028$ and $\sigma = 0.00724$ (Figure IV-36) and is independent of the wave height.

9. The significant wave height at the breakwater is limited to 5.0 m by water depth.

10. The number of individual waves during the monsoon season amounts to 960,000. During a hurricane it is assumed that 10,800 individual waves hit the structure.

THE BREAKWATER DESIGN

11. The basic breakwater design criteria are as follows. The breakwater was designed for a lifetime of 50 years. The rock size for the berm was designed on the basis of a 1/100 year design significant wave height of $H_s = 5.0$ m.

A value of $H_o = 2.75$, which is for berm breakwaters rather conservative, led, in combination with a Δ value of 1.57, to a choice of $D_{n50} = 1.15$ m ($M_{50} = 4.0$ tonnes).

12. The total longshore transport during the planned lifetime of the structure can be calculated by choosing an appropriate design wave and the number of waves in the lifetime N_{life} .

$$S_{life} = N_{life} * S \quad [stones] \quad (5)$$

13. The choice of the appropriate design wave for this case is far from easy. For the monsoon H_s and T_p values of 2.80 m and 13.3 s (1% wave steepness), a condition that is exceeded during 5% of the time, seem a reasonable choice. However, as for this combination $H_o T_o$ equals 38.85, the resulting longshore transport according to Equation (1) is zero.

The hurricane design condition of $H_s = 5.0$ m and $T_p = 10.7$ s is characterised by a value $H_o T_o$ of 86. As this value is smaller than 100 no transport is predicted for hurricane conditions either. So, no provision for the nourishment of the berm at the weather side of the breakwater has to be made.

However, it is imaginable that the design values are exceeded or that the coefficients of the transport equation (1) differ from the most likely values. Then the berm at the weather side might be quickly eroded away.

PROBABILISTIC APPROACH; A FIRST STEP

14. When the probability distribution of the wave height is known, the expected value of the longshore transport, expressed as the number of stones passing through a certain cross-section during the lifetime, should be calculated according to:

$$E(S_{life}) = \int_0^{H_{s,max}} \int_0^{s_{p,max}} N_{life} A(H_o T_o - B)^C f_{H_s}(H) f_{s_p}(s) dH ds \quad (6)$$

where: $f_{H_s}(H)$ = the probability density function (pdf) of H_s
 $f_{s_p}(s)$ = the pdf of s_p , the wave steepness defined on T_p at deep water

15. The expected value of the number of stones transported during the monsoon period over the entire lifetime of the structure can be calculated by substituting the pdf's of significant wave height and wave steepness, related to the Gumbel distribution (2), in the integral (6). When the integration is performed with the transport relation given by (1) and with the upper limits $H_{s,max} = 5.0$ m and $s_{p,max} = 0.05$, the expected value of the transport is 435 stones. This amount increases to 551 stones, when the integration is extended to $H_{s,max} = 7.0$ m.

In the longshore transport calculation of Equation (6) this H_s of 7.0 m is reduced to 5.0 m due to water depth limitations (see Paragraph 9). However, the influence on $H_o T_o$ of a deep water $H_s > 5.0$ m emerges if it is assumed that the deep water wave maintains its period while travelling to the breakwater location.

16. The difference between the result of the deterministic calculation of Paragraph 13 and the result reached here is caused by the fact that now the full range of wave height and steepness values are taken into account by the integration.

17. If the Gumbel pdf of the significant wave height is replaced by the pdf related to the Weibull distribution (3), the integration yields an expected value for the transport

of only 4.6 stones during the lifetime. An increase in the upper limit of integration to 7.0 m now has a negligible effect.

So, the expected value $E(S_{life})$ of the transport appears to be very sensitive to the form of the pdf of the significant wave height (Gumbel or Weibull) and the upper limit of integration $H_{s,max}$, which may point at an important question point in the design.

18. The expected value $E(S_{life})$ of the transport is also dependent on the uncertain values of A and B in Equation (1). If for the coefficients in the transport relation the following safe values are chosen: $A = 7.2 \cdot 10^{-5}$; $B = 80$, then the expected value of the transport for the Gumbel distributed wave height becomes 4,747 stones or $4,747 \cdot M_{50} = 19,000$ tonnes.

19. A similar approach is followed for the hurricane wave climate by substituting in the integral (6) the Frechet pdf related to (4) for the significant wave height and the Normal pdf for the steepness. Also in this case the transport is sensitive to changes in the upper limit of integration and to the substitution of safe values in the transport relation:

<i>Hurricane transport</i>	<i>upper limit $H_{s,max}$</i>	
	<i>15 m</i>	<i>17 m</i>
<i>average transport relation</i>	<i>668</i>	<i>841</i>
<i>"safe" transport relation</i>	<i>3,625</i>	<i>3,837</i>

20. As the stone transport by the monsoon and by the hurricane have to be added to find the amount of nourishment at the weather side, the following matrix should form the basis of the design.

<i>Total transport</i>	<i>upper limits $H_{s,max}$</i>	
	<i>low</i>	<i>high</i>
<i>average transport relation</i>	<i>1,103</i>	<i>1,392</i>
<i>"safe" transport relation</i>	<i>8,372</i>	<i>8,978</i>

The designer is confronted with a difficult decision.

PROBABILISTIC APPROACH; A SECOND STEP

21. The correct solution for the problem posed above is found by introducing the uncertainties described into the design equations in the form of additional pdf's.

Moreover, the uncertainties in the Δ and D_{n50} values (hidden in the dimensionless quantity $H_o T_o$) that will be realised during construction, and the exact amount of nourishment that will be supplied, can be included.

22. By means of a Level II probabilistic calculation (ref.3) the influence of the uncertainties in Δ , D_{n50} , the coefficients A and B in the transport relation and the integration limits $H_{s,max}$ on the expected transport, can be calculated. If the amount of material at the weather side to nourish the longshore transport is known, the probability of failure can be established.

23. To this end the following reliability function is defined:

$$Z = \text{Nourish} - E(S_{life,mons.}) - E(S_{life,hurr.}) \quad [\text{stones}] \quad (7)$$

where: Nourish = nourishment at t=0 [stones]

$E(S_{life,mons.})$ = expected value of the transport over the lifetime due to monsoon waves [stones]

$E(S_{life,hurr.})$ = expected value of the transport over the lifetime due to hurricane waves [stones]

24. For the constants A and B of the transport relation normal distributions are adopted with the following parameters based on the scarce experimental data:

	μ	σ
A	$4.8 \cdot 10^{-5}$	$2.4 \cdot 10^{-5}$
B	100.0	20.0

25. The uncertainties of the stone size D_{n50} and the relative density Δ are also modelled by normal distributions. The values for the standard deviations are based on the experience of the authors:

	μ	σ
D_{n50}	1.15	0.058
Δ	1.57	0.060

26. The upper limits of the integration are set by the maximum significant wave heights that will occur during the monsoon and during the hurricane in the lifetime of the breakwater of 50 years. These maximum significant wave heights during monsoon and hurricane over the entire lifetime follow extreme value distributions.

The lifetime contains $50 \text{ years} * 3 \text{ months} * 30 \text{ days} * 24 \text{ hours} / 3 \text{ hours} = 36,000$ independent realisations of the monsoon wave climate described by the Gumbel distribution (2), so the highest significant wave is distributed according to:

$$F_{H_{s,extr.}}(x) = F_{H_s}(x)^N \quad (8)$$

where: $N = 36,000$

Algebraically, the extreme value distribution is again a Gumbel distribution with the coefficients $A' = A + B \ln(N)$ and $B' = B$.

The upper limit of the hurricane climate is modelled following the same reasoning for $N = 50$ independent storms during the lifetime. The exact extreme value distribution is, in this case, easily derived to be a Fréchet distribution with parameters $A' = A$, $B' = B * N^{1/C}$ and $C' = C$.

27. The number of stones that is provided at the weather side of the breakwater at $t=0$ to provide nourishment for the transport occurring over the lifetime (the resistance side of the design problem), is modelled by a Normal distribution to account for construction tolerances:

	μ	σ
Nourish	2,500	100 [stones]

28. The Level II calculation shows (see Table 1) that the probability of failure is 28% in the lifetime of the breakwater. In this case, failure implies that the extra amount of nourishment provided at the time of construction is completely taken away during the design lifetime. The Level II calculation also shows the contributions of the variables to the standard deviation of Z in the column α^2 . The values in the column indicate that the greatest contribution comes from the B coefficient in the transport relation, with the D_{n50} in the second place. The integration limits, formed by the maximum significant wave heights due to the monsoon and the hurricane during the lifetime, are relatively unimportant.

29. From the table the conclusion may be drawn that further research should be done to establish the transport relation, especially the start of the movement modelled by the coefficient B. During construction the D_{n50} of the rock going into the berm should be strictly controlled by quality assurance measures to prevent errors in this variable to the lower side.

CONCLUSIONS

30. The paper shows that although the design of the cross-section of a berm breakwater is well defined by the work of Baird and Hall (ref.4), Van der Meer (ref.1) and others, the longshore transport caused by angular wave attack may pose a threat that must be addressed by the designer and the researcher of this type of structure.

31. On the basis of scarce data from Burcharth and Frigaard (ref.2) and from tests performed for a project in which the authors were involved, a simple longshore transport relation

for the armour rock of the berm has been derived. The influence of the angle of wave attack cannot be deduced from the data.

32. Statistical descriptions of the monsoon and the hurricane wave climates at the project location are given. A simple deterministic approach of the longshore transport of the berm material shows no transport.

33. A first step probabilistic approach, that takes into account the variability of the waves, proves, however, that the expected value of the longshore transport has a positive value and that nourishment has to be provided. It is shown that the decision on the amount of nourishment is far from simple in the light of the uncertainties in the transport relation and the maximum significant wave heights during monsoon and hurricane. The amount may vary from 1,103 stones to 8,978 stones depending on the optimism of the designer.

34. In a second step all uncertainties are included in a Level II probabilistic calculation. It is shown that a nourishment of 2,500 stones has a probability of failure of 29% in the lifetime. The Level II calculation shows further that the uncertainty of the transport relation contributes most to the failure probability. So, more research into this problem is needed. Secondly, the stone size has to be carefully controlled during construction by quality assurance procedures.

35. If the nourishment is increased to 5,000 stones the probability of failure is reduced to 18% (see Table 2). The designer has now to decide on the basis of probabilities and risks.

REFERENCES

1. VANDERMEER J.W. Rock slopes and gravel beaches under wave attack. Doctoral thesis, Delft University of Technology, Delft, the Netherlands, 1988. Also: Delft Hydraulics Communication No.396, the Netherlands, 1988.
2. BURCHARTH H.F. and FRIGAARD P. Reshaping breakwaters; on the stability of berm breakwater roundheads and trunk erosion in oblique waves. From: Berm breakwaters: unconventional rubble mound breakwaters; edited by D.H. Willis, W.F. Baird and O.T. Magoon, Canada, pp. 55-72, 1987.
3. CIRIA Rationalisation of safety and serviceability factors in structural codes. CIRIA report No.63, London, 1974.
4. BAIRD W.F. and HALL K.R. The design of armour systems for the protection of rubble mound breakwaters, Proc. Conf. on Breakwater design and construction, Inst. of Civ. Eng. London, 1983.

Table 1. Result of Level II probabilistic calculation; the nourishment amounts to 2,500 stones

$\beta = 0.550$

Probability of failure = $2.9 \cdot 10^{-1}$

Name	type	A	B	C	μ	σ	X	α^2		
Δ	N	0.000	0.000		0.000	1.570		0.060	1.564	0.037
D_{n50}	N	0.000	0.000		0.000	1.150		0.058	1.138	0.143
A	N	0.000	0.000		0.000	$4.8 \cdot 10^{-5}$		$2.4 \cdot 10^{-5}$	0.000	0.062
B	N	0.000	0.000		0.000	100.000		20.000	90.428	0.757
$H_{s_{max}, Monsoon}$	G	4.920	0.284		0.000	5.024		0.327	5.024	0.000
$H_{s_{max}, Hurr}$	F	0.000	7.926		3.388	8.832		3.001	8.832	0.000
<i>Nourish</i>	N	0.000	0.000		0.000	2500.000		200.000	2495.381	0.002

$Z(X) = -0.2689$ (X is the design point)

Number of iterations = 8

Table 2. Result of Level II probabilistic calculation; the nourishment amounts to 5,000 stones

$\beta = 0.923$

Probability of failure = $1.8 \cdot 10^{-1}$

Name	type	A	B	C	μ	σ	X	α^2		
Δ	N	0.000	0.000		0.000	1.570		0.060	1.560	0.034
D_{n50}	N	0.000	0.000		0.000	1.150		0.058	1.131	0.132
A	N	0.000	0.000		0.000	$4.8 \cdot 10^{-5}$		$2.4 \cdot 10^{-5}$	0.000	0.059
B	N	0.000	0.000		0.000	100.000		20.000	83.761	0.774
$H_{s_{max}, Monsoon}$	G	4.920	0.284		0.000	5.024		0.327	5.024	0.000
$H_{s_{max}, Hurr}$	F	0.000	7.926		3.388	8.832		3.001	8.832	0.000
<i>Nourish</i>	N	0.000	0.000		0.000	5000.000		200.000	4996.381	0.000

$Z(X) = 0.0018$ (X is the design point)

Number of iterations = 12

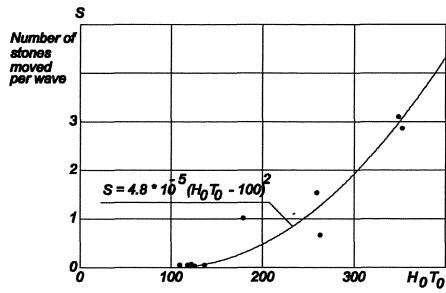


Figure IV-29. The longshore transport relation as fitted to model test data

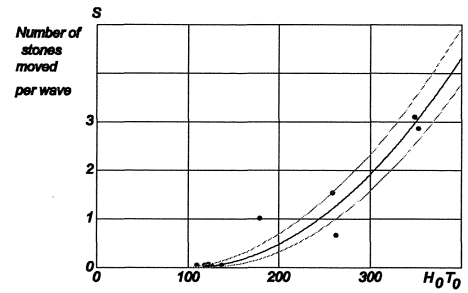


Figure IV-30. The effect of a change in the value of the coefficient B in the transport relation

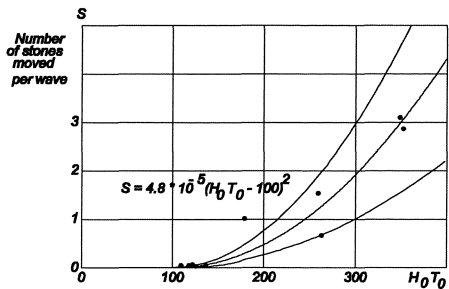


Figure IV-31. The effect of a change in the value of the coefficient A in the transport relation

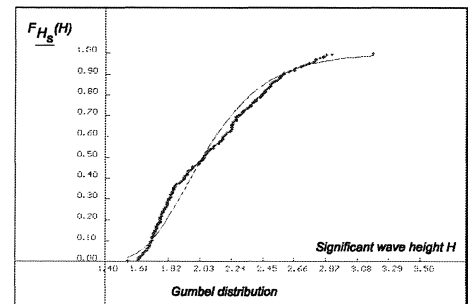


Figure IV-32. The distribution of the significant wave height during the monsoon

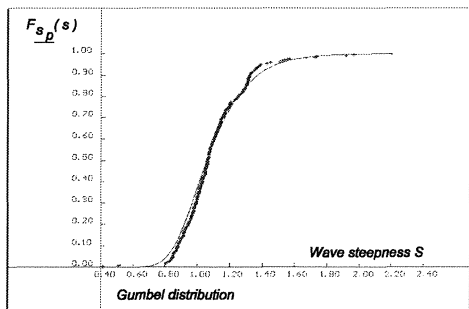


Figure IV-33. The distribution of the deep water wave steepness during the monsoon

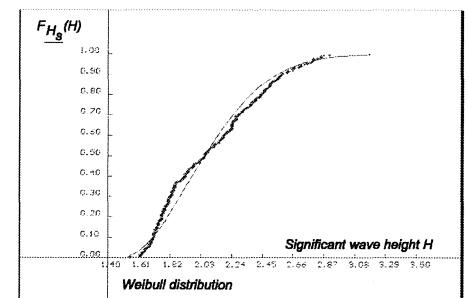


Figure IV-34. The alternative distribution of the significant wave height during the monsoon

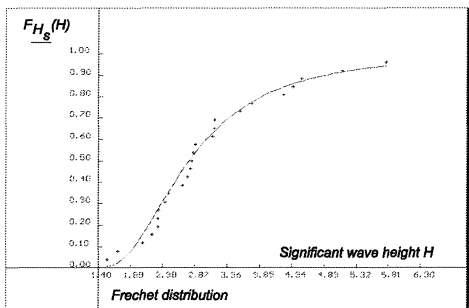


Figure IV-35. The distribution of the significant wave height during the hurricane

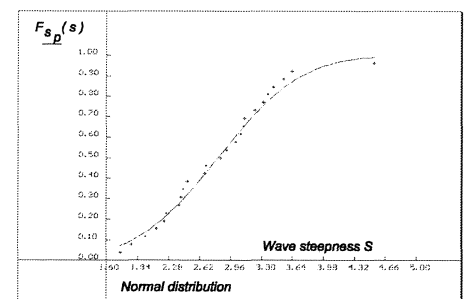


Figure IV-36. The distribution of the deep water wave steepness during the hurricane

V. LENGTH EFFECTS

V.1. INTRODUCTION

§ IV.1. already mentioned that, lengthwise, ostensibly homogeneous hydraulic structures such as breakwaters, dunes or dykes can be considered serial systems. The lengths of independent sections in these serial systems can be related to the nature of the load, to the strength properties or to both.

To stimulate discussion, a couple of lengths related to the load on a water defence are listed:

load	length of a section
water level	50 to 100 km
shower gust/ oscillation	5 to 10 km
wave climate	20 to 50 km
foreshore	5 to 10 km
location in stormdirection	1 to 5 km

The table below gives global indications of a couple of lengths related to the strength-properties of water defences, for which the corresponding property can be considered constant

streth	length of a section
crest height	0.2 to 0.5 km
grain diameter (D_{n50})	1 to 10 km
slope gradient	0.2 to 0.5 km
width	0.5 to 5 km
beach height	0.5 to 5 km

Within a statistically homogeneous course of a water defence structure a number of section or stretches are distinguished, see Figure V-1, with lengths equal to the "correlation distance" ¹⁾, i.e. the distance over which the statistical properties of the reliability function are assumed totally correlated.

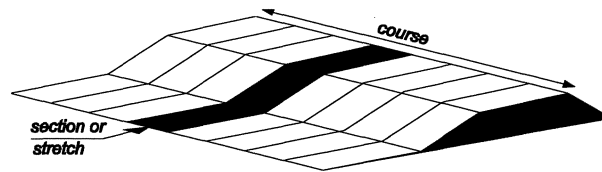


Figure V-1

For "course" in this figure one can think of the length of a water defence (see Figure IV-4: dyke with wave run-up bordering deep water or bordering water with a foreshore, a dune, a dyke without wave run-up, a lock, a coupure, high grounds, etc.).

By choosing the fluctuation scale as a "correlation distance", one section is assumed independent of every other one. The probability of failure of the water defence as a system is then determined by the weakest section, see Figure V-3. There are as many sections as fluctuation scale lengths fit into the course.

The fluctuation scale of the reliability function, $\underline{Z} = \underline{R} - \underline{S}$, is dependent on both the fluctuation scale of the strength properties, \underline{R} , and on the fluctuation scale of the load(s), \underline{S} . In Figure V-3a more failure modes per section are considered. This presentation is useful, as the length over which the strength properties fluctuate is small relative to the length over which the load(s) vary. In Figure V-3b the section length is determined for every mode. Every section is considered an independent structure, for which the probability of failure is determined according to the failure mode in question. The right figure bears a strong resemblance to Figure IV-5. The difference is that Figure IV-5 treats a whole construction as one section, whilst now a structure is assumed to consist of several sections.

¹⁾ Often, the characteristic \underline{x} is taken as a realisation of a stationary normally distributed process

and for $\rho_{\underline{x}, \underline{x}+\tau}$: $\rho_{\underline{x}, \underline{x}+\tau}(\tau) = e^{-\left(\frac{\tau}{D}\right)^2 \cdot \frac{\pi}{4}}$ is used

(see lecture notes: Probabilistic design, b3, TUD).

The **FLUCTUATION SCALE**, D , is defined as the surface below the auto correlation function:

$$D = \int_0^{\infty} \rho_{\underline{x}, \underline{x}+\tau}(\tau) d\tau$$

with: \underline{x} = the characteristic (crest height, friction resistance, bearing capacity, etc.) under consideration. "Collapse according to a certain failure mode" also qualifies as a "characteristic". (Familiarly said: "The Z- functions are correlated".)

τ = distance between the points (in time) which are taken into account, known as the lag.

$\rho_{\underline{x}, \underline{x}+\tau}$ = auto correlation function of \underline{x} .

For D the auto correlation within the fluctuation scale is approximately 50% or more. Furthermore, the fluctuation scale is about half the wave length, i.e. half the average distance between two "upward sections of the zero level", see Figure V-7.

The fault tree can be represented in two ways:

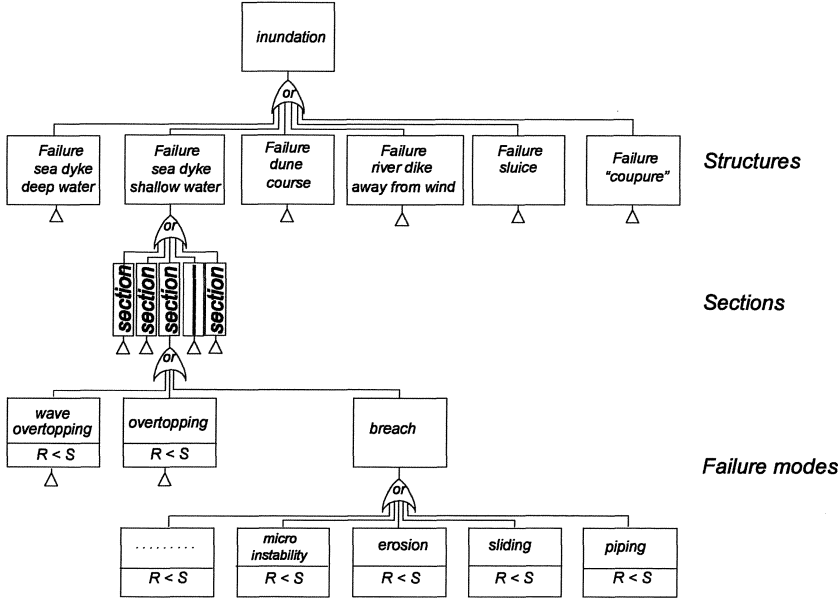


Figure V-3a

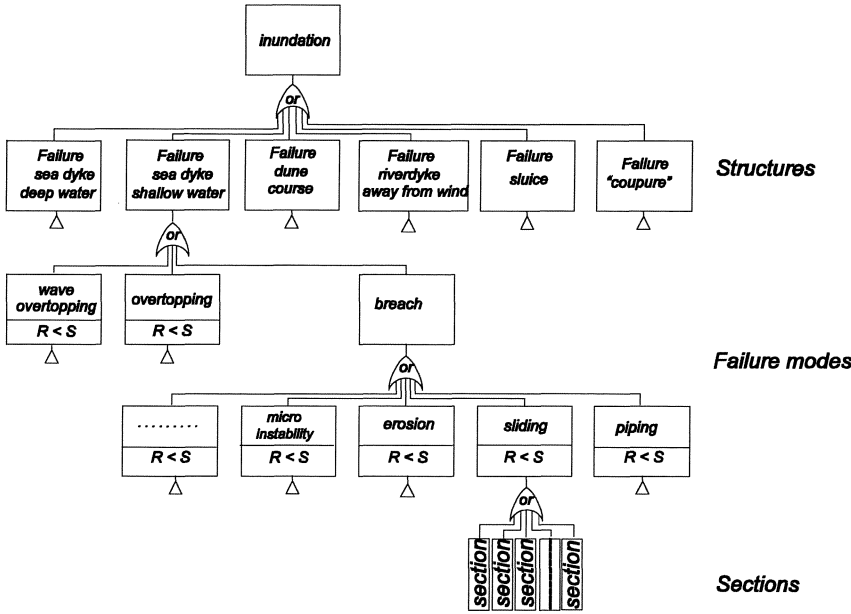
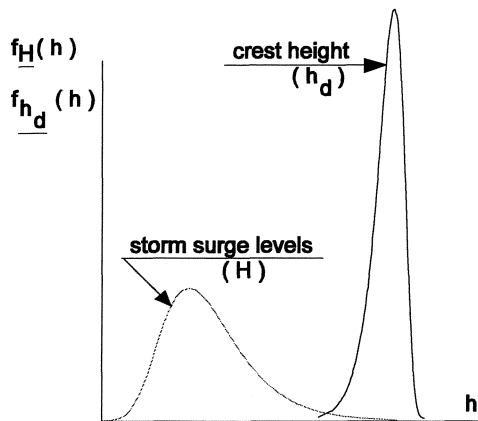


Figure V-3b

V.2. LENGTH EFFECTS AS A RESULT OF FLUCTUATING STRENGTH

STATISTICALLY HOMOGENEOUS COURSE. EXAMPLE: SEA DYKE.



A simple and greatly schematised case of the influence of fluctuating strength is treated as an example.

One failure mode for a sea dyke is considered, namely overtopping. For one section the reliability function is:

$$\underline{Z} = \underline{h_d} - \underline{H}$$

where $\underline{h_d}$ is the crest height and \underline{H} is the high water level above chart datum.

Figure V-4

The crest height is normally distributed with expected value $\mu_{h_d} = 5.0$ m. Two cases are regarded. The standard deviation of $\underline{h_d}$ is equal to $\sigma_{h_d} = 0.1$ m in the first case and equal to $\sigma_{h_d} = 0.2$ m in the second case. For the probability distribution of the storm surge levels in a year the probability for Hoek van Holland is assumed:

$$F_{\underline{H}}(h) = e^{-e^{-\frac{h-1.96}{0.33}}}$$

with:

$$\sigma_{\underline{H}} = \frac{\pi}{\frac{1}{0.33} \sqrt{6}} \approx 0.4.. m$$

ELEMENTARY LOWER AND UPPER LIMITS

With the data above, a refined level II calculation can be carried out for one section. The final results (design point values) are:

First case: $\sigma_{h_d} = 0.1$ m					
$\beta = 3.709$ $P_{b_i} = 1.04 \cdot 10^{-4}$	Variable	X (i)	$\frac{\partial Z}{\partial X_i}$	σ (i)	α^2 (i)
	h_d	4.97 m	1.00	0.1	0.01
	H	4.97 m	-1.00	1.299	0.99

Second case: $\sigma_{h_d} = 0.2$ m					
$\beta = 3.676$ $P_{b_i} = 1.18 \cdot 10^{-4}$	Variable	X (i)	$\frac{\partial Z}{\partial X_i}$	σ (i)	α^2 (i)
	h_d	4.89 m	1.00	0.2	0.02
	H	4.89 m	-1.00	1.278	0.98

The elementary lower and upper limits of the probability of collapse of the system (water defence as a serial system), consisting of N independent sections are:

$$\underset{i=1}{\overset{N}{MAX}} P_{b_i} \leq P_{defence} \leq \sum_{i=1}^N P_{b_i}$$

If all sections are assumed to originate from the same population (statistically homogeneous process in the course) so that all sections have the same inundation probability, the elementary lower and upper limit of the probability of inundation for the entire defence structure can be simplified to:

$$P_{b_i} \leq P_{defence} \leq N * P_{b_i}$$

Substituting the assumed numerical values gives:

Standard deviation of σ_{h_d}	elementary lower and upper limit
$\sigma_{h_d} = 0.1 \text{ m}$	$1.04 \cdot 10^{-4} \leq P_{defence} \leq N \cdot 1.04 \cdot 10^{-4}$
$\sigma_{h_d} = 0.2 \text{ m}$	$1.8 \cdot 10^{-4} \leq P_{defence} \leq N \cdot 1.18 \cdot 10^{-4}$

The development of the elementary limits as functions of the number of independent sections ¹⁾ is drawn in Figures V-7 and V-8.

APPROXIMATIVE METHOD ACCORDING TO DITLEVSEN

The method Ditlevsen (see lecture notes b3) gives closer boundaries. The reliability functions of two sections are:

$$\underline{Z}_i = \frac{h_{d_i} - H_i}{\sigma_{Z_i}}$$

$$\underline{Z}_j = \frac{h_{d_j} - H_j}{\sigma_{Z_j}}$$

The correlation coefficient is defined by:

$$\rho_{\underline{Z}_i, \underline{Z}_j} = \frac{cov(\underline{Z}_i, \underline{Z}_j)}{\sigma_{\underline{Z}_i} \cdot \sigma_{\underline{Z}_j}}$$

where $cov(\underline{Z}_i, \underline{Z}_j) = E \left[\left\{ \underline{Z}_i - E(\underline{Z}_i) \right\} \cdot \left\{ \underline{Z}_j - E(\underline{Z}_j) \right\} \right]$

where $E(\underline{X}) =$ expected value of \underline{X} .

¹⁾ Formally the upper limit is NOT VALID FOR $\rho = 0$ ((linear) independence) BUT FOR CASES WHEN "FAILURE" OF EVERY SECTION EXCLUDES "FAILURE" OF OTHER SECTIONS. If the events ("failure" of sections) exclude each other they are *not* independent! Independent events and events which exclude each other are not synonymous! When events exclude each other: one event occurring means the other, which is dependent on that, does *not* occur!

Further elaboration gives:

$$\begin{aligned}
 cov(Z_i, Z_j) &= E \left[\left(\underline{h}_{d_i} - \underline{H}_i - \mu_{\underline{h}_{d_i}} + \mu_{\underline{H}_i} \right) \left(\underline{h}_{d_j} - \underline{H}_j - \mu_{\underline{h}_{d_j}} + \mu_{\underline{H}_j} \right) \right] \\
 &= E \left[\left\{ \underline{h}_{d_i} - \mu_{\underline{h}_{d_i}} - \left(\underline{H}_i - \mu_{\underline{H}_i} \right) \right\} \left\{ \underline{h}_{d_j} - \mu_{\underline{h}_{d_j}} - \left(\underline{H}_j - \mu_{\underline{H}_j} \right) \right\} \right] \\
 &= \rho_{\underline{h}_{d_i}, \underline{h}_{d_j}} \sigma_{\underline{h}_{d_i}} \sigma_{\underline{h}_{d_j}} - \rho_{\underline{h}_{d_i}, \underline{H}_j} \sigma_{\underline{h}_{d_i}} \sigma_{\underline{H}_j} - \rho_{\underline{H}_i, \underline{h}_{d_j}} \sigma_{\underline{H}_i} \sigma_{\underline{h}_{d_j}} + \rho_{\underline{H}_i, \underline{H}_j} \sigma_{\underline{H}_i} \sigma_{\underline{H}_j} \\
 \sigma_{\underline{Z}_i} &= \sqrt{\sigma_{\underline{h}_{d_i}}^2 + \sigma_{\underline{H}_i}^2} & \sigma_{\underline{Z}_j} &= \sqrt{\sigma_{\underline{h}_{d_j}}^2 + \sigma_{\underline{H}_j}^2}
 \end{aligned}$$

- Now: $\sigma_{\underline{h}_{d_i}} = \sigma_{\underline{h}_{d_j}}$, assume $\sigma_{\underline{h}_d}$ (crest heights originating from the same population so the standard deviation of the crest heights is the same for all sections)
- $\sigma_{\underline{H}_i} = \sigma_{\underline{H}_j}$, assume $\sigma_{\underline{H}}$ (realisation of high water levels from one population, so that the standard deviation of the high water levels is the same for all sections)
- $\rho_{\underline{h}_{d_j}, \underline{H}_i} = \rho_{\underline{h}_{d_i}, \underline{H}_j}$ (symmetry of the correlation matrix)

so:

$$\rho_{\underline{Z}_i, \underline{Z}_j} = \frac{\rho_{\underline{h}_{d_i}, \underline{h}_{d_j}} \sigma_{\underline{h}_d}^2 - 2 \rho_{\underline{h}_{d_i}, \underline{H}_j} \sigma_{\underline{h}_d} \sigma_{\underline{H}} + \rho_{\underline{H}_i, \underline{H}_j} \sigma_{\underline{H}}^2}{\sigma_{\underline{h}_d}^2 + \sigma_{\underline{H}}^2}$$

For the determination of sharper upper and lower limits some assumptions are necessary:

- ◆ fluctuations in the dyke crest height and the storm surge levels are not correlated: $\rho_{\underline{h}_{d_i}, \underline{H}_j} = 0$.
- ◆ the defence structure is so "short" (shorter than the order of 50 to 100 km for "equal water level", see table on page V - 1), that all sections are threatened by the same storm surge level. Then: $\rho_{\underline{H}_i, \underline{H}_j} = 1$.

Working out the correlation coefficient gives:

$$\rho_{\underline{Z}_i, \underline{Z}_j} = \frac{\sigma_{\underline{h}_d}^2 \cdot \rho_{\underline{h}_{d_i}, \underline{h}_{d_j}} + \sigma_{\underline{H}}^2}{\sigma_{\underline{h}_d}^2 + \sigma_{\underline{H}}^2}$$

If the section lengths are chosen such that the dyke crest heights of the sections are (linearly) *independent* (see Figure V-2), then: $\rho_{\underline{h}_{d_i}, \underline{h}_{d_j}} = 0$.

The correlation coefficient for the modes in the sections i and j then becomes:

$$\rho_{\underline{Z}_i, \underline{Z}_j} = \frac{\sigma_{\underline{H}}^2}{\sigma_{\underline{h}_d}^2 + \sigma_{\underline{H}}^2} = \frac{\sigma_{\underline{H}}^2}{\sigma_{\underline{Z}}^2} = \alpha_H^2$$

This expression is equal to that for the factor α^2 in the level II calculation (see lecture notes CTWA4130/b3), which is the contribution of the uncertainty of the high water level to the total variance.

For $\sigma_{h_d} = 0.1$ m, respectively $\sigma_{h_d} = 0.2$ m, the contributions to the variance of the reliability function are given in the tables on page V - 5, where the probability of failure of one dyke section was considered:

Standard deviations crest heights	$\alpha^2_{\underline{H}}$ from level II	$\alpha^2_{\underline{H}}$ with \underline{H} Gumbel $\sigma_{\underline{H}} = 0.42..$ m (page V - 5 middle)
$\sigma_{h_d} = 0.1$ m	0.99	$\frac{0.42324..^2}{0.1^2 + 0.42324..^2} \approx 0.9471..$
$\sigma_{h_d} = 0.2$ m	0.98	$\frac{0.42324..^2}{0.2^2 + 0.42324..^2} \approx 0.8175$

N.B. When two reliability functions (Z_1 and Z_2) contain one common random variable X (and possibly other not common random variables), the correlation coefficient is equal to the product of the α s from the level II calculation:

$$\rho_{\underline{Z}_1, \underline{Z}_2} = \alpha_{\underline{X} \text{ in } \underline{Z}_1} \cdot \alpha_{\underline{X} \text{ in } \underline{Z}_2}$$

(Level II calculation means: linear (or *linearised*) probability function and all variables normally distributed, or **approximated** by normal distributions.)

According to the approximations by Ditlevsen, if $\beta_i = \frac{\mu_{Z_i}}{\sigma_{Z_i}} = \beta_j = \frac{\mu_{Z_j}}{\sigma_{Z_j}} = \beta$, as in this case:

$$P(\underline{Z}_i \leq 0 \cap \underline{Z}_j \leq 0) = 2 \cdot \Phi(-\beta) \cdot \Phi(-\beta^*)$$

Here: $\beta^* = \frac{1 - \rho_{\underline{Z}_i, \underline{Z}_j}}{\sqrt{1 - \rho^2_{\underline{Z}_i, \underline{Z}_j}}}$ and $\Phi(X)$ = standard normal distribution for the argument X.

An upper limit for a defence structure consisting of N equal sections, is, according to Ditlevsen:

$$P_{\text{defence}} \leq P(\underline{Z}_i < 0) + (N-1) \cdot \{P(\underline{Z}_i < 0) \cdot P(\underline{Z}_i < 0 \cap \underline{Z}_j < 0)\}$$

The lower limit follows from:

$$P_{\text{defence}} \geq \sum_{i=1}^N \{P(\underline{Z}_i < 0) - (i-1) \cdot P(\underline{Z}_i < 0 \cap \underline{Z}_j < 0)\} \text{ as long as the terms are positive}$$

The upper limits according to Ditlevsen have also been given in Figures V-7 and V-8. The lower limits according to Ditlevsen are practically equal to the elementary lower limits. They are not indicated in the figures.

AN EXACT SOLUTION

If one assumes that the water level, H , is equal for all sections and that the height of the water defence sections are independent amongst each other ¹⁾ but that they do originate from one population, an exact calculation is possible. The theory behind this was treated for extreme values (paragraph II-2 and further). For the calculation of the probability of failure (U.L.S. of for example the stability of the armour layer of a breakwater) the distribution of the maximum values of independent realisations (maxima of the highest significant wave or of a water level during a year or during the maintenance or planning period or during the lifetime) is of importance. Such a consideration can also be applied using length instead of time as a variable. However, in those cases the minima are often of importance, for example when the lowest of N independent dyke sections is wanted for a given length of the water defence.

The extreme value distribution of the lowest of N dyke sections is wanted. It is assumed that a sample of dyke crest heights can be described by a normal distribution. The probability that a section is higher than h equals:

$$P(\underline{h}_d > h) = 1 - \Phi_{\underline{h}_d} \left(\frac{h - \underline{\mu}_{h_d}}{\underline{\sigma}_{h_d}} \right)$$

Here $\Phi_{\underline{h}_d} \left(\frac{h - \underline{\mu}_{h_d}}{\underline{\sigma}_{h_d}} \right)$ is the standard normal distribution for the argument $\frac{h - \underline{\mu}_{h_d}}{\underline{\sigma}_{h_d}}$.

The probability that all N sections are higher than h is:

$$P(\underline{h}_{d_1} > h \cap \underline{h}_{d_2} > h \cap \dots \cap \underline{h}_{d_N} > h) = \prod_{i=1}^N \left\{ 1 - \Phi_{\underline{h}_d} \left(\frac{h - \underline{\mu}_{h_d}}{\underline{\sigma}_{h_d}} \right) \right\} = \left\{ 1 - \Phi_{\underline{h}_d} \left(\frac{h - \underline{\mu}_{h_d}}{\underline{\sigma}_{h_d}} \right) \right\}^N$$

From this, the probability that at least one of the N sections is lower than h follows:

$$P\left(\underline{h}_{d_{\min}} < h\right) = 1 - \left\{ 1 - \Phi_{\underline{h}_d} \left(\frac{h - \underline{\mu}_{h_d}}{\underline{\sigma}_{h_d}} \right) \right\}^N$$

The distributions for various values of N are displayed in Figure V-5.

¹⁾ This assumption is often *not* justified.

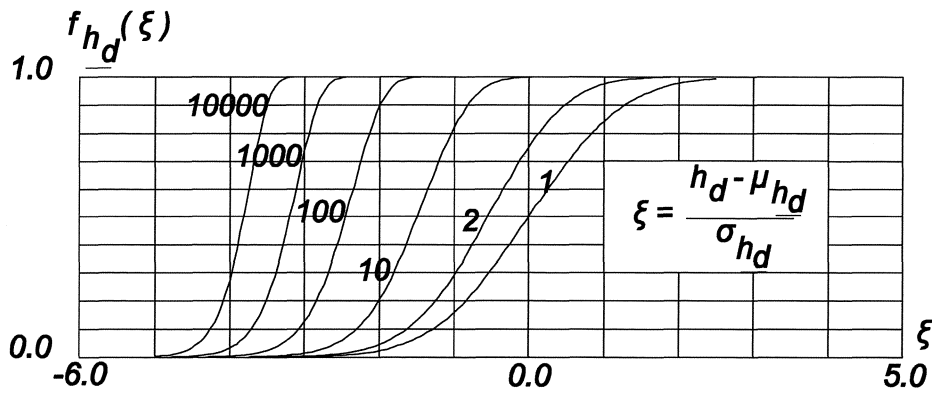


Figure V-5

The p. d. f. of the minima can be derived from the distribution :

$$\varphi_{\min h_d}(H) = \frac{d}{dH} \left[1 - \left\{ 1 - \Phi_{h_d} \left(\frac{H - \mu_{h_d}}{\sigma_{h_d}} \right) \right\}^N \right] = \frac{N}{\sigma_{h_d}} \cdot \left\{ 1 - \Phi_{h_d} \left(\frac{H - \mu_{h_d}}{\sigma_{h_d}} \right)^{N-1} \right\} \cdot \varphi_{h_d} \left(\frac{H - \mu_{h_d}}{\sigma_{h_d}} \right)$$

The probability density functions for various values of N are displayed in the figure below.

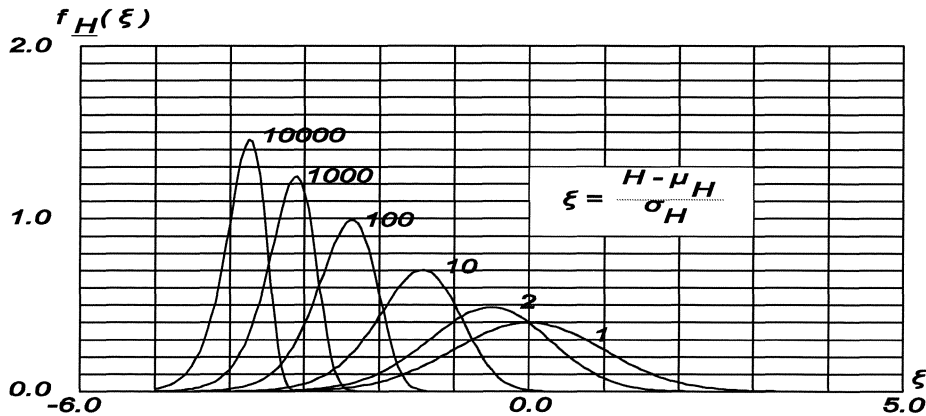


Figure V-6

The probability of inundation of the defence can be calculated by integration (level III):

$$P_{defence} = \int_{-\infty}^{+\infty} \int_H^{+\infty} \frac{N}{\sigma_{h_d}} \cdot \left\{ 1 - \Phi_{h_d} \left(\frac{H - \mu_{h_d}}{\sigma_{h_d}} \right)^{N-1} \right\} \cdot \varphi_{h_d} \left(\frac{H - \mu_{h_d}}{\sigma_{h_d}} \right) \cdot f_{SV}(HW) dHW dH$$

where $f_{SV}(HW)$ = probability density function of the storm surge levels. This double integral is numerically solvable. The solutions are sketched in Figures V-7 and V-8.

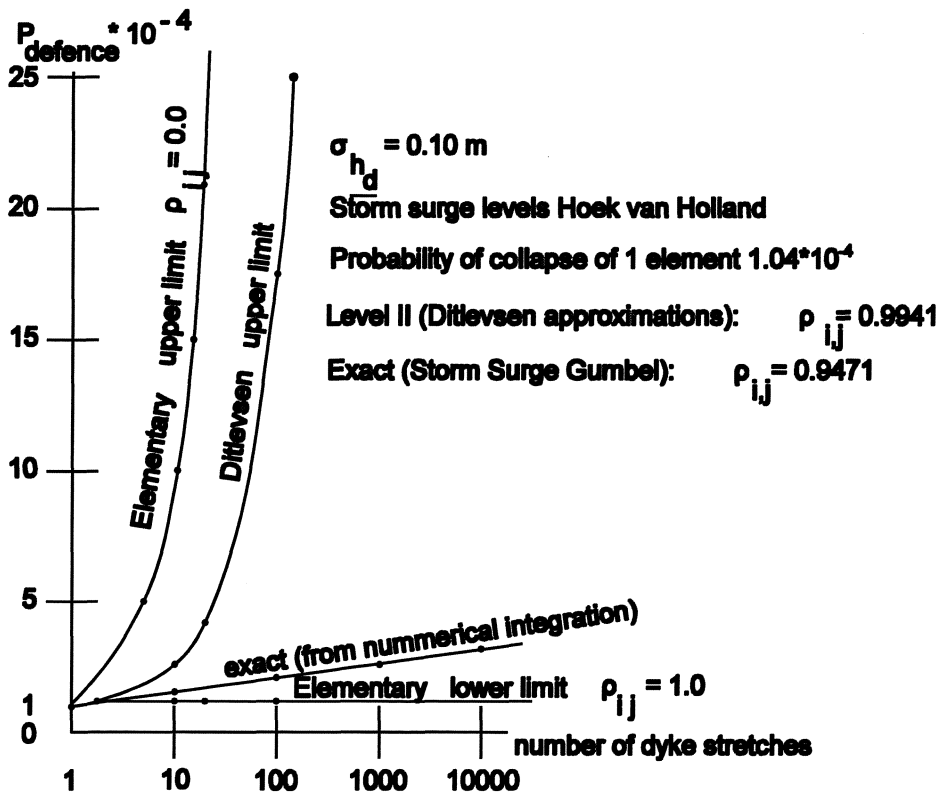


Figure V-7

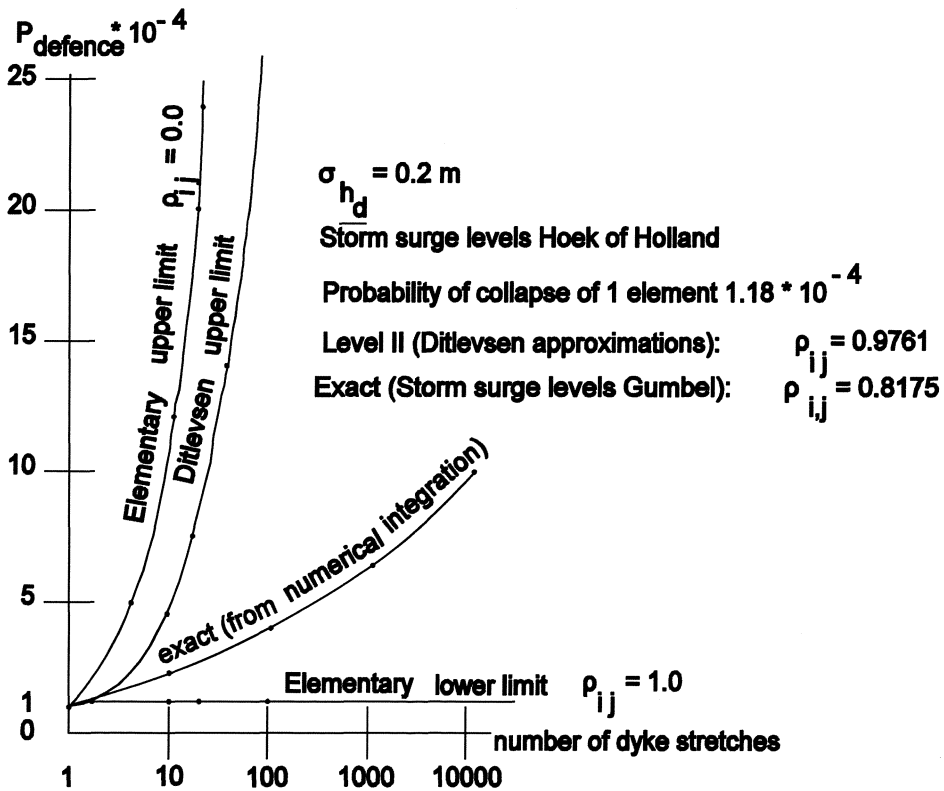


Figure V-8

SUMMARY OF THE RESULTS

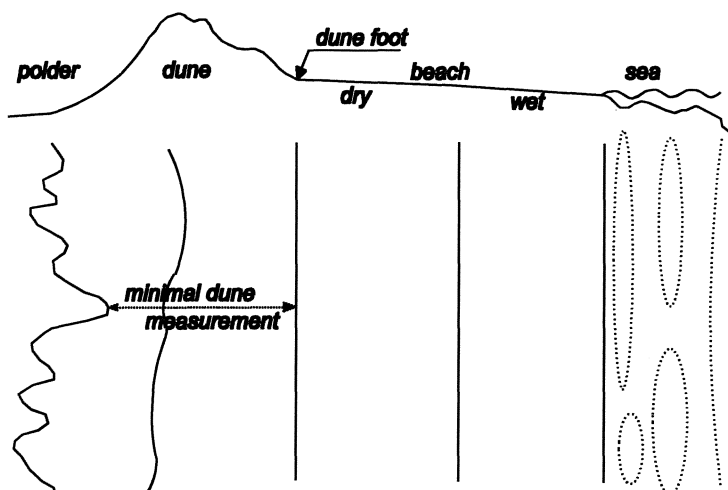
In the figures V-7 and V-8 the calculated elementary lower and upper limits, the upper limits according to Ditlevsen and the "exact solution" (storm surge levels Gumbel distributed) are displayed. In practice the upper limit approximations are used a lot, on the one hand because small probabilities of failure are then striven after, on the other hand because, if the correlation is not too great, the "exact solution" is often close to the upper limit. The calculated ratio between the upper limit of the probability of failure of the whole defence and the probability of failure of one section is resumed for 100 sections in the table below.

$\frac{P_{defence}}{P_{b_i}}$	elementary upper limit	upper limit according to Ditlevsen	"Exact solution" Storm surges Gumbel
$\sigma_{h_d} = 0.1 \text{ m}$	100	17	2
$\sigma_{h_d} = 0.2 \text{ m}$	100	32	4

From the preceding figures and the table it appears that the elementary upper limit is not always of practical use. The upper limit according to Ditlevsen also probably allows for a disproportionally large influence of the length effect. The "exact solution" shows that the length effect, even for a relatively small spread of the sections' crest heights is *not* negligible.

The practical question concerning the length of an independent section (and with that the question of the number of sections of the defence) remains unanswered, so the value of the choice of N = 100 sections (in the above table) can't be evaluated.

EXAMPLE OF A LOWER LIMIT APPROXIMATION : DUNE EROSION GUIDELINES



In the Dune Erosion Guidelines¹⁾ a lower limit approximation is selected, both for the distribution of the admissible probability of failure (10^{-5} in a year) over the sections and for within a section over the five failure modes. (In Figure IV-5 wave overtopping/ overtopping is considered one mode.) Firstly, the probability of collapse of a section is assumed equal to the probability of breach due to dune erosion.

The contributions of the other modes are kept so small by additional regulations (crest width 3 m, slope 1:2, etc.) that they can be neglected in further calculations.

As was previously demonstrated,

Figure V-9

this is justifiable under certain circumstances. Secondly, the length effect is taken into account in the guidelines by attributing the entire probability of failure to one section (the weakest). The probability of failure of the other sections have to be smaller by at least a factor 10. The probability of collapse of this section is tested according to the norm (10^{-5} in a year for Central Holland). According to the Dune Erosion Guidelines, such a test is only correct for a dune as a defence, if the *thinnest* (minimal) dune profile is checked for dune erosion. If the profile in the considered section is insufficient the entire defence (the dune) has to be adjusted and the thinnest profile remains the thinnest.

The new Dune Erosion Guidelines are a great step towards a practical application but the research into the probabilistic design of water defences is not yet completed.

¹⁾ The name for the guidelines is in fact an abbreviation. The literature reference reads: Technical Advisory committee for the Water defenses, Guidelines for the evaluation of the safety of dunes as a water defense (in Dutch: "Technische Adviescommissie voor de Waterkeringen, Leidraad voor de beoordeling van de veiligheid van duinen als waterkering"), the Hague, State publisher, 1984.

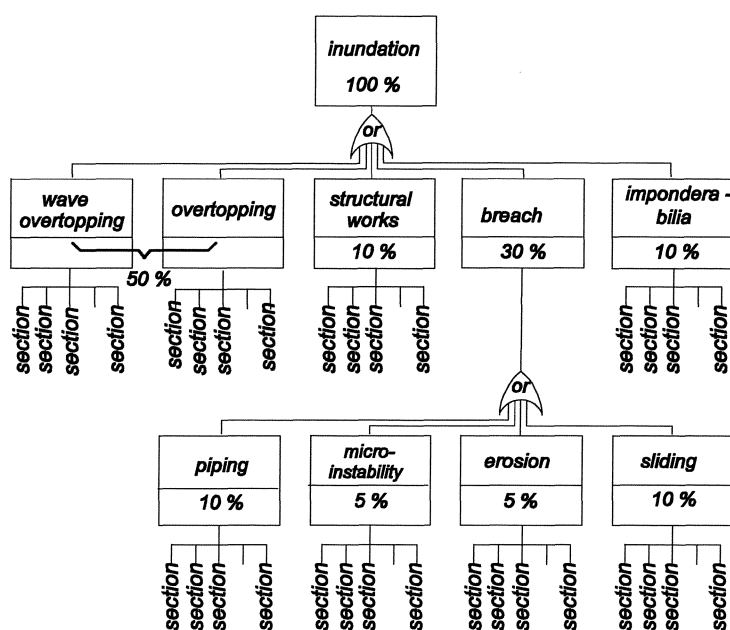


Figure V-10

For the probabilistic design of a water defence the length-effects as a result of the division into stretches is to be considered. Due to different defences (dyke, dune, construction, etc.) and different circumstances (bordering deep or shallow water, a sea, a transitory area or a river, etc.) different failure modes are involved, each to be schematised with its own independent dyke stretch length. In a fault tree, these parts of the water defence system, which can be considered separately, can each be indicated: see Figure IV-5.

The criteria tree in Figure V-10 is an extension of this. The added percentages for the contribution towards the probability of failure of the system form a so-called probability budget. This budget differs per case, dependent on the costs to be made to reduce a contribution towards the failure probability and on the extent of that contribution. The econometric aspects of raising a dyke, with several modes in a cross section, are treated further in § VI.4..

A possible failure probability budget for a dyke ring is given in the table below:

Failure mode	Start of failure (SLS) in multiples of the norm probability of inundation in a year	Total inundation (SLS) in multiples of the norm probability of inundation in a year
overtopping	} 1	0.5
wave overtopping		
sliding	1	0.1
piping	1	0.1
micro- instability	0.5	0.05
erosion outer slope	0.5	0.05
failure of structural works	1	0.1
imponderabilia	1	0.1

The term "imponderabilia" in the table above implies the "inestimable influences" such as trees, musk rats, ships collisions, etc..

There is an essential difference between a risk or a failure probability *budget* (i.e. a norm, a number of *criteria* which are to be satisfied) and a risk *analysis*. A criteria tree such as in Figure V-10 and a fault tree such as in Figure IV-5 or Figure V-3 may not be confused. In a criteria tree *requirements* to be met by the *failure probabilities* (the safety) of parts are posed. Using a fault tree, the *failure probability* of the structure is *calculated* from the failure probabilities of the parts.

Calculating the failure probability of a water defence system exactly is particularly difficult and in many cases still impossible with the current state of technology. Usually, though, upper and lower limit approximations can be given. The same is valid for criteria trees.

Often one opts for an **upper limit** approximation and one distributes the permitted probabilities of failure over the branches at every or-port. However, for a large number of elements this can lead to an unrealistically low requirement for the failure probability for every element. One can also choose for a **lower limit** approximation. In that case, virtually the entire failure probability is reserved for one (the weakest) element (part). Then, the other elements are allowed to have a much smaller failure probability.

The failure probabilities in the first column of the table at the bottom of the last page are the result of an upper limit approximation. They are found by addition of the failure probabilities of all sections in the dyke ring.

The permitted failure probability for every mode and for every section depends on the number of independent sections, on the transitory probability and on the accepted probability of inundation for the dyke ring area concerned. For the mode overtopping at least as many sections as threats (river, lake, sea) are distinguished. If a transitory area is involved, the number of sections is increased by one. These aspects are illustrated in Figure V-11.

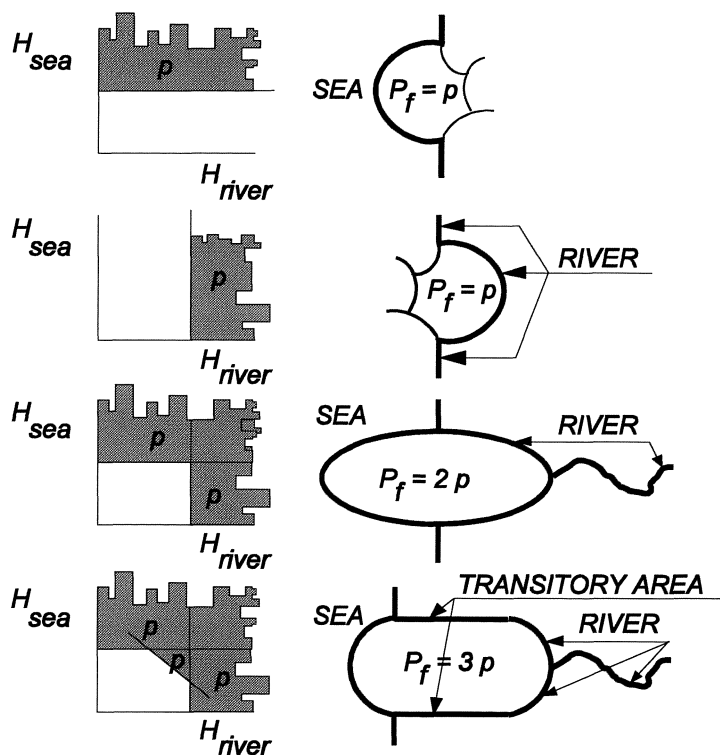


Figure V-11

For the mode overtopping, every section is threatened by the following, according to the table at the bottom of page V - 13 and Figure V-11:

sea and river:
$$P_b < \frac{10^{-5}}{2}$$

sea, transitory area and river:
$$P_b < \frac{10^{-5}}{3}$$

In the case of overtopping, a section can be defined as the entire stretch which has the same orientation, the same cross-section, and the same foreshore and where the wind speed (and the waves which are a consequence of it) and the water level are completely (linearly) correlated. In the case of river dykes this is difficult to imagine.

At sea, the number of possible orientations is limited and the wind(waves) and the water level are greatly (linearly) dependent. That is why the number of independent sections is limited to for example 6.

Around a polder in the river area the orientation of the dyke relative to the wind direction greatly varies. Hence, the number of independent sections is also greater. It will be around 16.

For the failure probability of every section according to the failure mode sliding, the same type of limitation of the contribution to the inundation probability of the dyke ring area is valid:

$$P_b < \frac{10^{-4}}{\frac{L}{l}}$$

with: l = section length for sliding
 L = length of the stretch.

Because, with respect to sliding, the part which is most sensitive to sliding is designed appropriately and because the reliability functions for the sections are correlated via the water level, a correction can be applied:

$$P_b < \frac{10^{-4}}{1 + \alpha * \frac{L}{l}}$$

with: α = correction factor.

Such reasoning, which leads to a (another) correction factor, is valid for the mode piping.

There is too little insight into the dependancies between variables which are of significance for the failure mode micro-instability.

The following condition could apply to a dyke ring which contains structural works:

$$P_b < \frac{10^{-5}}{1 + v * N}$$

with: N = number of structural works
 v = correction factor.

Given that the number of structures can increase in time, N is to be chosen sensibly. One could opt for an N per dyke ring which leaves space for future developments.

V.3. LENGTH AND TIME EFFECTS

Time and length effects (correlations in length and time) often occur in the same problem. The strength and the load(s) can be correlated in time and in place. Consider a sea dyke on the one hand and a dyke surrounding a pump accumulation basin (PAC- basin) on the other hand as examples. These dyke types appear to be extremes as far as the correlation is concerned.

The correlation of the reliability functions for the different sections was given by:

$$\rho_{Z_i, Z_j} = \frac{\rho_{h_{d_i}, h_{d_j}} \sigma_{h_d}^2 - 2 \rho_{h_{d_i}, H_j} \sigma_{h_d} \sigma_H + \rho_{H_i, H_j} \sigma_H^2}{\sigma_{h_d}^2 + \sigma_H^2} \quad (\text{page V - 6, middle}).$$

LENGTH EFFECT

In § V.2. a sea dyke was considered. The strength (height) of the sections was assumed uncorrelated: $\rho_{h_{d_i}, h_{d_j}} = 0$, and the same applied for the crest height and the water level: $\rho_{h_{d_i}, H_j} = 0$, whilst the sections were submitted to the same "load", the water level: $\rho_{H_i, H_j} = 1$.

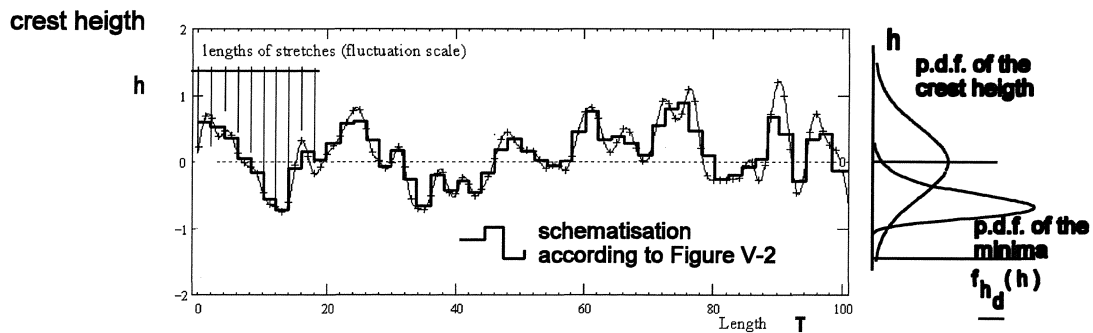


Figure V-12

The result was that the correlation coefficient $\rho_{Z_i, Z_j} = \frac{\sigma_H^2}{\sigma_{h_d}^2 + \sigma_H^2} = \frac{\sigma_H^2}{\sigma_Z^2} = \alpha_H^2$. For a sea dyke the spread of the load is very much greater than the spread of the strength: $\sigma_S \gg \sigma_R$ or $\sigma_H \gg \sigma_{h_d}$. A consequence is $\rho_{Z_i, Z_j} \approx 1$.

In the PAC basin the (high) water level is accurately managed and limited (by the spillway), so that $\sigma_S \ll \sigma_R$

or $\sigma_H \ll \sigma_{h_d}$. Inserted in $\rho_{Z_i, Z_j} = \frac{\sigma_H^2}{\sigma_{h_d}^2 + \sigma_H^2}$ this gives: $\rho_{Z_i, Z_j} \approx \frac{\sigma_H^2}{\sigma_{h_d}^2} \approx 0$ so that the sections are (practically)

independent in this case.

VI. OPTIMAL SAFETY

VI.1. NORMS

In the previous chapter, the starting point for the determination of permissible probabilities of failure per mode, per section was an acceptable probability of inundation of a dyke ring area ¹⁾ of, for example, 10^{-4} in a year. The choice of such a norm does not arise from existing laws. The Delta committee limited itself to indicating the exceedance frequency of the high water level (10^{-4} per year).

The probability of inundation of a dyke ring area in a year may not be confused with the exceedance frequency per year of the design water level at a certain point along the water defence. In the third part of the Delta report, the committee presents an economical consideration of the optimal inundation probability for Central Holland ($8 \cdot 10^{-6}$ in a year, see Van Dantzig and Kriens [1960]). For the Guidelines for the evaluation of the safety of dunes as water defences a probability of a breach of 10^{-5} in a year was selected as the norm.

The considerations of the River dykes Committee implicitly tend towards a probability of inundation equal to the probability of exceedance of the design water level, though this starting point has not yet been included in the Guidelines for the design of river dykes.

In a completely probabilistic approach to risky activities, the acceptable probability of the "fatal" event follows from an econometric consideration or from considerations regarding personally or socially acceptable risks. See Vrouwenvelder, A.C.W.M. and J.K. Vrijling, [1984].

The application of the probabilistic approach concerning the safety level leads to distinguishing between densely and sparsely populated polders, between polders with many industrial investments and polders of predominantly agricultural use. Such a differentiation must be reviewed, bearing in mind the principle that every Dutch national has a right to an equal minimum safety level. The criterion given above, concerning the personal risk, essentially does see to such an equal minimal safety level.

In the National Environmental policy plan, [1988], only the personal and the social risk are covered. The stated norms concerning the acceptable probabilities of accidents can be transformed into those given in the Lecture notes CTOW4130, see Vrouwenvelder, A.C.W.M., and J.K. Vrijling, [1995].

Literature:

Van Dantzig, D., and J. Kriens, 1960, The economical decision problem concerning the protection of the Netherlands against storm surges, Report by the Delta committee, Part 3, contribution II.2 (in Dutch, Het economisch beslissingsprobleem inzake de beveiliging van Nederland tegen stormvloed, Rapport van de Deltacommissie, Deel 3, bijdrage II.2), State printer, The Hague.

National Environmental policy plan, [1988]: Dealing with risks (in Dutch, Nationaal Milieubeleidsplan, [1988]: Omgaan met Risico's), Ministry of Housing, Spatial planning and the Environment, Central Management Information Service and External Relations, 1988.

Vrouwenvelder, A.C.W.M. and J.K. Vrijling, [1984]. Lecture notes b3, Probabilistic Design, Faculty of Civil Engineering, Technical University Delft, altered print, November 1984 (in Dutch).

Vrouwenvelder, A.C.W.M., and J.K. Vrijling, [1995]. Standards acceptable risk level, TNO report 95-CON-R0851 (in Dutch, Normstelling acceptabel risiconiveau, TNO rapport 95-CON-R0851), TNO-Bouw under the authority of Rijkswaterstaat-DWW, June 1995.

¹⁾ A dyke ring area is an area surrounded by primary water defenses.

In the econometric approach to the optimal safety level the loss of lives has to be expressed in monetary units. Though objective values such as the present value of the net national product per capita can be given for this, the question remains whether that constitutes a good interpretation of the involved social considerations. For this reason two approaches were developed, which give an acceptable probability of drowning due to inundation, based on accident statistics.

According to the first approach, an individual would determine the probability of drowning against the background of the risk of death for accidents in general. The formulation this so-called individual criterion is:

$$P_{\text{acceptable}} = \frac{\beta \cdot 10^{-4}}{P_{\text{df}}} \text{ in a year}$$

in which: $0,01 < \beta < 100$ = policy factor
 10^{-4} = probability of a fatal accident
 P_{df} = probability of drowning with occurring inundation.

The policy factor β allows for differentiation between voluntarily and involuntarily accepted risk and/or between existing and new situations.

Society reacts more strongly to an accident when people mourn for several deaths at the same time than for separate fatal accidents which take place spread over time and space. The social considerations for the evaluation of group risks must be modelled in a separate philosophy.

The probability of failure is acceptable if it is in the area defined as follows:

$$1 - F_{N_a}(X) \leq \frac{C}{X^2} \text{ with } C = \left[\frac{100 \cdot \beta}{c \cdot k \cdot \sqrt{N_a}} \right]^2$$

where: β = policy factor as given above
 $1 - F_{N_a}(X)$ = exceedance probability distribution of the number of deaths
 c = influence factor, determined by the distribution type of the number of deaths for given failure. For a deterministic number of deaths $c = 1$ and for an exponentially distributed number of deaths $c = 2$.
 k = probability condition or measure for risk aversion.
 N_a = number of places where the activity is carried out.

The acceptable probability of failure is proportional to the reverse of the square of the number of deaths. The formula can be derived from the Chebychev inequality, assuming that the expected value of the number of deaths is negligible relative to its standard deviation.

THE ACCEPTABLE PROBABILITY OF INUNDATION

To determine the acceptable probability of inundation of a polder, the three approaches have to be set side by side. The strictest criterion determines the acceptable probability of inundation. To illustrate this, the figure below indicates the results of the three approaches to the acceptable probability of inundation for the English town Whitstable (see § IV.1, page IV - 2), which has 5000 inhabitants. In the figure, the council's choice is also indicated. After all, the final determination of the acceptable inundation probability is up to the political authorities.

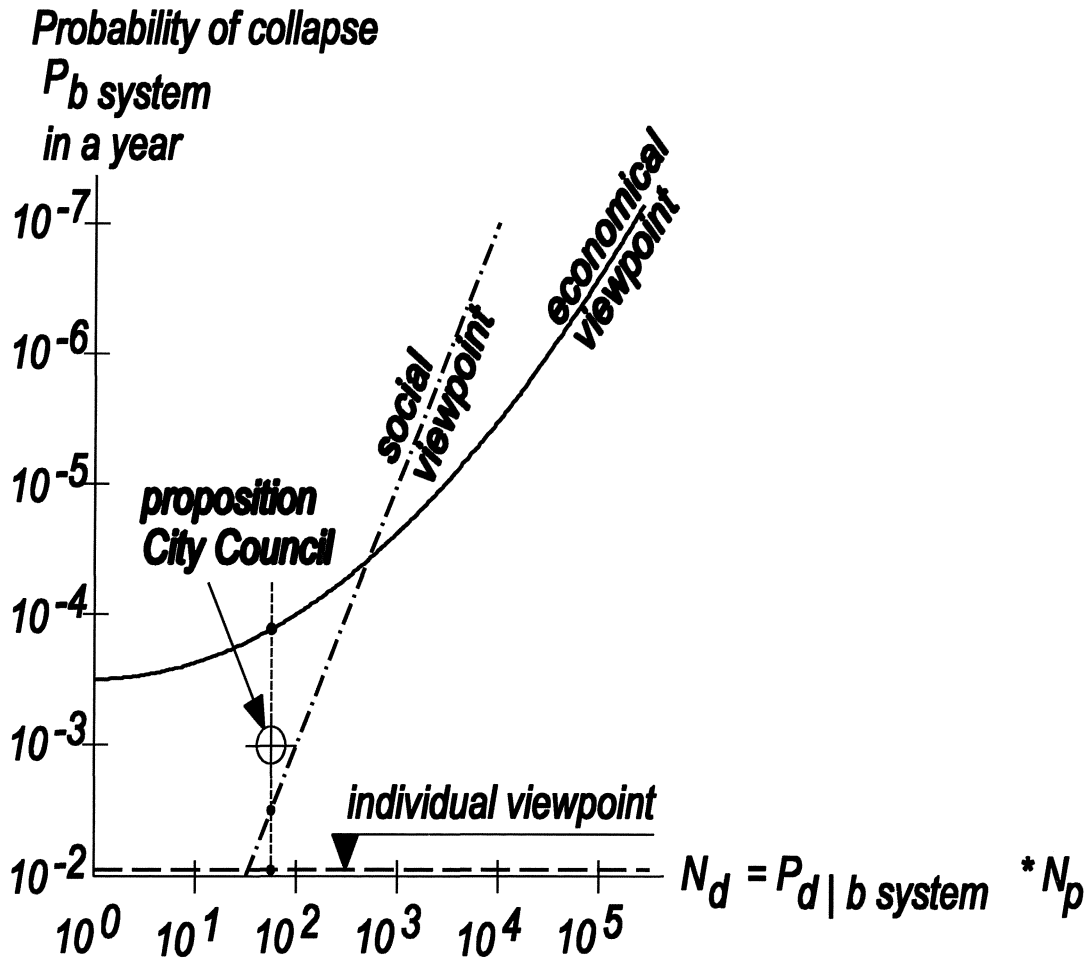


Figure VI-1

VI.2. ECONOMETRIC APPROACH

The econometric calculation of the optimal dyke height is as follows:

Risk is considered equal to the probability of inundation multiplied by its consequence (the damage):

$$Risk = P_b \cdot S(h)$$

with: P_b = probability of inundation

$S(h)$ = damage as a function of inundation with high water level h .

where h = inundation depth, which is also a function of the high water level.

The extent of the damage is dependent on the inundation depth: the higher the water level above the ground surface (up to a certain maximum) in the dyke ring area, the greater the damages. See the figure opposite. The influence of the inundation depth on the extent of the damage will not be treated in this course. It is assumed that, if inundation occurs, a fixed (deterministic) level of damage arises.

The inundation of a dyke ring area due to overtopping of a river dyke, which is not subjected to wave attack, is considered as an example. The probability distribution of the high water level of the river in a year is given by:

$$F_{HW}(H_r) = 1 - e^{-\frac{H_r - A}{B}}$$

The probability of the high water level, HW, of the river exceeding the crest height of the dyke, h_d , is:

$$P_b = e^{-\frac{h_d - A}{B}}$$

For comparison purposes the risk has to be discounted. The reduced interest rate (interest reduced by inflation and increased with the increasing economical growth in the dyke ring area) is r' .

The discounted value of the risk is:

$$CW_{risk} = \frac{P_b \cdot S}{r'} = \frac{e^{-\frac{h_d - A}{B}} \cdot S}{r'}$$

The construction costs amount to:

$$Bouwkosten = I_0 + I \cdot h_d$$

Here: I_0 = Initiation costs: costs for design, (laboratory) research, ground purchase, etc..

I = Variable costs: costs of excavation, profile works, revetment, etc..

h_d = Construction height of the defence.

It is assumed (by good approximation), that the variable costs are in proportion to the construction height of the dyke.

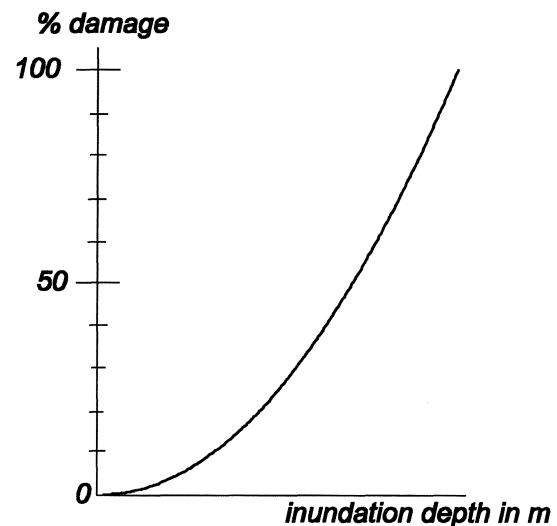


Figure VI-2.

The total costs are made up of construction costs and the discounted value of the risk:

$$C_{tot} = I_0 + I \cdot h_d + \frac{S \cdot e^{-\frac{h_d - A}{B}}}{r'}$$

The minimum of the total costs is found by presuming the derivative with respect to the height equal to zero:

$$\frac{\partial C_{tot}}{\partial H_d} = I - \frac{1}{B} \cdot e^{-\frac{h_d - A}{B}} \cdot \frac{S}{r'} = I - \frac{P_b \cdot S}{B \cdot r'} = 0$$

From this:

$$P_b \text{ optimal} = \frac{I \cdot B \cdot r'}{S} \text{ or } h_d \text{ optimal} = A - B \cdot \ln(P_b \text{ optimal})$$

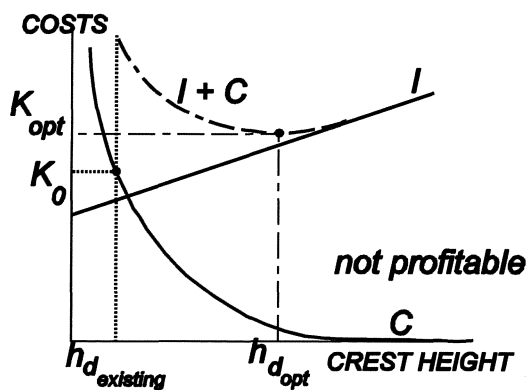
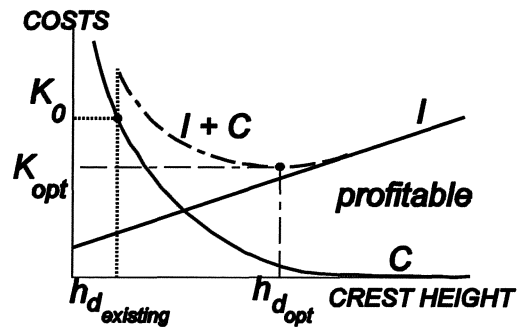


Figure VI-3

Subsequently, it must be established whether the sum of the costs at the optimal height is lower than the expected level of damage K_0 in the old situation (that is the existing state before raising the dyke). Only if this last condition:

$$\text{gain safety} > \text{costs dyke improvement}$$

is met, the dyke improvement is profitable. See Figure VI-3.

VI.3. MORE THAN ONE THREAT

VI.3.1. GENERAL

The sketched optimisation calculation can be extended to two (or more) threats. If a dyke ring area is threatened by two rivers, the two extremes sketched in Figure VI-4 can arise:

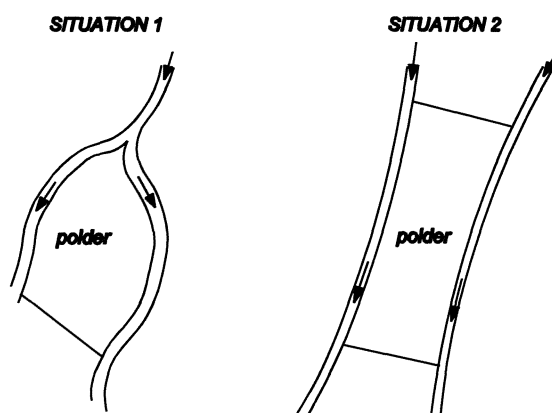


Figure VI-4

As determined (elementary lower and upper limit):

$$\max_{i=1}^2 P_{b_i} \leq P_{b_{\text{acceptable}}} \leq \sum_{i=1}^2 P_{b_i}$$

The left part of the equation concerns situation 1. There the dyke ring area is located downstream from a fork in a river. Both high water level threats are totally dependent. If high water occurs in one fork of the river, this is also the case in the other fork of the river. Depending on the width, the roughness, etc., of both forks one of both water levels (relative to a common reference level) will be highest. Assuming the polder ground surface is horizontal, one of both dykes will be highest. The probabilities of inundation for both defences are to be equal and smaller than the acceptable probability of collapse.

In situation 2 the river discharges are completely independent. This situation is represented by the right hand side of the equation given above. For these situations optimal heights of the defences can be given too.

SITUATION 1

For situation 1 the total costs are: $C_{\text{tot}} = I_0 + I_1 \cdot h_{d_1} + I_2 \cdot h_{d_2} + \frac{S}{r'} \cdot \left(\max_{i=1}^2 P_{b_i} \right)$.

The high water level exceedance curve in the one river fork is given by: $1 - F_{\underline{HW}_1}(h_{d_1}) = e^{-\frac{h_{d_1} - A}{B}}$ and in

the other river fork: $1 - F_{\underline{HW}_2}(h_{d_2}) = e^{-\frac{h_{d_2} - C}{D}}$

It is economically rational to choose equal exceedance frequency probabilities. This means: $P_{b_1} = P_{b_2} \leq P_{b_{\text{acceptable}}}$.

From this follows, for the high water levels: $\frac{h_{d_1} - A}{B} = \frac{h_{d_2} - C}{D}$.

The height of the one defence can then be expressed in the height of the other: $h_{d_1} = \frac{B}{D} \cdot (h_{d_2} - C) + A$.

These results substituted in the expression for the total costs gives:

$$C_{tot} = I_0 + I_1 \cdot \left\{ \frac{B}{D} \cdot (h_{d_2} - C) + A \right\} + I_2 \cdot h_{d_2} + \frac{S}{r'} \cdot e^{-\frac{h_{d_2} - C}{D}}$$

Making the derivative to the height of the defence equal to zero gives the optimal crest height or the optimal

probability of collapse: $\frac{dC_{tot}}{dh_{d_2}} = I_1 \cdot \frac{B}{D} + I_2 - \frac{S}{r' \cdot D} \cdot e^{-\frac{h_{d_2} - C}{D}} = 0.$

With $e^{-\frac{h_{d_2} - C}{D}} = P_{b_1} = P_{b_2} = P_{b_{optimal}}$ This leads to:

$$P_{b_{optimal}} = \frac{r'}{S} \cdot (I_1 \cdot B + I_2 \cdot D) \quad \text{or} \quad h_{d_2 \text{ optimal}} = C - D \cdot \ln(P_{b \text{ optimal}})$$

SITUATION 2

For situation 2 the total costs:

$$C_{tot} = I_0 + I_1 \cdot h_{d_1} + I_2 \cdot h_{d_2} + \frac{S}{r'} \cdot \left(\sum_{i=1}^2 P_{b_i} \right)$$

The high water level exceedance frequency curve in the one river fork is given by:

$$1 - F_{HW_1}(h_{d_1}) = e^{-\frac{h_{d_1} - A}{B}}$$

and in the other river fork:

$$1 - F_{HW_2}(h_{d_2}) = e^{-\frac{h_{d_2} - C}{D}}$$

Inserting this information in the expression for the total costs gives:

$$C_{tot} = I_0 + I_1 \cdot h_{d_1} + I_2 \cdot h_{d_2} + \frac{S}{r'} \cdot \left(e^{-\frac{h_{d_1} - A}{B}} + e^{-\frac{h_{d_2} - C}{D}} \right)$$

Posing the derivatives with respect to the defence heights (now plural, because the probabilities of failure for both defences are not equal) equal to zero leads to the optimal crest height or the optimal probability of collapse:

$$\frac{\partial C_{tot}}{\partial h_{d_1}} = I_1 - \frac{S}{B \cdot r'} \cdot e^{-\frac{h_{d_1} - A}{B}} = 0 \quad \Rightarrow \quad P_{b_1} = \frac{I_1 \cdot B \cdot r'}{S}$$

$$\frac{\partial C_{tot}}{\partial h_{d_2}} = I_2 - \frac{S}{D \cdot r'} \cdot e^{-\frac{h_{d_2} - C}{D}} = 0 \quad \Rightarrow \quad P_{b_2} = \frac{I_2 \cdot D \cdot r'}{S}$$

From these equations different failure probabilities with a fixed relation between each other are derived for both defences:

$$\frac{P_{b_1}}{P_{b_2}} = \frac{I_1 \cdot B}{I_2 \cdot D}$$

The optimal probability of failure for the dyke ring area in situation 2 is:

$$P_{b \text{ optimal}} = \frac{r'}{S} \cdot (I_1 \cdot B + I_2 \cdot D)$$

The total area safety is the same as in situation 1. In situation 1 the failure probabilities for both dykes are equal. In situation 2 the probability of inundation of the dyke ring area equals the sum of the probabilities of failure for both dykes.

VI.3.2. PREDOMINANT OBJECTION

There can be a predominant objection against raising one of the two defences, for example from the point of view of nature conservation or conservation of scenic beauty. In terms of inundation probabilities this means that the defence may not be raised (assume defence 2), the inundation probability is set at the existing level. Consider the probability of inundation P .

For situation 1 this makes: $C_{tot} = I_0 + I_1 \cdot h_{d_1} + \frac{S}{r'} \cdot \left\{ \max(P_{b_1}, P) \right\}$

The defence is raised until: $P_{b_1} = P$ provided the zero option (existing state, as it is) is not cheaper. Further raising of the defence won't reduce the total inundation probability of the dyke ring area.

For situation 2: $C_{tot} = I_0 + I_1 \cdot h_{d_1} + \frac{S}{r'} \cdot \left(e^{-\frac{h_{d_1} - A}{B}} + P \right)$

On the condition that the zero option is not more economical, the defence is raised as if there was only a question of one defence, i.e. to $h_{d_1} = A - B \cdot \ln(P)$.

VI.3.3. LIMITED BUDGET

The situation could arise where the employer only has a limited budget at his disposal to raise the defences.

Provided raising the defences is worthwhile (the zero option is more expensive), in situation 1:

$$P_{b_1} = P_{b_2} = \frac{r'}{S} \cdot (I_1 \cdot B + I_2 \cdot D) \cdot (1 + \lambda)$$

where λ has a value greater than 0 (zero), which indicates that the amount of money to be spent will be exhausted.

In situation 2 the optimum (provided the zero option is more expensive) can be determined with:

$$P_{f_1} = (1 + \lambda) \cdot I_1 \cdot B \cdot \frac{r'}{S}$$

$$P_{f_2} = (1 + \lambda) \cdot I_1 \cdot D \cdot \frac{r'}{S}$$

$$P_{b \text{ optimal}} = (1 + \lambda) \cdot \frac{r'}{S} \cdot (I_1 \cdot B + I_2 \cdot D)$$

The limitation is included in the calculation by enlarging all economical probabilities of failure by a factor $(1 + \lambda)$, which is just big enough to ensure that the budget for dyke improvement is exhausted.

VI.4. SEVERAL MODES IN ONE CROSS SECTION

If more than one mode can occur in one cross section, the calculation is analogous to the preceding.

Assume that for dyke section two modes are of importance, namely "overtopping" (dependent on the crest height, h_d) and "sliding over a deep sliding plane" (here presumed dependent on the inner slope angle, α) and that the modes are independent (quod non!). The crest height, h_d , and the slope angle, α , are called the optional variables.

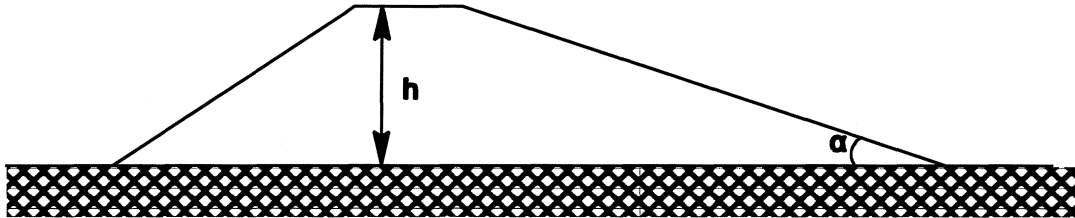


Figure VI-5

The construction costs are analogous to the preceding: $I_{tot} = I_0 + I_{h_d} \cdot h_d + I_{\alpha} \cdot \alpha$.

The present value of the risk is: $CW = \frac{(P_{\text{overtopping}}(h) + P_{\text{sliding}}(\alpha)) \cdot S}{r^j}$

The total costs are: $C_{tot} = I_0 + I_{h_d} \cdot h_d + I_{\alpha} \cdot \alpha + \frac{S}{r^j} \cdot (P_{\text{overtopping}}(h) + P_{\text{sliding}}(\alpha))$

Analogous to the preceding calculation we find

α_{opt} from: $\frac{\partial C_{tot}}{\partial \alpha} = 0$ and h_{opt} from: $\frac{\partial C_{tot}}{\partial h} = 0$.

On these grounds we can determine which crest height and which slope angle are optimal. The results can be incorporated in a criteria tree (Figure V-9).

N.B. The failure probabilities for the two modes are generally *not* equal.

VI.5. CONSEQUENCE VARYING AS A FUNCTION OF THE HIGH WATER LEVEL AND OF THE LOCATION OF THE BREACH

The previous sections were based on the assumptions that the ground surface of the dyke ring area is "horizontal" and that the height of the water defence system is on average equally high above the reference level. For a dyke ring area in or around the sea this, by approximation, will be the case. (See figure below, left side.) However, for river polders and polders in the "transitory area" this is not so. (See figure below, right side.) In case of a breach upstream the inundation depth will be greater than for a breach downstream. This implies that, for dyke ring areas that have "upstream and downstream sides", the upstream defences should have a smaller probability of breaching than the downstream defences or that building and settlement should be limited to the higher part. The latter is probably not a realistic option for the Netherlands, but in countries with less lack of space it is an alternative worth considering.

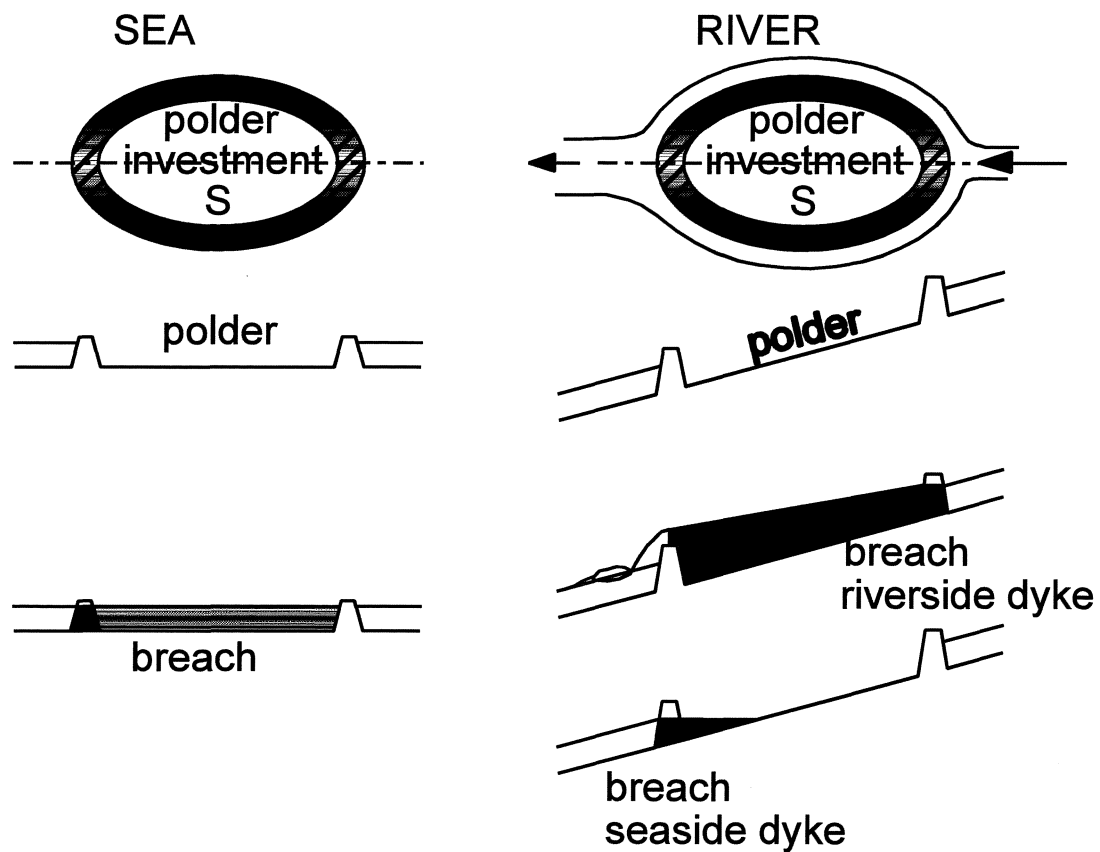


Figure VI-6

VII. BUDGETING AND TIME-PLANNING

VII.1. INTRODUCTION AND DEFINITIONS

The control of the costs and the duration of a civil engineering project is not simple (Vrijling [1990], Vrijling [1995]¹⁾). Apart from uncertainty concerning quanta and production tempi (uncertainty about technical aspects) unit prices or prices per quantum and wages (uncertainty involving economics) and "influences of the outside world" (essential changes of the design), this is caused by the long period over which a civil engineering project is stretched. This period starts when the social demand for change is felt and the first plan for the project is outlined. The end of the period can be set at the delivery of the final product and the settlement of the bill.

The estimate of the budget is always an approximation of the real costs. If all knowledge and facts have to be expressed in one single number, as is often required, discrepancies between the estimate and the finally realised costs cannot be avoided. Normally, in comparisons between the original estimate of the building costs and the total expenses at the end of the project, no correction is made for the overall increase in prices. In Table VII.1. the exceedence of the budgets for the hydraulic engineering parts of the reclamation of some IJsselmeerpolders (land reclamation works in The Netherlands) are given (Belgraver and Kleibrink [1984]):

Table VII.1.

Polder:	Exceedence
Wieringermeerpolder	12%
Northeast polder	16%
Easterly Flevoland	- 3%

in which:

$$\text{Exceedence} = \frac{\text{calculated costs after completion} - \text{estimate of budget in study-of-plan phase}}{\text{calculated costs after completion}} \cdot 100\%$$

The difference in accuracy between an estimate of the budget in an early stage of the project (the study-of-plan phase) and the final estimate (builder's specifications at the start of the engineering) is illustrated in the next table (Goemans en Smits [1984]):

Table VII.2.

Project	Difference in % of the final costs	
	Estimate in study-of-plan phase	Estimate in Builder's specifications phase
Haringvliet locks	77%	22%
Grevelingen dam	- 19%	22%
Volkerak dam	56%	23%
Brouwers dam	- 39%	- 18%

Often final project costs exceed their estimate. History of the estimate of the budget at the Ministry of Public Works in The Netherlands (Rijkswaterstaat) (Heezik [1994]) clearly shows the pattern of increase of costs and delay in the work (which, due to inflation and loss of interest, also increases the costs):

¹⁾ References to literature on estimating budgets and time-planning are added at the end of this chapter.

Table VII.3.

Project	Start	Planned		Reality	
		Mf	years	Mf	years
Noordhollands Canal	1818	4	5	12.5	7
Haarlemmer lake	1837	8.4	5 (?)	13.8	21
Nieuwe Waterweg	1858	5	5	36.8	38
Maas & Waal	1864	6.5	10	24.7	44

In road-construction projects there were (and there are) big fluctuations in the differences between the estimated budgets and the real costs as well. For road-construction projects in The Netherlands from 1980 up to and including 1985 differences between estimates in the pre-design phase and the real costs as a percentage of the real costs are given below:

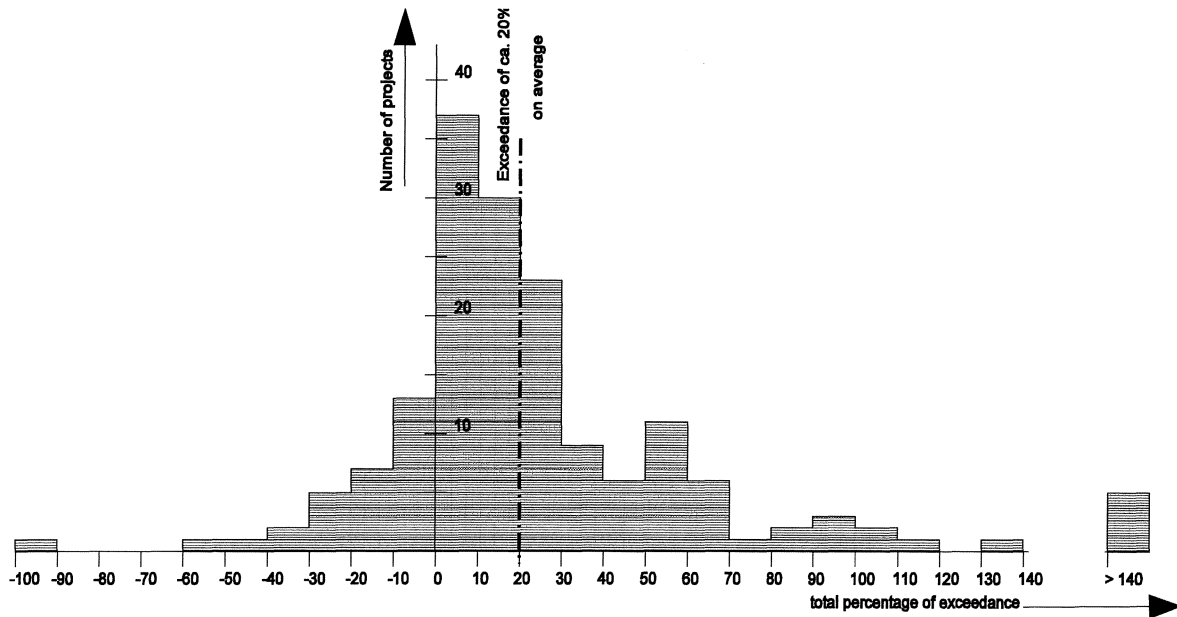


Figure VII-1

Publications on exceedance of the estimate of the budget in other countries show the same tendency. (The Economist [1989] and Merewitz [1973]).

VII.2. THE CLASSICAL APPROACH TO BUDGET ESTIMATES AND TIME-PLANNING

From early days, the calculation of estimates of the budget and time-planning schemes are based on most likely values. Uncertainty of the decision maker is expressed as an increase of the deterministic final amount by a certain percentage of that amount.

One's uncertainty regarding the budget estimate or the time-planning scheme is not constant during the project. The later in the project an estimate of the budget or a time-planning scheme is made, the more about the project is known and the decision maker's uncertainty concerning the estimated amounts of money and duration of the activities will be less than in the early stages of the project. A classification of project phases in order of time is given in Table VII.4. The project parts in the phase at hand are estimated or planned in detail, for other parts in other phases this is done roughly.

Table VII.4.

Class	Project phase
D	study-of-plan
C	pre-design
B	pre- builder's specifications
A	builder's specifications

Because of the decision maker's greater uncertainty in the early phases of the project, it is of no use to make detailed estimates and time-planning schemes for phases to come. Making an estimate of the budget in detail for builder's specifications when the project is still in the study-of-plan phase will turn out to be a waste of time, although in the early stages more detailed estimates and time-planning schemes (or parts of those) are made. Below some examples of specifications of budget estimates in several phases of a project are given.

Estimate of the budget, Class D Study-of-plan phase Estimate per unit

<i>1 viaduct</i>	×	<i>price of 1 viaduct</i>	=	<i>item viaduct</i>	
<i>5 km of road</i>	×	<i>price per km of road</i>	=	<i>item road</i>	
<i>1 tunnel</i>	×	<i>price per tunnel</i>	=	<i>item tunnel</i>	
					----- +
				<i>Total of Direct costs</i>	
				<i>Indirect costs</i>	
					----- +
				<i>Primary costs</i>	
				<i>Additional costs</i>	
				<i>Miscellaneous ¹⁾</i>	
					----- +
				<i>Basic estimate</i>	
				<i>Unforeseen ²⁾</i>	
					----- +
				<i>Estimate (ex. VAT)</i>	
				<i>VAT</i>	
					----- +
				<i>Study-of-plan phase estimate</i>	

In the successive phases the items of the class D- estimate are worked out in more detail. An example is given in the following class B- estimate.

¹⁾ In "Miscellaneous" those costs are categorized which are known but which are not specified. For a study-of-plan phase estimate these could be: land (has to be bought) preparation, deflection of conduit-pipes and water courses, temporary diversion of traffic, etc..

²⁾ "Unforeseen" is taken as an additional percentage on the Basic estimate here. If there is little insight in the character of the item Unforeseen then this way of calculation is applicable. In section VII.6.1. the amount of the percentage to be applied is discussed.

Estimate of the budget, class B. Pre- builders specifications phase. Estimate on the basis of quanta and unit prices

<i>800 m³ soil</i>	×	<i>price per m²</i>	=	<i>item "soil"</i>
<i>800 m³ concrete</i>	×	<i>price per m³</i>	=	<i>item "concrete"</i>
<i>1 ton reinforcement</i>	×	<i>price per ton</i>	=	<i>item "reinforcement"</i>
<i>800 m² formwork</i>	×	<i>price per m²</i>	=	<i>item "formwork"</i>
				----- +
				<i>Subtotal viaduct</i>

The other items are detailed analogously.

In a class A- estimate (estimate for builders specifications) the prices per m³, m² or ton are determined in more detail, based on working methods and quanta. In an estimate in this phase time and equipment are taken into consideration. Contractors prefer this method of estimating.

A sub- item of the item SOIL of the partial project ROAD from the class D- estimate (5 km of road) is chosen as an example of specification of an item in a class A- estimate:

For the delivery and processing of 80,000 m³ of soil for the partial project "road" the costs of the following means of production are estimated:

<i>Delivery at the quay by ship</i>	<i>80000 m³</i>	×	<i>price per m³</i>	=	<i>partial item 1</i>
<i>Lease of an unloading plant</i>	<i>80 days</i>	×	<i>day tariff</i>	=	<i>partial item 2</i>
<i>Transport to location (by cars)</i>	<i>800 days</i>	×	<i>day tariff</i>	=	<i>partial item 3</i>
<i>Equipment for processing and compaction</i>	<i>85 days</i>	×	<i>day tariff</i>	=	<i>partial item 4</i>
					----- +
					<i>Subtotal soil</i>

The price per m³ of processed soil is calculated by division by the volume in m³ (here: 80,000).

In principle, the estimate of Direct costs (an example of which was given for a class D- estimate at the bottom of the previous page) follows from an addition over all N partial items of the multiplication of quanta, h_i, and the prices per unit, p_i. See the calculation scheme of the budget estimate on the following page. Indirect costs can be calculated by an additional percentage, %₁, which is a fixed percentage of the Direct costs.

Additional costs and Miscellaneous can both be expressed as a percentage %₂ of the Primary costs. As stated above, additional costs are established as a percentage of the preceding part of the estimate. The Total estimate can thus be expressed as a function of the total of the Direct costs. A percentage of (the part of) the afore calculated estimate is called an additional percentage ¹⁾.

¹⁾ An additional percentage (for example the percentage Unforeseen) can be seen as a random variable or as a deterministic constant. For example the percentage VAT was fixed at 17.5% for a long time. It can be regarded as a fixed constant, unless it is expected to be changed in the future. Then, introducing the percentage VAT as a random variable is an option.

In any phase of the project such percentages can differ. Generally, the Total estimate, in which the additional percentages are included, is calculated from the total Direct costs:

$$Estimate = \left\{ \prod_{j=1}^M (1 + \%_j) \right\} \cdot \left\{ \sum_{i=1}^N h_i \times p_i \right\}$$

in which:

M = the number of additional percentages

$\%_j$ = the j^{th} addition over the foregoing subtotal

N = the number of cost items in the Direct costs

h_i = the quantum in the i^{th} item in the Direct costs

p_i = de unit price in the i^{th} item in the Direct costs.

A calculation scheme of the estimate looks like this:

<i>Calculation:</i>	$h_1 \times p_1$	
	$h_2 \times p_2$	
	
	$h_N \times p_N$	+

<i>Total of Direct costs:</i>	$\sum_{i=1}^N h_i \times p_i$	
<i>Addition for Indirect costs:</i>	$\%_1 \times \sum_{i=1}^N h_i \times p_i$	+

<i>Primary costs</i>	$(1 + \%_1) \times \sum_{i=1}^N h_i \times p_i$	
<i>Addition for</i>	+

<i>Total Estimate</i>	$\prod_{j=1}^M (1 + \%_j) \times \sum_{i=1}^N h_i \times p_i$	

TIME-PLANNING

At first sight, it seems that a time-planning of a project is more simple than a budget estimate. In an estimate of the budget the unit prices have to be multiplied by their quantum and then added. In a time-planning only the duration or the lengths of time of all activities have to be added and no multiplication is needed:

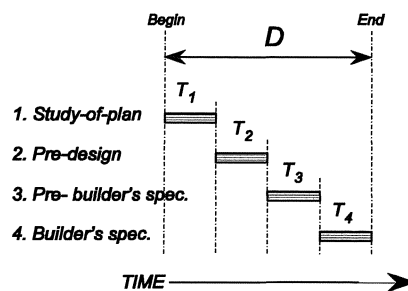


Figure VII-2

The duration of the project, D , equals:

$$D = \sum_{i=1}^N T_i$$

in which: i = rotation number of the activity

T_i = duration of the activity i

N = number of activities (in Figure VII-2: $N = 4$).

If the various activities succeed each other in time the time-planning is simple. Example: In a small building pit, pile driving cannot be started before digging of the pit is completed. The digging hinders pile driving too much.

Usually not all activities succeed each other in time. Various activities are (partially or totally) executed simultaneously. A consecutive activity can often only be started when more than one preceding activity have been completed.

In the figure below it is shown that the pre-builder's specifications phase can only be started when the pre-design phase has been completed and the licences have been granted. Both the activities have to be completed before the pre-builder's specifications phase can be started. If two activities are executed in parallel (in Figure VII-3: the pre-design phase and the granting of licences) the time-planning can be sketched as follows:

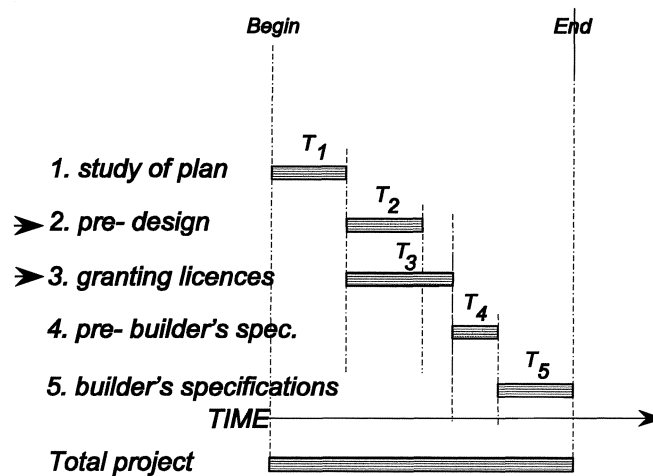


Figure VII-3

In this example there are two time-paths:

$$D_a = T_1 + T_2 + T_4 + T_5$$

$$D_b = T_1 + T_3 + T_4 + T_5$$

The total duration of the project, D_{tot} , is the maximum amount of time according to the duration of the various time-paths:

$$D_{tot} = \max(D_a, D_b)$$

In the example in Figure VII-3, the duration of the activities 1, 3, 4 and 5 determine the duration of the total project, D_{tot} . It is said that these activities form the *critical time-path* (critical path for short).

VII.3. UNCERTAINTY CONCERNING BUDGET ESTIMATES AND TIME-PLANNING

In order to express one's uncertainty about the estimate or the time-planning, probabilistic techniques are employed. If the random character of the cost items or the duration of the various activities are taken into account, the budget estimate or time-planning of the project is said to be statistically controlled.

The estimated amount of money or the planned duration of a project can be interpreted in various ways, depending on what the person who estimates or plans has in mind. Does he or she focus on an estimate of the mean costs or duration (the expected values) or on the amount that is most likely (the mode of the costs or the duration)? In the first case it is commonly assumed that the costs or the duration are normally distributed. The mean and the mode then coincide. In the second case other (skew) probability density functions are possible. Triangular probability density functions are often used for this purpose.

In addition to the mode or the mean of the estimate of the budget or the time-planning, the deviation from it (or the spread around it) is important. The size of the margin depends on the phase the project is in and on the required reliability with which the budget or the planned duration (quantification of the estimate or time-planning plus margin) will not be exceeded.

Section VII.8.3 comes back to the second point (reliability of the estimated amount of money or of the planned duration).

Consider the first point (size of the margin depends on the phase the project is in). In an early stage of the project one is much more uncertain about the budget estimate or the planned duration than in a later stage. Estimates and time-plans are often classified according to the phase of the project they were made in.

Characteristic numbers for the magnitude and for the spreading around costs items depend on the project phase. For time-planning such characteristic numbers are not (yet) available.

VII.3.1. CLASSIFICATION OF UNCERTAINTY

Uncertainty can be classified in three categories:

- ◆ uncertainty related to Normal events;
- ◆ uncertainty related to Special events;
- ◆ project uncertainty.

UNCERTAINTY RELATED TO NORMAL EVENTS

Although the costs items in a Basic budget estimate of a project become increasingly clear in the course of time, and the estimate becomes more accurate, many causes of uncertainty will remain as long as the project is not finished. With the necessary changes made, this can be applied to time-planning. The degree of uncertainty can be classified as follows:

1. There is no cause of uncertainty. The item concerned is deterministic. This concerns costs items or activities that are known exactly in size or duration. If, for example, the contract settling the purchase of land has been signed, this amount of money is known exactly. An "activity" with deterministic duration is the tide. The duration (along the North Sea coasts) is "exactly" 12 hours 25 minutes.

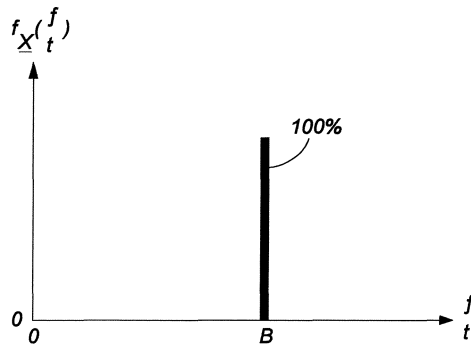


Figure VII-4

2. Often the costs are not so uniquely determined and one is uncertain about the duration of an activity. When the negotiations are still in progress, there is a notion about how much money the land (meant in point 1) will cost, but one cannot be certain. An example of uncertainty about the duration of an activity is a barge with heavy draught that has to be towed over a sill. Suppose this can only be done at high tide. (The keel clearance has to be sufficient). Usually the final costs or the spreading around the point in time of arrival at the sill will be within a band width. The probability density can then be as indicated in Figure VII-5.

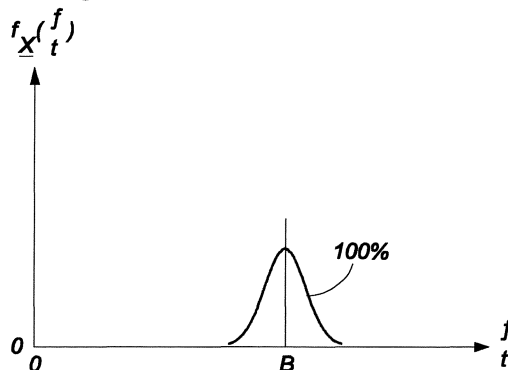


Figure VII-5

UNCERTAINTY RELATED TO SPECIAL EVENTS

Often another type of uncertainty plays a role with the evaluation of costs of a project or its duration, namely uncertainty caused by the Unforeseen or by Special events (mainly calamities). Two criteria characterize a Special event: the first is that it is not meant to occur and the second is that occurrence is not likely. The probability of occurrence, p , is small (less than 0.5), but if the event occurs, the consequence (damage or exceedence of the duration, B) is large. The probability of no occurrence (and accordingly: no damage or exceedence of the duration) is $1 - p$. In a "classical" estimate of the budget or time-planning such events are seldom taken into account. Contractors insure against such events, associated with small probabilities but with large consequences. In a statistically controlled estimate or time-planning the probabilities and the consequences can be indicated as follows:

3. Figure VII-6 shows the mass density of a Special event as a function of the damage or exceedence of the duration.

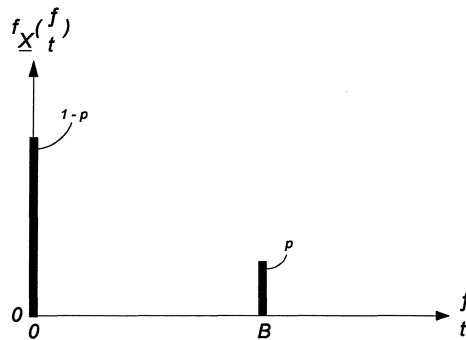


Figure VII-6

4. The probability density function of a "Special event", of which the consequences (the damage or the duration) are subject to uncertainty, could be as is illustrated in Figure VII-7.

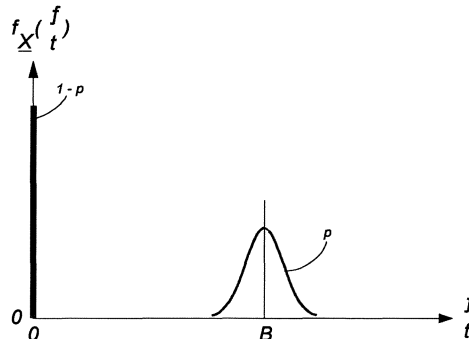


Figure VII-7

- In the study-of-plan phase several variants have to be considered and estimated (and sometimes planned). Beforehand, one is not certain which variant will be chosen (for example a tunnel, a ferry or a bridge for a road crossing of a river). Only at the end of the pre-design phase a decision is made. Awaiting the choice, elaborating and estimating (and eventually time-planning) several variants mainly meet the uncertainty. Sometimes, the decision between the variants is so unpredictable that all variants are considered equally likely. Sometimes one variant is preferential and it is unlikely that another one will be chosen.

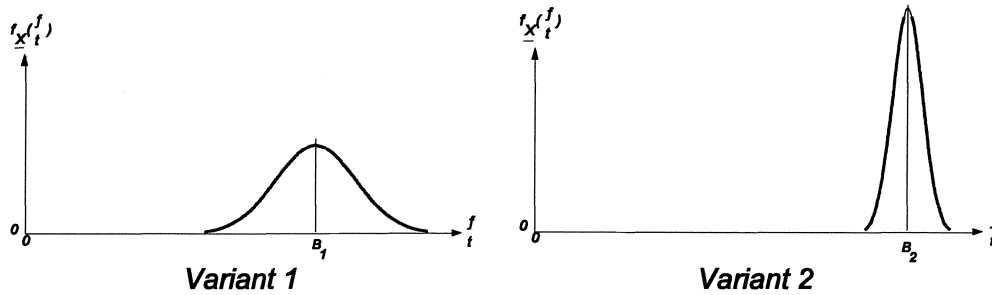


Figure VII-8

If more than one variant is estimated or planned, the problem could be that the estimate of the budget is required to be one total amount of money or the time-planning should be one total duration. One estimate of the budget or one time-planning (possibly with a margin or expressed as a probability density function) for presentational purposes is then acquired rationally by weighing each variant by its (estimated) probability of selection. The following figure presents the result for two variants.

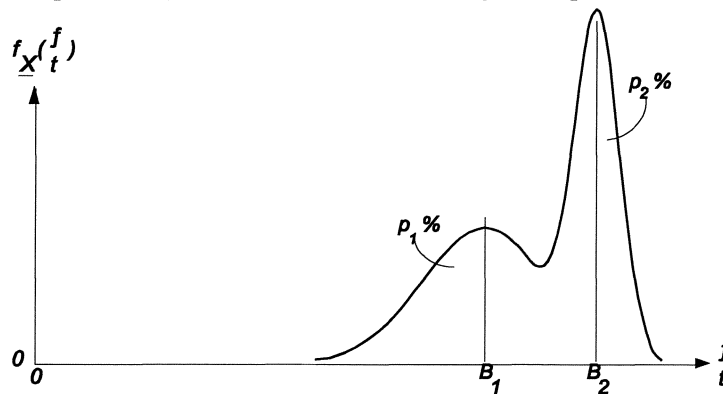


Figure VII-9

The disadvantage is that the result is not recognized as a reasonable estimate or time-planning of each of the individual variants.

The classified uncertainty and the formulae to calculate the associated means and the standard deviations of the probability-weighted consequence (the related risks) are summarized in the following table. Mutatis mutandis the formulae hold for a time-planning with only one time-path.

Table VII.5.

	Case	mean	standard deviation	Description
Normal events	1	B	0	A deterministic amount of money, B , expressed in units of money
	2	B	σ_B	A stochastic amount of money, with mean B , and some spreading, σ_B .
Special events	3	$p \times B$	$\sqrt{p \times (1-p) \times B^2}$	An event with probability of occurrence p that has a deterministic consequence B .
	4	$p \times B$	$\sqrt{p \times \left\{ (1-p) \times B^2 + \sigma_B^2 \right\}}$	An event with probability of occurrence p that has a statistic consequence with mean B and some spreading, expressed by σ_B .
Plan uncertainty	5	$p_1 \times B_1 + p_2 \times B_2$	$\sqrt{p_1 \times (B_1^2 + \sigma_{B_1}^2) + p_2 \times (B_2^2 + \sigma_{B_2}^2) - (p_1 \times B_1 + p_2 \times B_2)^2}$	There are two (or more) variants, each associated with a probability of realization, p_i . Their probabilities add up to one as it is certain that one of the variants will be selected.

As the formulae do not show directly how the ratios of the means and standard deviations alter, numerical values are filled in:

$$\begin{aligned}
 B (= B_1) &= 100 \text{ Mf}, & \sigma_B (= \sigma_{B_1}) &= 15 \text{ Mf} \\
 p (= p_1) &= 0,1 & p_2 &= 0,9 \text{ (One variant: } p_1 + p_2 = 1) \\
 B_2 &= 200 \text{ Mf}, & \sigma_{B_2} &= 30 \text{ Mf}
 \end{aligned}$$

Table VII.5a.

	Case	mean	stand. dev.
Normal events	1	100 Mf	0 Mf
	2	100 Mf	15 Mf
Special events	3	10 Mf	30 Mf
	4	10 Mf	33.5 Mf
Plan uncertainty	5	190 Mf	41.6 Mf

The spreading for an item of the estimate increases with the related uncertainty. In the first case in Table VII.5. one is absolutely certain about the size of the sum, B . The standard deviation equals zero. In the second case there is some uncertainty. The spreading, σ_B , is smaller than the expected value, B . (If this were not so, the estimate of the item was of no significance. It then suggests that there is not the vaguest idea of the size of B .) In case of Special events (cases 3 and 4), one is not certain if there will be costs (damage) at all. The probability that there will be costs is p ($p \ll 1$). There is a greater probability ($1 - p$) that there will be no costs. In fact the RISK¹⁾: (probability \times consequence = $p \times B$, see Vrijling and Vrouwenvelder [1984]) is estimated. If the Special event occurs, the estimated amount of money ($p \times B$) is not nearly enough to cover the costs (B). According to this, the third case is associated with a larger spread (in the order of $B \times \sqrt{p}$) than in the case of a Normal event. So the spreading for Special events is approximately $\frac{1}{\sqrt{p}}$ times the expected value $p \times B$.

1) From a mathematical point of view the estimates of Normal events are estimates of the risks as well. The probability of occurrence of Normal events is 1 (or 100% certainty).

VII.4. TIME PLANNING AND BUDGET ESTIMATES IN LEVEL II CALCULATIONS

If a planning has only one time-path, the duration of the project is approximately equal to the total of the time spaces of the individual activities. An estimate of the budget consists of summation of the multiplications of quanta and unit prices.

If a time-planning consists of only one time-path and the time space of any activity in it is normally distributed, a level II or FORM calculation is an exact solution of the probability of exceedence of the planned duration. If the time space of any activity, i , is normally distributed and all N activities are *independent*, the duration of the time-path is:

$$\mu_{time\ path} = \sum_{i=1}^N \mu_i \quad \sigma_{time\ path} = \sqrt{\sum_{i=1}^N \sigma_i^2}$$

Under the same assumptions and in case of *totally dependent* time spaces:

$$\mu_{time\ path} = \sum_{i=1}^N \mu_i \quad \sigma_{time\ path} = \sum_{i=1}^N \sigma_i$$

If the time spaces are partially correlated, the standard deviation per item can be split in a dependent part, α_i , and an independent part, $\sqrt{1 - \alpha_i^2}$. The dependent parts are added linearly and the independent parts are added quadratically. Finally the standard deviation of the total duration is calculated by adding the squares of the dependent and the independent parts and taking the square root:

$$\mu_{time\ path} = \sum_{i=1}^N \mu_i \quad \sigma_{time\ path} = \sqrt{\left(\sum_{i=1}^N \alpha_i \cdot \sigma_i\right)^2 + \sum_{i=1}^N (1 - \alpha_i^2) \cdot \sigma_i^2}$$

When considering the budget estimates, products of quanta and unit prices play a role. A general rule is: the expected value of a product is equal to the product of the expected values. If the variables are completely independent, the following holds: the square of the coefficient of variation of a product can be approximated²⁾ by the quadratic sum of the coefficients of variation. For the product of a quantum, h , and the unit price, p , of an estimate item, i , the coefficient of variation can be written as:

$$V_{\underline{z}}^2 = V_{\underline{h}}^2 + V_{\underline{p}}^2$$

¹⁾ This formula is elucidated on the next page.

²⁾ The exact formula of the square of the coefficient of variation of a product consisting of two variables is (Vrijling and Vrouwenvelder [1984]):

$$V_{\underline{z}}^2 = V_{\underline{x}}^2 + V_{\underline{y}}^2 + V_{\underline{x}}^2 \cdot V_{\underline{y}}^2$$

if $\underline{z} = \underline{x} \cdot \underline{y}$. In most cases $V_{\underline{x}}^2 \cdot V_{\underline{y}}^2$ is negligible.

PARTIAL DEPENDENCY OF ITEMS IN AN ESTIMATE

If the items in an estimate are partially dependent, the calculation procedure is as given in the scheme below:

Item	Expected value	Coefficient of variation	Variance	Dependent part	Independent part
1	$\mu_{h_1} \cdot \mu_{p_1} = \mu_1$	$V_{h_1}^2 + V_{p_1}^2 = V_1^2$	$\mu_1^2 \cdot V_1^2 = \sigma_1^2$	$\alpha_1 \cdot \sigma_1$	$(1 - \alpha_1^2) \cdot \sigma_1^2$
2	$\mu_{h_2} \cdot \mu_{p_2} = \mu_2$	$V_{h_2}^2 + V_{p_2}^2 = V_2^2$	$\mu_2^2 \cdot V_2^2 = \sigma_2^2$	$\alpha_2 \cdot \sigma_1$	$(1 - \alpha_2^2) \cdot \sigma_1^2$
...
i	$\mu_{h_i} \cdot \mu_{p_i} = \mu_i$	$V_{h_i}^2 + V_{p_i}^2 = V_i^2$	$\mu_i^2 \cdot V_i^2 = \sigma_i^2$	$\alpha_i \cdot \sigma_1$	$(1 - \alpha_i^2) \cdot \sigma_1^2$
...
N	$\mu_{h_N} \cdot \mu_{p_N} = \mu_N$	$V_{h_N}^2 + V_{p_N}^2 = V_N^2$	$\mu_N^2 \cdot V_N^2 = \sigma_N^2$	$\alpha_N \cdot \sigma_1$	$(1 - \alpha_N^2) \cdot \sigma_1^2$
	_____ + μ_{total}			_____ + $\sigma_{dependent}$	_____ + $\sigma_{independent}^2$
				$\sigma_{total} = \sqrt{\sigma_{dependent}^2 + \sigma_{independent}^2}$	

If $\alpha = 0$ in this scheme, complete independence of the costs items is assumed. If $\alpha = 1$, then all costs items are presumed to be completely dependent. If a spreadsheet program is used, the calculation is simple, as can be seen in the following example on page VII - 15.

The measure of dependency can be derived theoretically. It is very comprehensive, because there is a great resemblance with the correlation coefficient. Consider two costs items: y_1 and y_2 , and suppose that they have a component in common, for example the wages. In the example on page VII - 15, this can be the wages component in the viaduct (cost item y_1) and in the road (cost item y_2).

The wages component is the product of the number of hours (supposed to be different and independent for "viaduct" and "road") and the costs per hour. Suppose the costs per hour for both the costs items are the same. By this the costs of wages in items y_1 en y_2 are dependent. The first costs item is: $y_1 = h_1 \cdot p_1$, the second costs item is: $y_2 = h_2 \cdot p_1$.

Suppose the standard deviation of the first cost item is: σ_{y_1} and of the second cost item: σ_{y_2} . From the theory concerning level II- calculations it is known that the factor of influence on the wages component in the standard deviation of cost item y_1 is: $\alpha_{i_1} = \frac{h_1 \cdot \sigma_{p_1}}{\sigma_{y_1}}$. Analogously, the factor of influence on the wages component

in the standard deviation of cost item y_2 is: $\alpha_{i_2} = \frac{h_2 \cdot \sigma_{p_1}}{\sigma_{y_2}}$.

The square of the correlation coefficient is: $\rho_{1,2}^2 = \alpha_1 \cdot \alpha_2$. Furthermore, it is convenient to introduce the coefficient of variation because $h_i \cdot \mu_{p_i}$ equals the (expected value of) the wages in item y_1 . We can write:

$$\rho_{1,2}^2 = \alpha_{i_1} \cdot \alpha_{i_2} = \frac{h_1 \cdot \mu_{p_1} \cdot V_{p_1}}{\sigma_{y_1}} \cdot \frac{h_2 \cdot \mu_{p_1} \cdot V_{p_1}}{\sigma_{y_2}}$$

After dividing the nominator and the denominator by $\mu_{y_1} \cdot \mu_{y_2}$ the result is:

$$\rho_{1,2}^2 = \frac{\text{wages component}_1 \cdot V_{p_1}}{V_{y_1}} \cdot \frac{\text{wages component}_2 \cdot V_{p_1}}{V_{y_2}}$$

From this it is seen that the component causing dependency (here wage component i) has to be large in both cost items. Furthermore, the ratios of the coefficients of variation of the wage components, V_{p_1} , and V_{y_1} or V_{y_2} , respectively, have to be large. "Large" here means that both ratios have to be in the order of unity.

Even if a high value of 0.8 is assumed for both the wage components and for the ratios of the coefficients of variation, the result $\rho_{1,2}^2 = 0.8^4 = 0.4$ is small. The coefficient of correlation is $\rho = \sqrt{0.4} \approx 0.64$, the influence of the dependency on the spreading of the Total estimate will be very small.

EXAMPLE

	A	B	C	D	E	F	G	H	I	J	K	L	M	N	O	P	Q
1	Prices in kf	Probabilistic estimate of budget, dependent items															
2																	
3	item	quantity	unit	price/unit	total	v quan	v price	si quan	si price	si total	depend	si dep	si 1ndep	si indep^2	si tot^2	si tot	v total
4		(number)		kfl	kfl			kfl	kfl	kfl		kfl	kfl			kfl	
5	viaduct	3	piece	2500	7500.00	0	0.2	0	500	1500.00	0.7	1050	1071.21	1147500			
6	road	5	km	15000	75000.00	0.1	0.2	0.5	3000	1677-0.51	0.7	11739.3569	11976.54	143437500			
7	tunnel	1	piece	15000	15000.00	0	0.2	0	3000	3000.00	0.7	2100	2142.43	4590000			
8					----- +							----- +		----- +			
9	DIRECT COSTS				97500.00							14889.3569		149175000	3.71e+08	19257.9321	0.1975
10																	
11	indirect costs	0.3	1/1	97500	29250.00	0.1	0.1975	0.03	19257.9321	6475.63	0	0	6475.63	41933740.4			
12					----- +							----- +		----- +			
13	PRIMARY COSTS				126750.00							14889.3569		191108740	4.13e+08	20317.5217	0.1603
14																	
15	additional costs	0.15	1/1	126750	19012.50	0.1	0.1603	0.015	20317.5217	3592.05	0	0	3592.05	12902789.6			
16	miscellaneous	0.1	1/1	126750	12675.00	0.1	0.1603	0.01	20317.5217	2394.70	0	0	2394.70	5734573.14			
17					----- +							----- +		----- +			
18	BASIC ESTIMATE				158437.50							14889.3569		209746103	4.31e+08	20771.111	0.1311
19																	
20	hist. find	0.1	1/1	2000	200.00	0	0.1	0	200	603.32	0	0	603.32	364000			
21	polluted soil	0.1	1/1	3000	300.00	0	0.3	0	900	943.93	0	0	943.93	891000			
22	diamond find	0.05	1/1	-1000	-50.00	0	0.2	0	-200	222.49	0	0	222.49	49500			
23	design error	0.1	1/1	5000	500.00	0	0.2	0	1000	1532.97	0	0	1532.97	2350000			
24	pile rupture	0.1	1/1	5000	500.00	0	0.2	0	1000	1532.97	0	0	1532.97	2350000			
25	settlement	0.1	1/1	2000	200.00	0	0.2	0	400	613.19	0	0	613.19	376000			
26	installation error	0.1	1/1	5000	500.00	0	0.15	0	750	1518.63	0	0	1518.63	2306250			
27	formwork	0.2	1/1	1500	300.00	0	0.22	0	330	617.88	0	0	617.88	381780			
28	rupture of soil	0.25	1/1	500	125.00	0	0	0	0	216.51	0	0	216.51	46875			
29					----- +							----- +		----- +			
30	ESTIMATE				161012.50							14889.3569		218861508	4.41e+08	20989.3891	0.1306

Notice that the Special events (rows 20 up to and including 28) have been modelled as mentioned in point 4 of Table VII.5. For "Quantity" (column B, rows 20 up to and including 28) the probability of occurrence of the Special event is filled in. If the Special event occurs ("Unit" = probability 1/1 in column C), the costs are as given in column D. No spreading is assumed in the "Quantity" (variation in the probability of occurrence of the Special event), so the coefficient of variation of the "Quantity" (column F) is set at 0 (zero). However, spreading has been supposed in the costs. These are expressed as a part (column G) of the unit price of the Special event (column D). The standard deviation of the price of the Special event, given in column I (compare σ_B in Table VII.5.) is the coefficient of variation in column G, multiplied by the unit price from column D. In column J the calculation of the standard deviation of the cost price of the Special event takes place according to Table VII.5. point 4.

The modelling of the additional costs asks for some comment as well. Column B mentions (lines 11, 15 and 16) the additional percentages. The column "Price per unit" (column D) displays the total of the calculated costs. Cell D11 gives the amount of the Direct costs from cell E9: 97,500.00 kf and in cell D15 and cell D16 the Primary costs from cell E13: 126,750.00 kf appear. The additional costs in cells E11, E15 and E16 are calculated in the same way as for the Special events.

In column F some spreading in the quantities of the additions (= additional percentages) is taken into account. Cells F11, F15 and F16 give the applicable coefficients of variation.

The coefficients of variation of the prices of the additional costs cannot be chosen independently. They are equal to the coefficients of variation of the estimate calculated so far: cell G11 copies the content of cell Q9, cells G15 and G16 give the amount from cell Q13.

Column H contains the products of the values in columns B and F. The Indirect costs in cell H11 are the product of the contents of cells B11 and cell F11. For the additional costs, the content of cell H15, the product of cells B15 and F15 is calculated. For Miscellaneous, in cell H16, the product of cells B16 and F16 is calculated.

In column I, the product of the expected values of the price and the coefficient of variation of the price (product of the columns D and G) is given. For the Indirect costs, the content of cell I11, the product of the contents of cells D11 and G11 is calculated. For the additional costs in cell I15, the product of the contents of cells cell D15 and cell G15 is given. For Miscellaneous, the product of cells D16 and G16 is calculated and presented in cell I16.

The standard deviation of the total of each addition is mentioned in column J. Cell J11 presents the square root of {the square of the content of cell F11 plus the square of the content of cell G11} times the content of cell E11. The square root of the sum of squares of the coefficients of variation of the quantities and the unit prices is multiplied by the expected costs. Cell J15 gives the square root of {the square of the content of cell F15 plus the square of the content of G15} times the content of cell E15. Cell J16 presents the square root of {the square of the content of cell F16 plus the square of the content of G16} times the content of cell E16.

Finally, a remark is made concerning the dependency of the Primary costs items. Column K gives the dependencies of the items "viaduct", "road" and "tunnel" in rows 5, 6 and 7, namely 0.7, 0.7 and 0.7. These are the coefficients α_i from page VII - 14. Numbering the items: viaduct = 1, road = 2 and tunnel = 3, in the formula on the bottom of page VII - 14 we get:

$$\rho_{1,2}^2 = \alpha_1 \cdot \alpha_2 = 0.7 \cdot 0.7 = 0.49 = \rho_{1,3}^2 = \rho_{2,3}^2.$$

The coefficients of correlation are very low. The estimate will hardly differ from one in which the items are supposed to be uncorrelated.

EXAMPLE OF A CLASS A- ESTIMATE

As part of the development of a harbour project a quantity of sand of ca. 3,000,000 m³ has to be dredged by a hopper dredger. In the dredging industry the working week is seven days, with twenty four hours per day, so in a working week there are 168 hours.

Assuming a working week of 168 hours, the duration of the project, T, amounts to:

$$T = \frac{\text{quantity of sand}}{\text{working coefficient} \cdot \text{capacity} \cdot 168}$$

If the tariff on the hopper dredger is set by a fixed part (t_{fixed}) and by a variable part (t_{var}) per week, the costs, K, in total, amount to:

$$K = t_{\text{fixed}} \cdot (D + T) + t_{\text{var}} \cdot T + \text{overhead} \cdot (D + T)$$

For the calculation of the costs, a random delay, D, is added to the nett duration of the project.

Normal distributions with the following parameters model the probabilities of the variables:

Table VII.6.

variable	μ	σ	dimension
quantum	$3 \cdot 10^6$	$3 \cdot 10^5$	m ³
capacity	2060	300	m ³ /hour
t_{fixed}	$39 \cdot 10^4$	$39 \cdot 10^3$	f/week
t_{var}	$15 \cdot 10^4$	$20 \cdot 10^3$	f/week
overhead	$20 \cdot 10^4$	$20 \cdot 10^3$	f/week
delay	1	1	week
working coefficient	0.85	0.05	--

As was explained for "LOADS" (page II - 91, paragraph 2) the probability of exceedence of the costs can be calculated. In the problem at hand the costs technically fulfill the same role as the aforementioned loads. The reliability function is:

$$Z = K_{\text{fixed}} - \left\{ (t_{\text{fixed}} + \text{overhead}) \cdot (D + T) + t_{\text{var}} \cdot T \right\}$$

For K_{fixed} various deterministic values were substituted. The "probability of failure" (probability that the target of the costs, K_{fixed} , is exceeded) was plotted versus K_{fixed} . Some results of a level- II calculation for $K_{\text{fixed}} = 9 \text{ Mf}$ are given in the table below.

Table VII.7.

variable	type	μ	σ	design point value	α^2
t_fixed	N	390000 f/w	39000 f/w	395273.30 f/w	0.071
amount	N	3000000 m ³	300000 m ³	3068803.68 m ³	0.204
workcoef	N	0.85 --	0.05 --	0.843 --	0.075
cap	N	2060 m ³ /h	300 m ³ /h	1951.82 m ³ /h	0.505
D	N	1.00 w	1.00 w	1.17 w	0.110
t_var	N	150000 f/w	20000 f/w	151254.72 f/w	0.015
overhead	N	200000 f/w	20000 f/w	201386.80 f/w	0.019

In the column marked " α^2 " the contributions of the various variables to one's uncertainty about the project costs are listed. The largest contribution (0.505) comes from the uncertainty concerning the capacity of the dredger. The uncertainty about the total quantum of sand (0.204) plays an important role as well.

By repeating the calculation several times for various values of K_{fixed} the probability of exceedence of the costs can be established. The probability of exceedence is presented in Figure VII-10.

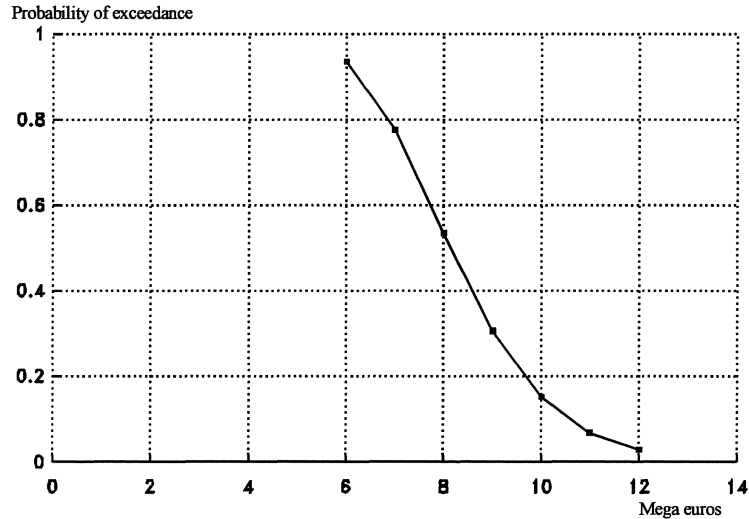


Figure VII-10

For the duration of the dredging project a probability of exceedence can be calculated analogously. The reliability function is:

$$Z = \frac{\text{quantity of sand}}{\text{working coefficient} \cdot \text{capaciteit} \cdot 168} - T_{plan}$$

Fixed values (in weeks) are substituted for T_{plan} , and the probability of exceedence of the planned time is calculated. The result is given in Figure VII-11.

A person (the "decision maker") who has to decide about the allocation of means (money) can use these results to get a good impression of the uncertainty about costs and the duration of the project. Moreover, it is clear from the column " α^2 " in Table VII.7., which variables contribute most to the total variance (which is a measure for one's uncertainty). Alterations concerning these variables should have preference if the total variance has to be decreased.

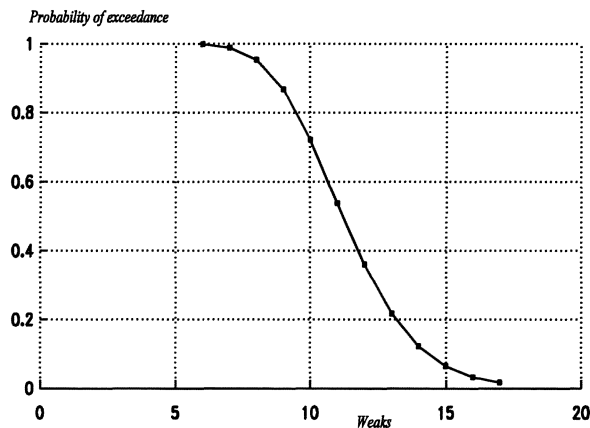


Figure VII-11.

In an approximate full distribution approach (AFDA- calculation) Special events cannot be treated satisfactorily as their probability density functions are discontinuous. The probability density functions (see Figures VII.6. en VII.7.) are replaced by normal distributions, the means and standard deviations of which are given in Table VII.5.. The replacement normal distributions, modelling calamities, are not good approximations. For correct modelling of Special events level III- methods are adequate. Often a Monte Carlo simulation is chosen.

STATISTICALLY CONTROLLED TIME-PLANNING

The reliability function of a time-planning in which more than one time-path plays a role, is not differentiable everywhere. The duration of the project, D , is the maximum of the time spaces of all time-paths, D_i :

$$\underline{D} = \max_{i=1}^N \{ \underline{D}_i \}.$$

Consequently, an exact level II- calculation is not possible. Time-planning problems are mainly analysed using a Monte Carlo- simulation.

In statistically controlled time-planning the time spaces of the activities are seen as random variables (given in Figure VII-12), in contrast to the deterministic approach, as sketched in Figure VII-2.. Generally, the expected value of the duration of the project is used for the duration, D . Sometimes, the mode is considered. If the independent time spaces of the various activities are normally distributed then there is a 50% probability that the duration of the project is exceeded.

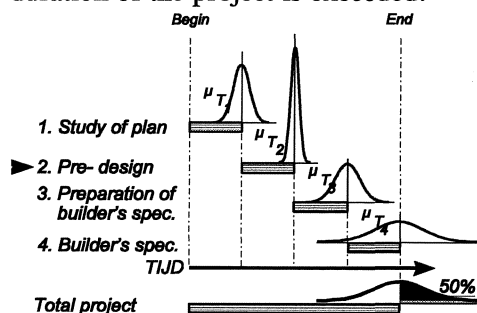


Figure VII-12

If the time spaces are independent and normally distributed, the mean and the standard deviation of the total duration of each time-path are:

$$\underline{\mu}_D = \sum_{i=1}^N \underline{\mu}_{T_i} \quad \underline{\sigma}_D = \sqrt{\sum_{i=1}^N \sigma_{T_i}^2}$$

Sometimes activities are carried out simultaneously, as was illustrated in Figure VII-3. Licences to lower the groundwater table, to dig, etc., can be acquired in parallel with the design "at the drawing board". The time-planning can be as shown in Figure VII-13.

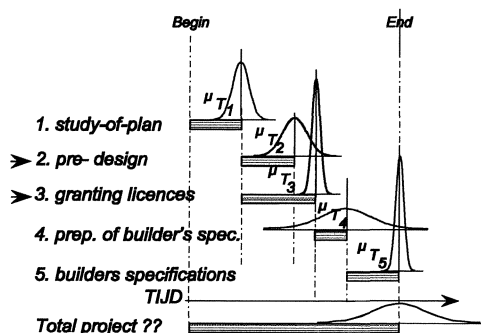


Figure VII-13

As stated on page VII - 7, there are two time-paths in this example:

$$\begin{aligned} D_a &= T_1 + T_2 + T_4 + T_5 \\ D_b &= T_1 + T_3 + T_4 + T_5 \end{aligned}$$

For the total project no ambiguous probability density function can be defined. It can not to be said, which one of the time-paths is "critical" (for which successive activities the total duration, D , is maximum). The duration to be considered depends on the mean duration and on the standard deviations of the simultaneous activities. In a probabilistic approach the concept of the "critical path" loses its significance. At most, it can be *a matter of probability that one of the time-paths will be critical*.

In theory, every activity is described by a different distribution. For activity i :

$$P(\text{duration act. } i \leq t_{\text{duration}_i}) = F_{D_i}(t_{\text{duration}_i})$$

The probability that activity i takes longer than t_{duration_i} is:

$$P(\text{duration act. } i > t_{\text{duration}_i}) = 1 - F_{D_i}(t_{\text{duration}_i})$$

According to section II-3, the probability that all n activities in one time-path have a greater duration than a given amount of time, T_{tot} , is:

$$P(\text{duration all } n \text{ act. } \geq T_{\text{tot}}) = \prod_{i=1}^n (1 - F_{D_i}(T_{\text{tot}}))$$

from which the probability distribution (extreme value distribution) of the maximum duration of all activities in one path can be calculated:

$$P(\text{duration all act. in time-path } j \leq T_{\text{tot}}) = F_{\text{tot. duration time path } j}(T_{\text{tot}}) = 1 - \prod_{i=1}^n (1 - F_{D_i}(T_{\text{tot}}))$$

in which i is the number of activities in time-path j . If there are N time-paths, the probability that the duration of the activities in one time-path is greater than T_{tot} is:

$$P(\text{duration all act. } \geq T_{\text{tot}}) = \max_{j=1}^N \left[\left\{ \prod_{i=1}^n (1 - F_{D_i}(T_{\text{tot}})) \right\}_j \right]$$

All time-paths are (in theory) described by different distributions, each with their own parameters. An example is given in Figure VII-14. Notice, that in Figure VII-14 there are two partial projects but there are three time-paths, each with their own distributions.

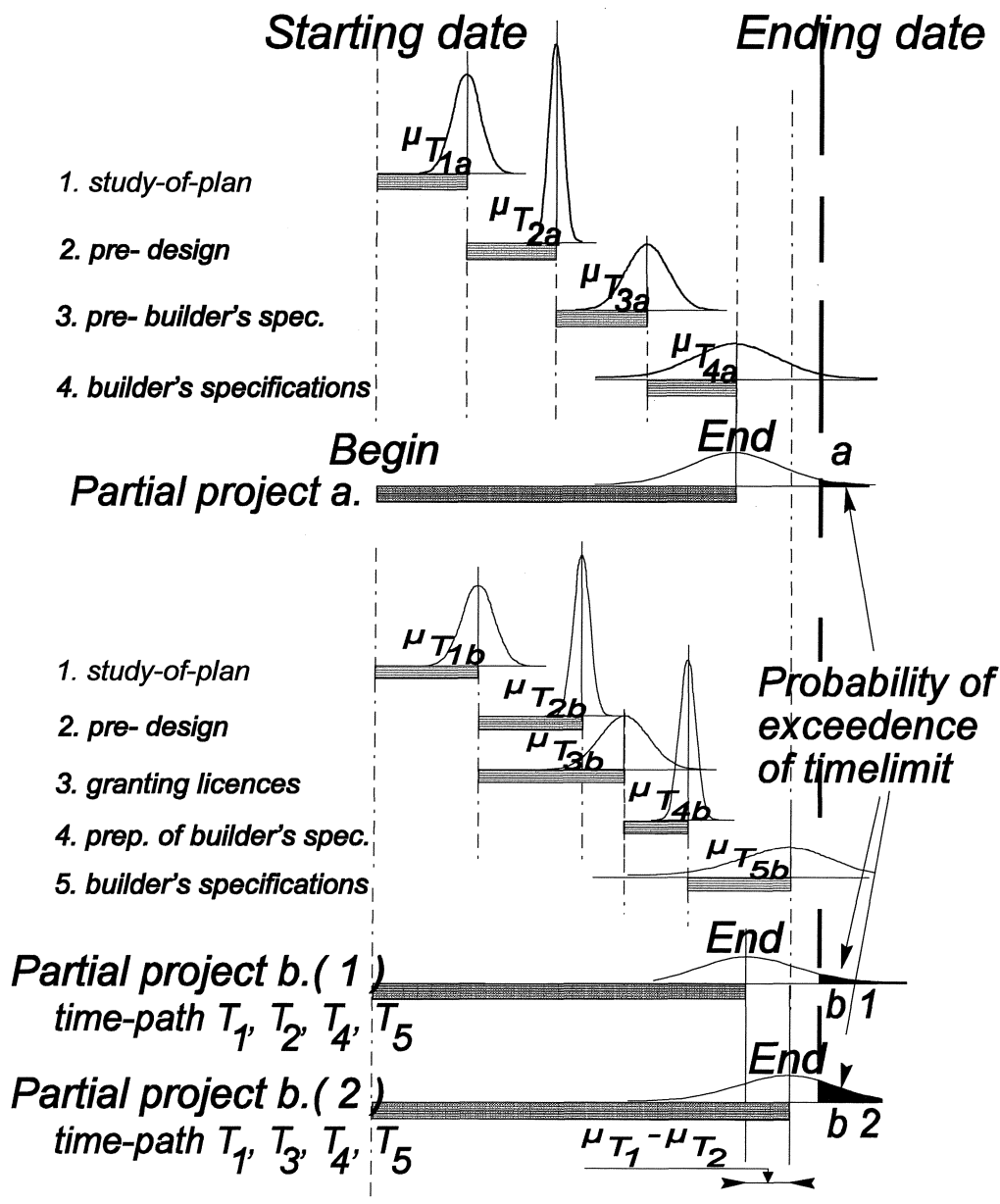


Figure VII-14

VII.5. VISUALISATION OF UNCERTAINTY

In the end, the calculated uncertainty has to be brought back into the framework of the estimate of the budget or the time-planning.

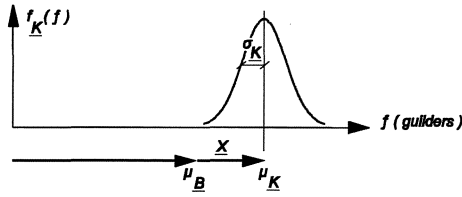


Figure VII-15

In Figure VII-15, \underline{B} represents the (stochastic) Basic estimate, made up at the end of a well defined phase of the project. The expected value of \underline{B} in Figure VII-15, i.e. $E(\underline{B})$ or $\mu_{\underline{B}}$, represents the estimate as it was traditionally calculated.. (It is often still calculated in this way.) \underline{X} is an unknown (random) amount of money that has to be added to the Basic estimate. In Figure VII-16, the variables from the definition sketch in Figure VII-15 are put into the context of an estimate.

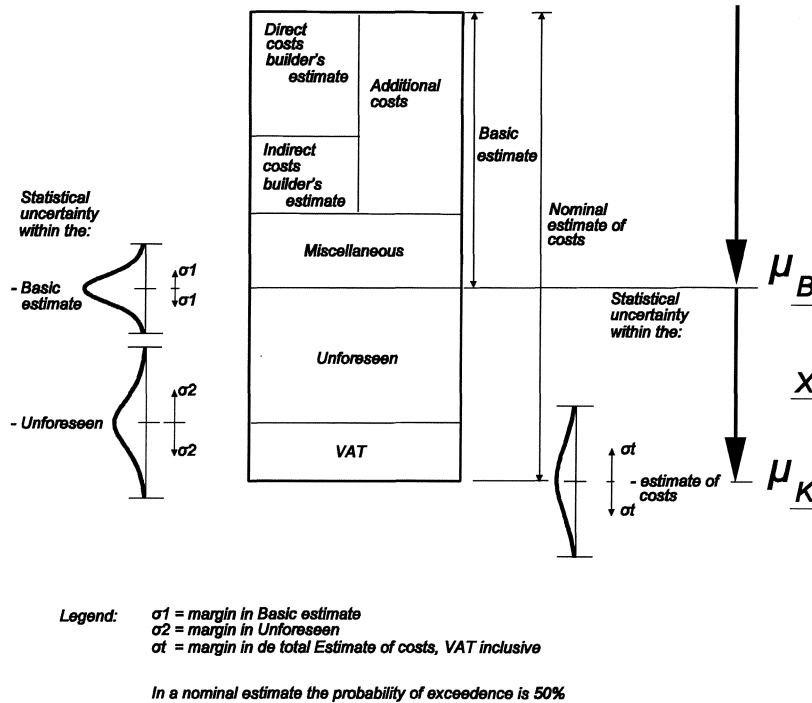


Figure VII-16

The real costs, \underline{K}^1 , will finally amount to:

$$\underline{K} = \mu_{\underline{B}} + \underline{X}$$

The expected value of the unknown amount of money, $\mu_{\underline{X}}$, appears to be a function of the expected value of the Basic estimate, $\mu_{\underline{B}}$. Furthermore, \underline{K} depends on the magnitude of the expected value of the Unforeseen, $\mu_{\underline{X}}$, and on the spreading of it, $\sigma_{\underline{X}}$, the latter two depend on the phase the project is in.

1) Notice that the spreading in the Basic estimate is accounted for in the spreading of the unknown amount of money, \underline{X} . Notice further that in the estimate of the budget no correction for inflation is taken into account.

VII.6. QUANTIFICATION OF THE ITEM UNFORESEEN

VII.6.1. EXPERIENCES WITH EXCEEDENCES OF COSTS

As can be seen in Figure VII-16, the deviation of the real costs from the estimate is mainly caused by two components:

1. the expected value of the items in Unforeseen. This deviation from the estimate is mainly referred to as "nominal Unforeseen".
2. the spreading. This concerns both the spread caused by the deviations from the assumed starting points (spreading in the Basic estimate) and by the incompleteness of the established extension of the project (spreading in the items in Unforeseen).

Mostly the VAT is seen as a fixed percentage that is calculated from and added to the Total estimate (ex VAT). This percentage, however, can be subject to uncertainty. This will not be dealt with here.

The real costs were modelled by (see Figure VII-16):

$$\underline{K} = \underline{\mu}_B + \underline{X}$$

The total estimate can be normalized:

$$\frac{\underline{K}}{\underline{\mu}_B} = 1 + \frac{\underline{X}}{\underline{\mu}_B}$$

in which $\frac{\underline{X}}{\underline{\mu}_B}$ is supposed to be normally distributed.

Starting from the normalized estimate and expressed in percentages of the expected values of the Basic budget estimates of many completed projects, the following values were found:

Table VII.10.

class	project phase	$\mu \left\{ \frac{\underline{X}}{\underline{\mu}_B} \right\}$ (nominal Unforeseen)	$\sigma \left\{ \frac{\underline{X}}{\underline{\mu}_B} \right\}$ (spreading in estimate)
D	study-of-plan phase	30%	50%
C	pre- design phase	20%	30%
B	pre- builder's specifications	10%	10%
A	phase builder's specifications phase	5%	5%

The phase the project is in is the only "entrance" to this table to establish the magnitude of the item Unforeseen. In practice, the table is used only if a detailed analysis is not needed.

Table VII.10. was calculated from data concerning large projects of various kinds. A great part of the data came from the building costs of chemical plants. The table contains expected values that are based on experience.

Such numbers do not have to be representative for specific projects, such as, for example, rail infrastructure projects. That is why an analysis of completed projects was undertaken by the Dutch Railways company. In the following table the results of the analysis of 20 projects are given as percentages of the expected values of the Basic estimate, B. The Dutch Railways company used a slightly different classification from the one used in section VII.2.1.1.:

Table VII.11.

class	project phase	nominal Unforeseen as % of μ_B	spreading in estimate in % of μ_B
0	costs indication	-7 ---> +22%	31 ---> 48%
1	cost price	2%	32%
2	credit request	7%	20%
3	estimate for construction	--	--

Considering the magnitude of the uncertainty the agreement with Table VII.10 is remarkably good.

VII.7. COMPARISON OF AN ESTIMATE CONTAINING SPECIAL EVENTS WITH EXPERIENCE ON COST EXCEEDENCES

Two methods were mentioned for the estimate of the item Unforeseen:

1. the estimates of the expected value and the standard deviation can be based on experience. Numbers can be as given in Table VII.10. The expected value and the spreading are then expressed as additions to the Basic estimate of the budget. Suppose the nominal Unforeseen is 25% of the Basic estimate (cell E18 on page VII-15), the addition is then: $0.25 \times 158\,437.50 = 39\,609.38\text{ k f}$.
2. the item can consist of Special events. (See the example on page VII-15, rows 20 up to and including 28).

The estimated totals of Unforeseen can be compared by means of the risk. This provides a good test for the assumption that the rough estimate of Unforeseen for a specific project correspond with the Special events. For simplicity sake it is assumed that the costs in the case of occurrence of a Special event are known. (Table VII.5, point 3).

The result of the Special event, G , is expressed as a fraction, f , of the Basic estimate, B :

$$G = f \times B$$

Usually N Special events will be foreseen, so, according to Table VII.5. point 3, the expected value of the risks of all Special events will equal $N \cdot p \cdot f \cdot B$. The standard deviation is:

$$\sigma = \sqrt{N \cdot p \cdot (1 - p) \cdot f^2 \cdot B^2}.$$

Take an estimate class C (pre-design phase) as an example. The question is, how many Special events, each having an expected probability of occurrence, p , and a potential consequence of G , are needed to justify a reservation for Unforeseen in the pre-design phase of 20% and a standard deviation, σ of 30% of the Basic estimate. (See Table VII.10.)

If the potential consequences of all Special events are equally large, the following combinations justify the reservations of 20% for Unforeseen in the pre-design phase (see formulae for G and σ):

Table VII.12.

Probability p	Number N	f = G/B
0.01	142	0.21
0.05	27	0.22
0.10	13	0.23
0.20	6	0.25
0.50	2	0.3

If the mean probability of a Special event, p , equals 0.1, then approximately 13 of such events are required (see Table VII.12.), each with consequence $G = 0.23 B$, to justify the reservation in the pre-design phase. During the course of the project it is to be expected that one or two of such events will indeed occur.

Upon a closer look at the scheme on page VII-15 it is conspicuous that the percentages, p , are all approximately 0.1 (see column B, "Quantity", lines 20 up to and including 28). The mean risk (column E) of the Special events is approximately 0.2. Only 9 Special events are listed, instead of 13. However, this cannot be the explanation of the discrepancy between the above-mentioned value of Unforeseen (39609.38 kf, see point 1.) and the addition of the mean values of the items Unforeseen in the example on page VII - 15 ($161012.5 - 158437.5 = 2575.00\text{ kf}$).

It could be interesting to compare the experiences, made in practice with this type of predictions stating that the Unforeseen is caused by one or two rarely occurring Special events with considerable consequences.

VII.8. RISK CONTROL MEASURES

VII.8.1. DESCRIPTION OF CONCEPTS

Risk control measures are measures that either lead to reduction of one's uncertainty (expressed as a standard deviation of the Total estimate of the budget or duration of the project) or lead to the reduction of the probability that the estimated costs exceed the budget or that the duration of the project is longer than planned. For shortness sake, risk control measures will only be discussed for budget estimates . For time-planning the method is (practically) analogous.

In the case the measures are taken in order to reduce the probability that the estimated costs exceed the budget, their aim is to increase the accuracy of the estimate of the budget. The accuracy of an estimate is the probability that the costs of a project do not exceed the budget. The costs are estimated. The decision maker defines a budget in such a way that the costs of the project are covered with a sufficiently small probability of exceedence. The formula in which this is expressed, reads:

$$Budget \geq \mu_{total} + k \cdot \sigma_{total}$$

μ_{total} and σ_{total} have been defined in the scheme on page VII - 14. μ_{total} is the expected value of the estimated costs. σ_{total} is a measure of the uncertainty of the decision maker. The factor k is a measure of his/her risk aversion. It indicates the decision maker's attitude to measures (which will add costs to the estimate) which reduce the probability of exceedence of the budget. This attitude can be positive, negative or neutral.

CLASSIFICATION OF THE MEASURES

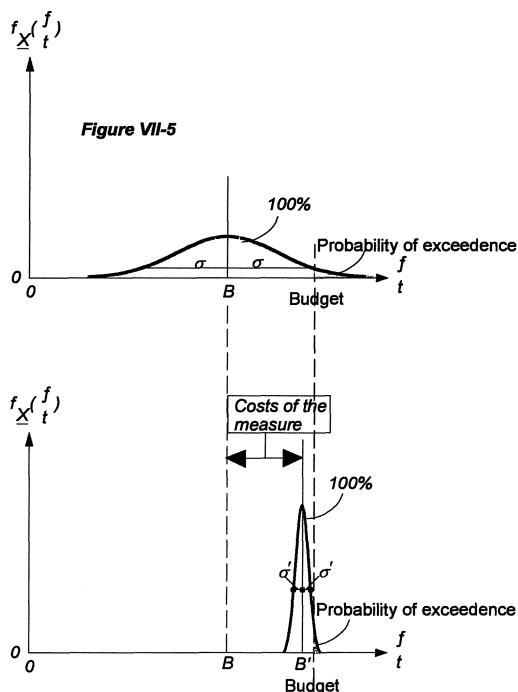
The decision maker can choose from two categories of risk control measures:

1. transfer of the risk to others for a fixed price. In this case his/her uncertainty about the item of the estimate is bought off by a deterministic (fixed) expenditure. Examples are forward contracts, lump sum contracts and insurances. In case of transfer the risk is limited by the juridical hardness of the agreement. If the hardness is total, cases 2, 3, 4 and(/or) 5 in Table VII.5. are replaced by case 1 in that table.
2. running the risk oneself and adapting the design if the risk is considered too great. The adaptation of the design requires an extra investment. In this case the uncertainty remains, but an attempt is made to sufficiently reduce the probability of exceedence of the budget by risk reducing measures (which cost money).

THE EFFECTS OF ADAPTATION OF THE DESIGN

If the decision maker is prepared to run (part of) the risk, it can be necessary to adapt the design. The effects of adaptation of the design are different for Normal and for Special events.

A. EFFECT ON THE RISK CONCERNING NORMAL EVENTS.



The measures concern an item categorized in case 2 in Table VII.5. (Figure VII.5). The variance of the estimate of the cost of a Normal event is determined by fluctuations in quanta and prices. The measures causing reduction of the variance have to be balanced against the costs of those measures. As it is certain that a Normal event will take place, the probability of occurrence, p , will be 100%.

The (expected value of the) estimate, B , is enlarged to B' . One's uncertainty, expressed in the standard deviation, σ , is decreased¹⁾ (provided the measure is effective). The cost of the measure and its effect on the probability density of the estimate of a Normal event is sketched in Figure VII-17. The probability of exceedence of the budget decreases by virtue of the measure of risk control.

Figure VII-17

B. EFFECTS ON THE RISKS CONCERNING SPECIAL EVENTS

Risk control measures concerning Special events reduce the probability of exceedence of the budget, as was the case for Normal events. In the latter case only the variance of the estimate was influenced. A measure to control a Special event can influence both the probability of occurrence and the consequence (damage). The damage can be:

1. deterministic. If the Special event occurs, the consequence is deterministic, to the order of B (Case 3 in Table VII.5., see Figure VII-6).

or

2. stochastic. This case is mentioned only for completeness sake. It concerns the Special event with an uncertain consequence. The consequence is a random variable. The mean is B and the standard deviation is σ_B . (Case 4 in Table VII.5., see Figure VII-7). The quantification of the costs of a measure and its effect is sketched in Figure VII-19. In the formula for the standard deviation

for Case 4 in Table VII.5, $\sqrt{p \times \{(1-p) \times B^2 + \sigma_B^2\}}$, the term σ_B^2 is negligible compared with $(1-p) \times B^2$.

The quantification, sketched in Figure VII-19 then coincides with the one in Figure VII-18. From the cases involving special events, mentioned in Table VII.5., only Case 3, represented in Figure VII-18, is taken into consideration.

1) For this reason it is of no use to try to reduce the risk associated with a Normal event that is a deterministic amount of money, B , as $\sigma_B = 0$ in that case. (See case 1 in Table VII.5., Figure VII-4).

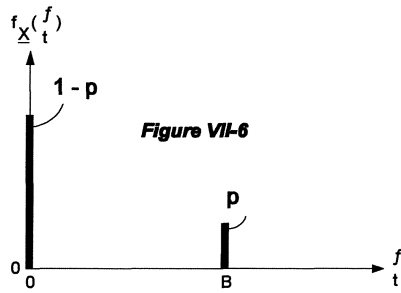


Figure VII-6

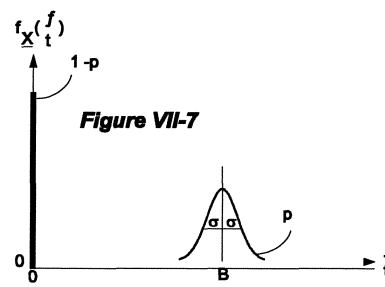


Figure VII-7

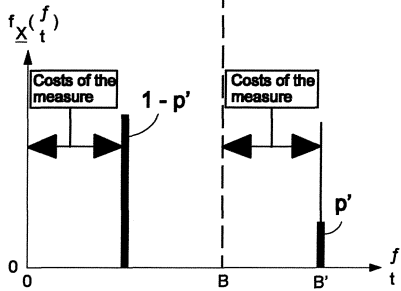


Figure VII-18

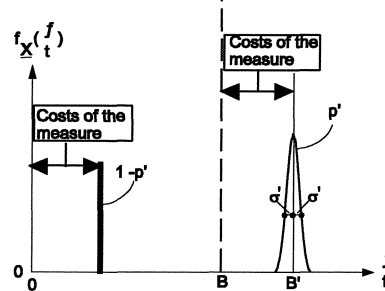


Figure VII-19

The measures concerning a deterministic damage in case of a Special event (see point 1 above) can aim: to

- a. decrease the probability of occurrence
- b. decrease the damage (the consequence)

Ad a: measure aims to decrease the probability of occurrence of the Special event.

Before the measure is taken, the probability of occurrence of the event is equal to p and the damage (if the event occurs) is B . If the measure is taken, the amount of money lost if the event takes place increases by the costs of the measure, but the probability of occurrence decreases to $p' < p$. If the event does not take place, the costs have been made in vain. The probability that this is the case is $1 - p'$. The quantification of the measures and their effects is sketched in Figure VII-18.

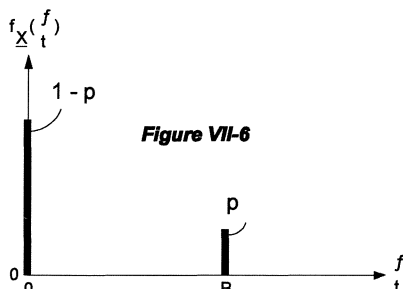


Figure VII-6

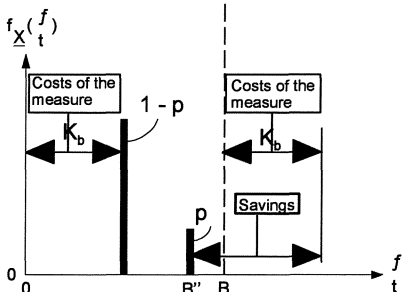


Figure VII-20

Ad b: measure aims to decrease the consequence of the Special event (leaving the probability of occurrence unchanged). Before and after the measure the probability of occurrence of the event is p . If the measure is taken, the amount of money lost when the event takes place is increased by the costs of the measure, K_B , but the consequences (damage after the measure is taken equals B) decrease. ("The consequences are - partly - taken beyond the reach of the threat.") The quantification of the measures and their effects are sketched in Figure VII-20.

The measures are named per item and their ways of quantification are explicitly stated. They can be introduced in (new) estimates. The result is an insight into the effect of each measure on the estimate: both on the mean, μ_{total} , and on the standard deviation, σ_{total} , of the estimate. The budget is taken as a standard, within which the project has to be financed. The decision maker will test if:

$$\mu_{total} + k \cdot \sigma_{total} \leq Budget$$

If the estimate is higher than the budget, one of the various measures can be selected.

VII.8.2. ANALYSIS OF THE INFLUENCE OF RISK CONTROL MEASURES

The risk control measures aim to reduce the influence of uncertainty on the estimate of the budget. The uncertainty is expressed in the standard deviation of that estimate. The standard deviation of the Total estimate is:

$$\sigma_{total} = \sqrt{\sigma_{Basic\ estimate}^2 + \sigma_{Unforeseen}^2}$$

If there are n items in the Basic estimate and m items in Unforeseen, then the standard deviation of the Total estimate can be written as:

$$\sigma_{total} = \sqrt{\left(\sigma_1^2 + \sigma_2^2 + \dots + \sigma_n^2\right)_{Basic\ estimate} + \left\{p_1(1-p_1)B_1^2 + p_2(1-p_2)B_2^2 + \dots + p_m(1-p_m)B_m^2\right\}_{Unforeseen}}$$

Starting from this formula the effect of risk control measures on the standard deviation of the Total estimate can be analysed.

INFLUENCE ON NORMAL EVENTS (concerning the Basic estimate).

One can try to reduce the standard deviation of the price per quantum and the standard deviation of the quantum of an item in the Basic estimate by risk control measures. The standard deviation of the price per quantum can be reduced by agreements on prices. The standard deviation of the quantum is smaller if "proven technology" is applied, for example by using standard solutions, that have been proven many times in comparable circumstances and with which a vast experience of material behaviour in working methods and in estimates has been built up. Reduction of the standard deviation of the price per quantum causes reduction of the standard deviation of the item concerned. The same is the case if the standard deviation of the quantum is reduced. This can be concluded from the scheme on page VII-14. If the standard deviation of the Total estimate is differentiated with respect to the standard deviation of the variable concerned, the result is:

$$\frac{d\sigma_{total}}{d\sigma_i} = \frac{\sigma_i}{\sigma_{total}}$$

in which i is the rotation number of the item concerned in the Basic estimate.

The standard deviation of the Total estimate, σ_{total} , as a function of the standard deviation of item i in the Basic estimate, σ_i , is an increasing function, as the derivative of σ_{total} with respect to σ_i is always positive. So decrease of the standard deviation of the price per quantum and/or reduction of the standard deviation of the quantum will result in reduction of the standard deviation of the Total estimate.

INFLUENCE ON SPECIAL EVENTS (concerning the Unforeseen)

MEASURES AIMED AT THE REDUCTION OF THE PROBABILITY OF OCCURRENCE

Page VII-9 states that the probability of occurrence of a Special event, p , is smaller than 0.5. Reduction of the probability of occurrence of a Special event associated with a deterministic consequence (Case 3 from Table VII.5) results in decrease of the standard deviation of the estimate of the item concerned,

as $\frac{d\sigma_{total}}{dp_i} = \frac{0.5 \cdot B_i^2 \cdot (1 - 2 \cdot p_i)}{\sigma_{total}}$ is always positive.

MEASURES AIMED AT THE REDUCTION OF THE CONSEQUENCE

Reduction of the consequence of the occurrence of a Special event with a deterministic consequence (Case 3 in Table VII.5.) always results in a decrease of the standard deviation of the item concerned:

$\frac{d\sigma_{total}}{dB_i} = \frac{B_i \cdot (p_i - p_i^2)}{\sigma_{total}}$ is always positive.

VII.8.3. ANALYSIS OF THE INFLUENCE OF RISK CONTROL MEASURES ON THE ACCURACY OF AN ESTIMATE or the sensitivity of the costs for risk control measures

The equality:

$$Budget = \mu_{total} + k \cdot \sigma_{total}$$

can be seen as the failure boundary of a "classical" reliability function:

$$Z = Budget - R \quad (R = N(\mu_{total}, \sigma_{total}))$$

In the above "budget" is the "strength" and "estimate", R, is the "load". The unwanted top event ("failure") is defined as "load exceeds strength". In this case this means that the budget is not sufficient to cover the estimated costs.

The safe region of the reliability function: $\frac{Budget - \mu_{tot}}{\sigma_{tot}} \leq k$, can be derived from the failure boundary.

The estimate, R, can be elaborated:

$$\begin{aligned} R &= \mu_{total} + k \cdot \sigma_{total} = \mu_{Basic\ estimate} + \mu_{Unforeseen} + k \cdot \sqrt{\sigma_{Basic\ estimate}^2 + \sigma_{Unforeseen}^2} \\ &= (\mu_1 + \mu_2 + \dots + \mu_n)_{Basic\ estimate} + (\mu_I + \mu_{II} + \dots + \mu_m)_{Unforeseen} + \\ &\quad k \cdot \sqrt{(\sigma_1^2 + \sigma_2^2 + \dots + \sigma_n^2)_{Basic\ estimate} + (\sigma_I^2 + \sigma_{II}^2 + \dots + \sigma_m^2)_{Unforeseen}} \\ &= (\mu_1 + \mu_2 + \dots + \mu_n)_{Basic\ estimate} + (p_1 \cdot B_1 + p_2 \cdot B_2 + \dots + p_m \cdot B_m)_{Unforeseen} + \\ &\quad k \cdot \sqrt{(\sigma_1^2 + \sigma_2^2 + \dots + \sigma_n^2)_{Basic\ estimate} + (p_1 \cdot (1 - p_1) \cdot B_1^2 + p_2 \cdot (1 - p_2) \cdot B_2^2 + \dots + p_m \cdot (1 - p_m) \cdot B_m^2)_{Unforeseen}} \end{aligned}$$

The summation of μ_{total} and $k \cdot \sigma_{total}$ can be sketched as follows:

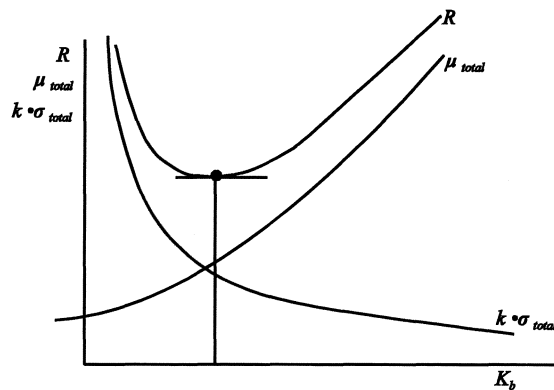


Figure VII-21

The accuracy of an estimate (with constant risk aversion, k, and in case of a deterministic target) increases if its expected value and/or its standard deviation are reduced.

Both the expected value of the price per quantum and the expected quantum play a role when the expected value of the item in the Basic estimate is calculated. The calculation of the expected value of an item in Unforeseen takes the probability of occurrence and the damage (consequence) of the Unforeseen item i into consideration. Decrease of the mean of the Basic estimate or of the mean of the Unforeseen leads to an increased accuracy of the estimate.

SENSITIVITY IN THE CASE OF NORMAL EVENTS

Differentiation of the last mentioned equation with respect to μ_i leads to:

$$\frac{dR}{d\mu_i} = \frac{d\mu_{total}}{d\mu_i} = 1$$

(The same holds for differentiation with respect to μ_j concerning the Unforeseen.)

The calculation of the standard deviation of the Total estimate takes the standard deviation of the price per quantum and the standard deviation of the quantum of an item from the Basic estimate into account in the same way. In both cases decreasing of the standard deviation of the item results in a decrease in the standard deviation of the Total estimate. From the expression for R (see preceding page) it follows:

$$\frac{dR}{d\sigma_i} = k \cdot \frac{d\sigma_{total}}{d\sigma_i} = \frac{k \cdot \sigma_i}{\sigma_{total}}$$

A DECISION RULE IN CASE OF NORMAL EVENTS.

The costs, K_b , of a measure concerning item i, increase the mean of that item by K_b :

$$\frac{d\mu_i}{dK_b} = 1$$

Differentiation of μ_{total} with respect to K_b according to the chain rule gives:

$$\frac{d\mu_{total}}{d\mu_i} \cdot \frac{d\mu_i}{dK_b} = 1 \times 1 = 1,$$

so the expected value of the estimate also increases just as much as the money spent on the measure.

The relationship between the costs of the measure, K_b , and the standard deviation, σ_i in item i can be written as:

$$\sigma_i = g_i (K_b)$$

In order to see if the measure causes a sufficient decrease in the standard deviation, $k \cdot \sigma_{total}$ is differentiated with respect to σ_i and subsequently with respect to K_b , according to the chain rule. The measure with respect to item i is sound if:

$$\frac{d \{k \cdot \sigma_{total}\}}{d\sigma_i} \cdot \left| \frac{d\sigma_i}{dK_b} \right| > \frac{d\mu_{total}}{d\mu_i} \cdot \frac{d\mu_i}{dK_b}$$

For Normal events this gives:

$$\frac{k \cdot \sigma_i}{\sigma_{total}} \cdot \left| \frac{d\sigma_i}{dK_b} \right| > 1$$

The given function $\sigma_i = g_i (K_b)$ and consequently $\frac{d\sigma_i}{dK_b} = \frac{d g_i (K_b)}{dK_b}$ can be substituted. For those values of K_b for which the inequality holds, risk control measures concerning item i are sound. All items in the Basic estimate can be taken into account in the optimization procedure. If there are n such items this leads to a n-dimensional minimization problem.

For each variable (item i in the Basic estimate) an estimation of the appropriate value of K_b will have to be made as a starting value in the iteration procedure. Depending on the risk aversion, k can be chosen as 1 or 2. The magnitude of $d\sigma_i$ is estimated in the order of $0.5 \cdot \sigma_i$.

The estimate of page VII-15 is taken as an example.

From: $\frac{k \cdot \sigma_i}{\sigma_{total}} \cdot \left| \frac{d\sigma_i}{dK_b} \right| > 1$ (see preceding page) follows:

$$dK_b \leq \frac{k \cdot \sigma_i}{\sigma_{total}} \cdot d\sigma_i$$

For the item "viaduct" (see page VII-15) σ_i : 1500 kfl (cell J5), σ_{total} : 19258 kfl (cell P9). For risk aversion $k = 2$ is chosen. A first estimation of an investment, dK_b , in a risk control measure which halves the standard deviation of item i : $d\sigma_i = 0.5 \cdot \sigma_i = 0.5 \cdot 1500 = 750$ kfl is found to be:

$$dK_b = \frac{2 \cdot 1500}{19258} \cdot 750 \approx 120 \text{ kfl}$$

In general the n -dimensional minimization problem is too complicated to be solved. The costs of this kind of risk control measures concerning Normal events are estimated in the given way and it is left at that. The minimization problem is not solved because:

- 1 the estimate consists of too many items (some hundreds) to be calculated successfully.
- 2 the functional relationships $\sigma_i = g_i(K_b)$ are not known in most cases.

SENSITIVITY IN THE CASE OF SPECIAL EVENTS

INFLUENCE OF RISK CONTROL MEASURES AIMED AT THE REDUCTION OF THE PROBABILITY OF OCCURRENCE

The probability of occurrence of a Special event is: $p < 0.5$. Decreasing the probability of occurrence of a Special event with a deterministic consequence (Case 3 in Table VII.5.) increases the accuracy

of the estimate as $\frac{dR}{dp_i} = B_i + \frac{k \cdot 0.5 \cdot B_i^2 \cdot (1 - 2 \cdot p_i)}{\sigma_{total}}$ is always positive.

This working method results in a m-dimensional minimization problem, as before. (It is supposed that the estimate contains m Unforeseen items.) For the same reasons the minimization problem cannot be solved in most cases. Thus we restrict ourselves to a rough estimate of the costs of risk control measures.

For the mean of the Special event, i , (see Figure VII-18):

$$\mu_i = p_i \cdot B_i + K_b$$

is found. Suppose $K_b \ll p_i \cdot B_i$ (investment small compared with the risk) then $\mu_i \approx p_i \cdot B_i$.

For the standard deviation (see Figure VII-18):

$$\sigma_i = B_i \cdot \sqrt{p_i(1-p_i)}$$

is found. As $p_i \ll 1$:

$$\sigma_i \approx B_i \cdot \sqrt{p_i}$$

The estimate of the i^{th} Special event is given by:

$$R_i = \mu_{R_i} + k \cdot \sigma_{R_i}$$

The following inequality has to be satisfied for the measure to be sound:

$$\left| \frac{dK_b}{dR_i} \right| \leq 1 \quad \text{or} \quad \left| \frac{dK_b}{dp_i} \right| \leq \frac{dR_i}{dp_i}$$

From this:

$$dK_b \leq \frac{dR_i}{dp_i} \cdot dp_i = B_i \cdot \left(1 + \frac{k}{2 \cdot \sqrt{p}} \right) \cdot dp_i$$

The probabilistic estimate on page VII-15 is again taken as an example.

For the item "contaminated soil": $p_i = 0.1$ (cell B21), B_i : 300 kfl (cell E21). Suppose again: $k = 2$. dp_i is estimated in the order of magnitude of $0.1 \cdot p_i$. A rough estimate of an investment in a risk control measure for contaminated soil is:

$$dK_b = 300 \cdot \left(1 + \frac{2}{2 \cdot \sqrt{0.1}} \right) \cdot 0.1 \approx 125 \text{ kfl}$$

INFLUENCE OF RISK CONTROL MEASURES, AIMED AT THE REDUCTION OF THE CONSEQUENCES (DAMAGE)

Reduction of the deterministic damage due to the occurrence of a special event with deterministic consequence

(Case 3 in Table VII.5.) will increase the accuracy of the estimate as $\frac{dR}{dB_i} = p_i + \frac{k \cdot B_i \cdot (p_i - p_i^2)}{\sigma_{total}}$ is always positive.

If $p_i \lll 1$ and $K_b \lll B_i$ then:

$$R_i = B_i \cdot p_i + k \cdot B_i \sqrt{p_i}$$

The following inequalities have to be fulfilled for the measure to be sound:

$$\left| \frac{dK_b}{dR_i} \right| \leq 1 \quad \text{or} \quad \left| \frac{dK_b}{dB_i} \right| \leq \frac{dR_i}{dB_i}$$

From this:

$$dK_b \leq \frac{dR_i}{dB_i} \cdot dB_i = \left\{ p_i + k \cdot \sqrt{p_i} \right\} \cdot dB_i$$

Again the probabilistic estimate on page VII-15 is taken as an example.

As on the previous page: $p_i = 0.1$, $B_i: 300$ kfl and $k = 2$. dB_i is estimated in the order of magnitude of $0.9 \cdot B_i$. A rough estimate of an investment in a risk control measure for contaminated soil, aimed at the reduction of the damage, is:

$$dK_b = \left\{ 0.1 + 2 \cdot \sqrt{0.1} \right\} \cdot 0.9 \cdot 300 \approx 200 \text{ kfl}$$

The measure can consist of electrically/chemically cleansing of the soil *before* contamination has been established.

VII.9. LITERATURE

Belgraver, H., H. Kleibrink, The Markerwaard, government investments in environmental ordering, (De Markerwaard, overheidsinvestering in de ruimtelijke ordening) in Dutch, Economische Statistische Berichten nummer 3445, February 1984

The Economist, Under water over budget, October 1989

Goemans, T., H.N.J. Smits, Costs control of a mega-project, the Eastern Scheldt works, (Kostenbeheersing van een mega-project: de Oosterschelde werken) in Dutch, Economische Statistische Berichten nr. 3478, October 1984

Heezik, A. van, 200 years of estimates at the Ministry of Public Works, an exploration, (200 jaar ramingen bij Rijkswaterstaat, een verkenning) in Dutch, Ministerie van Verkeer en Waterstaat, Directoraat-Generaal Rijkswaterstaat, 's Gravenhage, March 1994

Merewitz, I., Cost overruns in public works, Benefit/cost and policy analysis, Aldine Publishers, Chicago, 1973

Vrijling, J.K. en A.C.W.M. Vrouwenvelder, Lecture notes b3, Probabilistic Design, (Collegedictaat b3, Probabilistisch Ontwerpen) in Dutch, Faculty of Civil Engineering of the Technical University Delft, 1984.

Vrijling, J.K., Lecture for N.A.P. DACE (Dutch Association of Cost Engineers) seminar - 6 November 1990 - Are project costs controllable) Lecture IV: The influence of time on the controllability of projects, (Lezing voor N.A.P. DACE (Dutch Association of Cost Engineers) seminar - 6 November 1990 - Projects kosten beheersbaar? Lezing IV: De invloed van de tijd op de kostenbeheersing van projecten) in Dutch.

Vrijling, J.K., Syllabus for the course within the framework of the Project Estimates Infrastructure and in the framework of the Post Academical Course: "Foreseen, unforeseen or uncertain?", (syllabus bij de cursus voor het Project Ramingen Infrastructuur en bij de Post Academische Cursus: "Voorzien, onvoorzien of onzeker?") in Dutch, 1995.

Vrijling, J.K. et al., The RISMAN- method, a method for the management of risks of large infrastructure projects, (De RISMAN-methode, een instrument voor het risicomanagement van grote infrastructuurprojecten) in Dutch, gezamenlijke uitgave van Gemeentewerken Rotterdam, NS Railinfrabeheer, RWS Bouwdienst, RWS Directie Zuid-Holland, TU Delft en Twijnstra Gudde, 1996.

VIII. SAFETY COEFFICIENTS

PIANC committee

Safety factors for breakwater design

by: J.K. Vrijling, J.W. v.d. Meer, P. de Swart, W. v. Hengel

VIII.1. BOUNDARY CONDITIONS AND OTHER BASIC VARIABLES

Seven different wave climates have been used as boundary conditions for the level II calculations. The first four are based on observed data from real projects. The last three are theoretical extreme assumptions.

All wave climates have been modelled by means of a Gumbel distribution.

$$\Pr\{H_s < h\} = \exp(-\exp(-\frac{h-A}{B}))$$

If the given distribution models the highest significant wave in a year, then the distribution of the highest significant wave height in N Year is defined by:

$$\Pr\{H_s < h\} = \exp(-\exp(-\frac{h-A'}{B}))$$

Where $A' = A + B \cdot \ln(N)$

The parameter values for the seven wave climates are given below:

Data	A	A'	B	B/A'
Sines	8.30	13.74	1.39	0.101
Bilbao	5.99	7.90	0.49	0.062
Tripoli	4.53	10.95	1.64	0.150
DHI	6.65	9.66	0.77	0.080
Test 1	-	6.72	1.80	0.268
Test 2	-	11.55	0.75	0.065
Test 3	14.57	-	0.05	0.003

N.B.: $A' = A + B \cdot \ln(50)$

Table VIII.1.: The parameter values of the wave height distributions

The value of B/A' mentioned on the last column gives an impression of the variation of the significant wave height.

In the study the climates are ranked according to the B/A' value in Table VIII.2..

The parameters of the wave steepness distribution are chosen according to the conclusions of the ICCE meeting in Delft.

Data	A	A'	B	B/A'
Test 3	14.57	-	0.05	0.003
Bilbao	5.99	7.90	0.49	0.062
Test 2	-	11.55	0.75	0.065
DHI	6.65	9.66	0.77	0.080
Sines	8.30	13.74	1.39	0.101
Tripoli	4.53	10.95	1.64	0.150
Test 1	-	6.72	1.80	0.268

Table VIII.2.: The parameter values of the wave height distributions ranked according to B/A'

The Uncertainty of the significant wave height distribution was modelled by:

$$f_{H_s} \cdot H_s$$

The uncertainty is assumed to be normally distributed with the following parameters:

MU	SI
1.0	0.00
1.0	0.10
1.0	0.20

It should be discussed if the first class really exists or that the set 1.0, 0.05 is a better description of the state of the knowledge.

The parameters of the distributions of the other parameters loading as well as resistance are chosen according to the conclusions of the ICCE meeting in Delft.

VIII.2. THE ACCEPTABLE PROBABILITY OF FAILURE

The Level II calculations have been performed for three values of the acceptable or target failure probability of the breakwater armour during the lifetime of 50 years. The values that have been used, 10%, 20% and 40%, are high compared with target probabilities in building codes. In Holland a value of 1.0E-4 (beta = 3.6) is proposed for ULS and a target of 1% for SLS (beta=1.8).

The values used here are found by calibration of existing breakwaters. But looking to the histories of failure it seems wise to add 0.1% and 1% to the list of values. This may initiate a trend to safer breakwaters.

VIII.3. THE FORMAT OF THE PROPOSED CODE

Two slightly different formats have been studied for the stability of the armour layers. The first format is theoretically correctly derived, but leads to some tension between theory and practice. The second format is directly derived from the way it will be used in practice.

The first format:

$$R = 6.2 \cdot f_m \cdot P^{0.18} \cdot S^{0.2} \cdot \Delta \cdot D \cdot \cot a^{0.5}$$

$$S = f_{H_s} \cdot H_s \cdot N^{0.10} / s_z^{0.25}$$

$$\gamma_R = R_{kar} / R'$$

$$\gamma_S = S' / S_{kar}$$

where the characteristic values for all basic variables are equal to MU: $X_{char} = MU(X)$ except the characteristic value of the design wave.

For the characteristic value of the wave height two values have been studied:

$$H_{s_char} = A' \quad \text{return period 50 years}$$

$$H_{s_cha} = A' + B \quad \text{return period } 2,72 \cdot 50 \text{ years}$$

In practice the format will probably be used as follows:

$$Delta \cdot D / gamma_R = gamma_S \cdot H_s / N_stab$$

or

$$Delta \cdot D = gamma_S \cdot gamma_R \cdot H_s / N_stab$$

$$\text{where } N_Stab = 6.2 \cdot s_z^{0.25} \cdot P^{0.18} \cdot S^{0.2} \cdot \cot \alpha^{0.5} / N^{0.1}$$

The second format is derived following the application of the design formulae in practice as explained above. Using the same characteristic values for the basic variables the safety factors are defined as follows:

$$R = Delta \cdot D$$

$$S = H_s / N_stab$$

$$g_{aa} \quad R_R = \alpha \quad R / \quad ' \quad \quad \quad aa \quad S \quad S_S = d / \quad _$$

Theoretically this format is less precise, but now the factors show the importance of the terms on which they are applied. In the end the difference is nil because the product of the two factors is equal for both formats.

$$Delta \cdot D = gamma_S \cdot gamma_R \cdot H_s / N_stab$$

The difference is shown for the Bilbao case.

Format	g_R	g_S	g_R.S
1' format	1.103	1.114	1.224
2' format	1.034	1.184	1.224

In the report only the results for the first format are presented.

VIII.4. THE RESULTS

As a result of the calculations it appeared that the value of the damage number S did not influence the values of the factors. Therefore this variable has been omitted in the results presented.

In the Table A all relevant results of the Level II safety factor calculations are given. The values of Gamma_R, Gamma_S and Gamma_sk are printed in the respective columns.

The difference between the two load factors is explained by the two proposed choices for H_s_char.

$$H_{s_char} = A' \quad \quad \quad \Gamma_{S}$$

$$H_{s_char} = A' + B \quad \quad \quad \Gamma_{Sk}$$

In the horizontal direction the influence of F_H_s on the factors is shown in three steps.

In the fourth block the limited effect of the wave steepness increasing to 5% is clear.

Vertically, the variation of the wave height, expressed by B/A', increases per block.

Over the blocks the target probability of failure P_{ft} rises from 10% in the life time to 40%.

To provide a better insight into the results the factor values have been plotted as a function of B/A' and P_{ft} .

It is seen that Γ_R is fairly constant over the range of B/A' values.

Overlooking all results presented in Table A the value of Γ_R is bounded by $1.02 < - > 1.12$.

A value of $\Gamma_R = 1.05$ is proposed for all cases.

The value of Γ_S fluctuates strongly with B/A' in this figure and for all other cases. It seems impossible to choose one generally applicable value for this factor.

If, however, the definition of H_{char} is changed to $A' + B$ the behaviour of Γ_{Sk} is more restrained, and depending on the F_{H_s} class and the target failure probability a constant value might be chosen.

In Figure VIII-2 the factors are presented as a function of the uncertainty of the wave height distribution for the Sines wave climate.

Again it is concluded that Γ_R shows stability.

The factor Γ_{Sk} clearly increases with F_{H_s} , except for the highest value of the target probability of failure.

In Figure VIII-3 the most stable loading factor Γ_{Sk} is shown to be sensitive for the values of F_{H_s} and P_{Ft} . This sensitivity must be honoured in the code for technical as well as psychological reasons.

The extreme variability of Γ_S is clear from Figure VIII-4. If this definition of the factor is followed the idea of a fixed factor for all wave climates has to be abandoned.

The relative stability of Γ_R is clear from Figure VIII-5. Although the target probability of failure influences this factor, it seems appropriate to take a constant value for the sake of simplicity.

VIII.5. TENTATIVE PROPOSAL

The first choice to be tested further is $\Gamma_R = 1.05$.

For the loading factor Γ_{Sk} the following values are proposed, taking into account the considerations mentioned above.

Gamma_Sk P_f	0%	f_H _s 10%	20%
10%	1.10	1.15	1.25
20%	1.05	1.10	1.15
40%	1.00	1.00	1.00

As a first test the product of the loading and the resistance factors might be compared with the calculated results.

Gamma_Total P_f	0%	f_H _s 10%	20%
10%	1.15	1.20	1.30
20%	1.10	1.15	1.20
40%	1.05	1.05	1.05

VIII.6. DISCUSSION POINTS

- Format of the code
 - fixed factors
 - H_s charact.
- Minimal uncertainty of wave climate of 5%
- Additional P_f values of 0.1% and 1%
- The influence of dedicated model tests on the factors.

IX. MAINTENANCE THEORY

IX.1. INTRODUCTION

Before saying anything about maintenance it is wise to define this term.

Maintenance signifies:

All activities aimed at retaining an object's technical state or at reverting it back to this state, which is considered a necessary condition for the object to carry out its function.

These activities include both the repair of the structural strength, back to the starting level, and any inspections.

The costs of maintenance of civil engineering structures amounts to approximately 1 % of the founding costs per year. For a life-span of 100 years this means that the maintenance costs are of the same magnitude as the construction costs. Taking into account the decline in new housing development projects, maintenance costs are clearly becoming an increasingly greater share of the expenses.

A direct consequence is the desire to minimise maintenance costs.

In order to realise this, the optimal maintenance strategy has to be sought.

From the mechanical engineering maintenance theory, the following classification of strategies is known:

1. Curative maintenance - fault dependent maintenance
2. Preventive maintenance - use dependent maintenance
- condition dependent maintenance.

In the case of fault dependent maintenance, an object is repaired or replaced when it can no longer fulfil its function (see Figure IX-1). Thus, repair takes place after failure, therefore a failure norm is involved. The life of an object is fully exploited. An object's failure (and the associated costs) are accepted.

In hydraulic engineering this type of maintenance is usually not acceptable because, generally, the accepted probability of failure is limited. This type of maintenance can, however, be applied to non-integral construction parts (parts which do not contribute to the stability of the entire structure), with modest consequences of failure (provided reparation or replacement is not postponed for too long).

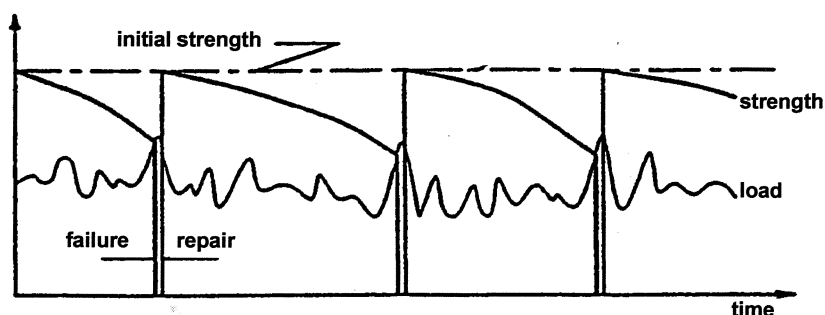


Figure IX-1 Possible course of strength with fault dependent maintenance

In the case of use dependent maintenance, maintenance is carried out after a period consisting of a previously determined number of usage units. The costs of maintenance and of the risk¹ generally determine the extent of this period. The life of the object is not totally exploited. In mechanical engineering, this type of maintenance is applied if the usage units can be registered, for example with a kilometre indicator, product counter, etc..

In hydraulic engineering, this is different. We can hardly register all loads for every construction to organise the maintenance around those registrations. In this case, the loads in a period are considered random variables. Subsequently, the life time is estimated and the time for repairs is determined for which the probability of failure is sufficiently small and for which the costs are minimal. Therefore, one should use the term time dependent maintenance (see Figure IX-2). A time norm is involved.

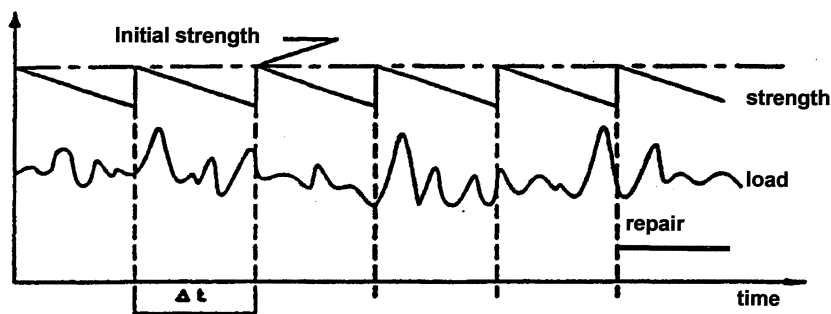


Figure IX-2 Possible course of the strength for time dependent maintenance

If loads which cause deterioration are registered, maintenance (inspection or repair) can be called for after an extreme large load or after a certain total amount of loading (cumulative). This is classified as load dependent maintenance, involving a load norm. In case the cumulative load plays a role, the possible courses of strength and load are given in Figure IX-3.

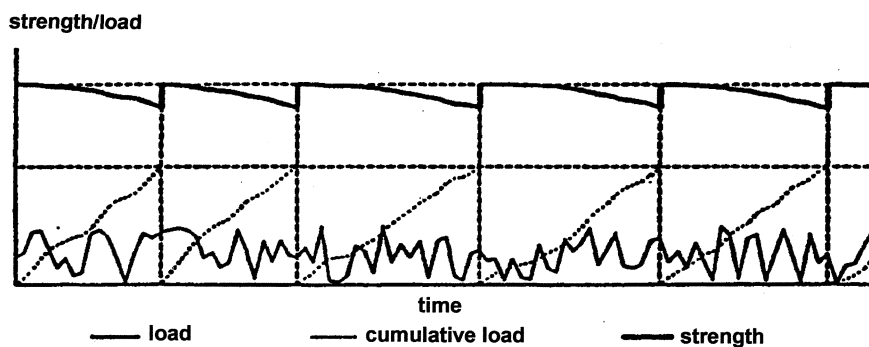


Figure IX-3 Possible course of the strength for load dependent maintenance

With condition dependent maintenance the state of the object is determined at set intervals, by means of inspections. The decision whether or not to carry out repairs is based on observations. The inspection intervals can be regular or dependent on the condition of the object. In the latter case condition parameters, indicating the condition of the object, have to be visible. The probability of failure in a period between two inspections has to be sufficiently small. Generally, the life time of the object can be better exploited than with usage dependent maintenance, but the costs of the inspections do have to be taken into account.

This type of maintenance also involves drawing up norms.

These norms concern (see Figure IX-4):

1. a limit state which leads to an increase of the inspection frequency (warning threshold)

¹ RISK = (PROBABILITY OF FAILURE) * (CONSEQUENTIAL DAMAGES)

2. a limit state which leads to carrying out repair works (action threshold)
 In fact this concerns strength norms. These norms result from an optimisation of the maintenance or correspond to a socially accepted failure probability in a year.

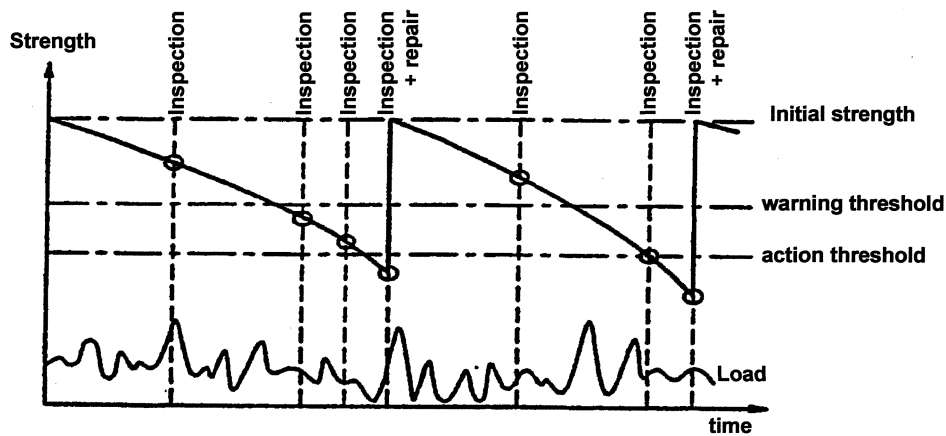


Figure IX-4 possible course of strength with condition dependent maintenance

The selection of the maintenance strategy to be used depends on factors such as:

- predictability of the life-span of the object;
- consequence of failure of the object;
- costs of replacement or repair;
- costs of inspection;
- visibility of the condition of the structure (damages or deterioration).

A first comparison of the different strategies, focussing on the usability is presented in Figure IX-5.

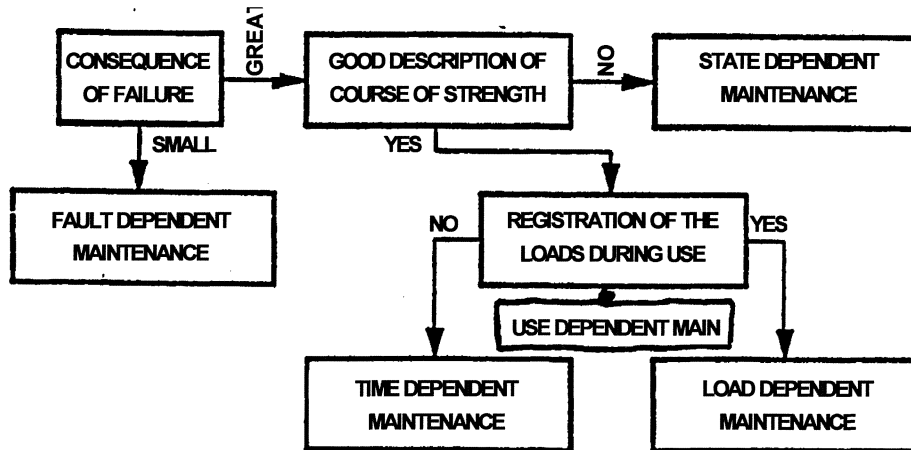


Figure IX-5 Global selection of the maintenance strategy

In hydraulic engineering a combination of two or more strategies appears to lead to a better result than simply applying a strategy selected using Figure IX-5. Thus, for example, a planning can be drawn up using the time dependent maintenance strategy, which can be adapted on grounds of observed loads, whilst the initiative to commence repair works is dependent on the strength according to inspection. Based on this example, one can state that the limits of applicability of the different strategies are flexible for hydraulic engineering.

Generally, however, statements can be made about the consequences of failure and with that the acceptance of fault dependent maintenance.

Choosing between time dependent and condition dependent maintenance is less simple.

Completely time dependent maintenance will be applied if inspection is not possible or if inspection is expensive relative to repairs.

Completely condition dependent maintenance will be carried out if it is not possible to make a prognosis of the strength in the course of time or if inspection is very simple and therefore inexpensive.

An important aspect of the condition dependent maintenance is collecting data concerning the strength in the course of time. This allows for better planning of the maintenance or the inspections.

This chapter will pay no further attention to the purely condition dependent maintenance, which requires no further knowledge of the wear of a construction.

The aim of this chapter is to give a method which can be used to determine an economically sound planning of the times of repair and/or inspection of a structure.

Existing design models will be used for the deterioration of the structure.

The expected value of the costs of repair, inspection and the risk are central. To determine these expected values of the costs, a grasp of basic statistical techniques is necessary. For this, the reader is referred to the lecture notes CTWa4130 - Probabilistic design (Vrouwenvelder, Vrijling - TUDelft).

IX.2. TERMINOLOGY

IX.2.1. TIME DEPENDENT STRENGTH

The strength of a structure is not independent of the point in time of evaluation. For a structure made of reinforced concrete, for example, the strength increases as the concrete hardens and decreases when the carbonation depth exceeds the cover, leading to corrosion of the reinforcement. For a steel structure, corrosion clearly also leads to a decrease of the strength of the structure. For structures which are not so much affected by the decay of materials, the strength can also be time dependent. Here, a typical example is the settlement of a dyke, where the crest height is the strength.

IX.2.2. PROBABILITY OF FAILURE

Failure is generally defined as exceeding a limit.

The limit state is a state, where the strength of and the load on the construction are equal. Two types of limit states can be distinguished, namely:

- a. the Ultimate Limit States (ULS) and
- b. the Serviceability Limit States (SLS).

When the ULS is exceeded, failure occurs as a result of collapse of the structure under extreme loads. Collapse of an earth body, the deflection of the structure and so on are ultimate limit states.

When the SLS is exceeded, the functional demands can no longer be met. Examples are limit states concerning: deflection of a floor, cracking in reinforced concrete, waves which are too high behind a breakwater etc..

Generally, failure can be defined as exceeding the strength with the loads. The state of a structure can be described using a reliability function:

$$Z = R - S$$

where: R = the strength
 S = the load

If the strength and/or the load are described with random variables, Z is also a random variable. If $Z < 0$ the structure fails. The probability of failure is:

$$\Pr\{Z < 0\} = \int_{-\infty}^0 f_z(\xi) d\xi$$

where: f_z = probability density of Z
 ξ = realisation of Z

The difficulty with the determination of the failure probability is the fact that the distribution function of Z usually can not be determined exactly. Only in a few cases, e.g. where all variables are normally distributed, the distribution of Z can be determined. However, there are techniques that make it possible to calculate the probability of failure or to approximate it. If the distributions of R and S are known:

$$\Pr\{Z < 0\} = \Pr\{R < S\} = \int_0^{\infty} (1 - F_S(\zeta)) \cdot f_R(\zeta) d\zeta$$

where: F_S = probability distribution of $S = \int_{-\infty}^{\zeta} f_s(v) dv$
 f_s = probability density function of S
 f_R = probability density function of R

This integral is known as the convolution integral.

In case the strength and/or loads consist of several random variables, the distributions of S and R are usually not exactly known. In these cases, the probability of failure is approximated by a Monte Carlo simulation or a level II calculation.

IX.2.3. DETERIORATION MODELS

The relation between strength and time is given by a deterioration model. The relation can be linear, exponential, logarithmic, etc..

In the case of development of the compression strength of cement stone, an asymptotic relation clearly exists (see Figure IX-6). After approximately 30 days, the compression strength of the cement stone almost equals the maximum value.

Settlement of a dyke on a thick, hardly permeable layer also involves a limit value of the strength which can be observed. The settlement approaches a final value (see Figure IX-7).

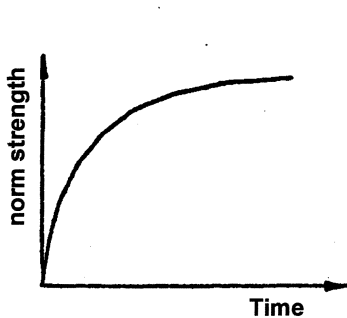


Figure IX-6 Course of the compression strength of cement stone

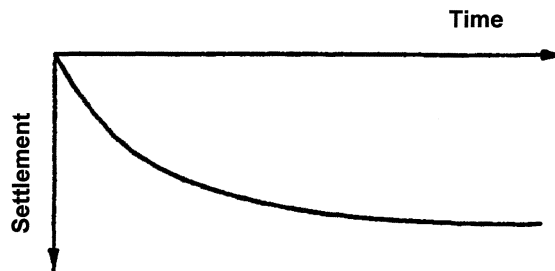


Figure IX-7 Course of settlement in time (consolidation)

The deterioration model thus determines the strength at every point in time. The model is an approximation of reality. The input required for the model is the starting strength and usually a number of parameters which describe characteristics of the material or the structure.

The parameters which serve as the input for the deterioration model are usually determined from tests or observations. They rarely have a certain value and can usually be best described by a random variable. This means that the strength at a certain time is a function of random variables and is thus a random variable itself.

IX.2.4 LIFE-SPAN OF A STRUCTURE WITHOUT MAINTENANCE

The life-span of a structure is the time which passes between the realisation of the structure and the failure of the structure. In Figure IX-8 this is clearly marked for time dependent strength and load, for which the exact values are known for every point in time. The intersection of the strength and the load determines the moment of failure of the structure.

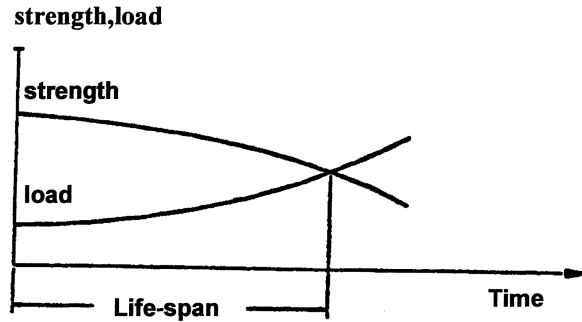


Figure IX-8 Life-span for an exactly known course of strength and load in time

In the case above, both strength and load are deterministic. The life-span is simple to determine, in that case. This is less so, when the load and/or the strength are random variables because, then, the life-span is also a random variable. The definition of the probability distribution of the life-span is:

$$F_L(t) = \Pr\{L < t\} = 1 - \Pr\{R > S \text{ for every } \tau \text{ in the interval } (0, t)\}$$

For the consideration of $\Pr\{R > S \text{ in the interval } (0, t)\}$ the load has to be defined as the dominating load in the period $(0, t)$. As t increases the average of the load in the interval $(0, t)$ will also increase. This way the dependence on the duration of the dominating load is incorporated in the probability distribution of the load. If the strength is also time dependent a new problem arises, namely the determination of the normative strength for the period $(0, t)$.

Given the probability distribution for the life-span, one can easily determine the probability density function from:

$$f_L(t) = \frac{dF_L(t)}{dt}$$

The expected value of the life-span can be found by integration:

$$\mu_L = \int_{-\infty}^{\infty} t \cdot f_L(t) dt = \int_0^{\infty} t \cdot f_L(t) dt$$

Multiplication of the probability density with dt gives the probability that the life-span ends between the moments t and $t + dt$:

$$f(t)dt = \Pr\{t < L < t + dt\}$$

The life-span ending in $(t, t + dt)$ means that $R < S$ in $(t, t + dt)$ and $R > S$ in $(0, t)$. In formulae this is:

$$f(t)dt = \Pr\{R < S \text{ in } (t, t + dt) \wedge R > S \text{ in } (0, t)\}$$

The probability density function of the life-span can also be seen as the probability of failure per time unit, i.e. the failure rate. In this case one refers to unconditional failure rate.

It is also possible to define the conditional failure rate ($r(t)$). Multiplication of the unconditional failure rate with dt again gives the probability of collapse in $(t, t+dt)$, but this time on the condition that in $(0, t)$ failure doesn't occur. in formulae:

$$r(t)dt = \Pr\{R < S \text{ in } (t, t + dt) | R > S \text{ in } (0, t)\}$$

The relation between $F_L(t)$, $f_L(t)$ and $r(t)$ is (the formulation of the conditional probability):

$$f_L(t)dt = (1 - F_L(t)) \cdot r(t)dt$$

This equation can also be written as:

$$r(t) = \frac{\frac{d}{dt} F(t)}{1 - F(t)} \Rightarrow \frac{d}{dt} F(t) + F(t) \cdot r(t) = r(t)$$

The solution to this differential equation is:

$$F(t) = 1 - \exp\left[\int_0^t -r(\tau)d\tau\right]$$

This equation enables us to establish the probability distribution and the probability density of the life-span if the load and strength are dependent on the duration.

To clarify this, we consider a construction for which the strength decreases in time but can be considered constant in an interval $(t, t+dt)$.

The strength in this interval is given by a deterioration model, on the condition that failure does not take place in the interval $(0, t)$. If this were the case, the structure would be replaced and deterioration would commence at another point in time.

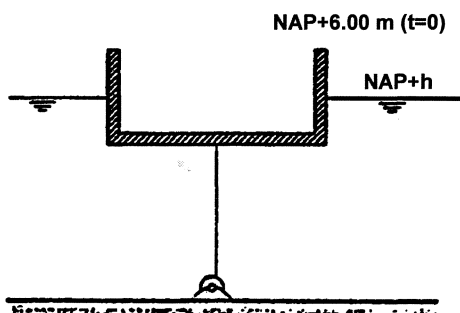
The load is defined using an extreme value distribution for maximums in a period lasting dt .

Because the strength is considered constant for a duration dt , the probability of failure in every interval $(t, t+dt)$ can be determined.

Because the strength in the interval $(t, t+dt)$ is conditional, the calculated probability of failure in the interval $(t, t+dt)$ is also conditional, i.e.:

$$\text{Calculated probability of failure} = \Pr\{R < S \text{ in } (t, t + dt) | R > S \text{ in } (0, t)\}$$

This is the exact formulation of $r(t) \cdot dt$. Dividing the calculated probability of failure in the interval $(t, t + dt)$ by dt gives the conditional failure rate. This serves to determine the probability distribution and the probability density of the life-span.



As an example, a strictly theoretical case is considered, involving a container, consisting of four sides and a bottom, floating on a lake. Chains attach the container to a winch at the bottom of the lake. At the beginning of every time unit the chain is pulled down 2 cm, after which the situation remains the same during one time unit (see Figure IX-9). At the time $t=0$ the top of the container is situated at NAP+6.00 m.

Figure IX-9 schematisation of the example

The maximum water level in a time unit is defined by a Gumbel distribution for maximums:

$$\Pr\{h > \xi\} = 1 - \exp\left(-\exp\left(-\frac{\xi - 1.98}{0.33}\right)\right)$$

with: h = water level

The structure fails if the lake water level exceeds the side of the container, thereby filling the container with water. It is now possible to calculate $r(t)dt$ for every point in time with:

$$r(t) \cdot dt = 1 - \exp\left(-\exp\left(-\frac{6 - 0.02 \cdot t - 1.98}{0.33}\right)\right)$$

The equation of the probability distribution of the life-span is:

$$F_L(t) = 1 - \exp\left(-\int_0^t r(\tau) \cdot dt\right) = 1 - \exp\left(-t + \int_0^t \exp(-\exp(0.0606 \cdot \tau - 12.1818)) dt\right)$$

and the probability density function is:

$$f_L(t) = \frac{d}{dt} F_L(t)$$

Figure IX-10 displays the numerical solutions of $F_L(t)$ and $f_L(t)$.

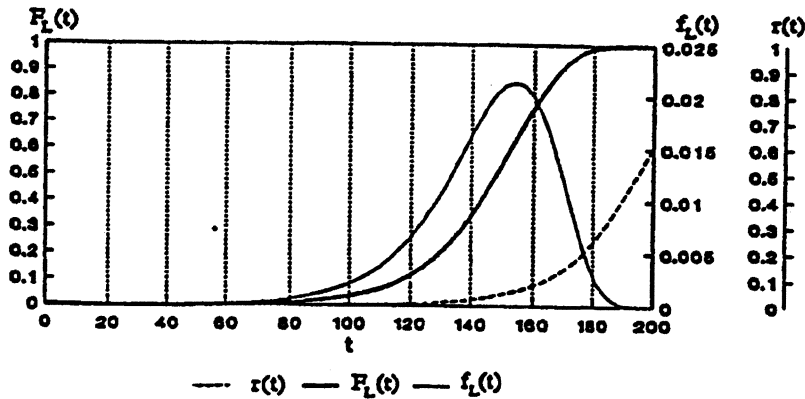


Figure IX-10 Probability distribution and probability density of the life-span

The expected value of the life-span is approximately 140 years.